Basics of Ship Manoeuvrability

S. Sutulo

April–June 1999/Revision: 2000/Revision and extension: 2007,
2009/Corrections: 2011, 2013

Abstract

A concise manual on the surface displacement ship manoeuvring motion theory based on a systematic exploitation of the mathematical model concept. Main manoeuvring properties are outlined and manoeuvring measures and criteria are commented. General principles of the creation of manoeuvring mathematical models are described and all the elements of mathematical models are introduced. Principles of computerized manoeuvring simulators are outlined and typical simulation results are presented and commented. Methods of determining and describing hydrodynamic forces acting upon a ship in her curvilinear manoeuvring motion are analyzed. Foundations of analytic study of the properties of linearized ship mathematical models are given. Also, briefly covered is manoeuvring in wind and current and commented are the IMO Manoeuvring Standards.

Remark: The text is subject to further revisions and extensions which is also true for the Table of Content.

Contents

List of Figures

List of Tables

Chapter 1

Introduction to Ship Manoeuvring

1.1 General

1.1.1 Subject of Ship Manoeuvrability

Many living creatures and multiple artificial objects can move and *manoeuvre* i.e. change the direction and magnitude of their motion. In many cases, a capability to manoeuvre is one of the most vital and important features of those objects. This is true for the overwhelming majority of transportation vehicles (such as: cars, trucks/lorries, buses, trains, tramways, aircraft, ships, ferries and many others), working vehicles (tractors, fishing vessels, fire-fighting airplanes and choppers, special purpose cars), and military hardware (naval surface ships, submarines, torpedoes, guided missiles, combat aircraft, tanks, armoured personal carriers etc.). All existing "manoeuvrable" objects can be clustered into several groups depending on their nature, and on their manoeuvring and dynamic properties. In the present course of lectures we shall only deal with the manoeuvrability of surface displacement ships (that is what the term *ship* will mean from now on!) with only occasional mentioning of some other objects, when this seems to be appropriate. At the same time, almost all surface displacement ships, irrespective of their purpose, size and special features, can be treated within a unified theory.

The concept of manoeuvring is intuitively clear and hardly requires search for some mathematically rigourous definitions. Moreover, different experts may stick on slightly different understandings of this and related terms (for instance, it is assumed in a popular reference book [7] that "manoeuvring" doesn't imply any controlled speed changes and a term "controllability" was introduced there to cover more general cases[1]). Nevertheless, it is important to emphasize that the manoeuvrability in the general sense includes also the motion stability property (which shouldn't be confused with a ship's stability in the hydrostatic sense!). This property is closely related to the *coursekeeping* process as the latter becomes easy and smooth just at a certain degree of the ship's directional stability.

At the same time, the ship manoeuvring is closely linked to the control theory as the ship

[1]This term is, however, rarely used by most manoeuvring experts maybe because of danger of confusing it with the (full) controllability of a dynamic system as defined in the control theory.

motion is probably the first thing subject to a careful and permanent control performed by specially trained operators (helmsmen, navigators) although often with the assistance of automatic control systems.

1.1.2 Specific Dynamic Properties of Surface Displacement Ships

It is intuitively clear that the surface ships exhibit in the process of manoeuvring some characteristic features which are not necessarily typical for other moving objects. Many of these features have strongly influenced the content of the discipline and it would be useful to list them here:

1. **A surface ship's manoeuvring motion is plane.** Of course, any ship is attached to the water surface which will be treated here as a horizontal plane[2]. Here lies the main difference between dynamics of surface ships and submarines as the latter can manoeuvre in space (a *surfaced* submarine must and can be treated as a surface displacement ship). So, any ship has *three* main degrees of freedom (DOF) and her current position can be unambiguously defined with **three** generalized coordinates[3]. In fact, manoeuvring motions of surface ships in the horizontal plane can be accompanied with secondary motions in vertical planes (dynamic roll and sometimes sinkage and trim) but these are of lesser importance and always limited in their amplitude.

2. **The surface displacement ships are relatively large and slow objects.** In general, they are even the largest and the slowest means of transportation. This statement is backuped by the analysis of the values of a specific parameter called *the reference time* T_{REF} defined in the following way:

$$T_{REF} = \frac{L}{V} = \sqrt{\frac{L}{g}}\frac{1}{\mathsf{Fn}}, \tag{1.1}$$

   where L is the ship's reference length (in most cases it is the length between the perpendiculars); V is the ship speed's magnitude; g—the acceleration of gravity; Fn is the Froude number.

   Some typical values of the reference time are listed in Table 1.1.

   Pay attention that all the values will become larger at partial speeds. The reader is also invited to estimate reference time values for some other moving objects, including living ones (cars, bats, birds, fish, insects, etc.).

3. **Most of the surface displacement ships are *roughly* directionally marginally stable.** This property will be discussed later in more details and here we must only

[2] Actually it is rather a spherical surface and this is accounted for in the navigation but the ship manoeuvring theory does only deal with the length scales comparable with the ship length or exceeding it by one order—in both cases the free surface's curvature is negligible.

[3] One needs 6 generalized coordinates to describe the position of a submarine. On the other hand, it is hard to imagine a moving object with only two meaningful degrees of freedom but one-DOF cases are evident: trains, tramway and any other rail transport. The paradox is explained by the existing relationships between the space dimension and the corresponding number of degrees of freedom (i.e. 1D—1DOF, 2D—3DOF, 3D—6DOF).

Table 1.1: Reference Time for Some Aeronautical and Marine Manned Objects

Vehicle	*Reference time at full speed in seconds*
Supersonic fighter	0.02–0.03
Heavy subsonic aircraft	0.15–0.25
Airship	2–4
Air-cushion vehicle	1–3
Destroyer-class naval surface displacement ship or a nuclear-powered submarine	6–8
Fast displacement catamaran	2–4
Typical general cargo ship	12–20
Very large full-bodied vessel	40–60

mention that this is has some connection with the previous feature and determines many of dynamic peculiarities of the displacement ships.

4. **Hydro- and aerodynamic forces dominate in the analysis of the surface ship manoeuvring.** This property is, of course, true for most marine and aeronautical objects but surface displacement ships operate just on the air-water interface and it turns out that the both media contribute substantially when the ship is under wind action (the latter is in fact even more typical than the still weather conditions).

1.1.3 Ship Manoeuvring Applications

Finally, it is worthwhile to note that the manoeuvring theory is closely related to the ship navigation and navigational safety: there have been in the history of shipping enough examples of damages caused by poor manoeuvring capabilities of the involved ships. Mathematical models for ship manoeuvring constitute an important component of the software of all computerised manoeuvring simulators used for training navigators and for the harbour design. Although traditionally manoeuvring issues have never been of primary importance in the ship design, they could not be completely disregarded either. This is especially important for the river-going vessels but after introduction of the *Interim Standards for Ship Manoeuvring* by the International Maritime Organization (IMO) [40] one could witness a significant grow of attention payed to the manoeuvring performance of the merchant sea-going ships.

1.1.4 Links to Other Fields of Ship Hydrodynamics and Dynamics

Certain analogies and common points between the theory of ship manoeuvring and the theory of ship motions in waves can also be established as they both cover just somewhat different aspects of the ship dynamics. However, many factors prevent these two fields from complete fusion and main distinctions will be analyzed in these lectures as well as the similarities.

Another possible look at the ship manoeuvring is that it presents itself a certain generalization of the ship resistance and propulsion. The main difference between these two disciplines can be formulated as follows: while the former studies arbitrary ship motions, the latter deals exclusively with the specific case of rectilinear translatory motion along a ship's centreplane. One evident consequence of this connection is that most of the manoeuvring mathematical models use some results and data obtained from resistance and propulsion analysis. Thus, the ship manoeuvring is a kind of integrating discipline which crowns the cycle in ship hydrodynamics and there is no wonder it is typically studied the last.

1.1.5 Approaches, Methods, and Tools

Problems of manoeuvrability, similarly to all other topics of the ship hydrodynamics and dynamics, can be and are studied both experimentally and theoretically. Probably for the ship manoeuvring, the importance of experimental methods is especially high due to extreme complexity of the flow structure around a manoeuvring object. The viscous effects are here of primary importance and the picture is further complicated with interactions between the hull, the propeller, and the rudder (or some other control device). It is now generally acknowledged that the only match to the experiment could be the computational fluid dynamics (CFD) methods developed for the Reynolds averaged Navier–Stokes equations (RANSE). By the time of writing this text lines (February 2007) manoeuvring-oriented CFD codes were only used by few researchers and mainly for testing purposes. All practically significant manoeuvring mathematical models had been developed on the basis of experimental data. However, collection of experimental data is not that easy either as the experimental facilities suitable for manoeuvring studies and these studies themselves are very complicated and expensive. Such a situation was one of strong reasons for developping simpler, though approximate, theoretical methods for estimating hydrodynamic coefficients of ships' hulls and rudders at early design stages. Most of these methods are based on the wing theory and on the slender-body theory and result in simple formulae providing, however, very rough but often realistic estimates of manoeuvring forces. Several attempts have been made to raise the accuracy by applying various vortex-lattice methods to actual ship hulls but the results were usually disappointing. This can be explained primarily by difficulties and uncertainties in implementing the Kutta condition on typical hull forms[4]. Actually, much better results were obtained by introducing empirical corrections into the slender-body-theory formulae and this approach is still used very often in practical calculation methods.

Similarly to the theory of seakeeping, the ship manoeuvrability not only contains a hydrodynamic but also a dynamic part. In the dynamic problems, all the forces are supposed to have been estimated and the ship motion analysis becomes the main target. The dynamic problems, as compared to the hydrodynamic ones, are more treatable with theoretical and/or numerical tools, including the numerical time-domain simulations. Methods and concepts of the control theory turned out to be especially suitable for the manoeuvring motion analysis. This is true even when dealing with the so-called uncontrolled motion, leave alone studies of the closed-loop systems modeling manoeuvring ships steered by helmsmen or autopilots. Dynamic experiments,

[4]The same vortex-lattice methods showed perfect performance in the cases when the Kutta condition could be surely and unambiguously formulated as e.g. for the airplane wings and propeller blades.

mainly in form of the free-running model tests, are also used for validation of theoretical evaluations. Of course, the most expensive full-scale manoeuvring trials are traditionally considered as the ultimate criterion of truth.

1.1.6 Brief Historical Notes

The theory of ship manoeuvring and control was the last area of the ship hydrodynamics to be born. During centuries, ships were being designed and built without special considerations of manoeuvring performance. Satisfactory controllability was achieved through following traditional rules and recipes and the naval architects did not feel any sensible pressure from that side, in spite of some occasional failures when a ship happened to have either a bad turning ability, or a poor directional stability. In short, before the World War 2, nothing was known about the ship manoeuvring except for several empiric formulae part of which even recognized later as substantially wrong . But at the end of 40s and at the beginning of 50s, development of the surface ship manoeuvring theory gained momentum. It is interesting to note that this followed even a more dramatic boost in studies of the submarine and marine weapons dynamics. The latter was pre-determined by the vital importance of better dynamic qualities of the high-speed after-war subs which were critical not only for their enhanced combat efficiency but also from the viewpoint of their survivability. As it was very soon understood that the submarines were going to become one of the most important strategic component of the modern navy, large investments were made into the construction of advanced experimental facilities and into the current support of numerous research projects. Firstly, it happened in the USA and in Russia but somewhat later the "manoeuvring boom" spread over other developed countries. It is also worth mentioning that first studies in the field of submarine dynamics were based on the conversion of the results obtained earlier for the airships having suffered sharp decline approximately in the same period.

Of course, further diffusion of new knowledge and tools over broader research area covering various surface ships was natural and inevitable and since the end of fourties, the surface ship manoeuvring has been developing rapidly enough to become by now one of the most interesting and promising research areas in the ship science.

1.2 Review of Ship Control Devices

1.2.1 General Remarks

It is absolutely clear and it follows from the general Newtonian laws that in order to change parameters of the motion of a ship (i.e. to make her manoeuvre), some additional forces and/or moments are to be applied. This can be done either explicitly through **generating** some additional forces with **active control devices**, or implicitly, by means of alterating some already acting forces with **passive control devices**. In the latter case, changed are the forces produced by ship propellers and/or forces acting upon a ship's hull (with all the appendages). It is clear that the active control devices must consume some energy to produce a steering force and they can be interpreted as some special kind of propellers. Active devices are, in principle, effective independently of the advance speed, although some of them can lose their effectiveness at normal speed and are used mainly in low-speed manoeuvring. As, on the contrary, the apparent effectiveness of passive control devices increases with the speed, it can be said that these two groups of control means complement each other. Of course, all control devices used on displacement ships are *hydrodynamic*[5]. The hydrodynamic issues, however, will be covered more in detail later while in this section we shall limit ourselves with a brief and rather superficial review of the most popular controls. As to details of the design and construction of the devices, these are covered in other naval architecture disciplines while in the ship manoeuvrability are only mentioned their most important features which may become useful for the development of their mathematical models.

1.2.2 Active Devices

The most popular active control devices are jet thrusters mounted inside transverse tunnels piercing a ship's hull (Fig. 1.1).

A small reversible propeller driven by means of an angular transmission (Fig. 1.2) produces a jet and generates a reaction force acting at the opposite direction. For the majority of modern vessels, such thrusters are located near the ship's bow to create a larger steering moment (they are then supposed to operate together with the main propellers and rudders). When some ship is expected to manoeuvre frequently in complicated harbour areas, additional stern thrusters are also desirable. If a ship is equipped with both bow and stern thrusters, she can not only freely manoeuvre at zero speed but can also keep her position under wind and/or current action without recourse to anchors. This process is called **dynamic positioning** and it is a typical operation mode for drilling ships, mine hunters, and research vessels.

At the same time, tunnel thrusters have their effectiveness degraded at a non-zero speed. This is caused by additional suction which is due to vortices generated by the deflected jet (Fig. 1.3) as which produces a force directed opposite to the thrust. On Fig. 1.4 borrowed from [26] four zones of additional pressure (disappearing at zero speed) are shown.

The suction in the zone A has just been mentioned. The additional pressure C is caused by velocities' reduction ahead of the jet and the zones B and D are caused by the inflow

[5]The evident exception are sailing boats where the sail in fact combines propulsive and controlling functions

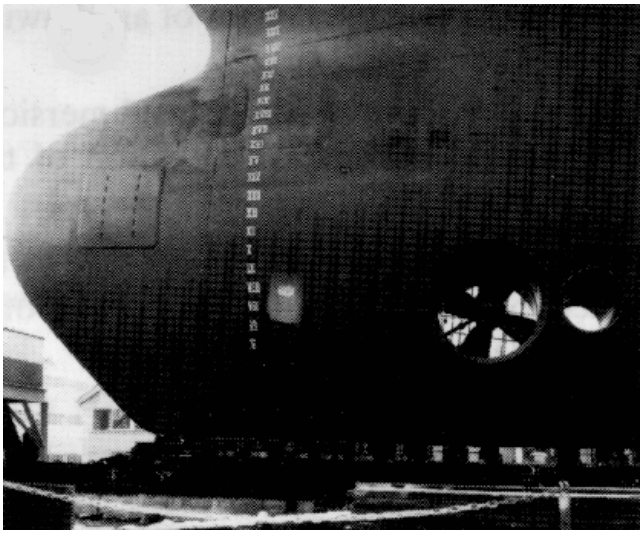

Figure 1.1: Bow thruster arrangement (with a suction tunnel behind)

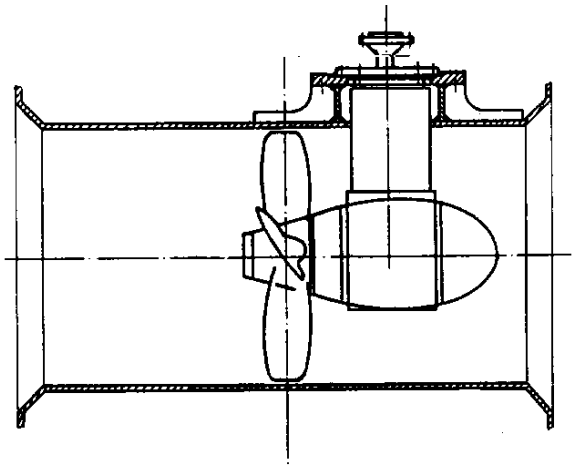

Figure 1.2: Tunnel thruster: schematic view

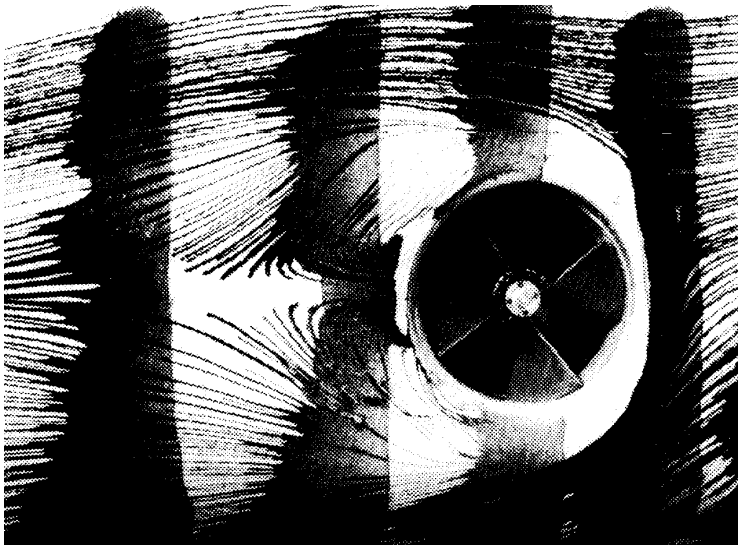

Figure 1.3: Streamlines on the hull in the vicinity of a thruster's inlet in ahead run

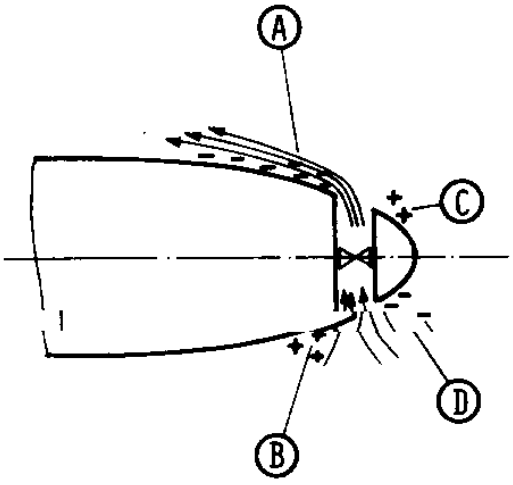

Figure 1.4: Bow thruster at non-zero ahead speed: pressure zones

acceleration near the inlet (the additional velocity is added to the main flow in the zone D but is subtracted in the zone B). However, the resulting effect depends greatly on the hull shape in the vicinity of the thruster's inlet and outlet, and, according to the experimental data presented in [26], the reduction varies from 10 to 70 percent for the side force. It is interesting to note that the force's moment doesn't vary in full compliance with the side force as the resulting centre of pressure can be shifted (there are cases when the moment is increased at non-zero speeds). The so-called suction tunnels (see Fig. 1.1) are sometimes envisaged to reduce the deterioration effects. Anyway, it is generally believed that any tunnel thrusters become ineffective at normal operating speed especially compared with the effectiveness of passive devices. An important consequence of this is that navigators should not rely on the thrusters trying to augment a ship's turning ability in emergency situations.

As an alternative, azimuthing thrusters (Fig. 1.5 and Fig. 1.6) can also be used in low-speed manoeuvring but they are only installed on special vessels or another floating objects (platforms). Sometimes, and there is a trend to make it even common, they are used as main "vectoring thrust" propellers or "azipods" eliminating any need in passive controls.

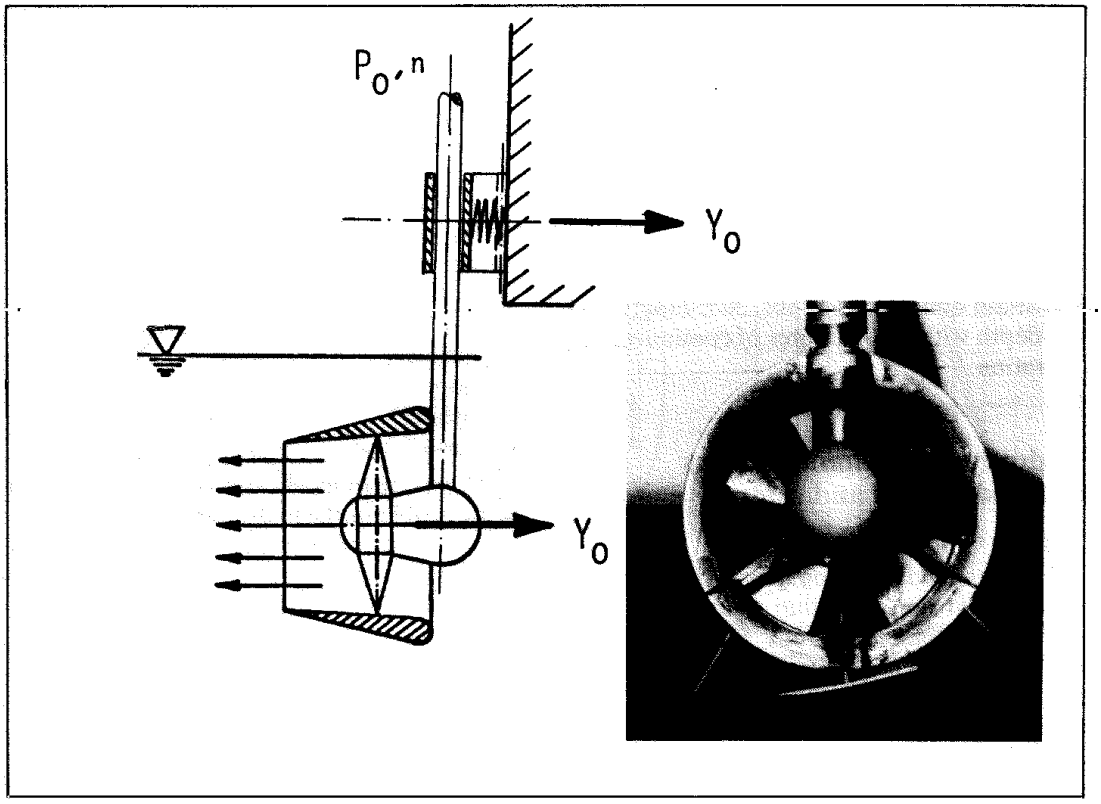

Figure 1.5: Ducted azimuthal thruster: Y_0 —thrust; P_0 —torque

1.2.3 Passive control devices

The bow thrusters and other active means of control appeared relatively recently. During centuries, the ships have been equipped exclusively with *rudders* which still are the most typical

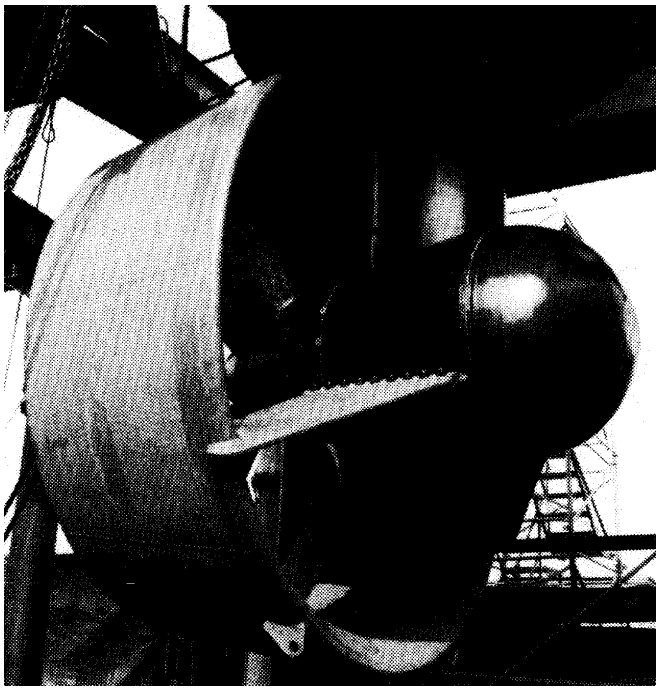

Figure 1.6: A powerful azimuthal thruster

passive or *main* ship control devices. In most cases, the rudder can't be competed as an effective, reliable and convenient tool for performing normal nautical manoeuvres at non-zero speeds. In fact, when the rudder is located behind the propeller and is working in the slipstream, its applicability area is even somewhat extended: navigators are using the so-called "kick ahead" manoeuvre when the propeller starts running for a short time at the deflected rudder and zero ship speed. The result is that the ship is getting a significant angular momentum while the speed remains practically null.

A great variety of ship rudders have been designed, created, and installed on ships but, leaving aside special high-performance rudders (flap rudder, rotating cylinder rudder, active rudder[6], Schilling's rudder, see [26] for details) one can only discover on most of the sea-going vessels the types shown on Fig. 1.7. Even more, the type D (rudder hung on the post) shown on the figure is now rarely used although it was very popular on earlier designs of single-screw merchant ships. Another somewhat obsolete type of rudder used on twin-screw vessels is the **skeg rudder** (Fig. 1.8).

Some comments should be made about the horn rudder (type C; see also Fig. 1.9 and Fig. 1.10) which is used on many modern merchant and naval vessels. This rudder is often called *semi-balanced* against "simplex" rudders (type A) which are considered as *balanced*. However, such a terminology can be misleading as basically a rudder is called balanced when its stock moment (steering gear torque) is compensated. The degree of the compensation depends on the relationship between the whole movable rudder area and its part ahead of the stock axis. So, it is clear that a horn rudder can be made not "semi-" but full-balanced while the stock moment for all movable rudders A and B might be only partly compensated.

[6]This is rather an active-passive hybrid.

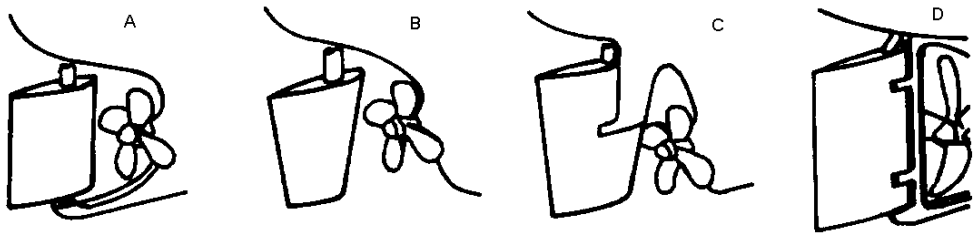

Figure 1.7: Main rudder types: A—all-movable "simple" rudder with heel bearing; B—underhung all-movable spade rudder; C—underhung horn rudder; D—"rudder post" arrangement

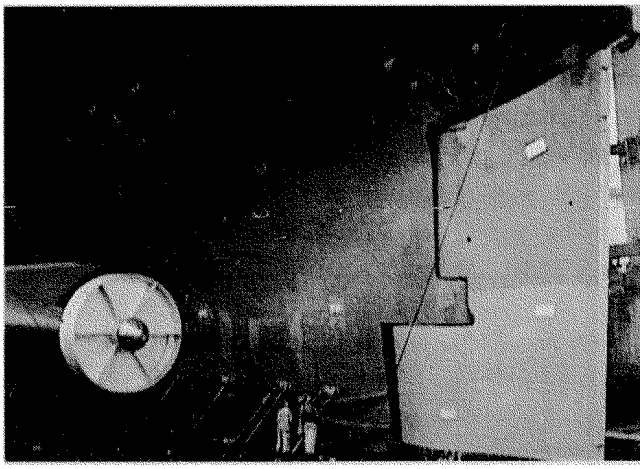

Figure 1.8: Skeg rudder on a twin-screw vessel

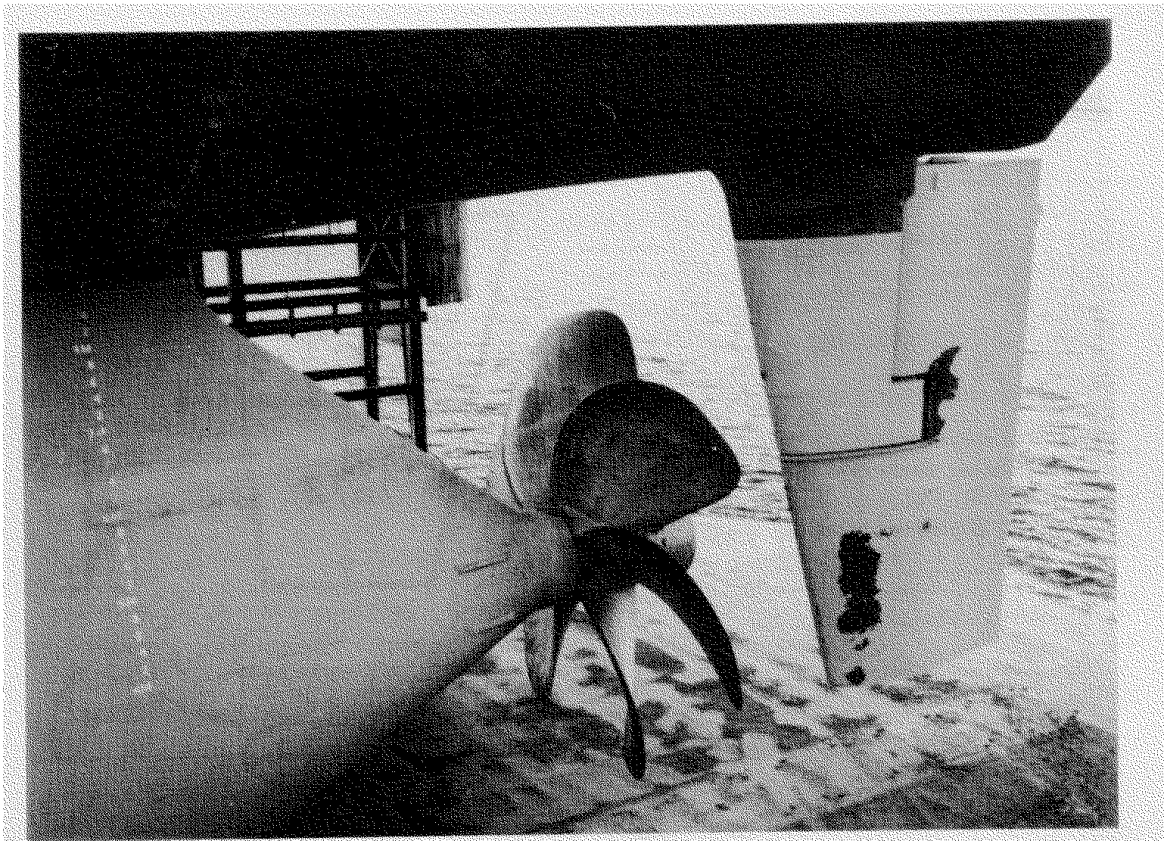

Figure 1.9: A horn rudder on a single-screw ship

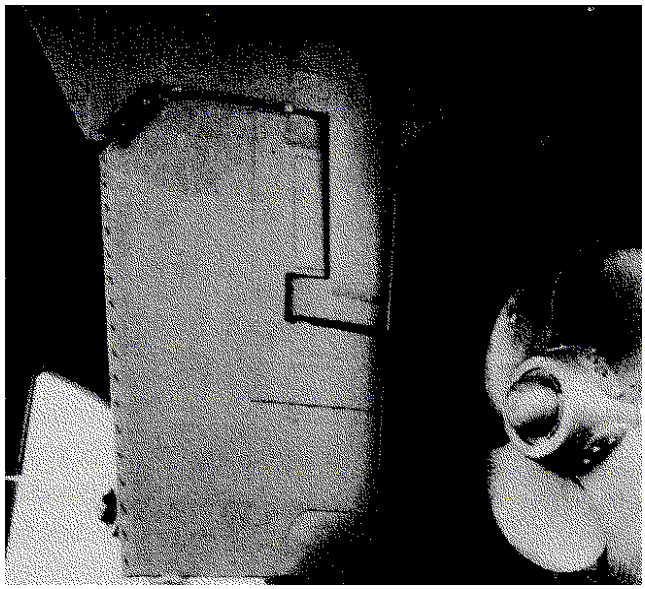

Figure 1.10: The starboard horn rudder on a twin-screw vessel

The rudders can be placed inside the propeller race (slipstream) or outside it. The latter case is typical for twin- and quadruple-screw ships. The rudder is then somewhat less efficient because it is missing the increased flow velocity in the slipstream. However, this variant can be even preferable if low acoustic signature is required as considerable periodic forces induced by the propeller plades cannot be avoided otherwise (the periodicity of the flow field is clearly seen on Fig. 1.11 where cavitating tip vortices are passing through the rudder one after another—the cavitation erosion can then become another deteriorating side effect).

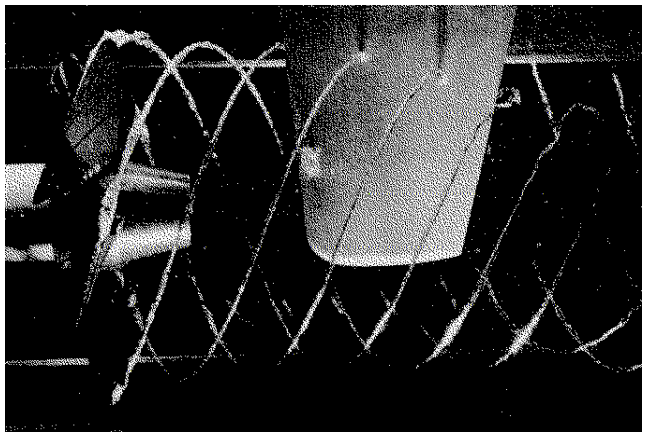

Figure 1.11: A rudder in the propeller race: tip-vortex cavitation visualizes the flow

The steering nozzles (Fig. 1.12 and Fig. 1.13) are also used as main passive control devices especially with small-diameter heavily loaded propellers and are often fitted with fins which mainly serve for torque compensation (balancing).

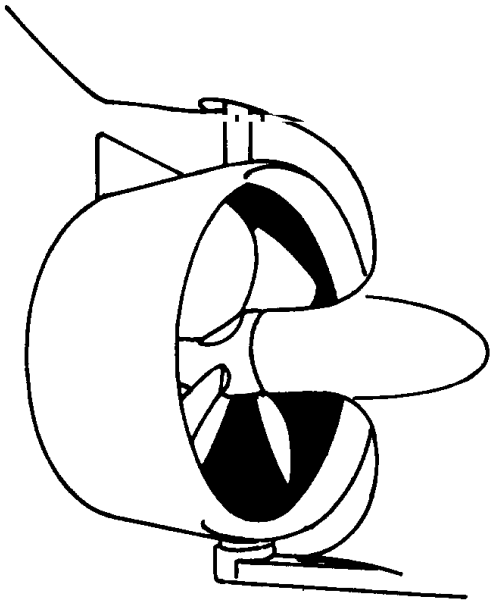

Figure 1.12: Steering nozzle with a fin: schematic view

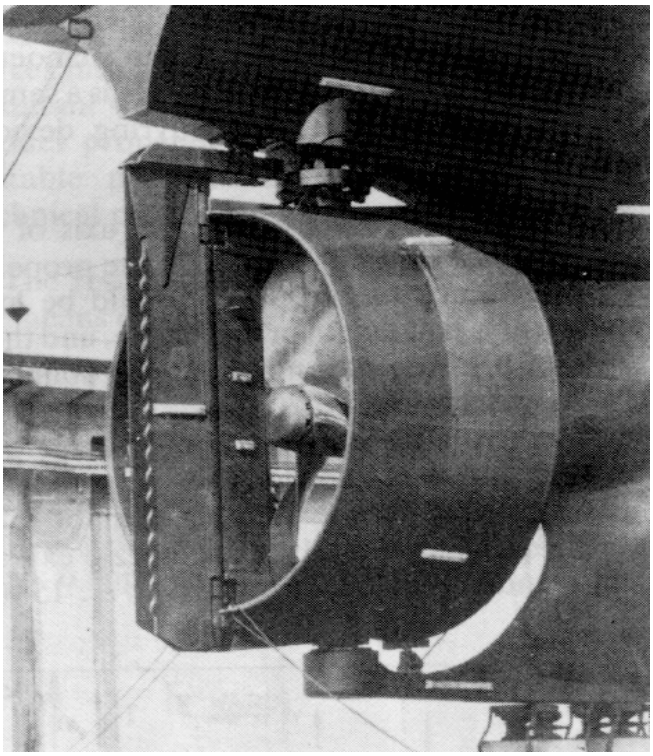

Figure 1.13: Steering nozzle with a flapped fin

Their main advantage is that they combine the steering properties with increasing a propeller's efficency at high loads. Similar nozzles are also used to deflect jets produced by water-jet propulsors being then their integrated part.

Sea-going vessels are usually equipped with a single rudder or steering nozzle or—much more seldom—with twin rudders. The river-going ships require good manoeuvring performance at shallow draught and, to achieve this, rather complicated arrangements including several rudders and/or steering nozzles can be applied.

Summing up the review, one can notice that the controlling parameter of any passive control device is the *deflection angle*. Special *steering gears* are used to deflect a rudder or a nozzle. As the stock torques (*residual* ones in case of balanced rudders) are considerable and the gear's power is always limited, the deflection cannot be executed instantaneously (typically, it takes around 15 seconds for a full rudder deflection which is in most cases equal to 30–45 degrees). From now on, we shall assume by default, unless there be special remarks, that the generic ship we are dealing with in our theoretical studies is equipped with a single plain rudder though almost all the conclusions will keep consistent for other steering arrangements.

Finally, pay attention that rudders or steering nozzles are always placed **at the stern** of a ship (except bow rudders on some ferries which, however, are used in *astern* run only). This is not occasional and is closely linked with fundamental dynamic properties of the surface displacement ships that will be analyzed later.

The information about the ship steering devices, which was presented above, is sufficient to continue studying ship manoeuvrability but the most important issues related to rudder

hydrodynamics will be elaborated later.

1.3 Standard Manoeuvres and Full-Scale Trials of Ships

1.3.1 General remarks

Most of the manoeuvres described in this section cannot be called normal nautical manoeuvres: they are usually used to assess, to check, and to compare manoeuvring performance of ships. We shall only consider here the most widely known and recognized manoeuvres and there parameters following mainly *The ITTC*[7]*-75 Manoeuvring Trial Code* (see [26], Appendix C). General requirements to the full-scale manoeuvring trials will be also given as well as the parameters which are to be recorded during the tests.

1.3.2 Turning manoeuvre

The *turning manoeuvre* (or *circulation*) is probably the most popular. It is sometimes executed in normal ship operation but very rarely long enough to have all its phases completed.

A standard turn is started from the so-called *approach phase* (the leg from the point 1 to the point 2 on Fig. 1.14) when the ship is keeping straight course with a constant *approach speed*. At the moment corresponding to the ship's position at the point 2, the order is given:

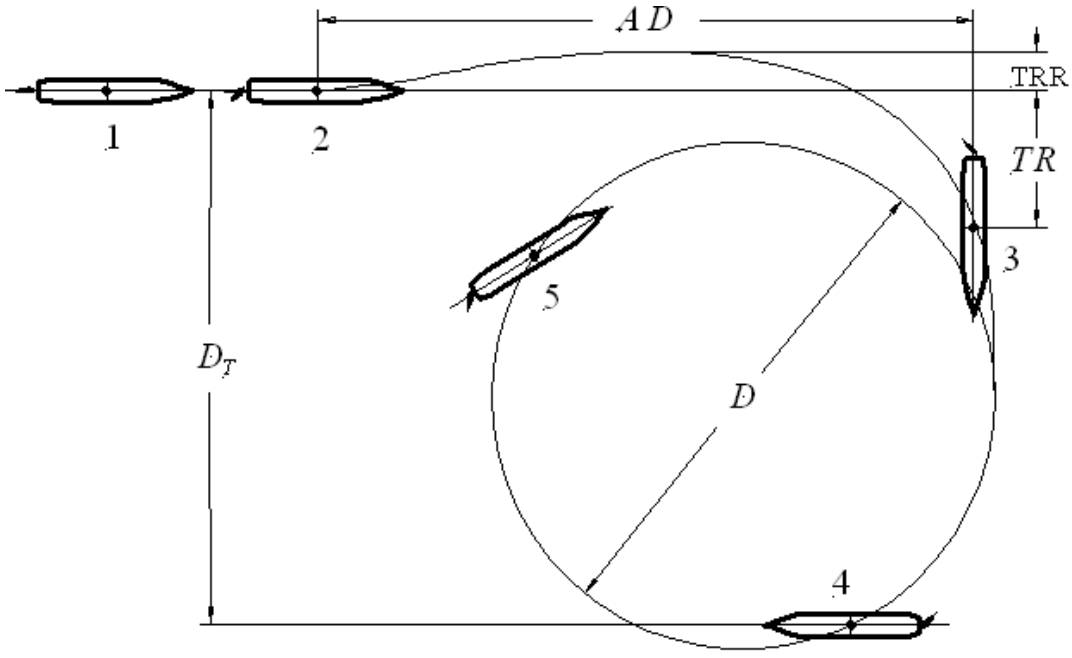

Figure 1.14: Turning manoeuvre trajectory (deformed)

"Rudder—NN [degrees] starboard (portside)!" and the deflection starts. The rudder must be deflected at the maximum possible rate. Sometimes, the period of time when the rudder is

[7]International Towing Tank Conference—serial international conferences which form permanent international bodies charged with working out guidelines and standards for the research work in the field of ship hydrodynamics.

being deflected is called *first* or *manoeuvring* phase of turn. But this phase is still not very interesting as the ship's parameters of motion do not vary substantially. However, the meaning of this phase is that only during this time the ship is actively controlled—after that, the rudder is kept steady at the ordered deflection until the end of the turning.

However, from the very beginning of the rudder's deflection, the ship's motion becomes unsteady and remains so during some period after the rudder's deflection is completed. That period starting at the point 2 is called the *second phase* of the turn or the *evolution* and continues until the motion becomes again steady. The ship is then supposed to follow a perfect citcular path. The endpoint of the second period cannot be shown on the sketch (see Fig. 1.14) with certainty as its position is somewhat fuzzy and depends on many factors but approximately it is located between the points 4 and 5. A good criterion of transition to the steady turn regime (which is also called *third phase of the turn*) is the stabilization of the ship speed after its decrease during the evolution phase. This decrease is inevitable even if the engine controls remain untouched (standard situation) because of the increased resistance in curvilinear motion. The steady turn can continue practically infinitely as the ship will follow the same circular trajectory but practically the turn can be completed after $1\frac{1}{2}$ full circles though 2–3 full circles are desirable in the case of non-perfect testing conditions (wind and current).

Several numerical measures are associated with the turning manoeuvre which are also considered as measures of a ship's turning ability. All the parameters are shown on Fig. 1.14 and the following comments can be made on them:

- The *reverse transfer* TRR is the least evident parameter as its value varies from merely zero to $\frac{B}{2}$, where B is the breadth of the ship. In most cases this parameter is rather close to zero and is only clearly revealed in numerical simulations while in the full-scale trials it is practically impossible to register it. That is why, it is sometimes not even shown on the turning manoeuvre's sketches and has no practical meaning. At the same time, its theoretical meaning is significant as it helps to understand the play of forces in manoeuvring motion: at first moments after the rudder's deflection only rudder forces are significant and the transverse rudder force directed opposite to the direction of the rudder deflection initially pushes the ship **left** in the case of a **right turn** which results in the reverse transfer. But the hull forces develop very soon and they create together with the rudder transverse force the moment turning the ship to the right.

- The *transfer* TR is the distance from the initial course line to the position 3 where the ship's heading is incremented by 90 degrees. This transfer is significant enough and its magnitude typically (for see-going ships) varies from $1.5L$ to $3.5L$.

- The *advance* AD is also measured to the position 3 but **along** the approach course line from the position 2 where the deflection started. Typical values are from $3L$ to $5L$. The advance is a very important measure of a ship's turning ability and is especially characteristic for collision avoidance manoeuvre.

- The *tactical diametre* D_T or TD is the lateral distance from the initial course line to the position 4 where the ship's heading is reversed (i.e. altered by 180 degrees). It is probably the most popular practical measure of a ship's turning ability with numerical

values varying from $3L$ to $7L$. However, the definition "tactical" is used traditionally and this measure doesn't have any special meaning in modern naval tactics.

- The *steady turn diametre* or simply *diametre of turn*, D or STD, is just the diametre of the resulting circular trajectory (see Fig. 1.14). The range of numerical values is the same as for the tactical diametre ($3L$–$7L$) but, of course, these two parameters are, generally, not identical, although correlated. The steady turn diametre shows how curved can be the path the ship is able to track but it's major meaning is theoretical as it characterizes the ship's behaviour in a simpler special case of steady curvilinear motion.

The following additional remarks can be made:

1. River-going vessels or ships with special high-performance control devices usually possess better turning abilities: turning diametres can be reduced to 1.5L–2L.
2. Turning manoeuvres can be executed with different approach speeds and rudder orders but the most often three values of speed are considered (maximum, minimum stable and medium) combined with two values of rudder orders (full rudder and 15 deg) to both port and starboard.
3. The turning manoeuvre can be completed with a *pull-out* manoeuvre i.e. when the steady turning is judged to be sufficient, the rudder is set amidship (or to the neutral position[8] if known). The manoeuvre continues until the rotation stops completely or attains some small steady rate. The latter is the manoeuvre's main output.
4. Turning tests from *zero speed* are also sometimes performed. The turning is then accompanied with acceleration. In most cases the engine is ordered half ahead while the rudder is deflected fully. As the steady turn period will be the same as at a normal turn, the zero-speed turn is normally completed when the heading change of 180 deg is achieved.

1.3.3 Zigzag manoeuvre

Different kinds of zigzags are widely used in naval operations as, for instance, a counter-submarine zigzag or a zigzagging during search missions. But the zigzag manoeuvre described here has nothing in common with practical manoeuvring—this is a specially designed manoeuvre (first proposed by Kempf in 1944 and it is sometimes also called *Kempf's Z-test*) aiming at generating a periodic substantially unsteady motion of a ship. The trajectory presents no interest in this manoeuvre and it is itself described in terms of time histories of two variables: the current rudder deflection angle and the current heading angle (Fig. 1.15).

Each zigzag manoeuvre is defined with two constant parameters: the *heading deviation* and the *rudder angle deviation*. In general, these parameters can be assigned arbitrary values but, mostly, either both are taken equal to 10 degrees (one speaks then about a 10–10 zigzag), or to 20 degrees (20–20 zigzag). The manoeuvre starts from a straight course approach run deflecting the rudder either to the starboard or to the portside up to the prescribed value of the

[8] Due to possible lack of flow symmetry, the neutral rudder position is not necessarily amidship.

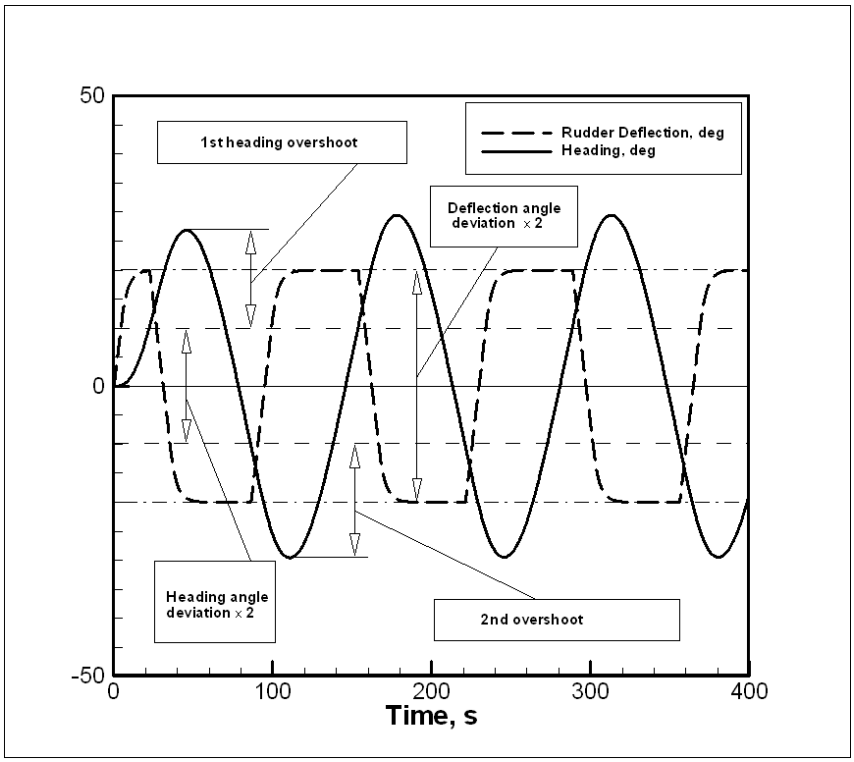

Figure 1.15: Zigzag manoeuvre time histories

rudder deviation (see Fig. 1.15; again, the deflections must be performed as fast as possible) . The heading begins to change in the same direction and when it reaches the nominal deviation value, the rudder is deflected to the opposite side (reversed) until it reaches the same deviation magnitude but with the opposite sign. The heading cannot follow the rudder instantly because of the ship's inertia and, after the counter-rudder is applied, it keeps increasing in the same direction but with decreasing rate until some maximum deviation is attained. The difference between this maximum deviation and the nominal deviation represents the so-called "heading overshoot". Then, the heading resumes changing in compliance with the rudder deflection and the process is being repeated. Very soon (approximately after the second half-period), the process becomes periodic and normally not more than 4–5 switches have to be executed.

Overshoot angles (usually the first and second overshoots are considered) are main numerical measures of a ship's dynamic qualities in the zigzag manoeuvre. For a 10–10 zigzag, for instance, the first overshoot normally varies from 5 to 20 degrees and the second one—from 5 to 35 degrees. However, these overshoot angles can reach 70–80 degrees for especially bad vessels. In the 20–20 zigzag the overshoot angles lie mostly within the 10–30 degrees range.

Less common are some additional measures of the zigzag: the zigzag *period* defined similarly to any periodic process (the initial transient must be skipped), the *reach* which is the time elapsed from the starting moment up to the first return to the initial heading, and some other characteristic time intervals (see [26] for details).

Of great interest are gentle zigzags (say, 5–5) as they are especially relevant to the course keeping process but they are often difficult to perform because they are especially sensitive to

the wind action.

1.3.4 Spiral manoeuvres

There are two different kinds of spiral manoeuvres: the *direct spiral* (or simply *spiral*, or the *Dieudonné spiral*), and the *Bech reverse spiral*. The direct spiral is in fact a consequence of steady-turn phases as if extracted from a set of turning manoeuvres. Usually the spiral is started from a right turn at full rudder. After the steady turn state is attained, the rudder angle is decreased by a certain value (say, by 5 deg) and again the steady turn is reached. Then the rudder angle is decreased further, and so on, until the ships executes the tightest steady turn to the opposite side. After that, the procedure is repeated in another direction and finishes with the ship turning again in the initial direction. This manoeuvre is very interesting from the theoretical viewpoint but consumes much time and is therefore difficult to perform. As to the output information, it will be described later after some additional concepts are introduced. The same holds for the overall description of the Bech spiral. It is only worthwhile to note that the trajectory in itself presents no interest for the analysis of the results of the spiral tests but it can become useful for planning trials in a restricted area.

1.3.5 Stopping manoeuvres

These manoeuvres are important both for the practice and for manoeuvring studies. However, there can be some difference in execution: while in practical manoeuvring the operator is usually trying to keep the ship on the initial straight course (this can fail because most passive control devices become ineffective with reversing propellers), in trials the rudder is kept steady amidship until the ship's speed becomes zero.

Normally, two kinds of stopping manoeuvres are considered:

1. *Crash stop* or the emergency propeller reversing from the maximum speed ahead (this manoeuvre is avoided in normal navigation).
2. *Low-speed stopping* from half and slow ahead with reversing to full astern but according to a normal (engine saving) reversing program.

In both cases the time to the full stop is registered and the trajectory (Fig. 1.16) is recorded. Three main evident numerical measures are: the head reach, the lateral deviation, and the track reach. The latter is measured along the curvilinear path and considered as normal if it doesn't exceed $15L$ for the crash stop. The lateral deviation's magnitude can attain 20–30 percent of the head reach value for single-screw ships.

1.3.6 Course change manoeuvres

It goes about changing a ship's heading by a given value (it is assumed that the ship goes straight before and after the manoeuvre: Fig. 1.17). This manoeuvre is of great practical significance

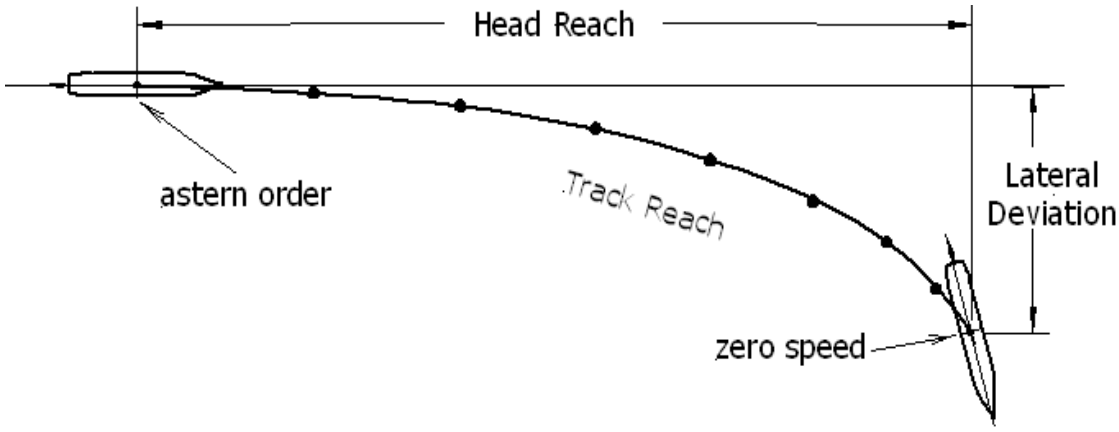

Figure 1.16: Trajectory in a stopping manoeuvre

but very seldom executed in trials because it requires rather complicated steering and its results depend not only on the manoeuvring qualities of the ship but also on the helmsman's skills or on the quality of the control laws if an automated heading change is applied. That is why some substitutes were proposed (now practically abandoned) where the rudder was deflected and then reversed with prescribed orders according to some simple program and the resulting heading change was then the output.

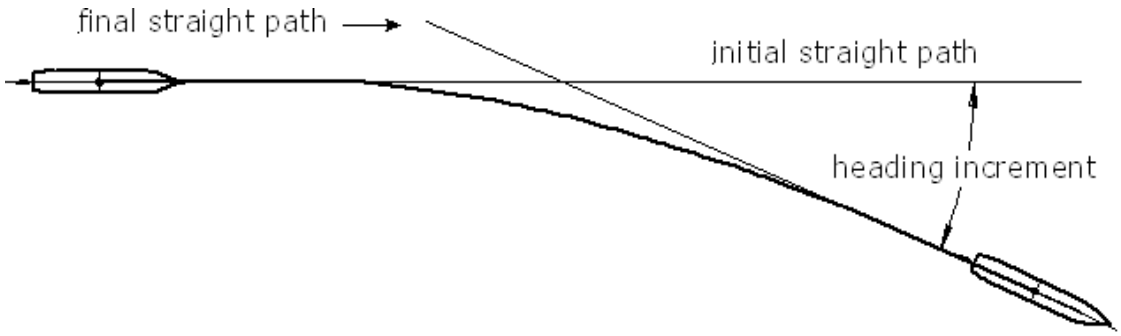

Figure 1.17: Trajectory in a heading change manoeuvre

1.3.7 Coordonate manoeuvre

This manoeuvre is navigational and is often executed by naval ships in group sailing but it is also used by practically all the vessels as part of passing and overtaking manoeuvres. In some sense, the coordonate manoeuvre is an extension of the heading change manoeuvre but instead of the heading, changed is the straight course or *lane* (Fig. 1.18). In a true coordonate the lateral shift is the pre-ordered parameter and a relatively sophisticated control law is required to perform this shift with high quality of transient.

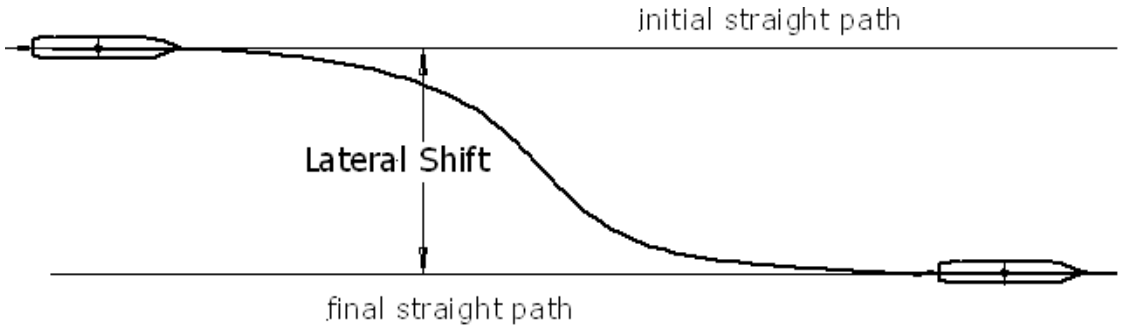

Figure 1.18: Trajectory in a coordonate manoeuvre

1.3.8 Full-scale manoeuvring trials: general guidelines

There are certain rules which have to be followed to carry out full-scale trials with good quality and to provide reliable results.

Ship load conditions

It is usually recommended to carry out tests, first of all, at full and, when possible, at ballast load condition. However, in many cases the researcher has no choice and is forced to test the ship at some occasional, often intermediate, conditions. But in any case it is strongly recommended to take readings from the draught marks to determine the ship's mean draught and trim. The transverse metacentric height and the centre's of gravity applicate must be estimated (the best is to perform an inclining experiment). If necessary (for example, when a significant fuel consumption is expected), this procedure must be fulfilled twice: before and after the trials.

Weather and current conditions

Of course, it is highly desirable that the tests be performed in perfect conditions i.e. without any current, in still air and calm sea but again, actual conditions can occur not ideal.

Uniform current is the least harmful as it only deforms the resulting trajectory and necessary corrections can be introduced relatively easily. Moreover, if the chart information is unavailable, the current speed and its non-uniformity can be estimated from the extended turning manoeuvres by comparing a ship's positions with 360 degrees heading difference (the same compass heading) as described, for instance, in [13] (the IMO Circular *Explanatory Notes for the Manoeuvring Standards*). According to the cited circular, a non-uniform current can be accepted if its mean velocity doesn't exceed 20 percent of the testing speed.

Sea waves can be accepted if the sea state is not over 3 (the significant wave height below 1.25 m) but according to [13] ships exceeding 150 m in length can be tested also at sea state 4 (waves up to 2.5 m). Moderate waves do not distort test results but they introduce additional noise and make random errors bigger.

The wind is of major concern in manoeuvring trials as it leads to biased estimates and

unlike the current cannot be accounted for in a simple way. Various sources indicate different acceptable levels of the wind speed. For instance, the ITTC 75 Trial Code requires that the wind force do not exceed Beaufort 4 (16 knots) for any manoeuvres. Moreover, the Beaufort number 2 (7 knots) and lower is required for reverse spirals, zigzags, pull-outs and bow thruster tests. And completely calm weather is necessary to obtain good results from direct spiral tests [26]. The IMO weather requirements [13] are somewhat more loose: wind force within Beaufort 4 (14 knots) is allowed in any case and if a ship is longer than 150 m **or** her lateral windage area is less than $\frac{3}{2}$ of her lateral underwater area, even stronger winds (Beaufort 5 —up to 20 kn) are considered acceptable[9]. Of course, all the recommendations are very approximate and fuzzy. In fact, the acceptability of some given weather conditions for any particular trials has to be analyzed individually.

Water depth

Normally, manoeuvring trials are executed in deep water. According to the IMO [13], it means the depth shouldn't be less than 5 draughts of the tested ship but it can be insufficient in the case of fast displacement ships. On the other hand, sometimes the trials are deliberately carried out in shallow water to obtain information on its influence onto manoeuvring characteristics. In this case it is highly desirable to choose an area with a horizontal flat bottom as otherwise the results will be difficult to analyze.

Measuring and recording requirements

As full-scale trials are always an expensive and difficult enterprise, it can be advised to collect as much information as possible. Here is the list of the kinematic parameters that can be measured and recorded during the trials with brief comments on the necessary instrumentation.

1. Ship's trajectory. The global positioning system with differential correction (DGPS) is out of competition for this purpose except maybe for the ship inertial navigation system (SINS) but the latter is available on very few objects.

2. Current time—system clock is normally used at computer recording but the time generated by the DGPS can be also recorded; it is very important to synchronize current time records within all the files.

3. Ship's speed with respect to the seabed, which is also called *Speed Over the Ground—SOG* and her true course (*Course Over the Ground—COG*)—the both parameters are also taken from the DGPS unit.

4. Ship's speed with respect to water—taken from the ship hydrodynamic log.

5. Heading angle—taken from the ship gyro-compass (the gyro can have some constant deviation which must be taken account of).

[9] However, the exemption made for large ships (over 150 meters) doesn't look logical

6. Rate of turn (rate of yaw)—using a rate-gyro is highly desirable (the heading angle signal must be numerically differentiated otherwise which can present a problem).
7. Propeller rotation rate (for each propeller on multi-screw ships).
8. Propeller's current pitch (for controllable-pitch propellers).
9. Rudder deflection angle—taken from the steering gear circuit or from a special gauge connected to the rudder's stock or helm.
10. Instantaneous roll angle—from a special inclinometer.
11. Instantaneous relative wind speed and direction—from a specially installed wind gauge.

Very rarely are also measured some dynamic parameters: thrust and torque on each propeller shaft, and torque on the rudder stock (very important would be also to measure rudder force components but this is an extremely difficult task).

In practice, some of the parameters can be dropped depending on the situation (for instance, there is no need to record a ship's trajectory in zigzag manoeuvres; the roll angle will be negligible at slow speed and/or large metacentric height; in case of calm weather wind parameters present no interest, etc.).

Chapter 2

Mathematical Models for Description of Ship Manoeuvring Motion

2.1 Kinematics of Manoeuvring Motion

2.1.1 Initial definitions: frames of reference and primary kinematic parameters

General three-dimensional case

Any detailed study of the three-dimensional manoeuvring lies beyond the scope of these notes but taking this general case as the starting point, makes the two-dimensional case more clear.

To describe an instantaneous position of any marine object with respect to the shore or to the seabed, it is necessary to introduce some steady Earth-fixed frame of reference. It is reasonable to use in this purpose a Cartesian coordinate frame $O\xi\eta\zeta$ with the ζ-axis directed vertically downward and with the both remaining axes lying on the undisturbed water free surface (Fig. 2.1). The latter is assumed to be absolutely flat, i.e. not spheric, as characteristic lengths in manoeuvring problems are, at most, of the order of several nautical miles[1]. The ξ-axis can be oriented arbitrarily[2]—for instance, it is convenient to chose it coinciding with the approach course when some manoeuvre is analyzed.

Body-fixed axes $Cxyz$ must be attached to each explored object. Normally, this is another Cartesian frame which is assumed to coincide (at least, it should *almost* coincide: certain initial displacement along one of the axes can be accepted) with the Earth-fixed frame at some initial time moment. The origin C of the body axes can be, in principle, put anywhere within the body but reasonable choice can help to avoid unnecessary complications. **The centre of mass**

[1] As has been already mentioned, the spheroidal shape of the water surface cannot be neglected in navigational tasks dealing with distances measured in hundreds and thousands of miles but at such a scale the ship is represented by a moving point, all the details of her kinematics are then lost, and any conventional manoeuvring model becomes irrelevant.

[2] But, again, this is the issue of great importance in navigation where this axis is usually directed along the true meridian.

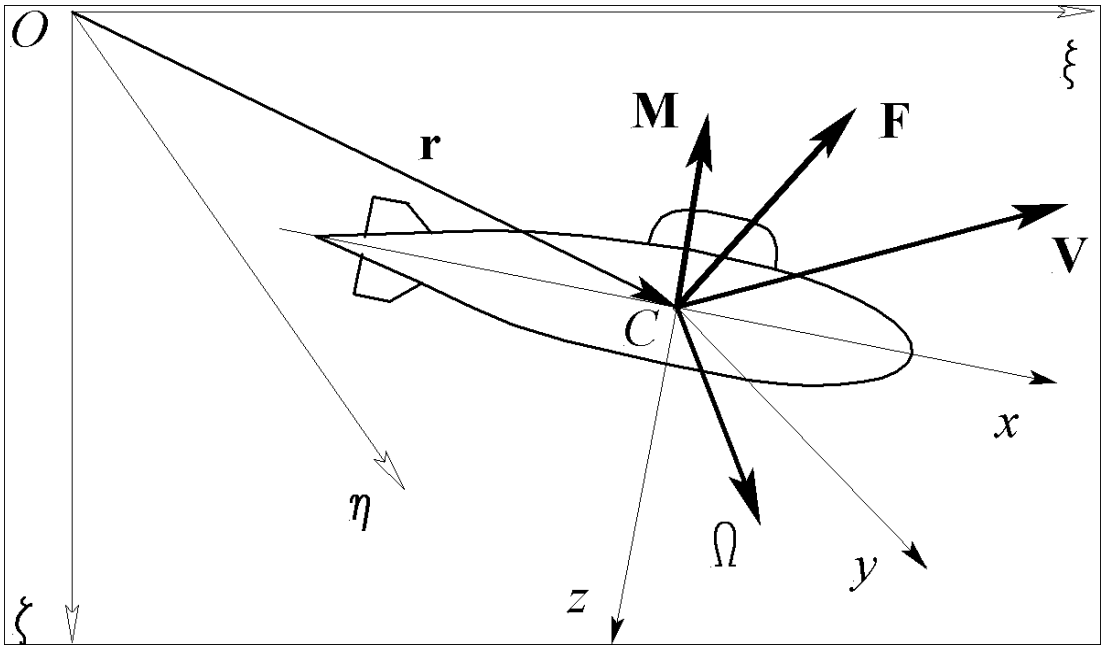

Figure 2.1: Coordinate frames: 3D case

is the most popular standard option but this choice loses part of its advantages if this centre can be displaced during the operation. For instance, some longitudinal shift of the centre of mass lies behind the action of trimming systems installed on submarines and other underwater vehicles. In such cases, the centroid of the submerged volume can be a good choice.

At some arbitrary given moment of time t, the current position of any free moving object is defined by 6 *general coordinates* (in accordance with 6 degrees of freedom). Three of these coordinates are linear displacements of the moving origin C: ξ_C, η_C, and ζ_C which are forming the position vector

$$\mathbf{r} = \xi_C \mathbf{e}_\xi + \eta_C \mathbf{e}_\eta + \zeta_C \mathbf{e}_\zeta, \tag{2.1}$$

where $\mathbf{e}_\xi$, $\mathbf{e}_\eta$, and $\mathbf{e}_\zeta$ are orthogonal unit vectors corresponding to the axes.

Another three general coordinates describing an object's rotation are Euler angles. These parameters can be defined in somewhat different ways depending on the order of three consecutive turns. The angles that are commonly used in ship dynamics are defined from the following sequence of rotations:

1. 1st rotation: around the ζ-axis — the *heading angle* ψ;
2. 2nd rotation: around the new position of the η-axis — the *pitch angle* θ;
3. 3rd rotation: around the last position of the ξ-axis — the *roll angle* φ.

The motion of the object at the time moment t can be described with two vectors: $\mathbf{V}(t)$—the velocity of the origin C, and $\mathbf{\Omega}(t)$—the angular velocity vector. The magnitude of the former $V = |\mathbf{V}|$ is usually called *speed* and the magnitude of the angular velocity $\Omega = |\mathbf{\Omega}|$—*rotation*

rate. The velocity vector $\mathbf{V} = \frac{d\mathbf{r}}{dt}$ can be decomposed in the steady axes:

$$\mathbf{V} = V_\xi \mathbf{e}_\xi + V_\eta \mathbf{e}_\eta + V_\zeta \mathbf{e}_\zeta = \dot{\xi}_C \mathbf{e}_\xi + \dot{\eta}_C \mathbf{e}_\eta + \dot{\zeta}_C \mathbf{e}_\zeta, \tag{2.2}$$

where V_ξ, V_η, and V_ζ are time derivatives of the general coordinates which are called *general velocities*.

The vector $\mathbf{\Omega}$ can also be decomposed similarly but the resulting projections **in no way are** general velocities and do not have any application.

Both $\mathbf{V}$ and $\mathbf{\Omega}$ can be also decomposed in the body axes with $\mathbf{e}_x$, $\mathbf{e}_y$, and $\mathbf{e}_z$ being the corresponding orthogonal unit vectors:

$$\begin{aligned} \mathbf{V} &= u\mathbf{e}_x + v\mathbf{e}_y + w\mathbf{e}_z, \\ \mathbf{\Omega} &= p\mathbf{e}_x + q\mathbf{e}_y + r\mathbf{e}_z. \end{aligned} \tag{2.3}$$

Here, traditional notations are used for the velocities components and they are also called *velocities* or, less frequently, *quasi*-velocities. The meaning of the last term is to oppose these projections to general velocities as they **are not** time derivatives of **any** general coordinates. The relationship between general velocities and quasi-velocities can be established and as the former are the general coordinates's time derivatives, this relationship is represented by the following set of kinematic differential equations (evaluations are skipped here as they are standard and can be found in many books on advanced mechanics and mathematics, see e.g. [20]):

$$\begin{aligned} \dot{\xi}_C &= u\,\cos\psi\,\cos\theta + v\,(\cos\psi\,\sin\theta\,\sin\varphi - \sin\psi\,\cos\varphi\,) \\ &+ w\,(\cos\psi\,\sin\theta\,\cos\varphi + \sin\psi\,\sin\varphi\,); \\ \dot{\eta}_C &= u\,\sin\psi\,\cos\theta + v\,(\sin\psi\,\sin\theta\,\sin\varphi + \cos\psi\,\cos\varphi\,) \\ &+ w\,(\sin\psi\,\sin\theta\,\cos\varphi - \cos\psi\,\sin\varphi\,); \\ \dot{\zeta}_C &= -u\,\sin\theta + v\,\cos\theta\,\sin\varphi + w\,\cos\theta\,\cos\varphi\,; \\ \dot{\psi} &= q\,\frac{\sin\varphi}{\cos\theta} + r\,\frac{\cos\varphi}{\cos\theta}; \\ \dot{\theta} &= q\,\cos\varphi - r\,\sin\varphi\,; \\ \dot{\varphi} &= p + q\,\tan\theta\sin\varphi + r\,\tan\theta\cos\varphi\,. \end{aligned} \tag{2.4}$$

All the velocities defined by eq. (2.3) bear special traditional names:

u—velocity of surge;

v—velocity of sway;

w—velocity of heave;

p—velocity of roll;

q—velocity of pitch;

r—velocity of yaw.

Now, let's study in more detail the case of a surface ship, manoeuvring with not more than 4 effective degrees of freedom. This is sufficient for most surface ship manoeuvring problems as the heave and pich motions can be neglected without sensible loss of the model's adequacy.

Kinematics of surface ship manoeuvring

Frames of reference and dimensional parameters. We shall assume that the surface ship has 4 degrees of freedom: surge, sway, yaw and roll. The same frames of reference as in the previous subsection can be used under the condition that $\theta \equiv \zeta_C \equiv 0$. The origin C of the body axes is supposed to be always located at the intersection of the centreplane with the waterplane. There are two reasonable options concerning its longitudinal location: either in the midship plane, or in the same transverse plane where the centre of mass is located.

However, in most cases it is preferred to exploit the fact that the rolling motion in manoeuvring is of secondary importance and of limited amplitude. Then, it appears more convenient not to fix completely the moving frame to the ship but to let it follow the object in the horizontal plane but not to track the roll motion[3] (Fig. 2.2). The reality is, however, even more complicated. As we shall see later, to obtain properly the inertial forces, we have even to assume that the frame is **completely fixed in terms of velocities distribution** but **not inclined by the current roll angle**. The axis Cz remains then always vertical and the rate of yaw

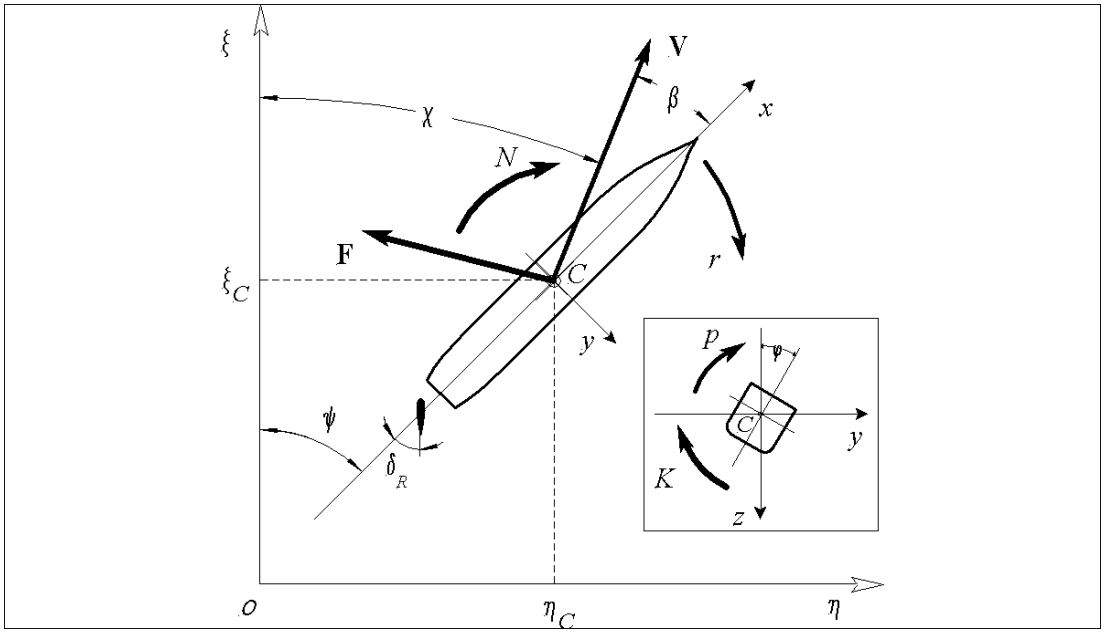

Figure 2.2: Coordinate frames: surface ship case (all shown angles and angular velocities are positive)

r is measured in the horizontal plane. Then, the components w and q will be also identically zero and the kinematic equations (2.4) are simplified dramatically:

$$\begin{aligned} \dot{\xi}_C &= u\cos\psi - v\sin\psi\,; \\ \dot{\eta}_C &= u\sin\psi + v\cos\psi\,; \\ \dot{\psi} &= r; \\ \dot{\varphi} &= p. \end{aligned} \tag{2.5}$$

[3] As this partially-body-fixed frame dominates in surface ship manoeuvring, we shall use for the axes the same notation as for the genuine body-fixed axes but this must be specified in any problem statement.

Besides the heading and roll angles, there are some other angular parameters shown on Fig. 2.2: the *course angle* χ, the *drift angle* β, and the *rudder deflection angle* (or simply *the rudder angle*) δ_R. An evident relationship follows from the sketch:

$$\psi = \chi + \beta. \tag{2.6}$$

Further,

$$\begin{aligned} \dot{\xi}_C &= V\cos\chi; \\ \dot{\eta}_C &= V\sin\chi \end{aligned} \tag{2.7}$$

and

$$\begin{aligned} u &= V\cos\beta; \\ v &= -V\sin\beta. \end{aligned} \tag{2.8}$$

It is also clear that

$$V = \sqrt{u^2 + v^2}. \tag{2.9}$$

So, along with the set (u, v, r) it is possible to use alternatively the combination (V, β, r) for full description of a ship's motion in the horizontal plane.

Finally, the following remarks can be made on the dimensional kinematic parameters:

- The heading angle ψ and the course angle χ can be represented in the traditional compass form varying from 0 to 2π (0 to 360 degrees) or as a deviation from some given direction varying from $-\pi$ to $+\pi$ (positive when the deviation is clockwise). In the latter case the heading angle is also often called *yaw angle,* especially when it has a relatively small magnitude.
- The sign rule for the angles defining a ship's position and motion is taken standard i.e positive in the clockwise direction. But this rule must not be necessarily applied to the rudder angle as it is an internal rudder parameter not related directly to the ship motion. We shall, as prefer most researchers, consider the rudder angle **positive** when it is deflected to the **starboard**[4].

2.1.2 Dimensionless kinematic parameters.

Dimensionless kinematic parameters play important role in the ship manoeuvring theory as they help to eliminate a great part of the scale influence and to make possible comparing manoeuvring performance of ships with different size and speed, including geosim models.

Any nondimesionalizing must be based on some characteristic (reference) dimensional quantities. In the present case, we need some characteristic length and a characteristic velocity. As to the characteristic length, the natural choice is the ship's wetted length or its length between the perpendiculars. It is somewhat more complicated with the characteristic speed: here two different options can be used here: the ship's speed V or a more complicated parameter defined below.

[4]The opposite sign rule is, however, not a rarity (see [7]).

Standard dimensionless parameters.

If the current (instataneous) ship speed V is taken as the characteristic one, the following "primed" dimensionless velocities can be defined (the symbol "$\stackrel{d}{=}$" means "equal by definition"):

$$\begin{aligned} u' &\stackrel{d}{=} \frac{u}{V}; \\ v' &\stackrel{d}{=} \frac{v}{V}; \qquad (2.10) \\ r' &\stackrel{d}{=} \frac{rL}{V}. \qquad (2.11) \end{aligned}$$

The first two dimensionless velocities are not completely independent as

$$u'^2 + v'^2 \equiv 1 \qquad (2.12)$$

but it is not possible to drop one of them unless **the sign** of the other is fixed. When arbitrary manoeuvres are expected, it can be more convenient to use the drift angle which in fact is also non-dimensional and is connected with the linear dimensionless velocities:

$$\begin{aligned} u' &= \cos\beta; \\ v' &= -\sin\beta. \end{aligned} \qquad (2.13)$$

The inversion of this set of equations leads to the formula

$$\beta = \begin{cases} -\arcsin v' & \text{at} \quad u \geq 0 \\ -\pi \ \text{sign}\ v' + \arcsin v' & \text{at} \quad u < 0. \end{cases} \qquad (2.14)$$

If the drift angle's absolute values do not exceed 20 degrees, which is the case in most normal manoeuvres, a simpler relation holds:

$$\beta \approx -v' \qquad (2.15)$$

and these two parameters become then practically interchangeable.

When $V \equiv 0$, the parameters u' and v', as well as the drift angle, are not defined though some their limiting values can be obtained in calculations.

Finally, the dimensionless time t' can be introduced. It was found that the most consistent way to do it is to use the following definition for the infinitesimal increment

$$\mathrm{d}t' \stackrel{d}{=} \frac{V(t)\mathrm{d}t}{L}, \qquad (2.16)$$

which means that the current dimensionless time must be found from the differential equation

$$\dot{t}' = \frac{1}{L}V(t). \qquad (2.17)$$

Only when the ship's speed is constant or varying slowly, the following approximate explicit formula for the dimensionless time can be used:

$$t' \approx \frac{Vt}{L}. \qquad (2.18)$$

Modified dimensionless angular velocity of yaw

Some manoeuvres are executed at a very low speed of advance or even at zero speed ("pure rotation"). The linear dimensionless velocities and the drift angle remain then finite but the dimensionless angular velocity r' becomes unlimited and inconvenient to use. This problem can be removed by changing the reference velocity in the parameter's definition. If we introduce the *modified* or *generalized* characteristic velocity as

$$V_{mod} \stackrel{d}{=} \sqrt{V^2 + r^2 L^2}, \tag{2.19}$$

we can define the *modified* or *generalized* dimensionless rate of turn r'':

$$r'' \stackrel{d}{=} \frac{rL}{V_{mod}} = \frac{rL}{\sqrt{V^2 + r^2 L^2}}. \tag{2.20}$$

It is clear that $|r''| \leq 1$ and is connected with r' by the equation

$$r'' = \frac{r'}{\sqrt{1 + r'^2}} \tag{2.21}$$

and thus defines a mapping $(-\infty, \infty) \mapsto [-1, 1]$.

It is also possible to define the modified dimensionless time t'' in an obvious way but, contrary to the modified angular velocity, it is practically of no use.

2.1.3 Classification of ship manoeuvres by their "strength"

The terms "normal manoeuvres" and "arbitrary manoeuvres" have been already used but it is now possible to give them a much better definition with the help of the introduced dimensionless parameters. Let us consider the plane $\beta - r''$ (Fig. 2.3). The rectangle $[-\pi, \pi] \times [-1, 1]$ in that plane contains **all possible** manoeuvres. So, we call a manoeuvre *arbitrary*, or *hard*, or *strong* if no restrictions are imposed on the drift angle and on the dimensionless rotation rate. As in practice, certain combinations of the drift angle and of the rotation rate can only be achieved at very slow speed, such manoeuvres are also called *low-speed manoeuvres* and in most cases they can only be executed by means of active control devices or tugs.

The trials show that if a ship is steered by passive control devices, the drift angle's magnitude seldom exceeds 15–20 deg even at largest rudder angles while the corresponding absolute value of the dimensionless rotation rate r' lies below 0.5–1.0 (or below 0.5–0.7 in terms of the modified velocity r'')[5]. The manoeuvres with the parameters not exceeding the given limits by absolute value are called *normal* or *moderate*. The region of moderate manoeuvres is approximately shown on Fig. 2.3 as the intermediate hatched rectangle.

Further, we shall call manoeuvres *gentle* or *weak* if $|\beta| \leq$3–5 deg and $|r'| \leq$0.1–0.15. Such manoeuvres result from small rudder deflections by 5–10 deg and are typical for the course keeping and small heading corrections. They correspond approximately to the small solid rectangle on Fig. 2.3.

[5]These limits can be exceeded in certain cases such as river-going vessels.

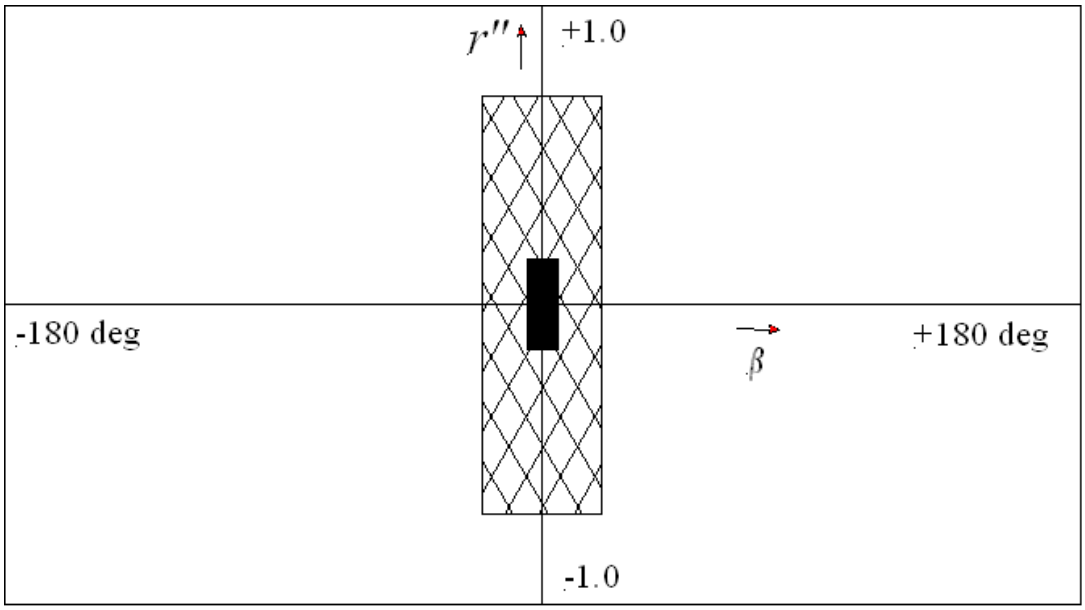

Figure 2.3: Manoeuvring regions in the β—r'' plane (the shown boundaries are approximate)

Remarks.

- All given range values are somewhat fuzzy and no standards on the manoeuvres classification have been worked out so far.
- Although the domains of moderate and gentle manoeuvres are shown as rectangles, it doesn't necessarily mean that all their inner points are reachable. On the contrary, in all typical calm water manoeuvres the observed combinations of v' and r'' tend to concentrate around the rectangle's diagonal directed from the first to the third quadrant. But this is no lnger true when the ship is manoeuvring in wind.

2.1.4 Local kinematics in manoeuvring motion

As the manoeuvring motion is something more than the pure translation, the linear velocities of various points belonging to the ship will vary. All the linear velocities we were talking about so far, referred to the moving origin C. It is known from the rigid body kinematics that for any given point A fixed to the moving body with the location with respect to the body-fixed frame defined by the position vector

$$\mathbf{r}_A = x\mathbf{e_x} + y\mathbf{e_y} + z\mathbf{e_z}, \tag{2.22}$$

the local velocity vector $\mathbf{V}(\mathbf{r}_A)$ will be

$$\mathbf{V}(\mathbf{r}_A) = \mathbf{V}(x, y, z) = \mathbf{V} + \mathbf{\Omega} \times \mathbf{r}_A. \tag{2.23}$$

As in our case the motion is restricted to 4 degrees of freedom and $w \equiv q \equiv 0$, the resulting formulae for the local velocities are

$$u(x, y, z) \;\; = \;\; u - yr,$$

$$\begin{aligned} v(x,y,z) &= v + xr - pz, \\ w(x,y,z) &= yp. \end{aligned} \tag{2.24}$$

These equations, however, are only valid if the frame $Cxyz$ is fully fixed to the ship. In the special non-rolling frame, p will not influence the local velocities[6] and it can be set equal to zero. The remaining equations can be re-written in the non-dimensionalized form (dimensionless local velocities are based on the same speed V and length L; pay attention that $u \equiv u(0,0,0)$ and $v \equiv v(0,0,0)$):

$$\begin{aligned} u'(x,y) &= u' - y'r', \\ v'(x,y) &= v' + x'r', \end{aligned} \tag{2.25}$$

where $x' = \frac{x}{L}$ and $y' = \frac{y}{L}$.

As in moderate manoeuvring u' is close to unity and in most cases $|y'| \ll 1$, the transverse distribution of the longitudinal velocity is most often neglected (it is to be taken into account in hard manoeuvring of ships with lateral propellers or rudders and/or for catamaran). But the linear longitudinal distribution of the transverse velocity is of primary importance in hydrodynamics of the manoeuvring motion.

For each value of x we can consider the following useful local parameters:

- local total velocity with respect to water

$$\mathbf{V}(x) = u\mathbf{e_x} + v(x)\mathbf{e_y}; \tag{2.26}$$

- its magnitude

$$V(x) = \sqrt{u^2 + v^2(x)}; \tag{2.27}$$

- local drift (sidewash) angle

$$\beta(x) = \begin{cases} -\arcsin\frac{v(x)}{V(x)} & \text{at} \quad u(x) \geq 0 \\ -\pi \text{ sign } v(x) + \arcsin\frac{v(x)}{V(x)} & \text{at} \quad u(x) < 0. \end{cases} \tag{2.28}$$

In the case of moderate manoeuvring on can write

$$\beta(x') \approx \beta - x'r' \tag{2.29}$$

i.e. the sidewash angle is approximately linearly distributed along the hull.

[6] In fact, this influence exists and if, for instance, we want to detect the roll's influence onto the rudder's kinematics, we have to use the equations (2.24). On the other hand, this influence is neglected in most existing mathematical models for the hull forces.

Pivot point. It is clear that for every given v' and r' there exists some point P with the abscissa x_P at which $\beta(x_P) = v(x_P) = 0$. This point is called the *pivot point* and its dimensionless abscissa is

$$x'_P = -\frac{v'}{r'}. \tag{2.30}$$

An empirical fact was established that in steady turn the pivot point's dimensionless abscissa varies in most cases within the range $(0.3, 0.5)$ irrespective of the turning diametre (i.e. it is located near the ship's stem or slightly behind it) . This property can often be used to check the results of tests and computations. However, besides that, the pivot point is not so important for the manoeuvrability theory. As to the manoeuvring practice, some people pretend to see that the ship is rotating around this point in the circulating motion. This, however, depends on the observer's imagination as the real centre of rotation in steady turn is exactly the centre of the circle trajectory while the pivot point is the centre of rotation but **in the relative motion** if the pivot point is chosen as the translated pole (Fig. 2.4).

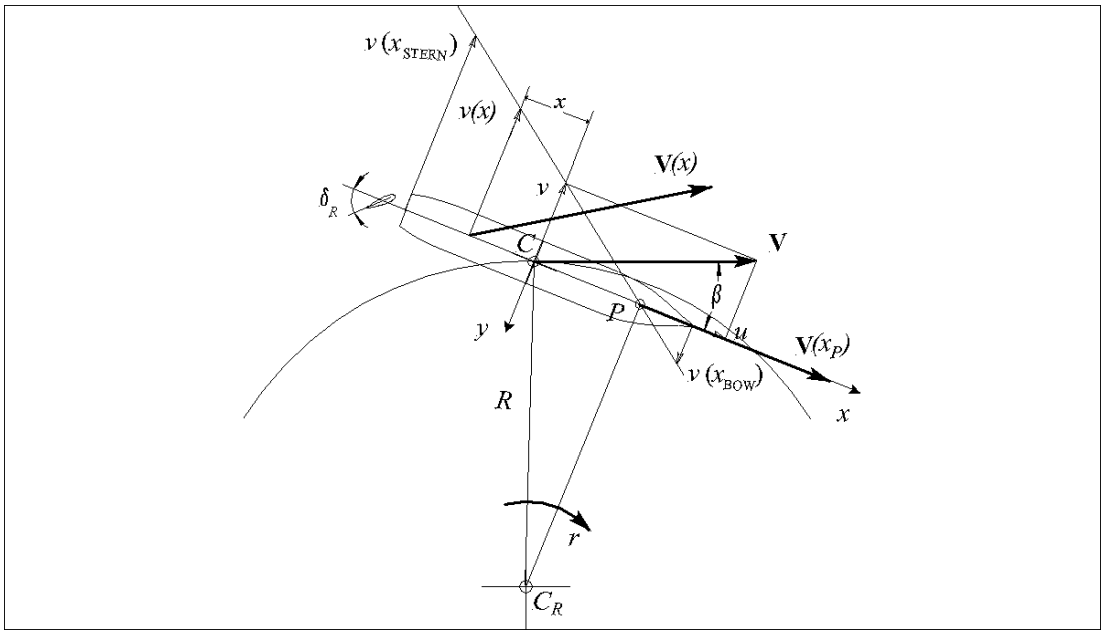

Figure 2.4: Distribution of velocities in circular motion

Remark.

- All the considerations concerning the local kinematics remain correct for **arbitrary-translated** manoeuvring motion as long as the **instantaneous** values of all the varying parameters are assumed. The radius R on Fig. 2.4 is then the trajectory's local radius of curvature.

Dimensionless rate of yaw and radius of steady turn. Another interesting and useful property can be obtained from (Fig. 2.4). One can see directly that

$$V = Rr, \tag{2.31}$$

where $R = \frac{D}{2}$ is the steady turning radius. It yields immediately

$$r' = \frac{L}{R}. \tag{2.32}$$

The last relation is very useful for linking numerical values of r' to the steady turn diametre values which are more common in practical assessments. For instance, a "normal" value $D = 4L$ corresponds to $r' = 0.5$. However, it is important to remember that the dimensionless angular velocity and the curvature radius are thus connected in steady turn only!

2.2 Dynamic Equations for Ship Manoeuvring Motion

2.2.1 Euler equations for a ship

General 3D case

Any marine object can be treated as the free rigid body moving under action of the external force $\mathbf{F}$ applied at the origin C of the body-fixed axes (see Fig. 2.1) and of the moment $\mathbf{M}$ around this origin. The force and the moment can be decomposed as:

$$\begin{aligned} \mathbf{F} &= X\mathbf{e}_x + Y\mathbf{e}_y + Z\mathbf{e}_z, \\ \mathbf{M} &= K\mathbf{e}_x + M\mathbf{e}_y + N\mathbf{e}_z \end{aligned} \tag{2.33}$$

where X, Y and Z are respectively the surge, sway and heave forces, and K, M and N are the roll, pitch and yaw moments.

The Euler equations of arbitrary motion of a free rigid body well known from general mechanics are applicable to our case and for any object symmetric about the centreplane Cxz they are:

$$\begin{aligned} m\,\dot u + mz_G\,\dot q - m\,vr - mx_G\,r^2 + mz_G\,pr + m\,wq - mx_G\,q^2 &= X \\ m\,\dot v - mz_G\,\dot p + mx_G\,\dot r + m\,ur - m\,wp + mx_G\,pq + mz_G\,qr &= Y \\ m\,\dot w - mx_G\,\dot q - m\,uq - mz_G\,q^2 + m\,vp + mx_G\,pr - mz_G\,p^2 &= Z \\ -mz_G\,\dot v + I_{xx}\,\dot p - I_{xz}\,\dot r + mz_G\,wp + (I_{zz} - I_{yy})\,qr - mz_G\,ur - I_{xz}\,pq &= K \\ m\,z_G\dot u - mx_G\,\dot w + I_{yy}\,\dot q + mx_G\,uq + mz_G\,wq + (I_{xx} - I_{zz})\,pr & \\ + I_{xz}\,(p^2 - r^2) - mz_G\,vr - mx_G\,vp &= M \\ mx_G\,\dot v - I_{xz}\,\dot p + I_{zz}\,\dot r + mx_G\,ur - mx_G\,wp + (I_{yy} - I_{xx})\,pq + I_{xz}\,qr &= N, \end{aligned} \tag{2.34}$$

where m is the mass of the object; x_G, y_G, z_G are the centre-of-mass' coordinates; I_{xx}, I_{yy}, I_{zz}, and I_{xz} are the moments of inertia.

If the origin C coincides with the centre of mass G then $x_G = y_G = z_G = 0$ and the left-hand side of the equations will look simpler.

Case of surface ship

The 4 DOF case (i.e. with heave and pitch excluded), which we are going to treat as basic for the surface ship, turns out to be somewhat artificial. To evaluate the corresponding equations of motion, we should, first, follow tightly the concept of the body-fixed axes. The absence of heave means that $\zeta_C \equiv \dot\zeta_C \equiv 0$ and the absence of pitch—that $\theta \equiv \dot\theta \equiv 0$. The general coordinates will be nullified automatically provided the initial conditions are zero. Nullifying the general velocities in eq. (2.4) results in two constraints imposed onto the quasi-velocities. Then,

$$\begin{aligned} w &= -v\tan\varphi, \\ q &= r\tan\varphi \end{aligned} \tag{2.35}$$

and

$$\begin{aligned} \dot{w} &= -\dot{v}\tan\varphi - vp\,\frac{1}{\cos^2\varphi}, \\ \dot{q} &= \dot{r}\tan\varphi + pr\,\frac{1}{\cos^2\varphi}. \end{aligned} \tag{2.36}$$

Substituting the formulae (2.35) and (2.36) into the equations (2.34) eliminates two variables, the set becomes overdefined and, hence, two equations can be dropped. Of course, the most reasonable is to drop the equations with Z and M components at the right-hand sides which results in

$$\begin{aligned} m\,\dot{u} + mz_G\tan\varphi\,\dot{r} - m\frac{1}{\cos^2\varphi}\,vr - mx_G\frac{1}{\cos^2\varphi}\,r^2 + mz_G(1+\frac{1}{\cos^2\varphi})\,pr &= X \\ m\,\dot{v} - mz_G\,\dot{p} + mx_G\,\dot{r} + m\,ur + m\tan\varphi\,vp + mx_G\tan\varphi\,pr & \\ +mz_G\tan\varphi\,r^2 &= Y \\ -mz_G\,\dot{v} + I_{xx}\,\dot{p} - I_{xz}\,\dot{r} - mz_G\,ur - mz_G\tan\varphi\,vp + (I_{zz}-I_{yy})\tan\varphi\,r^2 & \\ -I_{xz}\tan\varphi\,pr &= K \\ mx_G\,\dot{v} - I_{xz}\,\dot{p} + I_{zz}\,\dot{r} + mx_G\,ur + mx_G\,\tan\varphi\,vp + (I_{yy}-I_{xx})\tan\varphi\,pr & \\ +I_{xz}\tan\varphi\,r^2 &= N. \end{aligned} \tag{2.37}$$

Exploiting now the assumption that the body axes are not inclined, we can assign $\varphi = 0$ and the resulting set of dynamic equations with 4 degrees of freedom is

$$\begin{aligned} m\,\dot{u} - m\,vr - mx_G\,r^2 + 2mz_G\,pr &= X \\ m\,\dot{v} - mz_G\,\dot{p} + mx_G\,\dot{r} + m\,ur &= Y \\ -mz_G\,\dot{v} + I_{xx}\,\dot{p} - I_{xz}\,\dot{r} - mz_G\,ur &= K \\ mx_G\,\dot{v} - I_{xz}\,\dot{p} + I_{zz}\,\dot{r} + mx_G\,ur &= N. \end{aligned} \tag{2.38}$$

As $|I_{xz}|$ is small for normal ships, the corresponding terms are usually removed from the equations. Further simplifications can be achieved in the case of central body axes when the origin is at the centre of mass:

$$\begin{aligned} m\,(\dot{u} - vr) &= X \\ m\,(\dot{v} + ur) &= Y \\ I_{xx}\dot{p} &= K \\ I_{zz}\dot{r} &= N. \end{aligned} \tag{2.39}$$

The last two sets of equations of motion look very simple but this is just their general form. To make the equations usable, it is necessary to expand the force and moment components in the right-hand sides. In general, these will be rather complicated functions[7] of the general coordinates ξ_C, η_C, ψ and φ, velocities u, v, p and r, accelerations $\dot{u}$, $\dot{v}$, $\dot{p}$ and $\dot{r}$; and they will also depend on the rudder deflection angle δ_R, propeller rotation frequency n, and, possibly, on some other variables. Our next task will be to provide appropriate description of the acting forces and to outlie means for their estimation.

[7] Of course, they are **real** in the mathematical sense of the word!

2.2.2 Classification of forces acting upon the ship

Let us introduce a special notation Φ for the generic force/moment component i.e. $\Phi = X, Y, K, N$. Any component can be decomposed in the following way:

$$\Phi = \Phi_{\text{HYDRO}} + \Phi_{\text{AERO}} + \Phi_{\text{others}}, \tag{2.40}$$

where the first component stands for the *main* hydrodynamic forces on the underwater part of the ship and the second one represents all aerodynamic forces acting upon the upper hull and superstructures. The third component assembles all the forces of special origin though some of them can be hydrodynamic as well. The following forces are usually treated as "others":

- Forces produced by active auxiliary control devices (especially bow and stern thrusters);
- Reactions from quay fenders;
- Forces from the tug tow lines or those directly from tugs in pushing mode;
- Forces from a mooring line and/or anchor chains;
- The hydrostatic and gravitational rolling moment;
- Hydrodynamic interactions with:
  - other ships (passing by, meeting, and overtaking);
  - side banks;
  - bottom irregularities;
- The wave excitation forces;
- Naval guns' recoil.

Most of the listed forces can be very important at simulating a ship's motion in the real world but from the viewpoint of the ship manoeuvring theory they are not of primary concern as most of the ship manoeuvring properties can be established and studied in the so-called "canonic" environment which means, for instance: deep water, calm sea, still air, unlimited area, and steering by means of the main passive devices[8]. Let us assume, unless the opposite is stated, that the hydrodynamic forces are analyzed and determined for this canonic case. Aerodynamic forces will be studied later in the framework of the problem of the ship manoeuvring in wind as this requires introduction of some additional kinematic notions.

The static (hydrostatic+gravitational) rolling moment K_s can be described without major problems and is usually taken in the form

$$K_s = -mg\,GM\varphi, \tag{2.41}$$

where g is the acceleration of gravity, and GM is the metacentric height, but using a more accurate approximation for the righting arm is also possible.

A much more lengthy discussion is required for the hydrodynamic components.

[8] Another two canonic cases are those of constant wind velocity and/or of shallow water with a flat horizontal bottom.

Hydrodynamic forces

So, we shall analyze in more detail the hydrodynamic component Φ_{HYDRO} which is assumed to be a function of the following parameters:

$$\Phi_{\text{HYDRO}} = f(\varphi, u, v, p, r, \dot{u}, \dot{v}, \dot{p}, \dot{r}, \delta_R, n). \tag{2.42}$$

Several important observations can be made regarding the arguments' list.

1. In the unbounded water area (the canonic case!) only one general coordinate in the 4DOF model (the roll angle) can affect the hydrodynamic forces.

2. No pre-history influence is shown i.e. just the current instantaneous values of the parameters affect the forces. Strictly speaking, this is not accurate because it is clear that, in principle, both the wave and vortex wakes left in the fluid can affect the forces. However, special experiments carried out by Scragg [36] showed that such influence is negligible for normal ship forms in normal manoeuvring motion[9]. This property is also extended to arbitrary manoeuvres and no serious evidence against this has been reported so far.

3. Higher-order time derivatives of the velocities are not included due to general mechanics considerations. In the Newtonian mechanics, the forces are only engendered by first-order time derivatives of the velocities. The same conclusion can be drawn from the Lagrange equations valid for mechanical systems of very general nature.

4. It was assumed in eq. (2.42) that the ship is single screw with single rudder. If this is not the case, there will be several propeller rotation rates and/or deflection angles in the arguments list.

To make the mathematical model suitable for any practical use, the forces must be described in such a way that they could be actually computed at any combination of the kinematic parameters. Methods of such description of the forces will be discussed in the next subsection. It will be shown that large number of factors (arguments) considerably complicates the task. That is why, here comes a preliminary analysis aiming at finding possibilities for reasonable decomposition of the problem and reduction of the effective number of factors.

The full hydrodynamic force can be studied as one entity acting on the whole hydrodynamic configuration (the "integrated" approach) or it can be decomposed in the following way:

$$\begin{aligned} \Phi_{\text{HYDRO}}(\varphi, u, v, p, r, \dot{u}, \dot{v}, \dot{p}, \dot{r}, \delta_R, n) &= \Phi_H(\varphi, u, v, p, r, \dot{u}, \dot{v}, \dot{p}, \dot{r}) \\ &+ \Phi_P(u, v, r, n) + \Phi_R(u, v, p, r, \delta_R, n), \end{aligned} \tag{2.43}$$

where Φ_H is the hull force/moment component; Φ_P —the propeller component; Φ_R —the rudder component.

This decomposition defines the so-called "modular approach". One of its advantages is due to reduced arguments lists which can be seen above for each separated contribution. Of course, certain hydrodynamic interaction is always present and these interaction effects are usually included into P- and R-components. Propeller and rudder forces will be, however, studied later while here we shall focus on the hull forces.

[9] This is not true for ship motion in waves where retardation integral operator terms have to be introduced for adequate modeling—the difference lies in the Strouhal number values.

Structure of hull forces. Further decomposition of the hull forces can be based on the separation of various physical effects (the same approach is followed in ship resistance and seakeeping). This can be done in the following way:

$$\Phi_H = \Phi_{Hi} + \Phi_{Hv} + \Phi_{Hw}, \tag{2.44}$$

where additional subscripts stand for: i — hydrodynamic inertial forces; v — viscous forces, and w — wave forces.

Hydrodynamic inertial forces are of primary importance in manoeuvring and they are always substantial. These are the only hydrodynamic forces applied to the body "manoeuvring" in the unbounded perfect fluid. The fluid viscosity gives birth to the second component which, however, is often thought of in terms of lifting effects and is associated with vortices accompanying any manoeuvring motion. Wave effects are believed to be negligible for the Froude numbers not exceeding 0.25 but in fact even at the Froude number values as high as 0.5 they mainly mark their presence through the ship's dynamic squat.

However, the representation (2.44) is very difficult to use in practical purposes because in all existing theoretical and experimental methods of determination of the hull forces, all the effects (inertial, wavemaking, viscousity) are considered mixed although this comes somewhat contrary to expectations inspired by the component separation typically used in the classic ship resistance theory. As if to introduce even more confusion, some authors, as Newman [28] consider separately lifting forces as caused by some analogue of the Kutta–Zhukovsky condition and viscous forces as those caused by friction and flow separation. But such discrimination does not seem to be justified as the Kutta condition itself is due to the fluid's viscosity. Indeed, if we consider any body, no matter with or without tail stabilizers, steadily moving with a drift (or attack) angle in the inviscid unbounded fluid, the lift, side force and the resistance all will be exactly zero and the Kutta condition will not take place. However, viscosity, always present in the real fluid, changes the situation acting partly through friction, partly through activating the Kutta condition, partly through possible flow separations.

For practical purposes, it is more reasonable not to insist on complete separation of components and more useful proved to be a decomposition of the following type:

$$\Phi_H = \Phi_{Ha}(\varphi, u, v, p, r, \dot{u}, \dot{v}, \dot{p}, \dot{r}) + \Phi_{Hq}(\varphi, u, v, p, r), \tag{2.45}$$

where the first term is supposed to vanish at $\dot{u} = \dot{v} = \dot{p} = \dot{r} = 0$ and the second term (the quasi-steady part) doesn't depend on the quasi-accelerations at all.

At first sight, it looks like the quasi-steady part is much simpler than the accelerations-dependent part. But a special assumption is usually made simplifying the latter part dramatically. This assumption is usually called the "quasi-steadiness hypothesis" and means the following:

1. The unsteady part of the hull force does **only** depend on the quasi-accelerations, and
2. This dependence is strictly **linear**.

It all means that the following representation can be used:

$$\Phi_{Ha} = \Phi_{Ha}(\dot{u}, \dot{v}, \dot{p}, \dot{r}) = \Phi_{\dot{u}}\dot{u} + \Phi_{\dot{v}}\dot{v} + \Phi_{\dot{p}}\dot{p} + \Phi_{\dot{r}}\dot{r}, \tag{2.46}$$

where the coefficients are often called the *acceleration derivatives*[10]. These are supposed to be constant for any given hydrodynamic configuration and they are associated with the added mass coefficients known from the potential theory. Moreover, the added masses can serve as a very good approximation to the acceleration derivatives (seakeeping added mass coefficients are suitable if taken at zero frequency). The unsteady parts of the force components are then presented as follows:

$$\begin{aligned} X_{Ha} &= -\mu_{11}\,\dot{u}, \\ Y_{Ha} &= -\mu_{22}\,\dot{v} - \mu_{24}\,\dot{p} - \mu_{26}\,\dot{r}, \\ K_{Ha} &= -\mu_{42}\,\dot{v} - \mu_{44}\,\dot{p} - \mu_{46}\,\dot{r}, \\ N_{Ha} &= -\mu_{62}\,\dot{v} - \mu_{64}\,\dot{p} - \mu_{66}\,\dot{r} \end{aligned} \tag{2.47}$$

(the account is made for the centreplane symmetry of the ship) and the acceleration derivatives then only differ from the added masses by their sign and notation i.e. $X_{\dot{u}} = -\mu_{11}$, ..., $Y_{\dot{p}} = -\mu_{24}$ etc. If the added masses are determined by means of the potential theory, the usual symmetry relations are valid:

$$\mu_{24} = \mu_{42}; \qquad \mu_{26} = \mu_{62}; \qquad \mu_{46} = \mu_{64} \tag{2.48}$$

but this is not necessarily confirmed by experimental estimation of the same coefficients.

In general, all the accumulated knowledge on the ship manoeuvring forces, proves that the quasi-steadiness hypothesis works well for normal (i.e. slender) ship forms in normal (moderate) manoeuvring. This is less certain for substantially unsteady low-speed manoeuvring but in practice this hypothesis can still be applied with satisfactory results.

Remark. The accelerations-dependent force as defined by eq. (2.46) or eq. (2.47) can be extracted not only from the hull force but also from the total hydrodynamic force (the quasi-steady nature of the propeller and rudder forces is confirmed by many theoretical and experimental studies) and the latter is then represented as

$$\begin{aligned} \Phi_{\mathrm{HYDRO}}(\varphi, u, v, p, r, \dot{u}, \dot{v}, \dot{p}, \dot{r}, \delta_R, n) &= \Phi_{Ha}(\dot{u}, \dot{v}, \dot{p}, \dot{r}) + \Phi_q(\varphi, u, v, p, r, \delta_R, n) \\ &= \Phi_{\dot{u}}\,\dot{u} + \Phi_{\dot{v}}\,\dot{v} + \Phi_{\dot{p}}\,\dot{p} + \Phi_{\dot{r}}\,\dot{r} \\ &+ \Phi_q(\varphi, u, v, p, r, \delta_R, n), \end{aligned} \tag{2.49}$$

where the quasi-steady part $\Phi_q()$ of the total hydrodynamic force is what one deals with within the "integrated" approach.

2.2.3 Modified equations of motion

Acceleration-dependent unsteady forces can be introduced into the left-hand side of the set (2.38). For simplicity, let us consider the case when only hydrodynamic forces act upon the

[10] The term "derivatives" is of historical origin that will be clear from the later material.

ship. Then, substituting eq. (2.49) and (2.47) into the mentioned set we shall get

$$\begin{aligned}
(m+\mu_{11})\,\dot{u} - m\,vr - mx_G\,r^2 + 2mz_G\,pr &= X_q \\
(m+\mu_{22})\,\dot{v} + (-mz_G+\mu_{24})\,\dot{p} + (mx_G+\mu_{26})\,\dot{r} + m\,ur &= Y_q \\
(-mz_G+\mu_{42})\,\dot{v} + (I_{xx}+\mu_{44})\,\dot{p} + (-I_{xz}+\mu_{46})\,\dot{r} - mz_G\,ur &= K_q \\
(mx_G+\mu_{62})\,\dot{v} + (-I_{xz}+\mu_{64})\,\dot{p} + (I_{zz}+\mu_{66})\,\dot{r} + mx_G\,ur &= N_q.
\end{aligned} \tag{2.50}$$

Of course, alternative acceleration derivatives symbols can be used instead of the classic added mass notation.

2.2.4 Dimensionless Hydrodynamic Forces

The lists of arguments for hydrodynamic forces we were dealing with so far were not exhaustive. They included only kinematic parameters, the rudder deflection angle and the propeller rotation rate. But in fact, the hydrodynamic forces always depend also on various physical constants (density ρ, acceleration of gravity g, and kinematic viscosity ν), and on the dimensions and shape of the body in concern.

Then, taking the same reference velocity V_{REF} as in the kinematical analysis (i.e. V or V_{mod} depending on the class of manoeuvres in concern), the same characteristic length L and introducing the reference area as $A_{\mathrm{REF}} = LT$, where T is a ship's draught, we can write for the generic quasi-steady force component:

– in the case of normal manoeuvring

$$\Phi_q = \Phi'_q(\mathsf{Rn}, \mathsf{Fn}, \varphi, v', p', r', \delta_R, J)\,\frac{\rho V^2}{2} L^\ell T, \tag{2.51}$$

where Φ'_q is the dimensionless force component or the force coefficient; $\mathsf{Rn} = \frac{VL}{\nu}$ is the Reynolds number; $\mathsf{Fn} = \frac{V}{\sqrt{gL}}$ —the Froude number; J —the propeller's advance ratio as defined in ship propulsion; $\ell = 1$ at $\Phi = X, Y$ and $\ell = 2$ at $\Phi = K, N$;

– in the low-speed manoeuvring case of, when the dependence on the roll motion and the roll equation itself can then be dropped,

$$\Phi_q = \Phi''_q(\mathsf{Rn}, \mathsf{Fn}, \beta, r'', \delta_R, \gamma_P)\,\frac{\rho V_{\mathrm{mod}}^2}{2} L^\ell T, \tag{2.52}$$

where Φ''_q is the modified force coefficient; γ_P is the propeller advance angle[11]

The following remarks can be made cocerning these representations:

1. The Reynolds number dependence manifests presence of the scale effect. It is clear that it cannot be accounted for in physical modeling as the full-scale and model values of this number differ by 3–4 orders of magnitude. Unlike the traditionally deep concern

[11] Normally designated as β in the screw propeller theory.

of the scale effect in ship resistance, it is still much worse studied in manoeuvring and is simply neglected in most cases. The latter is possible because of looser accuracy requirements compared to those regarding the speed prediction. Nevertheless, using the largest available model in the tank experimentation is strongly recommended.

2. The Froude number influence may become substantial for high-speed vessels and can be modeled. However, for the great majority of surface ships the zero-Froude-number assumption works well and then the Froude number can then also be omitted from the arguments list.

3. The representation (2.51) is not applied to the roll moment in the existing approaches as the form used in seakeeping is preferred for this component.

4. While the instantaneous roll angle φ can influence substantially the sway force and yaw moment coefficients, this is less likely for the rate of roll p and the latter is not usually present in the arguments lists.

5. As was demonstrated by numerous experiments, the surge force is not significantly influenced by either φ or p.

Hence, we can write down the following expressions for the horizontal plane force components in moderate manoeuvring:

$$\begin{aligned} X_q &= X'(v', r', \delta_R, J)\,\frac{\rho V^2}{2} LT, \\ Y_q &= Y'(\varphi, v', r', \delta_R, J)\,\frac{\rho V^2}{2} LT, \\ N_q &= N'(\varphi, v', r', \delta_R, J)\,\frac{\rho V^2}{2} L^2 T. \end{aligned} \tag{2.53}$$

2.2.5 Description of forces in the equations of motion

As the equations of manoeuvring motion are ordinary differential equations with the time as independent variable, they are, first of all, supposed to be integrated numerically[12] in the time domain. This means that the forces acting on the ship have to be effectively computed at every integration step and this can be done in the following ways:

1. A computational fluid dynamics (CFD) numerical procedure computing the forces is called at every step—this approach can, in principle, allow the closest and the most precise modeling of real physical processes but is very inefficient from the viewpoint of computational speed unless very simple (and, hence, inaccurate!) methods are implemented.

2. The values of the forces are pre-calculated or measured experimentally with some discrete step and at all the expectable combinations of the values of the parameters the forces depend on. The set of these values forms a so-called *grid function* or a multi-entry table. In

[12] Analytic integration is the alternative but it can be performed very rarely.

course of the numerical integration of the equations of motion, the closest suitable values are searched on the grid and, if necessary, interpolated. This approach is reliable, requires no preliminary information and assures the fastest computing but is not convenient as the databases are often bulky and not very portable. More serious problems arise in the case of many input parameters as the number of experiments necessary to fill the grid can become unacceptable.

3. The most often, used are some relatively simple approximating equations. In the case when they are obtained from experimental data containing some random errors they are also called equations of regression or *regression models*. Although the approximations can look rather lengthy and can sometimes contain several dozen parameters, they are always much more observable than the grid functions and can effectively handle complicated cases with large numbers of arguments.

Whatever method of description of the forces is chosen, in any case they are to be estimated and we shall focus on the estimation methods in the next section.

2.3 Hydrodynamic Forces in Curvilinear Motion

2.3.1 Preliminary remarks.

Accurate and reliable prediction of hydrodynamic forces is never an easy task but the situation faced in ship manoeuvring is especially complicated as compared to other fields of ship hydrodynamics. In ship seakeeping, for instance, some effective theoretical models were developed and they even dominate in practical use. This was possible because in these applications, the potential linear wave effects are forming the main part of most of the hydrodynamic forces. Also, many effective and sufficiently accurate solutions have been obtained in the theory of screw propellers where the classic wing theory, although generalized and extended, is applicable. But the situation in ship resistance theory is already much worse as here involved are viscous and nonlinear wave forces and although a great progress has been achieved in the development of sophisticated computer codes, the towing tank experiments are still considered as the most reliable method for a ship's speed prediction.

But manoeuvring hydrodynamics includes all the resistance complexities and is even much worse because of a very complicated flow structure in curvilinear motion. An impression on this flow structure can be obtained from Fig. 2.5 where presented are the vortex patterns sketched on the basis of measurements and observations in rotating-arm captive model tests carried out by Nikolayev and Lebedyeva [29]. Here, one can observe four different free vortex filaments (marked by numbers 1 through 4) whose configuration depends strongly on the relationship between the drift angle and the path curvature. As the filaments appear as result of the flow separation, which is mainly governed by viscousity, any consistent numerical algorithm for calculating manoeuvring forces must be based on the Reynolds Averaged Navier–Stokes equations (RANSE). However, nowadays (2000 and the same keeps correct for 2007) these methods are only used in research purposes and are unlikely to be applied for practical manoeuvring computations still in the nearest future.

The scaled-model experiments are therefore the only practical mean to provide a relatively reliable information on hydrodynamic forces but these require operation of special costly and complex experimental facilities and, in many cases, rather sophisticated methods of data handling.

Very often, estimation of manoeuvring performance with reasonable accuracy is required when dedicated model tests cannot be afforded. Then, approximate estimation methods based on available databases of experimental results obtained from the model series tests can be used—most of existing "practical" methods for manoeuvring calculations work this way.

Approximate analytic methods stemming from the slender-body approach are also sometimes useful for very rough but still reasonable estimates.

Part of the material of this section relates to either the bare hull, or to the hull equipped with the rudder and/or propeller and necessary comments will be always provided. However, simple but reliable methods for calculation of the forces produced by the rudder and/or propeller will also be presented.

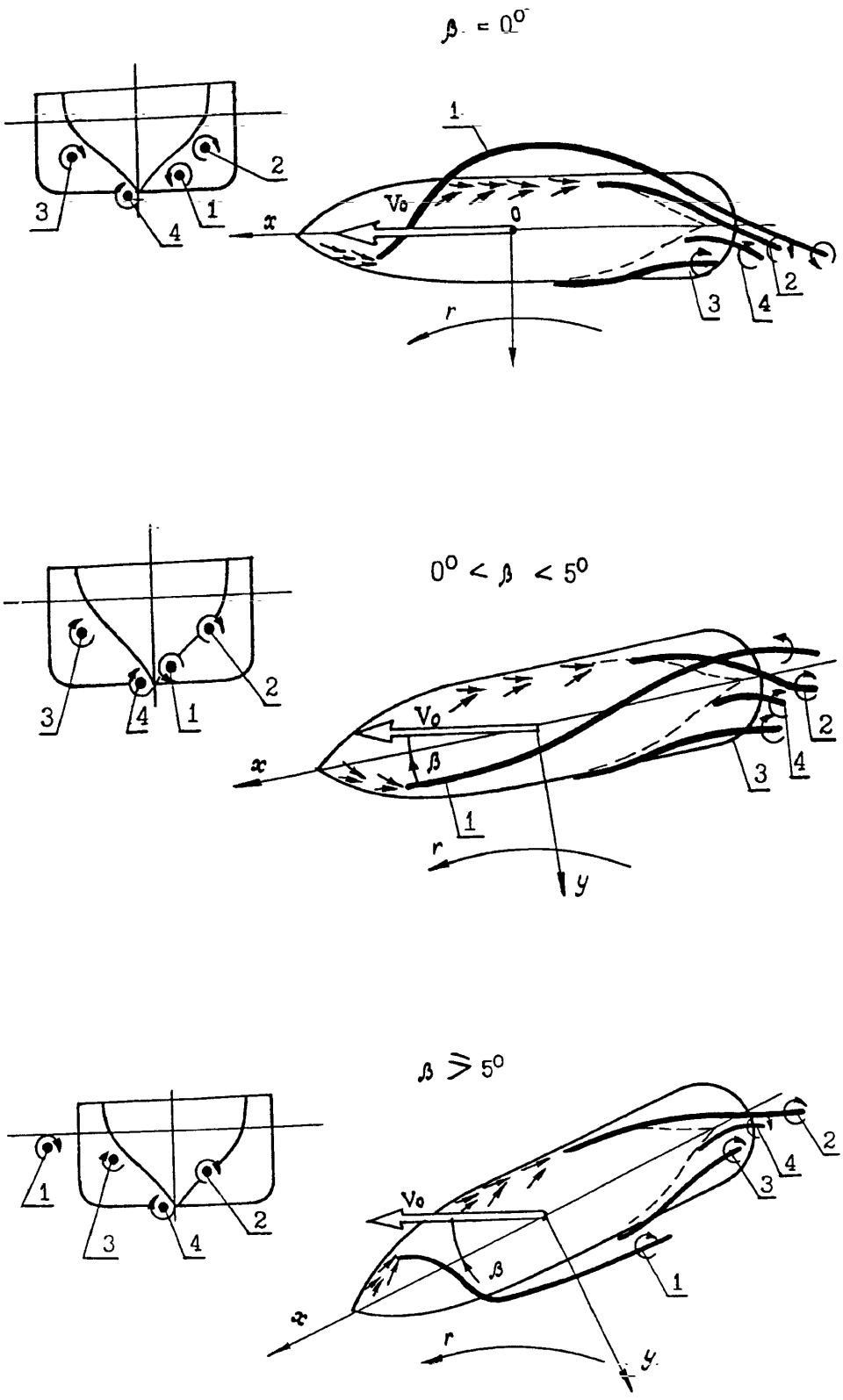

Figure 2.5: Sketch of the vortex pattern around the ship hull: from captive model test runs on a rotating arm

2.3.2 Numerical Computational Methods

All methods developed in the computational fluid dynamics (CFD methods) which were ever applied to manoeuvring problems, can be subdivided into two groups:

- Viscous fluid methods.
- Inviscid fluid methods.

Only methods of the first group have enough potential for reliable and adequate prediction of the manoeuvring hydrodynamic forces in the future. However, at the moment of writing this text (2007) they are still considered as not quite matured, the existing applications to manouvring are all of testing nature, and only model (i.e. not full-scale) values of Reynolds number are reachable in most cases as the required computer resources are proportional approximately to Rn^3. But even at lower reynolds numbers, hardware requirements are very high and real-time simulations are impossible with the common computers.

The viscous flow around a 6.437 m model of the *Mariner* ship and of a series 60 ship equipped with rudders was studied by Cura Hochbaum [9]. The cases of the steady oblique straight motion and of the steady circular motion with zero drift angle with $\mathsf{Rn} = 1 \times 10^7$ and $\mathsf{Fn} = 0.2$ were explored. RANSE were the governing equations and two turbulence models (Cebeci—Smith and Wilcox) were used alternatively. The finite volume method (FVM) was applied to solve the boundary value problem and the finest computational grids included about 480,000 cells. The stern part of the grid is shown on Fig. 2.6. The rudder is there approximated

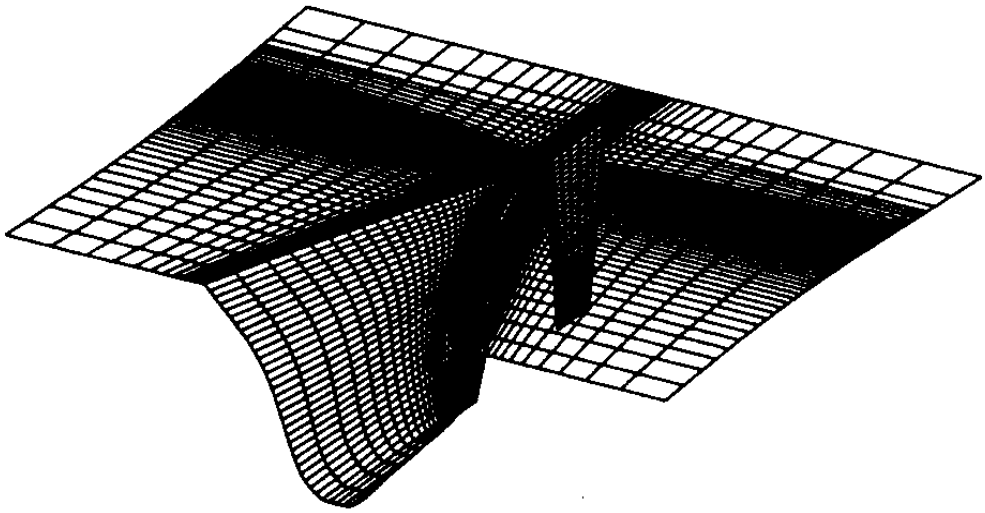

Figure 2.6: *Mariner* ship: Computational grid at the stern

with a zero-thickness flat plate. The computed results were compared with experimental ones obtained in the Hamburg Model Basin and they showed good qualitative and—in many cases—even satsifactory quantitative agreement (flow fields are compared on Fig. 2.7 (this is also

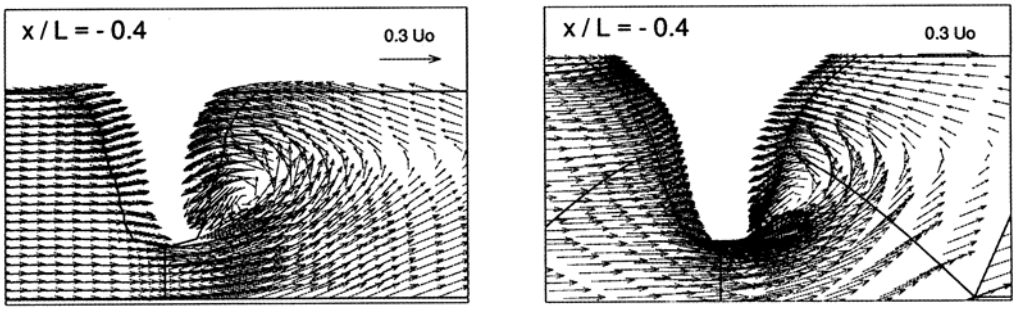

Figure 2.7: Series 60 afterbody: velocity field (left—measurements, right—computations; $\beta =$ 10 deg, $\mathsf{Fn} = 0.16$, $\mathsf{Rn} = 2.67 \times 10^6$)

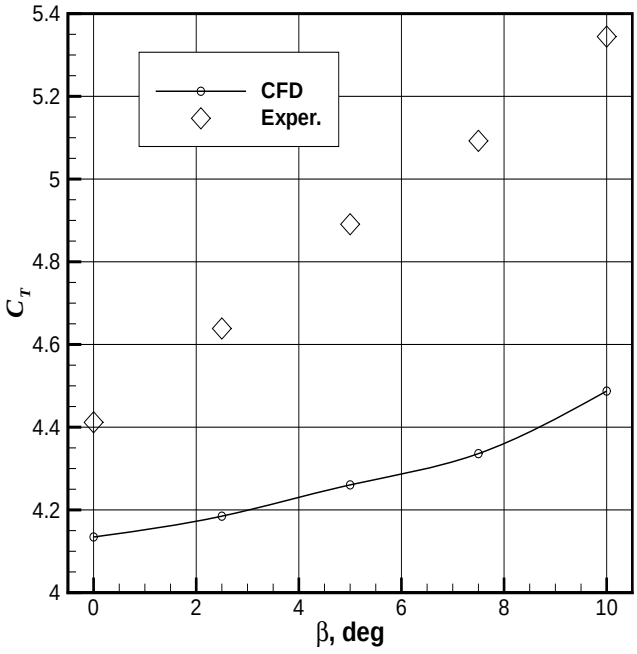

Figure 2.8: Series 60: measured and computed values of the total drag coefficient ($C_B = 0.6$, $\mathsf{Fn} = 0.16$, $\mathsf{Rn} = 2.67 \times 10^6$)

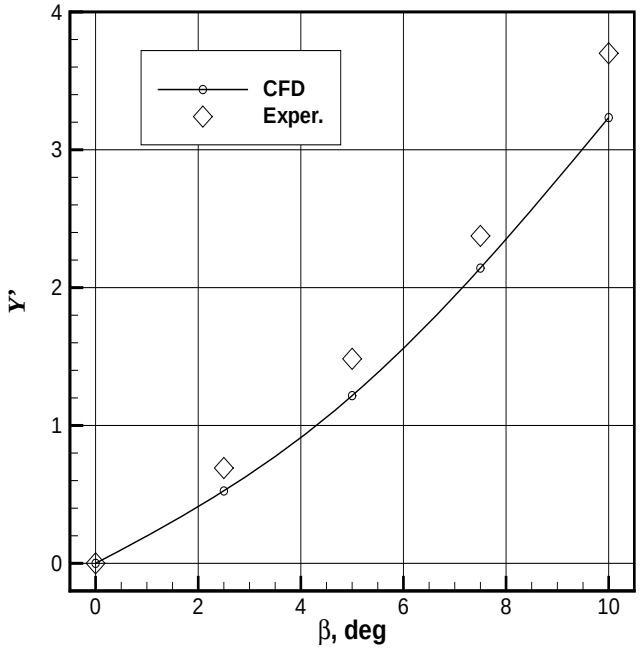

Figure 2.9: Series 60: measured and computed values of the sway force coefficient

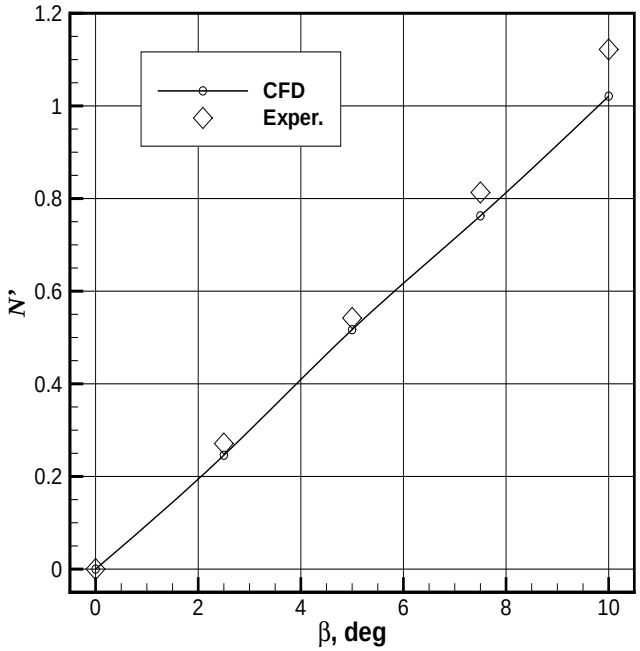

Figure 2.10: Series 60: measured and computed values of the yaw moment coefficient

worthwhile comparing with sketches on Fig. 2.5) and the forces—on Fig. 2.8–2.10. where C_T stands for the total resistance coefficient as defined in the ship resistance theory. It can be seen the the agreement is good for the sway force and yaw moment. For the total resistance it is somewhat worse: the discreapancy exceeds here 20%. However, regarding the needs of manoeuvring problems it is less important because the resistance can be relatively easily and reliably estimated by other means including standard towing tests .

Another interesting solution was obtained by Sato et al. [35] again by the FVM but in this case explored were two VLCC models SR221-A and B used earlier for numerous case studies. Only the bare hull was modeled in the RANSE computations at $\mathsf{Rn} = 1 \times 10^6$ and $\mathsf{Fn} = 0.138$. The both models had the same main particulars: ($L/B = 5.52$, $B/T = 3.0$, $C_B = 0.802$, $C_P = 0.806$. However the aft prismatic coefficient C_{Pa} and the longitudinal centre of buoyancy position LCB are different: 0.7504 and -2.45% for the model "A", and 0.7557 and -2.61% for the model "B" respectively. Comparison of the measured and computed distribution of the transverse force at a 9 deg drift angle is shown on Fig. 2.11 and Fig. 2.12 where can be seen a

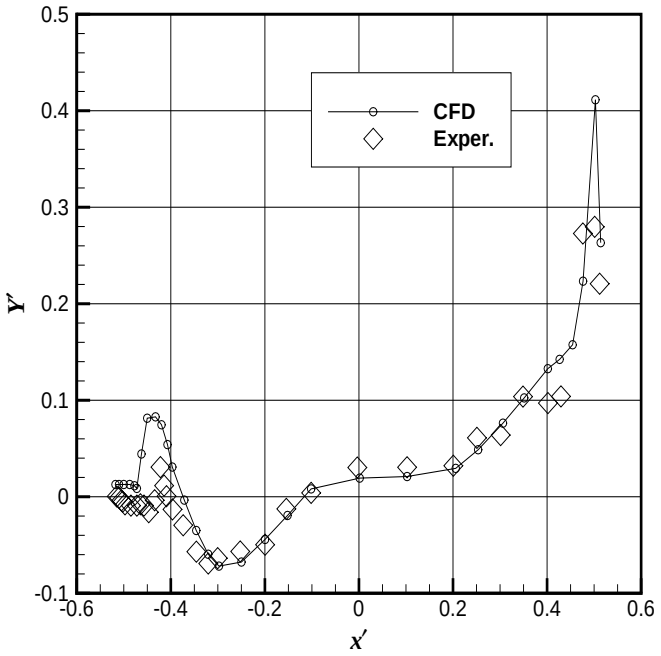

Figure 2.11: Longitudinal distribution of transverse force on Model-A

qualitatively good reproduction of a typical load distribution along the ship hull in pure drift motion.

In this study, probably for the first time ever, the RANSE solver was linked to a manoeuvring motion simulation program which used, however, relatively crude empiric methods for calculating rudder and propeller forces.

Another examples of applying RANSE codes to manoeuvring problems can be found in the surveys [2] and [23].

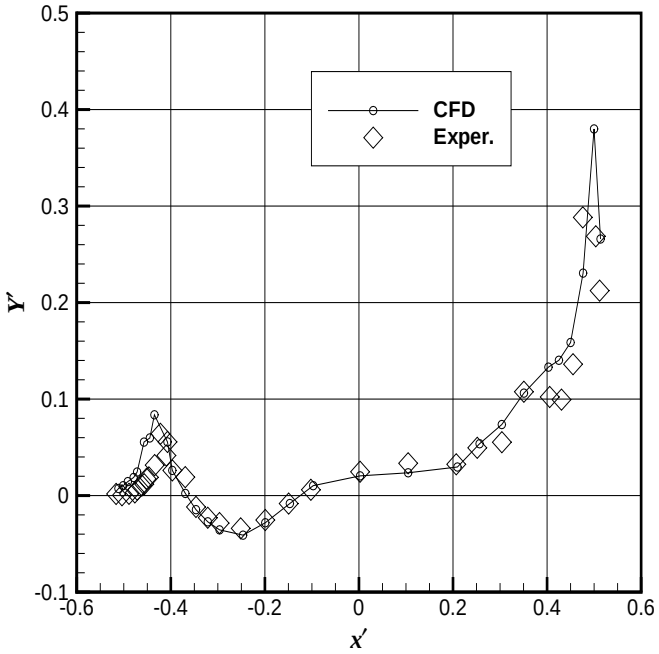

Figure 2.12: Longitudinal distribution of transverse force on Model-B

In the latter paper, presented was also a review of several inviscid flow codes. Of course, as the lifting effects are here very important, as they are responsible for the sway force and yaw moment, all these codes presume presence of some vorticity whose strength is to be determined by means of the Kutta–Zhukovsky condition. All those programs are in fact based on the panel method with various variants of the singularities distribution, namely:

- Hull surface vorticity distribution alone.
- Source and vorticity distributions over the centerplane (in the case of the zero source strength, this approach reduces to the lifting surface theory: the hull is then substituted with its centerplane interpreted as a very small aspect ratio ($k = T/L$) wing.
- Hull surface source distribution + centerplane vorticity distribution (the latter then serves exclusively for satisfying the Kutta condition).

In the sharp hull forms cases with the skeg and/or rudder amidship, it is possible to define unambiguously the flow separation lines. The Kutta condition is then well defined and the vortex methods can give surprisingly good results. But in general, this is rather a matter of luck as separation regions are not known in advance (see Fig. 2.5) and, although some analogue of the Kutta condition still holds, it becomes too unclear, fuzzy and poorly defined and that is why large uncertainties are inevitable.

Anyway, no one perfect fluid method can estimate satisfactorily the surge force which must then be estimated additionally with some other means.

2.3.3 Experimental Methods

Elements of regression analysis

The regression analysis plays a very important role in processing the experimental results and even in planning the experiments themselves. By all means, this is true for every scientific discipline dealing with experiments including all ship hydrodynamics but it is especially important in ship manoeuvring. The most basic notions and results of the regression analysis will be explained or, at least, reviewed here but we recommend the books [27] and [10] for more detailed information.

Let us introduce the *vector of factors* x which is represented as the column matrix:

$$\mathsf{x} = (x_1, x_2, \ldots, x_k)^T, \tag{2.54}$$

where the elements of the matrix are the input variables or *factors* (for instance, $x_1 = \beta$, $x_2 = r'$, $x_3 = \delta_R$, and so on), T is the transposed matrix symbol, and k is the number of factors which is also interpreted as the dimension of the factor space.

The *response* is the variable (or several variables) measured during the experiment and which can be estimated with the help of some approximation (we shall use for a scalar response the general notation y; in manoeuvring problems y can be any force/moment component, i.e. X, Y, K, N). It is common to say that we can create a regression model if the response can be explicitly represented as

$$y = f(\mathsf{x}, \mathsf{b}), \tag{2.55}$$

where

$$\mathsf{b} = (b_1, b_2, \ldots, b_m)^T \tag{2.56}$$

is the regression coefficients vector and $f()$ is some arbitrary function.

Linear regression models. Linear regressions, for which the function $F(\mathsf{x}, \mathsf{b})$ is linear with respect to the coefficients but not necessarily with respect to the factors, constitute a very important particular case. Any linear regression model can be represented as

$$y = \mathsf{fb}, \tag{2.57}$$

where

$$\mathsf{f}(\mathsf{x}) = (f_1(\mathsf{x}), f_2(\mathsf{x}), \ldots, f_m(\mathsf{x}))^T \tag{2.58}$$

is the vector of the *regressors* which are some arbitrary functions of the factors. The linear regression equation is completely defined if defined are both the regressors and the regression coefficients. Usually, the regressors are supposed to be defined *a priori* (we shall elaborate this later) but to define the coefficients, measurements of the response are to be carried out.

Let $\mathsf{x}^{(i)} = (x_1^{(i)}, \ldots, x_k^{(i)})^T$ be the vector of factors at the ith test run, where $i = 1, \ldots, N$ and N is the overall number of test runs. All combinations of the factors tried during the experiment form the following *factor matrix*:

$$\mathsf{X} = ((\mathsf{x}^{(1)})^T, \ldots, (\mathsf{x}^{(N)})^T)^T = \begin{pmatrix} x_1^{(1)} & \cdots & x_k^{(1)} \\ \vdots & \ddots & \vdots \\ x_1^{(N)} & \cdots & x_k^{(N)} \end{pmatrix}. \tag{2.59}$$

It is common to say that any factor matrix defines some *experimental design*. When the factor matrix and the vector of regressors are both defined, it is possible to construct the following *design matrix*:

$$\mathsf{F} = \begin{pmatrix} f_1(\mathsf{x}^{(1)}) & \cdots & f_m(\mathsf{x}^{(1)}) \\ \vdots & \ddots & \vdots \\ f_1(\mathsf{x}^{(N)}) & \cdots & f_m(\mathsf{x}^{(N)}) \end{pmatrix}. \tag{2.60}$$

If y_i is the response obtained in the ith test run, and the vector of responses (observations, measurements) is $\mathsf{y} \stackrel{d}{=} (y_1, \ldots, y_N)^T$ then we can write down the following for our linear regression model:

$$\mathsf{y} = \mathsf{F}\mathsf{b}. \tag{2.61}$$

It could be expected that the regression model will accurately reproduce the experimental response if the true values of the regression coefficients b are known. However, even then the equality (2.61) can be only fulfilled approximately as the measurements do always contain some random errors which we did not consider so far. But this equation can be used for estimating the regression coefficients if we treat it as a matrix linear algebraic equation with respect to b. Usually $N > m$ and the unique solution can be found with the least-square method:

$$\hat{\mathsf{b}} = (\mathsf{F}^T\mathsf{F})^{-1}\mathsf{y}, \tag{2.62}$$

where a hat over $\hat{\mathsf{b}}$ means the estimated value.

The number of unknown regression coefficients is never very large (below 20–30 for most cases) and, in principle, they all can be estimated even when $N = m$. The experimental design is then called *saturated*. However, in practice it is safer to use somewhat redundant designs which are less sensitive to outliers (wild points) and make possible some statistical analysis of the regression coefficients' estimates (see [27] and [43] for details). The success of the estimation procedure depends also substantially on the experimental design's quality. If the number of factors does not exceed 3–4, the *classic designs* are most often used i.e. the factors are just being changed with certain steps independent of each other. The measured response values can then be used either to build a grid function or to obtain good estimates of the regression coefficients.

Quality of the approximation depends also on which set of regressors is used or, in other words, on the regression model's *structure* which can be more or less adequate in any particular case. The are no formal techniques to set up regression model structures and intuitive considerations can be very important.

Structures of ship manoeuvring regression models

Polynomial models for moderate manoeuvring In normal manoeuvring, all kinematic parameters are limited in magnitude: in most cases $|v'| \leq 0.35$, $|r'| \leq 0.7$, $|\delta_R| \leq 0.7$. Also, for the majority of ships, the dependence of the forces on the factors is smooth and the corresponding functions can be expanded into multivariate Taylor series at the straight motion point. Although the procedure remains similar for any number of factors, we shall assume here

for simplicity that any dimensionless quasi-steady hull force component depends only on the velocities of sway and yaw and then

$$\begin{aligned}\Phi'_q(v',r') &= \Phi'_q(0,0)+\left(\frac{\partial\Phi'_q}{\partial v'}\right)(0,0)\,v'+\left(\frac{\partial\Phi'_q}{\partial r'}\right)(0,0)\,r'+\frac{1}{2!}\left(\frac{\partial^2\Phi'_q}{\partial v'^2}\right)(0,0)\,v'^2\\ &+ \frac{1}{2!}\left(\frac{\partial^2\Phi'_q}{\partial r'^2}\right)(0,0)\,r'^2+\frac{1}{2!}\left(\frac{\partial^2\Phi'_q}{\partial v'\partial r'}\right)(0,0)\,v'r'+\frac{1}{3!}\left(\frac{\partial^3\Phi'_q}{\partial v'^3}\right)(0,0)\,v'^3\\ &+ \frac{1}{3!}\left(\frac{\partial^3\Phi'_q}{\partial r'^3}\right)(0,0)\,r'^3+\frac{1}{3!}\left(\frac{\partial^3\Phi'_q}{\partial v'^2\partial r'}\right)(0,0)\,v'^2r'+\frac{1}{3!}\left(\frac{\partial^3\Phi'_q}{\partial v'\partial r'^2}\right)(0,0)\,v'r'^2+\dots.\end{aligned}\tag{2.63}$$

The expansion (2.63) is used as a basis for creating polynomial regression models. To complete the construction process, only the terms whose power does not exceed some certain value (3 in the majority of implementations) are retained in the equation and also somewhat more convenient notation is introduced: $\Phi'_0 \stackrel{d}{=} \Phi'_q(0,0)$, $\Phi'_v \stackrel{d}{=} \left(\frac{\partial\Phi'_q}{\partial v'}\right)(0,0),\dots,\Phi'_{vv} \stackrel{d}{=} \frac{1}{2!}\left(\frac{\partial^2\Phi'_q}{\partial v'^2}\right)(0,0),\dots,$ $\Phi'_{vvv} \stackrel{d}{=} \frac{1}{3!}\left(\frac{\partial^3\Phi'_q}{\partial v'^3}\right)(0,0),\dots,\Phi'_{vrr} \stackrel{d}{=} \frac{1}{3!}\left(\frac{\partial^3\Phi'_q}{\partial v'\partial r'^2}\right)(0,0),\dots$. The last retained term power is called the model's order and in the considered example the third-order polynomial regression model looks like

$$\begin{aligned}\Phi'_q(v',r') &= \Phi'_0+\Phi'_v v'+\Phi'_r r'+\Phi'_{vv}v'^2+\Phi'_{rr}r'^2+\Phi'_{vr}v'r'\\ &+ \Phi'_{vvv}v'^3+\Phi'_{rrr}r'^3+\Phi'_{vvr}v'^2r'+\Phi'_{vrr}v'r'^2,\end{aligned}\tag{2.64}$$

where the regression coefficients are traditionally called the *hydrodynamic* or *manoeuvring derivatives* and it is clear why. However, in fact they are not derivatives anymore: once the structure of the model is defined, its Taylor-expansion origin can be forgotten and the coefficients must be estimated from experiment. Only the first-order coefficients Φ'_v and Φ'_r keep some properties related to their initial definition and they are sometimes called the *positional derivative* and the *rotational derivative* respectively).

Symmetry considerations. If a ship is completely symmetric with respect to the centre plane (it means in practice that the ship is either twin-screw or quadruple-screw), the following symmetry/antisymmetry relations are valid for the force components:

$$\begin{aligned}X(v,r) &= X(-v,-r),\\ Y(v,r) &= -Y(-v,-r),\\ K(v,r) &= -K(-v,-r),\\ N(v,r) &= -N(-v,-r).\end{aligned}\tag{2.65}$$

Then, the regressors, which do not satisfy these conditions, must be removed from corresponding regression models. This results in

$$\begin{aligned}X'_q(v',r') &= X'_0+X'_{vv}v'^2+X'_{rr}r'^2+X'_{vr}v'r',\\ \Phi'_q(v',r') &= \Phi'_v v'+\Phi'_r r'+\Phi'_{vvv}v'^3+\Phi'_{rrr}r'^3+\Phi'_{vvr}v'^2r'+\Phi'_{vrr}v'r'^2,\end{aligned}\tag{2.66}$$

where $\Phi = Y, K, N$.

The situation is somewhat more complicated with single- and triple-screw vessels which are not quite symmetric hydrodynamically. In this case, the safest strategy would be to use identical full models for all components but just introduction of the constant term Φ'_0 into models for the sway force and yaw moment may become sufficient with resonable accuracy.

Modified polynomial models. It is possible to use the following modification of the polynomial model (2.64):

$$\begin{aligned}\Phi'_q(v', r') &= \Phi'_0 + \Phi'_v v' + \Phi'_r r' + \Phi'_{vv} v'^2 + \Phi'_{rr} r'^2 + \Phi'_{vr} v' r' \\ &+ \Phi'_{v|v|} v'|v'| + \Phi'_{r|r|} r'|r'| + \Phi'_{|v|r} |v'|r' + \Phi'_{v|r|} v'|r'| \end{aligned} \tag{2.67}$$

i.e. the cubic terms are replaced with quadratic ones but with the absolute value function applied. Technically, the model is of second order unlike the previous third-order model but it is no longer analytic (in the sense of the theory of analytic functions) and, strictly speaking, is not polynomial (such models can be called *quasi-polynomial*). This modification does not have any sensible advantages or drawbacks compared to the normal polynomial models and the choice is rather matter of taste. However, model containing absolute values become much less convenient when it is supposed to differentiate them which may become necessary in the stability or sensitivity analysis. And in no case can it be recommended to mix absolute-value-quadratic and cubic terms within the same regression, although such examples can be found in the literature, as their effects are very similar and such compound models can suffer from the so-called multi-collinearity and bring problems into the coeffcients estimation process.

Dimensional polynomial models. Sometimes, regression models created directly for the dimensional force components are preferred. The difference is that in this case the longitudinal velocity u is always present as an additional factor. If the model is supposed to represent forces in the neighbourhood of the approach speed $V_0 \equiv u_0$ and $\Delta u \stackrel{d}{=} u - u_0$ is the velocity alteration in manoeuvring, the third-order polynomial regression will be

$$\begin{aligned}\Phi_q(\Delta u, v, r) &= \Phi_0 + \Phi_u \Delta u + \Phi_{uu} (\Delta u)^2 + \Phi_{uuu} (\Delta u)^3 + \Phi_v v + \Phi_r r \\ &+ \Phi_{uv} \Delta u v + \Phi_{ur} \Delta u r + \Phi_{uuv} (\Delta u)^2 v + \Phi_{uur} (\Delta u)^2 r \\ &+ \Phi_{vv} v^2 + \Phi_{rr} r^2 + \Phi_{vr} v r \\ &+ \Phi_{uvv} \Delta u v^2 + \Phi_{urr} \Delta u r^2 + \Phi_{uvr} \Delta u v r \\ &+ \Phi_{vvv} v^3 + \Phi_{rrr} r^3 + \Phi_{vvr} v^2 r + \Phi_{vrr} v r^2. \end{aligned} \tag{2.68}$$

The equation in the dimensional form is more complicated and looks less elegant but in this case the quadratic dependence of forces on the ship speed is no longer assumed which can result in a more adequate fit at high Froude numbers. Historically, just these dimensional manoeuvring regressions came first and they are usually associated with the name of Abkowitz [7].

Trigonometric models for low-speed manoeuvring. To approximate forces in arbitrary manoeuvres, trigonometric linear regression models can be more convenient. The idea of using

multivariate Fourier expansions is exploited at the construction of these regressions. Special attention must be payed to a thorough selection of terms which should be performed in such a way that all the relevant details of experimental responses be reproduced though keeping the model as simple as possible. It is important that the structure keep adequacy in the limiting cases: for instance, at the zero-speed rotation none of the force components is allowed to structurally depend on the limiting residual value of the drift angle.

Here is an example of such a regression model:

$$\begin{aligned}
\Phi''(\beta, r'') &= \Phi''_0 + \Phi''_1 r'' + \Phi''_2 \sin \pi r'' + \Phi''_3 \cos \frac{\pi}{2} r'' + \Phi''_4 r''^2 + \Phi''_5 \sin 2\pi r'' \\
&+ \Phi''_6 \cos \frac{3\pi}{2} r'' + \Phi''_7 \sin \pi r''^2 + \Phi''_8 \sin\beta \sin \pi r'' + \Phi''_9 \cos\beta \sin \pi r'' \\
&+ \Phi''_{10} \sin\beta \cos \frac{\pi}{2} r'' + \Phi''_{11} \cos\beta \cos \frac{\pi}{2} r'' + \Phi''_{12} \sin 3\pi\bar{r} + \Phi''_{13} \cos \frac{5\pi}{2} r'' \\
&+ \Phi''_{14} \sin 2\pi r''^2 + \Phi''_{15} \sin\beta \sin 2\pi r'' + \Phi''_{16} \cos\beta \sin 2\pi r'' \\
&+ \Phi''_{17} \sin\beta \cos \frac{3\pi}{2} r'' + \Phi''_{18} \cos\beta \cos \frac{3\pi}{2} r'' + \Phi''_{19} \sin\beta \sin \pi r''^2 \\
&+ \Phi''_{20} \cos\beta \sin \pi r''^2 + \Phi''_{21} \cos \frac{7\pi}{2} r'' + \Phi''_{22} \sin 2\beta \cos \frac{\pi}{2} r'' \\
&+ \Phi''_{23} \cos 2\beta \cos \frac{\pi}{2} r'' + \Phi''_{24} \sin 2\beta \sin \pi r''^2 + \Phi''_{25} \sin 2\beta \cos \frac{3\pi}{2} r'' \\
&+ \Phi''_{26} \cos 2\beta \cos \frac{3\pi}{2} r'' + \Phi''_{27} \sin 2\beta \sin 2\pi r'' + \Phi''_{28} \cos 2\beta \sin 2\pi r'' \\
&+ \Phi''_{29} \sin 2\beta \cos \frac{5\pi}{2} r'' + \Phi''_{30} \sin 2\beta \sin 2\pi r''^2 + \Phi''_{31} \sin 4\beta \cos \frac{\pi}{2} r'' \\
&+ \Phi''_{32} \cos 2\beta \cos \frac{5\pi}{2} r'' + \Phi''_{33} \cos 2\beta \sin 2\pi r''^2 + \Phi''_{34} \cos 4\beta \cos \frac{\pi}{2} r'' \ ,
\end{aligned} \tag{2.69}$$

where $\Phi''_i,\ i = 0, \ldots, 34$ are the regression coefficients and r'' is the generalized dimensionless yaw rate as introduced above.

Similar models containing the absolute value function are also possible.

Experimental facilities

Some tests providing information on manoeuvring forces can be carried out on such "general purpose" installations as conventional towing tanks and wind tunnels with a model fixed at some incidence (drift) angle. However, these *oblique towing* tests are of limited value as they cannot account for the path curvature which is an undetachable feature of manoeuvring motions. The method of curved models (i.e. models with curved centre planes) was proposed and used in some hydrodynamic centres to solve the problem but it appeared to be inconvenient as every value of the path curvature required manufacturing another model. Nowadays, manoeuvring hydrodynamic characteristics are obtained exclusively on special facilities capable to reproduce the model's curved motion. These facilities are mostly used for the so-called *captive-model tests* i.e. the model is forced to execute some pre-determined curvilinear motion while the model's reactions received by the driving mechanism are measured and used for estimation of hydrodynamic forces and moments.

There are two substantially different kinds of such installations: the *Rotating Arm* (or the *Circulating Tank*)[13], and the *Planar Motion Mechanism (PMM)*. Each of the installations requires suitable experimental techniques and data processing methods.

Rotating arm. The idea of the rotating arm is evident and simple: a special radial arm towing a model is rotating around a fixed axis over the water surface in a circular or rectangular tank (Fig. 2.13 and 2.14). The model can be fixed at different points along the arm and

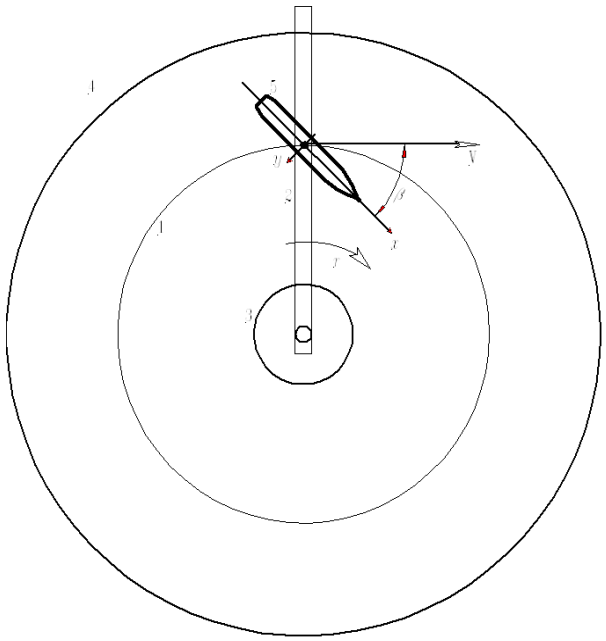

Figure 2.13: Scheme of Rotating Arm Facility: 1—model's circular trajectory; 2—rotating arm; 3—central support (island); 4—outer boarder of the circulating tank; 5—scaled ship model

at different angles with respect to it. As the arm can rotate with various rates, the three

[13]In fact, the rotating arm is operated in the circulating tank

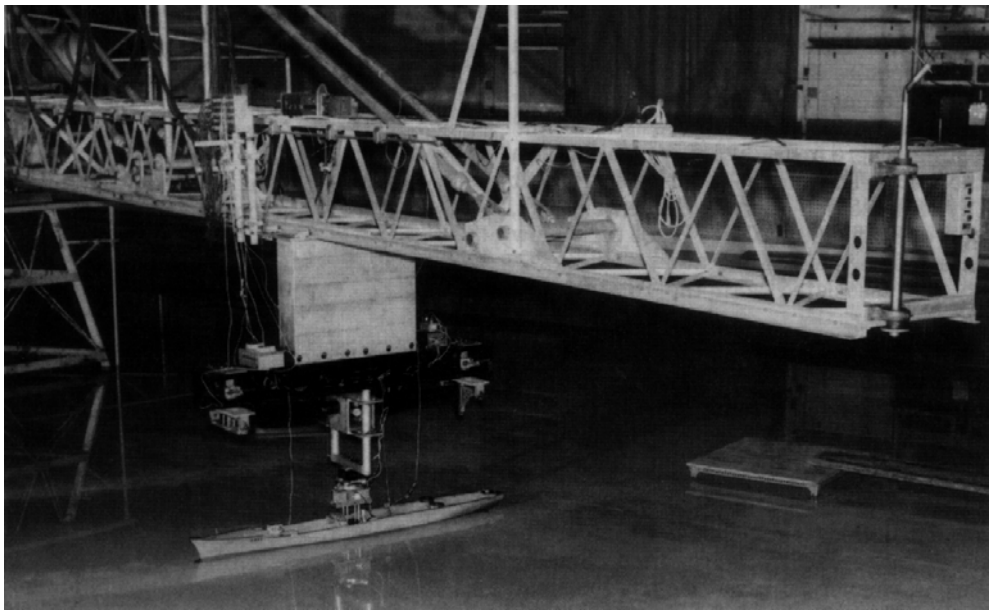

Figure 2.14: View of 22 m Diametre Rotating Arm at Davidson Laboratory (USA)

parameters (Fn, β, and $r' = L_{\text{MODEL}}/R_{\text{ROTATION}}$) can be set independently at each test run. To obtain small values of r' at a given model length[14], large values of R are required and this predetermines large diametres of the best facilities of this kind (the record is 80 m for the circulating tank at the David Taylor Model Basin (USA)).

The model is connected to the arm by means of dynamometric elements and up to 6 force/moment components can be measured at each test run for fully fixed models. However, in most cases, to reduce the number of factors, models of surface ships are given freedom in roll, heave, and pitch. Not only bare hulls, but also models equipped with rudders and propellers can be tested. Of course, the centrifugal force of the model itself must be estimated and subtracted from the dynamometer readings.

The steady circular motion only can be reproduced on the rotating arm. Thus, the quasi-steady force/moment components alone can be estimated directly for any given combination of kinematic parameters. The standard regression technique can be further applied for estimating the manoeuvring derivatives.

Planar motion mechanisms. The most advanced and sophisticated representatives of the PMM family are the so-called *Computerized Planar Motion Carriages (CPMC)* or xy-carriages. The idea of the facility is again very simple and straightforward: a conventional towing-tank carriage (x-carriage) supports transverse railways for a secondary y-carriage. The latter, however, carries an additional Δx "incremental" subcarriage with a rotating platform (ψ-drive) (Fig. 2.15 and 2.16). The model is attached to the end of this combination of carriages by means of dynamometers and can be given arbitrary forced motion in the horizontal plane including, for instance, the same circular paths which are obtained with the rotating arms.

[14]It is acknowledged that models should not be smaller then 6 m length—otherwise the scale effect may become unacceptable.

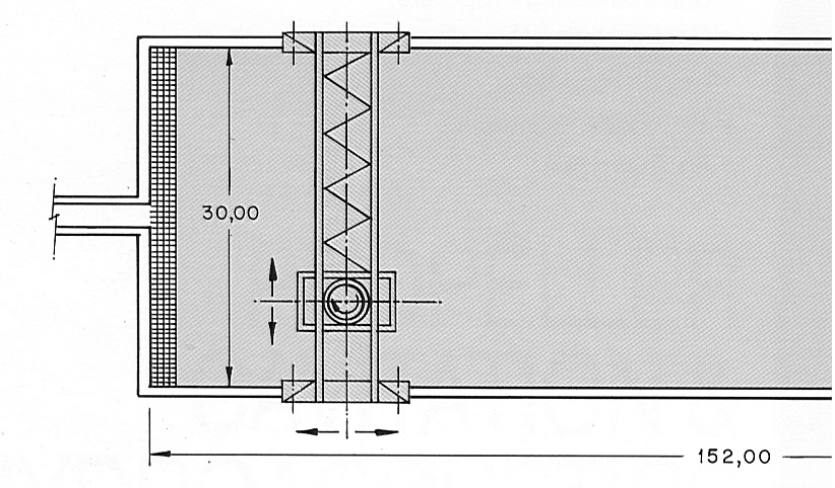

Figure 2.15: Scheme of XY-carriage (CPMC) of El Pardo Model Basin (Spain)

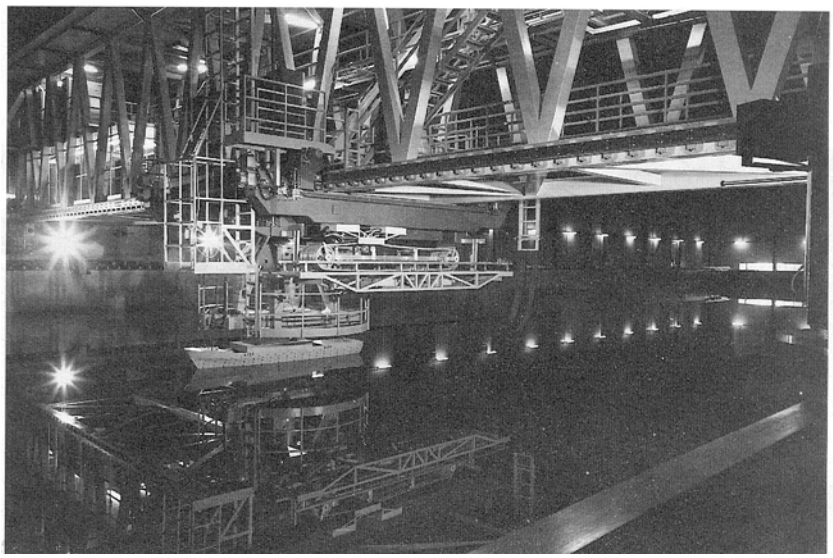

Figure 2.16: View of CPMC facility of El Pardo Model Basin (Spain)

Implementation of this scheme is, however, not so simple as it requires using high precision electric drives controlled by a complicated digital system synchronizing all the motions to produce desired "manoeuvres" (there are special control programs for automated execution of standard tests). The positioning accuracy is very high. For instance, the tolerances for linear displacements do not exceed ±5 mm for the CPMC installed in 1992 in the El Pardo Model Basin (CEHIPAR) in Spain[15].

The CPMC can be used not only for captive model tests but also for the precise tracking of self-propelled free-running models: in this mode the control computer manipulates the drives in such a way that the dynamic interaction between the rotating platform and the model continously measured by the dynamometers remain negligible.

Another advantage of CPMC (and of also any other PMM) is that, unlike rotating arms, they do not require special tanks: the facility can be installed either in a seakeeping tank and be used also for seakeeping tests (CEHIPAR), or in a conventional, i.e. resistance/propulsion, tank as it is done at HSVA (Hamburg, Germany).

Less sophisticated conventional PMMs (the first unit was built in USA at the beginning of 50s) are of much simpler design: they are in fact mechanical two-coordinate (transversal + rotational) oscillators with hydraulic drives and a helicoidal gear. The PMM is attached to a normal towing tank carriage and is involving the connected model into forced harmonic oscillations in sway and yaw. The amplitudes are, however, limited and much smaller than those attainable with the CPMC (usually not more than 1.0–2.5 m for sway). The both forms of oscillations can only have the same pre-set frequency but the phase shift between the transverse and the angular motions can be adjusted to produce different kinds of forced oscillations. As the traditional PMM are much less complex than the CPMC and so are their control systems, they are less expensive and are nowadays the most common devices for conducting captive model tests.

Estimating hydrodynamic forces after harmonic oscillations tests, which are the only option on simpler PMM, has certain peculiarities. Creation of a grid function is in this case problematic because the motion is substantially unsteady and the velocities and accelerations effects are mixed. That is why, the PMM technique has been always associated with using regression models.

Depending on the resulting form of oscillations, different kinds of tests can be performed. The most informative is the so-called *combined sway—yaw test* when the "heading angle" of the model is changed harmonically, say

$$\psi = \psi_0 \sin \omega t, \tag{2.70}$$

where ψ_0 is the amplitude and ω is the frequency while the drift angle β remains constant during the run (to get this, angular oscillations have to accompanied with transverse ones and the model looks zigzagging in the tank; the particular case when $\beta \equiv 0$ is called "pure yaw test". Then

$$r = r_0 \cos \omega t, \tag{2.71}$$

[15]The first facility of this kind was created in Germany in 1976 and is in operation in the Hamburg Model Basin (HSVA).

where $r_0 = \omega\psi_0$ is the angular velocity amplitude, and

$$\dot{r} = -r_0\omega \sin \omega t. \tag{2.72}$$

Then, it is clear that the rate-of-yaw signal has the phase shifted by $\frac{\pi}{2}$ or it is *out of phase* with respect to the heading angle signal while the acceleration is practically *in phase* with it as the shift by π can be easily compensated through the sign change.

The output signals i.e. the measured force components $\Phi(t)$ are also $\frac{2\pi}{\omega}$-periodic but they can also have non-zero mean values and higher harmonics[16]. In other words, any component measured during the PMM oscillatory tests can be represented in form of Fourier series:

$$\Phi(t) = \Phi_{\mathrm{MEAN}} + \Phi_{\mathrm{IN}} \sin \omega t + \Phi_{\mathrm{OUT}} \cos \omega t + \Phi_{\mathrm{IN2}} \sin 2\omega t + \Phi_{\mathrm{OUT2}} \cos 2\omega t + \ldots. \tag{2.73}$$

One of the most efficient and simple ways to extract the information contained inside the time histories of the responses is to compute their Fourier coefficients. These are (higher harmonics have never been analyzed):

– the mean value

$$\Phi_{\mathrm{MEAN}} = \frac{1}{T} \int_0^T \Phi(t)\, \mathrm{d}t; \tag{2.74}$$

– the in-phase first harmonic's amplitude

$$\Phi_{\mathrm{IN}} = \frac{2}{T} \int_0^T \Phi(t) \sin \omega t\, \mathrm{d}t; \tag{2.75}$$

– the out-of-phase first harmonic's amplitude

$$\Phi_{\mathrm{OUT}} = \frac{2}{T} \int_0^T \Phi(t) \cos \omega t\, \mathrm{d}t; \tag{2.76}$$

– the in-phase second harmonic's amplitude (not used in practice)

$$\Phi_{\mathrm{IN2}} = \frac{2}{T} \int_0^T \Phi(t) \sin 2\omega t\, \mathrm{d}t; \tag{2.77}$$

– the out-of-phase second harmonic's amplitude

$$\Phi_{\mathrm{OUT2}} = \frac{2}{T} \int_0^T \Phi(t) \cos 2\omega t\, \mathrm{d}t, \tag{2.78}$$

where $T = \frac{2\pi}{\omega}$ is the main period.

[16] Subharmonics can probably also exist but there have still been no reports confirming their presence.

The Fourier analysis on classic PMM is often carried out partly in analogous way with the help of sine-cosine rotating transformers. In any case, the values of Φ_{MEAN}, Φ_{IN}, Φ_{OUT}, and Φ_{OUT2} are automatically computed and registered after each test run or obtained numerically through the post-processing of the recorded time histories.

The regression models (2.46) and (2.64) must be also transformed to produce responses for Fourier coefficients. To perform this, the equations (2.71) and (2.72) have to be substituted into the sum of the models (2.46) and (2.64), then the transforms (2.74)–(2.76) and (2.78) are evaluated. Finally , the following regressions can be obtained for the Fourier coefficients (those related to quasi-steady components are non-dimensionalized):

$$\begin{aligned}
\Phi'_{\text{MEAN}} &= \Phi'_0 + \Phi'_v v' + \Phi'_{vv} v'^2 + \frac{1}{2}\Phi'_{rr} r'^2_0 + \Phi'_{vvv} v'^3 + \frac{1}{2}\Phi'_{vrr} v' r'^2_0, \\
\Phi_{\text{IN}} &= -\Phi_{\dot{r}} \omega r_0, \\
\Phi'_{\text{OUT}} &= \Phi'_r r'_0 + \Phi'_{vr} v' r'_0 + \frac{3}{4}\Phi'_{rrr} r'^3_0 + \Phi'_{vvr} v'^2 r'_0, \\
\Phi'_{\text{OUT2}} &= \frac{1}{2}\Phi'_{rr} r'^2_0 + \frac{1}{2}\Phi'_{vrr} v' r'^2_0.
\end{aligned}$$

Then, if a consistent set of sway–yaw tests for various (v', r'_0) combinations is performed, most of the regression coefficients can be estimated with the least-square technique. The only exception are acceleration derivatives $\Phi_{\dot{v}}$ which require at least one *pure sway test* i.e. transverse oscillations of the model without rotation.

For the considered sample regression model, the information supplied by the second-order out-of-phase amplitudes turned out to be redundant but these can still be involved into the analysis mainly for checking purposes. A more detailed discussion of this estimation algorithm can be found in [34], [44] and [45].

The described procedure was set up and tested in [43] but so far more popular in hydrodynamic centres are traditional methods based on a consecutive estimation of the manoeuvring derivatives. The reasons are mainly historical: an extensive computerised numerical analysis was problematic in 50s when first PMM started operating. A variant of such intuitive approach is described in detail in [7]. At the same time, there are suggestions of even more complicated methods based on a direct analysis of time histories obtained after arbitrary forced unsteady motions [41], [12].

2.3.4 Slender-Body Theory

A relatively simple analytic method for predicting hydrodynamic forces on the ship hull in manoeuvring motion is described below. Of course, such a method is not capable to provide good and reliable estimates for any ship forms but the estimates obtained are often reasonable and sometimes even better then those withdrawn from serial tests data bases [26]. Even more important is that this method supplies some *canonic* values of hydrodynamic derivatives for schematized hull forms which are often useful themselves as very rough estimates.

The method exploits the ship hull's slenderness and is in fact a variant of the strip theory well known in ship seakeeping. In some respects, the manoeuvring implementation is even simpler as the manoeuvring motion in the horizontal plane is relatively slow (i.e. with low values of the Strouhal number) and all free-surface effects can be neglected. On the other hand, the method must be applicable to moderate manoeuvres (at least!) and must describe certain nonlinearities. The latter is achieved through splitting the method into two parts:

1. The classic slender-body theory based on the perfect fluid dynamics and usually associated with Munk who had applied this approach for analyzing airship transverse loads before the WW2, and
2. The so called *cross-flow theory* which assuming a simplistic hydrodynamic model for vortex separation.

The Munk method is closely connected to the seakeeping strip method and, at the same time, to the theory of wings with extremely small aspect ratio. The cross-flow part takes its origin in experiments with not streamlined bodies, especially cylinders recoursing to data on the drag and flow picture around such cylinders in the cross flow. Although the considered flow structures associated with each of these two theories are very different and cannot combine in real conditions, it is assumed (and it is a very strong assumption!) that the partial force estimates can be superimposed. As result, the classic Munk approach provides the linear part with respect to the kinematic parameters, while the cross-flow theory only results in nonlinear terms thus complementing the first submethod. In other words, the total estimated hull hydrodynamic force is represented as the sum:

$$\Phi_H = \Phi_{HM} + \Phi_{HCF}, \tag{2.79}$$

where $\Phi = Y, N$ (the X-component cannot be estimated with any strip method and the roll moment is dropped here for simplicity—details concerning this component can be found in [26]), Φ_{HM} is the Munk component, and Φ_{HCF} is the cross-flow component.

The zero Froude number assumption is applied here. This means that the boundary condition on the free surface is identical to that on the rigid wall and instead of the underwater part of the hull near the free surface, we can deal with the doubled hull in the unbounded fluid (Fig. 2.17). This doubled hull can be treated as a low aspect ratio wing with the span $2T$, the chord L and with the thickness B. Its reference area is usually defined as $2TL$ and the aspect ratio k_H is

$$k_H = \frac{2T}{L}. \tag{2.80}$$

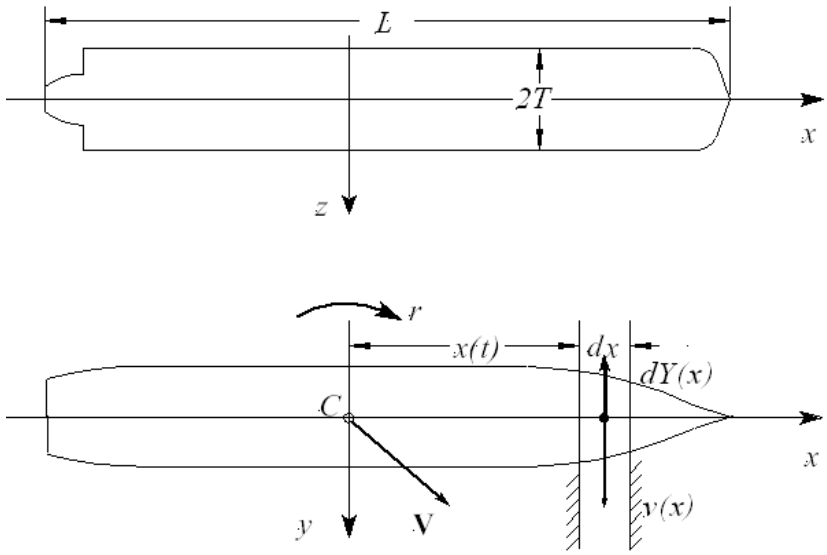

Figure 2.17: Mirrored Ship Hull in Curvilinear Motion—Munk method

Munk forces

If the doubled hull performs an arbitrary manoeuvring motion in the horizontal plane, it can be imagined that it is piercing, at some arbitrary time moment t, two imaginary parallel planes fixed with respect to Earth (see Fig. 2.17). The both planes are supposed to be **at this given time moment** perpendicular to the axis Cx, the gap between them is infinitesimal (equal to $\mathrm{d}x$) and the instantaneous coordinate of each plane can then be assumed the same and equal to $x(t)$. Let us consider the perfect fluid's motion between those planes. Its momentum is

$$\mathrm{d}Q = \mu_{yy} v(x)\,\mathrm{d}x, \tag{2.81}$$

where μ_{yy} is the cross-sectional transverse added mass coefficient and, as expected, $v(x) = v + xr$.

As follows from the second Newton law, the elementary hydrodynamic reaction $\mathrm{d}Y_{HM}$ acting onto the section will be

$$\mathrm{d}Y_{HM} = \gamma_{HM}(x)\,\mathrm{d}x = -\frac{\mathrm{d}}{\mathrm{d}t}\mathrm{d}Q[t, x(t)] = -\frac{\mathrm{d}[\mu_{yy}(x)v(x,t)]}{\mathrm{d}t}\mathrm{d}x, \tag{2.82}$$

where $\gamma_{HM}(x)$ is the transverse distributed hydrodynamic load.

As Q depends on time not only directly but also through the changing distance $x(t)$, the time derivative in eq. (2.82) must be taken in the following form:

$$\frac{\mathrm{d}}{\mathrm{d}t} = \frac{\partial}{\partial t} + \frac{\mathrm{d}x}{\mathrm{d}t}\frac{\partial}{\partial x} = \frac{\partial}{\partial t} - u\frac{\partial}{\partial x} \tag{2.83}$$

which is the usual representation of the time derivative in the moving frame. It will be natural then to divide the transverse loading similarly:

$$\gamma_{HM} = \gamma_{HMa} + \gamma_{HMq}, \tag{2.84}$$

where the additional subscripts a and q stand, as before, for the accelerations-dependent and the quasi-steady parts respectively. Substituting eq. (2.81) into eq. (2.82) we can obtain after simple evaluations

$$\begin{aligned} \gamma_{HMa} &= -\mu_{yy}\,\dot{v} - x\mu_{yy}\,\dot{r}, \\ \gamma_{HMq} &= \mu_{yy}\,ur + \frac{\partial \mu_{yy}}{\partial x}\,uv + x\frac{\partial \mu_{yy}}{\partial x}\,ur. \end{aligned} \tag{2.85}$$

First, consider the accelerations-dependent part of the load. It is evident that the corresponding sway force and yaw moment are

$$Y_{HMa} = \int_L \gamma_{HMa}(x)\,\mathrm{d}x; \qquad N_{HMa} = \int_L x\gamma_{HMa}(x)\,\mathrm{d}x \tag{2.86}$$

or

$$\begin{aligned} Y_{HMa} &= -\mu_{22}\,\dot{v} - \mu_{26}\,\dot{r}, \\ N_{HMa} &= -\mu_{26}\,\dot{v} - \mu_{66}\,\dot{r}, \end{aligned} \tag{2.87}$$

where, assuming that the origin C lies in the midship plane, the doubled hull's added masses are:

$$\mu_{22} = \int\limits_{-\frac{L}{2}}^{\frac{L}{2}} \mu_{yy}(x)\,\mathrm{d}x; \qquad \mu_{26} = \int\limits_{-\frac{L}{2}}^{\frac{L}{2}} x\mu_{yy}(x)\,\mathrm{d}x; \qquad \mu_{66} = \int\limits_{-\frac{L}{2}}^{\frac{L}{2}} x^2\mu_{yy}(x)\,\mathrm{d}x \tag{2.88}$$

In fact, the last equations define a method for calculating the ship added masses. The required sectional added mass can be borrowed from the seakeeping data using the zero-frequency values.

It is somewhat more complicated with the quasi-steady loading. It was found appropriate to split it further into two components:

$$\gamma_{HMq} = \gamma_{HMq1} + \gamma_{HMq2}, \tag{2.89}$$

with

$$\begin{aligned} \gamma_{HMq1} &= \mu_{yy}\,ur, \\ \gamma_{HMq2} &= \frac{\partial \mu_{yy}}{\partial x}\,uv + x\frac{\partial \mu_{yy}}{\partial x}\,ur. \end{aligned} \tag{2.90}$$

While the load γ_{HMq1} depends on the added mass distribution and is supposed to be purely inertial, the second part γ_{HMq2} is function of the added mass longitudinal gradient and is thought to be influenced by the viscosity. The latter can be demonstrated in the case of the oblique straight motion of the ship hull. While the transverse load distribution in the perfect fluid would be relatively close to being antisymmetric (Fig. 2.18), in the real fluid the antisymmetry disappears: due to viscosity, actual loads become much smaller in the aft part of the hull while the forebody loads are predicted much better, see also Fig. 2.11 and 2.12. As the picture is very similar to that reproducing chordwise load distributions on a thin flat plate without and with circulation, one can conclude that some circulation around the ship hull also exists and some kind of the Kutta condition is to be applied here. However, the Kutta condition is defined much less certainly for a thick slender hull than for a classic wing, and is usually formulated as follows (see [14] for additional comments):

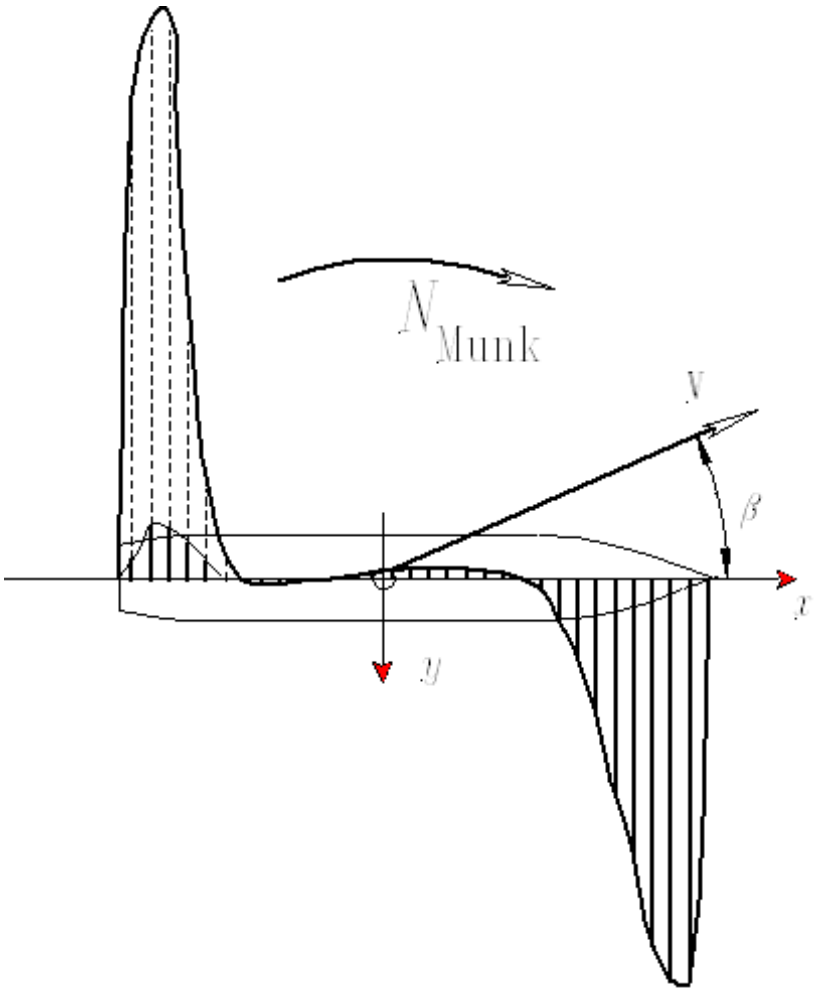

Figure 2.18: Scheme of Transverse Load Distribution: solid lines—real fluid; dashed lines—perfect fluid

The transverse hydrodynamic load of the second kind (γ_{HMq2}) must not be integrated along some aft part of the body where the separation occurs and the presence of the load is not confirmed with the experiments.

Then, the quasi-steady parts of the sway force and yaw moment will be

$$\begin{aligned} Y_{HMq} &= \int_{-\frac{L}{2}}^{\frac{L}{2}} \gamma_{HMq1}(x)\,\mathrm{d}x + \int_{-\frac{L}{2}}^{\frac{L}{2}} \lambda(x)\gamma_{HMq2}(x)\,\mathrm{d}x, \\ N_{HMq} &= \int_{-\frac{L}{2}}^{\frac{L}{2}} x\gamma_{HMq1}(x)\,\mathrm{d}x + \int_{-\frac{L}{2}}^{\frac{L}{2}} \lambda(x)x\gamma_{HMq2}(x)\,\mathrm{d}x, \end{aligned} \tag{2.91}$$

where $\lambda(x)$ is the correction weighting function most often defined as

$$\lambda(x) \stackrel{d}{=} \begin{cases} 1 & \text{at} \quad x > x_e \\ 0 & \text{at} \quad x < x_e \end{cases}, \tag{2.92}$$

and where x_e is the abscissa of the section aft of which viscous effects are supposed to eliminate the transverse load of the second kind. Cosistent definition of the value of this parameter presents one of the most serious challenges of the Munk theory. Of course, better would be to take it directly from the experiment but such an approach would kill most of the rationale of the slender body theory which is supposed to provide predictions in absence of the test data! Hence, in practice, some general recommendations are followed. The most common of them are:

- x_e is the abscissa of the beginning of the region with strong negative pressure gradient which can be e.g. the end of the parallel body of fuller ship bodies;
- x_e is the abscissa of the station with the largest added mass;
- x_e—the abscissa of the maximum draught station;
- $x_e = 0$ i.e. the load is only assumed to exist on the forward part of the ship's hull (i.e. forward of the midship section).

It can be noticed that all these recommendations, although not quite equivalent, do not heavily contradict each other.

Anyway, these guidelines should be followed with some care and not blindly: for instance, the transverse load shouldn't be completely removed aft of the midship section on sharp hull forms without a cylindrical part (parallel middle body), or along the most part of the hull of a ship trimmed by the bow independently on where the maximum draught is currently located.

The force and the moment can be expressed through their dimensionless coefficients in the standard way[17]:

$$Y_{HMq} = Y'_{HMq}(v', r')\,\frac{\rho V^2}{2} LT,$$

[17]These formulae are valid for a real ship hull. The reference area must be $2TL$ when operating with the doubled hull as at the evaluation of the dimensionless derivatives given below.

$$N_{HMq} = N'_{HMq}(v', r')\,\frac{\rho V^2}{2}L^2T. \tag{2.93}$$

As the Munk theory is linear, and is supposed to be rigorously valid for only small drift angles and curvatures, it will be then possible to assume $u' = 1$ and then the coefficients can be represented as

$$\begin{aligned} Y'_{HMq} &= Y'_{Hv}\,v' + Y'_{Hr}\,r', \\ N'_{HMq} &= N'_{Hv}\,v' + N'_{Hr}\,r'. \end{aligned} \tag{2.94}$$

It is reasonable to introduce the following additional dimensionless parameters:

– the dimensionless longitudinal coordinate $x' \stackrel{d}{=} x/L$;

– the dimensionless sectional added mass coefficient

$$\mu'_{yy} \stackrel{d}{=} \frac{2\mu_{yy}}{\rho\pi T^2(x)}, \tag{2.95}$$

where $T(x)$ is the local draught and the denominator is the added mass of a doubled elliptic cross section;

– the dimensionless local draught $T'(x) \stackrel{d}{=} T(x)/T$ (usually $T \equiv T(0)$).

Linear manoeuvring derivatives are then represented as

$$\begin{aligned} Y'_{Hv} &= \frac{\pi k_H}{2}\left[\int\limits_{-\frac{1}{2}}^{\frac{1}{2}} \lambda(x')\frac{\partial}{\partial x'}[\mu'_{yy}(x')T'^2(x')]\,\mathrm{d}x'\right], \\ Y'_{Hr} &= \frac{\pi k_H}{2}\left[\int\limits_{-\frac{1}{2}}^{\frac{1}{2}} \mu'_{yy}(x')T'^2(x')\,\mathrm{d}x' + \int\limits_{-\frac{1}{2}}^{\frac{1}{2}} x'\lambda(x')\frac{\partial}{\partial x'}[\mu'_{yy}(x')T'^2(x')]\,\mathrm{d}x'\right], \\ N'_{Hv} &= \frac{\pi k_H}{2}\left[\int\limits_{-\frac{1}{2}}^{\frac{1}{2}} x'\lambda(x')\frac{\partial}{\partial x'}[\mu'_{yy}(x')T'^2(x')]\,\mathrm{d}x'\right], \\ N'_{Hr} &= \frac{\pi k_H}{2}\left[\int\limits_{-\frac{1}{2}}^{\frac{1}{2}} x'\mu'_{yy}(x')T'^2(x')\,\mathrm{d}x' + \int\limits_{-\frac{1}{2}}^{\frac{1}{2}} x'^2\lambda(x')\frac{\partial}{\partial x'}[\mu'_{yy}(x')T'^2(x')]\,\mathrm{d}x'\right]. \end{aligned} \tag{2.96}$$

The equations (2.96) can be used for practical estimation of the linear manoeuvring derivatives. Sometimes, it can be desirable to transform the integrals containing $\frac{\partial}{\partial x'}[\mu'_{yy}(x')T'^2(x')]$ through integrations by parts in such a way that the derivatives be eliminated from the integrands. Introducing some additional corrections like those proposed by Söding [26, P. 181–183] can also somewhat improve the predictions.

However, as was mentioned earlier, the slender-body technique is rarely used for practical calculations but rather for deriving some "canonic" estimates for schematized hull forms as is demonstrated below.

The theory above was developed for the zero-Froude-number assumption i.e. no wavemaking effects can be estimated in this way. This can be a limitation especially when considering forces on fast displacement ships operating at Froude numbers up to 0.5. Several attempts to create a generalized theory of the slender body or of the small-aspect-ratio wing moving with drift and yaw near the free surface or intersecting it have been undertaken but without major success. Remaining as crude as the classic Munk theory, those theories loose, however, all its simplicity. Moreover, it was discovered that the velocity dependent sinkage and trim are more influencing the hull forces than the wave making per se.

Canonic values of linear hydrodynamic derivatives Let us make the following assumptions about the hull shape:

1. All the cross sections are elliptic (the ship's local breadth, however, can vary and even reach the zero value).
2. The hull has no trim and the centerplane is perfectly rectangular.

The loading function is then

$$\mu'_{yy}(x')T'^2(x') = \begin{cases} 1 & \text{at} \quad x' \in (-\frac{1}{2}, \frac{1}{2}) \\ 0 & \text{at} \quad x' \notin (-\frac{1}{2}, \frac{1}{2}) \end{cases} \tag{2.97}$$

and its derivative is

$$\frac{\partial}{\partial x'}[\mu'_{yy}(x')T'^2(x')] = \delta(x' + \frac{1}{2}) - \delta(x' - \frac{1}{2}), \tag{2.98}$$

where $\delta()$ is the Dirac δ-function.

The δ-functions emerged above are located at the very extremities but still **inside** the hull as the rectangular centre plane should be interpreted as a limiting configuration resulting from uprighting the inclined stem and stern lines at a fixed waterplane length. It is evident that in this case the viscosity correction function $\lambda(x')$ must only remove the aft δ-function i.e.

$$\lambda(x')\frac{\partial}{\partial x'}[\mu'_{yy}(x')T'^2(x')] = -\delta(x' - \frac{1}{2}). \tag{2.99}$$

Substituting eq. (2.97) and eq. (2.98) into eq. (2.96) yields after simple evaluations

$$Y'_{Hv} = -\frac{\pi k_H}{2}; \quad Y'_{Hr} = \frac{\pi k_H}{4}; \quad N'_{Hv} = -\frac{\pi k_H}{4}; \quad N'_{Hr} = -\frac{\pi k_H}{8}. \tag{2.100}$$

These values are also valid for a thin very low aspect ratio wing (the Jones theory) and they can be alternatively obtained from the lifting surface theory.

It is interesting to check where the transverse force is applied. In the pure sway case:

$$x'_v = \frac{N'_{Hv}}{Y'_{Hv}} = +\frac{1}{2} \tag{2.101}$$

and in the case of pure yaw

$$x'_r = \frac{N'_{Hr}}{Y'_{Hr}} = -\frac{1}{2}. \tag{2.102}$$

It means that in the considered schematic case, the force caused by the sway (drift) is concentrated near the stem of the ship while the force produced by the rotation (yaw) is located at the stern. It also means that once some small drift angle appears (for instance, due to the rudder action), the resulting sway force on the hull will act increasing that initial drift angle—that is how the turn starts. But at the same time, the ship starts rotating and the force caused by rotation will produce a counteracting moment limiting the yawing rate or, in other words, "damping" the yaw motion. That is why, the rotational forces and moments are also called *damping forces*[18].

Besides the case of the rectangular centerplane, some other simple cases can be treated analytically. For instance, let us consider the case of a trimmed hull with elliptic cross sections. As the trim angle is always small, it is possible to assume that the bow and stern lines remain approximately vertical. Then, within the hull's length

$$T'(x') = 1 - \frac{2}{k_H}\theta x' = 1 - \tau x', \tag{2.103}$$

where

$$\tau \stackrel{d}{=} \frac{2(T_{\text{stern}} - T_{\text{bow}})}{T_{\text{stern}} + T_{\text{bow}}} \tag{2.104}$$

is the relative trim. Evidently,

$$\mu'_{yy}(x')T'^2(x') = \begin{cases} 1 - 2\tau x' + \tau^2 x'^2 & \text{at} \quad x' \in (-\frac{1}{2}, \frac{1}{2}) \\ 0 & \text{at} \quad x' \notin (-\frac{1}{2}, \frac{1}{2}) \end{cases} \tag{2.105}$$

and

$$\frac{\partial}{\partial x'}[\mu'_{yy}(x')T'^2(x')] = -2\tau + 2\tau^2\, x' + (1 + \frac{\tau}{2})^2\, \delta(x' + \frac{1}{2}) - (1 - \frac{\tau}{2})^2\, \delta(x' - \frac{1}{2}). \tag{2.106}$$

If the correction function $\lambda(x')$ is taken the same as in the previous case (i.e as the aft delta-function remover), the resulting formulae for the hydrodynamic derivatives will be:

$$\begin{aligned} Y'_{Hv} &= -\frac{\pi k_H}{2}\,(1 + \tau + \frac{1}{4}\tau^2), \\ Y'_{Hr} &= \frac{\pi k_H}{4}\,(1 + \tau + \frac{1}{4}\tau^2), \\ N'_{Hv} &= -\frac{\pi k_H}{4}\,(1 - \tau - \frac{1}{12}\tau^2), \\ N'_{Hr} &= -\frac{\pi k_H}{8}\,(1 + \frac{1}{3}\tau + \frac{1}{4}\tau^2). \end{aligned} \tag{2.107}$$

[18]It is clear that the term "damping" has somewhat different meaning in manoeuvring as compared to seakeeping.

The nonlinear terms can be neglected in most cases.

Cross-flow forces

The cross-flow concept is based on some analogy between the flow around a cross section of the hull and the transverse flow around cylindrical bodies (see, for instance, Fig. 2.5). Kinematics is assumed to be the same as it was at deriving the Munk forces (Fig. 2.17) but the interpretation of the fluid action is very different. The existence of the longitudinal velocity u is completely neglected and every cross section (or a slice with the thickness $\mathrm{d}x$) is supposed to be subject to the drag produced by the cross flow with the velocity magnitude $|v(x)|$. This drag determines the *cross-flow transverse loads* on the manoeuvring ship hull. As the sections are not streamlined, separation is supposed to occur (this corresponds to existence of the free longitudinal vortices around the ship hull) and the "drag" is expected to be significant.

If the cross-sectional drag coefficient is $C_D(x)$ and the related reference area for the double body slice is $2T(x)\mathrm{d}x$ then the elementary cross-flow transverse force is

$$\mathrm{d}Y_{HCF}(x) = \gamma_{HCF}(x)\,\mathrm{d}x = -C_D(x)\frac{\rho}{2}v^2(x)\ \mathrm{sign}\ v(x)(2T(x))\,\mathrm{d}x \tag{2.108}$$

or the transverse cross-flow load on the underwater hull can be represented as

$$\gamma_{HCF}(x) = -\frac{\rho}{2}\,C_D(x)T(x)\,v(x)|v(x)| = -\frac{\rho}{2}\,C_D(x)T(x)\,(v+xr)|v+xr|. \tag{2.109}$$

The cross-flow force component is then expressed as follows:

$$\begin{aligned} Y_{HCF} &= \int\limits_{-\frac{L}{2}}^{\frac{L}{2}} \gamma_{HCF}(x)\,\mathrm{d}x = -\frac{\rho}{2}\int\limits_{-\frac{L}{2}}^{\frac{L}{2}} C_D(x)T(x)\,(v+xr)|v+xr|\,\mathrm{d}x, \\ N_{HCF} &= \int\limits_{-\frac{L}{2}}^{\frac{L}{2}} x\gamma_{HCF}(x)\mathrm{d}x = -\frac{\rho}{2}\int\limits_{-\frac{L}{2}}^{\frac{L}{2}} xC_D(x)T(x)\,(v+xr)|v+xr|\,\mathrm{d}x. \end{aligned} \tag{2.110}$$

These dimensional equations can be used in all the situations including low and zero speed manoeuvres. However, in the case of moderate manoeuvring it is also possible to operate with the standard dimensionless coefficients:

$$\begin{aligned} Y'_{HCF} &= -\int\limits_{-\frac{1}{2}}^{\frac{1}{2}} C_D(x')T'(x')\,(v'+x'r')|v'+x'r'|\,\mathrm{d}x', \\ N'_{HCF} &= -\int\limits_{-\frac{1}{2}}^{\frac{1}{2}} x'C_D(x')T'(x')\,(v'+x'r')|v'+x'r'|\,\mathrm{d}x'. \end{aligned} \tag{2.111}$$

As the cross-flow theory is heuristic and approximate, it would be inappropriate to import values of C_D from wind-tunnel test databases. Better estimates can be obtained when the

function $C_D(x')$ is defined from the condition of the best fit of the results of manoeuvring captive-model tests. If some parametric approximation of this function is assumed, the formulae (2.111) represent, in fact, some specific regression models. However, there is no evidence of any advantage of these regressions over more common ones at the equal number of parameters. The real value of eq. (2.111) is its capability to provide rough but reasonable predictions of the nonlinear force in the absence of any measurements. Some general guidelines for choosing C_D values are then followed: according to Söding [26, P. 182–183] C_D averaged along the hull varies in most cases from 0.5 to 1.0 (larger values are typical for full or sharp sections). Then, assuming, say, $C_D(x')T'(x') \equiv 1$ eq. (2.111) one can use them for fast qualitative estimations. The integrals can be calculated numerically or analytically. The latter results in

$$\begin{aligned}
\int_{-\frac{1}{2}}^{\frac{1}{2}} (v' + x'r')|v' + x'r'|\,\mathrm{d}x' &= \frac{1}{3r'}\left[\left|v' + \frac{r'}{2}\right|^3 - \left|v' - \frac{r'}{2}\right|^3\right], \\
\int_{-\frac{1}{2}}^{\frac{1}{2}} x'^j\,(v' + x'r')|v' + x'r'|\,\mathrm{d}x' &= \frac{1}{2^{j+1}}\left[\left(\frac{v'^2}{1+j} + \frac{r'^2}{4(3+j)}\right)\,\mathrm{Sign}_+\,(v', r', j)\right. \\
&+ \left.\frac{v'r'}{2+j}\,\mathrm{Sign}_-\,(v', r', j)\right], \quad j = 1, 2, \ldots,
\end{aligned} \tag{2.112}$$

where

$$\mathrm{Sign}_\pm\,(x, y, j) = \mathrm{sign}\,(x + \frac{y}{2}) \pm (-1)^j\,\mathrm{sign}\,(x - \frac{y}{2}). \tag{2.113}$$

Pay attention that the result of the integration at $j = 0$ is neither polynomial, nor quasi-polynomial, but rather a sort of rational function!

2.3.5 Methods Based on Serial Model Tests

Considerable cost of captive model tests makes unrealistic conducting them every time hydrodynamic characteristics of ship hulls are required. Definitely, it cannot be done at all when some of the parameters of hull form are not yet fixed. Systematic series of hull shapes are a common tool for circumventing such difficulties in ship hydrodynamics, especially in ship resistance, where many hull form series have been tested in course of decades supplying sufficient information for predicting the ship speed at early design stages. However, the situation is much less favourable in manoeuvring because of several reasons. First, instead of only one residual drag coefficient, it is necessary to estimate a considerable number of manoeuvring derivatives and, second, the influence of the hull shape parameters can be more complicated and less predictable.

Nevertheless, some methods for estimation of manoeuvring derivatives based on systematic tests have been proposed. One of the most widely known is a method presented by Japanese scientists Inoue et al. [18]. It was later reproduced by many researchers and described in numerous publications including the reference book [7]. This method is supposed to be valid for single-screw merchant vessels with more or less usual particulars and with the block coefficient C_B varying from 0.6 to 0.8. The regression models for the sway force and yaw moment coefficient are here taken in the form[19]:

$$\begin{aligned} Y'_q(v',r') &= Y'_v\,v' + Y'_r\,r' + Y'_{v|v|}\,v'|v'| + Y'_{v|r|}\,v'|r'| + Y'_{r|r|}\,r'|r'|, \\ N'_q(v',r',\varphi) &= N'_v\,v' + N'_r\,r' + N'_{vvr}\,v'^2r' + N'_{vrr}\,v'r'^2 + N'_{r|r|}\,r'|r'| \\ &+ N'_\varphi\,\varphi + N'_{v|\varphi|}\,v'|\varphi| + N'_{r|\varphi|}\,r'|\varphi|. \end{aligned} \tag{2.114}$$

Regressions of linear derivatives on the form parameters were proposed in [18]. They are supposed to be affected by the relative ship trim τ and can be represented as

$$\begin{aligned} Y'_v &= Y'_{v0}\,(1+b_1\tau), \\ Y'_r &= Y'_{r0}\,(1+b_2\tau), \\ N'_v &= N'_{v0}\,(1+b_3\tau), \\ N'_r &= N'_{r0}\,(1+b_4\tau), \end{aligned} \tag{2.115}$$

where: $b_1 = \frac{2}{3}$, $b_2 = \frac{4}{5}$, $b_3 = -\frac{0.27N'_{v0}}{Y'_{v0}}$, $b_4 = 0.3$.

The zero-trim linear derivatives depend on the double-hull aspect ratio k_H and on the special fullness parameter $C_{BL} = \frac{C_B B}{L}$, where C_B is the block coefficient and B is the ship width. It can be clearly seen that the slender body theory was involved in devising the regression structures although significant empiric corrections were introduced as well:

$$\begin{aligned} Y'_{v0} &= -\frac{\pi k_H}{2} - 1.4\,C_{BL}, \\ Y'_{r0} &= \frac{\pi k_H}{4}, \\ N'_{v0} &= -k_H, \\ N'_{r0} &= -0.54\,k_H + k_H^2. \end{aligned} \tag{2.116}$$

[19] The surge force and the roll moment are treated there in a somewhat different way which will be explained later.

Two additional form parameters are necessary to approximate nonlinear derivatives:

$$\begin{aligned} C_{BT} &= (1 - C_B)\,\frac{T}{B}, \\ D_{BT} &= C_B\,\frac{T}{B}. \end{aligned} \tag{2.117}$$

The following approximations valid for $C_{BL} \in [0.0615, 0.2]$, $C_{BT} \in [0.02, 0.15]$, $D_{BT} \in [0.078, 0.4]$ were obtained by the author from the fairing curves presented in [18]:

$$\begin{aligned} Y'_{v|v|} &= -6.65\,C_{BT} + 0.0735, \\ Y'_{v|r|} &= 1.73\,C_{BT} - 0.443, \\ Y'_{r|r|} &= -0.5\,C_{BT}, \\ N'_{vvr} &= \begin{cases} 23.7\,C_{BL} - 2.23 & \text{at} \quad C_{BL} \in [0.071,\, 0.088] \\ -91.5\,C_{BL}^2 + 21.15\,C_{BL} - 1.294 & \text{at} \quad C_{BL} \in (0.088,\, 0.143] \\ -2.88\,C_{BL} + 0.268 & \text{at} \quad C_{BL} \in (0.143,\, 0.2], \end{cases} \\ N'_{vrr} &= 0.43\,D_{BT} - 0.0637, \\ N'_{r|r|} &= \begin{cases} 0.675\,C_{BL} - 0.1015 & \text{at} \quad C_{BL} \in [0.0615,\, 0.113] \\ -6.9\,(C_{BL} - 0.156)^2 - 0.112 & \text{at} \quad C_{BL} \in (0.113,\, 0.2]. \end{cases} \end{aligned} \tag{2.118}$$

Rough averaged estimates were obtained for the roll-dependent part of the yaw moment:

$$\begin{aligned} N'_{\varphi} &= -0.0076, \\ N'_{v|\varphi|} &= 1.72\,N'_v, \\ N'_{r|\varphi|} &= -2.35\,N'_r. \end{aligned} \tag{2.119}$$

In some cases, Inoue's approximations can provide reasonable and even good estimates of manoeuvring derivatives but very large errors are also possible especially on full vessels. Experimental studies aimed at creation of more accurate methods based on extended series of models involving more form parameters are being undertaken but, due to sensitivity of the hull forces to slight changes of the body lines, this task is unlikely to be accomplished in the nearest future.

2.3.6 Forces Produced by Propellers and Rudders

General Remarks

As was already mentioned, all manoeuvring relevant hydrodynamic forces acting on rudders and propellers are, in a very good approximation, quasi-steady forces and do only depend on the instantaneous velocities. However, accurate computations of the forces present a very tough problem as both devices work, in general, inside the non-homogeneous and curled flow field after the ship hull. For the screw propeller it will be a more or less standard prediction problem with an additional complication due to oblique inflow. As result, not only the thrust and torque but also the side force are expected as response components. As to the rudder, the problem of estimating the force and the stock moment is basically that of the wing hydrodynamics yet with two complicating factors. The first complication is caused by the hull influence and the second one occurs if the rudder works in the propeller race that is very common for merchant ships. Consistent computational methods aiming at rigourous computation of the flow around the rudder must be based on the RANSE as the oncoming flow very rarely can be treated as potential. One of the first attempts of attacking this problem is described in [39]. However, in practice, simplified mathematical models based on experimental data for propellers and rudders are still preferred and they will be described in this subsection.

Basics of Propeller Hydrodynamics in Manoeuvring motion

Inflow kinematics. According to the simplified approach, the screw propeller is supposed to work inside some equivalent uniform oblique flow depending on the propeller's instantaneous velocity with respect to the undisturbed water

$$\mathbf{V}_P = u_P\,\mathbf{e_x} + v_P\,\mathbf{e_y}, \tag{2.120}$$

where its components are:

$$u_P = u, \tag{2.121}$$
$$v_P = v + x_P r \tag{2.122}$$

with x_P being the propeller abscissa in the body axes[20]. The propeller drift angle β_P can be determined with the help of eq. (2.28).

However, due to the hull's influence, the propeller apparent velocity

$$\mathbf{V}_{PA} = u_{PA}\,\mathbf{e_x} + v_{PA}\,\mathbf{e_y} \tag{2.123}$$

will be different from V_P by both its magnitude and direction. The following relations are usually assumed:

$$u_{PA} = u\,(1 - w_P), \tag{2.124}$$
$$v_{PA} = \kappa_{Pv}\,v + \kappa_{Pr}\,x_P\,r, \tag{2.125}$$

[20]It is assumed in eq. (2.121) that the propeller's lateral offset is negligible even if the propeller is not located in the centerplane. This assumption is less accurate for catamarans.

where w_P is the usual effective propeller wake fraction as defined in ship propulsion [47] and the parameters κ_{Pv} and κ_{Pr} are called the *flow straightening factors*.

Literature on the ship propulsion contains many data on the wake fraction w_{P0} for the straight motion but in general w_P was found to depend on the local drift angle β_P. According to Inoue et al. [19]

$$w_P(\beta_P) = w_{P0}\, e^{-4\beta_P^2}. \tag{2.126}$$

Data on the propeller straightening factors are less available and in most cases they are assumed to be the same as corresponding factors for the rudder which will be presented later.

Thrust and torque estimation. The effective thrust T_E (which is in fact an alias for the longitudinal propeller force X_P as present in the equation of motion) can be represented in the standard way:

$$T_E \equiv X_P = T_P\,(1 - t_P), \tag{2.127}$$

where T_P is the open water thrust and t_P is the thrust-deduction fraction [47]. The former is weakly affected by the transverse velocity and in the moderate manoeuvring case can be represented as

$$T_P = \rho n^2 D_P^4\, K_T(J), \tag{2.128}$$

where n is the propeller rotation rate (in revolutions per second), D_P — the propeller diametre, K_T — the thrust coefficient, and J is the advance coefficient defined as

$$J = \frac{u_{PA}}{nD_P}. \tag{2.129}$$

The propeller torque Q_P is expressed similarly to eq. (2.128):

$$Q_P = -\rho n^2 D_P^5\, K_Q(J), \tag{2.130}$$

where the minus sign is often dropped in the ship propulsion but it is important for correct coupling with the engine.

The propeller characteristic curves $K_{T,Q}(J)$ can be obtained experimentally and approximated with multivariate algebraic polynomials (additional factors are: the pitch ratio, the area ratio, and the number of blades; an example of such polynomials for the popular Wageningen B-screw series can be found in [47, P. 191]) .

In the case of arbitrary manoeuvres when both the longitudinal velocity and the rotation rate can become zero and change their signs, it is necessary to apply another representations for the thrust and torque based on trigonometric approximations. A simple mathematical model of this kind was proposed by Oltmann and Sharma [30]. The thrust and torque are then represented as

$$T_P = \frac{\rho}{2} A_d\, C_T(\gamma_B)\, V_B^2, \tag{2.131}$$

$$Q_P = -\frac{\rho}{2} A_d D_P\, C_Q(\gamma_B)\, V_B^2, \tag{2.132}$$

where $A_d = \frac{\pi D_P^2}{4}$ is the propeller disk area, C_T and C_Q are the generalized thrust and torque coefficients represented as

$$C_{T,Q} = \begin{cases} C_{T,Q0} + C^c_{T,Q}\cos\gamma_B + C^s_{T,Q}\sin\gamma_B & \text{at } \cos\gamma_B \geq 0.9336 \\ C^{cc}_{T,Q}|\cos\gamma_B|\cos\gamma_B + C^{ss}_{T,Q}|\sin\gamma_B|\sin\gamma_B & \text{otherwise} \end{cases}, \tag{2.133}$$

where γ_B is the effective blade advance angle, V_B is the effective total blade velocity, and $C_{T0},\ldots,C^{ss}_Q$ are constant regression coefficients.

When the propeller's axial velocity with respect to water u_{PA} and its rotation rate n are known, the blade's total velocity will be

$$V_B = \sqrt{u_{PA}^2 + V_{CP}^2}, \tag{2.134}$$

where the effective circumferential blade's velocity V_{CP} is

$$V_{CP} = 0.7\pi\, D_P\, n \tag{2.135}$$

and the sine and cosine functions of advance angle can be expressed as

$$\sin\gamma_B = \frac{u_{PA}}{V_B}; \qquad \cos\gamma_B = \frac{V_{CP}}{V_B}. \tag{2.136}$$

The published values of 10 regression coefficients in (2.133) (see [30]) are only valid for a 5-blade propeller with a pitch ratio value 0.745 and with the expanded area ratio equal to 0.6. Somewhat different data for C_T and C_Q for a number of various propellers can be found in [4] and [22]. The used regression models are the truncated Fourier series:

$$C_T = 0.01\left[A_0^T + \sum_{i=1}^{30}\left(A_i^T\cos i\gamma_B + B_i^T\sin i\gamma_B\right)\right], \tag{2.137}$$

$$C_Q = -0.001\left[A_0^Q + \sum_{i=1}^{30}\left(A_i^Q\cos i\gamma_B + B_i^Q\sin i\gamma_B\right)\right]. \tag{2.138}$$

and the database for the regression coefficients $\{A_i^{T,Q}\}_{i=0}^{30}$ and $\{B_i^{T,Q}\}_{i=1}^{30}$ can be found in [4]. This database does not cover e.g. all B-series propellers but Roddy et al. [33] have developed a neural network extrapolation procedure which makes possible obtaining reasonable 4-quadrant responses for propellers with arbitrary number of blades, pitch ratio and disk area ratio.

Transverse force and yaw moment. In the general case, the propeller is working in oblique flow with a transverse velocity component v_P. Then, analyzing the flow over a blade element at its upper and lower positions, one can figure out that at $v_P > 0$ and with the clockwise rotating propeller the attack angle of the blade element will be greater when the blade is at its lowest position and is moving against the sidewash stream. Both drag and lift will then be larger which will result, first, in some downward shift of the thrust action line and, second—in some resultant force directed collinearly with the sidewash velocity. The former effect is trimming the ship, insignificantly in fact, but the latter may be quite sensible on high-speed ships with

large diametre screw propellers. The mentioned kinematic analysis can be used as basis for a method of estimating the propeller transverse force which is sometimes called the *Glauert force* and it is clear that its direction does not depend on the propeller rotation direction. Empirical data can also be used. However, in many cases the Glauert force appears to be negligible and we shall assume in the following that

$$Y_P = N_P = 0 \tag{2.139}$$

in ahead run.

When the ship is reversing i.e. the propeller produces a jet directed ahead onto the ship's stern, another kind of the transverse force emerges on single and triple screw ships. This kind of force is not applied to the propeller itself but is created by the pressure fields on the afterbody surface. If the propeller rotates counterclockwise in reversing, the force will be directed to the portside turning the ship to the starboard. This phenomenon is often called the Hovgaard effect and the thus generated force is called the Hovgaard force. This force cannot be neglected in simulation of hard manoeuvres (by the way, it produces the effect shown on Fig. 1.16) and is normally estimated from model tests (see [26, P. 51]). As first approximation it can be recommended to estimate this side force' absolute value as $|Y_P| = \kappa_H |X_P|$, where κ_H is the empiric Hovgaard coefficient ($\kappa_H = 0.35$ can be assumed in absence of other data but appropriate tuning is recommended whenever possible), its sign must be chosen as minus for the propeller with right rotation and plus in the opposite case. Of course, the Hovgaard force is zero at $X_P > 0$.

Wake velocity distribution. The propeller action is not limited by the forces and moments it produces directly or through inducing additional pressures on the ship's hull. If the rudder is located fully or partly in the propeller race, of primary importance are also velocities induced by the propeller. In practical schemes used in ship manoeuvring the following rather crude assumptions concerning the slipstream velocity field are usually made:

1. Only axial induced velocities are relevant (some remarks on the tangential velocities are made in the next paragraph but the radial velocities are completely ignored).
2. The induced axial velocity is supposed to be uniformly distributed over the jet's sectional area.
3. The ideal propeller (actuator disk) theory is supposed to be applicable.

These above were common features of most practical models for the propeller slipstream but there are slight differences in various specific implementations, sometimes mostly apparent. The model described below is compilation and generalization of several published schemes. It is relatively physically transparent and also has an advantage of being applicable to arbitrary (four-quadrant) flow regimes.

Let A_0 be the area of the thin actuator disk and let it be placed into the uniform flow with the velocity $\mathbf{V}_A$ directed along the normal to the disk. The disk is somehow generating

a uniform jet with the straight axis continuing downstream to infinity in the same direction as $\mathbf{v}_A$. The jet velocity at infinity $\mathbf{u}_\infty$ is collinear to $\mathbf{V}_A$ and its signed module is

$$u_\infty = V_A + w_{a\infty} = u_{PA} + w_{a\infty}, \tag{2.140}$$

where all the terms are always supposed to be of the same sign, $u_{PA} \equiv v_A$ is, as before, the surge velocity of the propeller with respect to water i.e. with account to the wake fraction, and $w_{a\infty}$ is the so-called axial induced velocity at infinity.

According to the classic actuator disk theory,

$$w_{a\infty} = u_{PA}(\sqrt{1 + C_{TA}} - 1), \tag{2.141}$$

where

$$C_{TA} = \frac{2|T|}{\rho u_{PA}^2 A_0} \tag{2.142}$$

is the standard loading coefficient. Substituting eq. (2.142) and eq. (2.141) into eq. (2.140) it is possible to get the formula

$$u_\infty = \sqrt{u_{PA}^2 + w_{a0\infty}^2}, \tag{2.143}$$

where

$$w_{a0\infty}^2 = \frac{2T}{\rho A_0} \tag{2.144}$$

is the squared axial induced velocity at infinity in bollard regime. Then the actual axial induced velocity at infinity is

$$w_{a\infty} = u_\infty - u_{PA}. \tag{2.145}$$

In general, the induced axial velocity w_a is varying along the jet. Theoretically, according to the actuator disk theory, it reaches its maximum value $w_{a\infty}$ at infinity downstream and its value in the actuator disk $w_{a0} = \frac{1}{2} w_{a\infty}$. The jet's sectional area is varying inversely due to the mass conservation law, so the theoretical slipstream section area at infinity $A_\infty = \frac{1}{2} A_0$. Of course, this idealized picture is not conserved in real fluid: while at a distance up to 2–3 propeller diametres the jet is really contracting, but further its dissipation starts. this involves additional fluid in to the slipstream but the velocity drops acordingly and at infinity no induced velocity can be detected and all kinetic energy of the slipstream finally ends transformed into thermal form which, in course of time also dissipates. However, as the rudders are located relatively close to screw propellers, the idealized model of infinite contracting propeller race is considered fully applicable for estimating its influence on the rudder forces.

The dimensionless propeller–rudder distance parameter can be defined as

$$\bar{x} = \frac{2(x_P - x_R)}{D_P} \operatorname{sign} T. \tag{2.146}$$

It is clear that this parameter is positive when (1) the rudder is located behind the propeller and (2) the propeller is working ahead, that is producing positive thrust.

The axial induced velocity at arbitrary distance from the propeller can be represented as

$$w_a(\bar{x}) = \frac{1}{2} \kappa_w k_w(\bar{x}) w_{a\infty}, \tag{2.147}$$

where κ_w is the empiric correction factor which is often set equal to 1 although, for instance, Kose [21] recommended 0.68 for single-screw ships, $k_w(\bar{x})$ is the velocity change function which must tend to 2 as $\bar{x} \to \infty$ and must be equal to 1 at $\bar{x} = 0$. This function can be obtained approximating measured values or from a simple vortex theory of the screw propeller with infinite number of blades. A suitable explicit approximation was suggested by Fedyaevsky and Sobolev [14] and, with appropriate generalizations, it can be represented as

$$k_w(\bar{x}) = \left[\left(1 + \frac{\bar{x}}{\sqrt{1+\bar{x}^2}}\right)\kappa(T)\right] \text{ sign } T, \tag{2.148}$$

where

$$\kappa(T) = \begin{cases} 1.0 & \text{at} \quad \bar{x}T \geq 0, \\ 0.7 & \text{at} \quad \bar{x}T < 0 \end{cases} \tag{2.149}$$

is another empiric correction factor. It is introduced because the formula (2.148) is qualitatively valid not only behind but also ahead of the propeller. Practically this situation occurs when the rudder is located behind the propeller working astern i.e. in the reversed mode. There is no jet from the suction side of the propeller disk which can then be approximately represented as disk of sinks inducing velocities in all the space except for the jet. These velocities will, obviously, vanish at infinity which is captured by eq. (2.148) but introduction of an additional empiric correction factor was found reasonable.

Finally, the equivalent velocity of surge u_{RP} for the rudder (or its part) immersed in the slipstream or in the suction stream ahead of the propeller will always be

$$u_{RP} = u_{PA} + w_a. \tag{2.150}$$

As to the corresponding sway velocity it can be assumed to be inaffected by the propeller in the suction zone i.e. ahead of the propeller ($\bar{x} < 0$)

$$v_{RP} = v_{RA}. \tag{2.151}$$

The latter formula is often applied also to the rudder inside the jet assuming that the jet is deflected by the oblique flow. However, the experiments show that in the propeller's vicinity the jet is not affected by the outer flow and is always directed along the propeller axis deflecting only gradually and the full deflection is only reached at some distance from the propeller's disk. As the tangent to the jet is also co-axial with the propeller axis near the disk, one can assume the following dependence for the rudder effective sway velocity for $\bar{x} \geq 0$:

$$v_{RP} = \kappa_v(\bar{x})\, v_{RA} = \frac{\bar{x}^2}{a + \bar{x}^2}\, v_{RA}, \tag{2.152}$$

where a is the empiric constant. Then, the magnitude of the effective rudder velocity in the propeller slipstream V_{RP} is defined from the following relation:

$$V_{RP}^2 = u_{RP}^2 + v_{RP}^2. \tag{2.153}$$

As the slipstream velocity is growing from the propeller disk downstream, its diameter $D_S(\bar{x}$ is decreasing and can be found from the continuity (mass conservation) equation as

$$D_S(\bar{x}) = \sqrt{\frac{u_{RP}(0)}{u_{RP}(\bar{x})}} D_P. \tag{2.154}$$

Information about the slipstream radius cane be used to determine the rudder's washed area behind the propeller. When the rudder is located upstream of the propeller (as typically happens in the reversed regime), the whole rudder area should be considered as washed by the flow to the disk of sinks modelling the propeller in this situation.

However, the analysis above is only valid for the perfect fluid. In the real fluid, the effect of the jet's contraction will be accompanied with the effect of turbulent mixing and expansion of the slipstream. Söding [26] suggested the following empiric correction ΔD_S to the slipstream's diameter as function of the dimensional distance between the propeller and rudder:

$$\Delta D_S(|x_P - x_R|) = 0.3\,|x_P - x_R|\frac{u_{RP}(\bar{x}) - u_{PA}}{u_{RP}(\bar{x}) + u_{PA}}. \tag{2.155}$$

Then, the corrected average slipstream velocity $u_{RP}^{\rm cor}$ can be estimated through application of the momentum conservation principle to the axial induced velocity:

$$u_{RP}^{\rm cor}(\bar{x}) = (u_{RP}(\bar{x}) - u_{PA})\left(\frac{D_S(\bar{x})}{D_S(\bar{x}) + \Delta D_S}\right)^2 + u_{PA}. \tag{2.156}$$

Almost all of the existing practical methods for estimating rudder forces in the propeller race are based on the equations written above. However, the appearance can be different as, for instance, the thrust loading coefficient can be expressed through the thrust coefficient K_T, and the advance J or the slip ratio

$$s = 1 - \frac{J}{P/D_P}. \tag{2.157}$$

Asymmetric effects on single-screw ships. On surface displacement ships, any propeller works in a non-uniform wake with transverse velocity components being present. In most cases the transverse velocity is directed upwards and causes the thrust's shift to the starboard for a clockwise rotating propeller (the ship will then tend to turn to the portside). However, at the same time, the local wake fraction will be greater for the upper part of the propeller disk and this will create a transverse force directed to the portside and turning the ship astarboard. The resulting effect is uncertain as it depends on the actual stern configuration and propeller arrangement. Moreover, there are additional sources of the asymmetry stemming from the propeller—rudder interaction which will be commented later. However, most single-screw ships tend to turn better to the starboard and the principal part of the asymmetry is supposed to be accounted for through the introduction of some non-zero *neutral* or *balance* rudder angle δ_{R0}. On twin-screw ships, all these effects will be mutually compensated as the propellers rotate in opposite directions but triple-screw vessels will again show some asymmetry.

Elementary Hydrodynamics of Rudders

Main geometric parameters. The most important geometric parameter of a ship rudder is its lateral area A_R which in most cases constitutes between 1 and 4 percent of the area LT (from many viewpoints it is desirable to have as small rudder as possible; larger relative

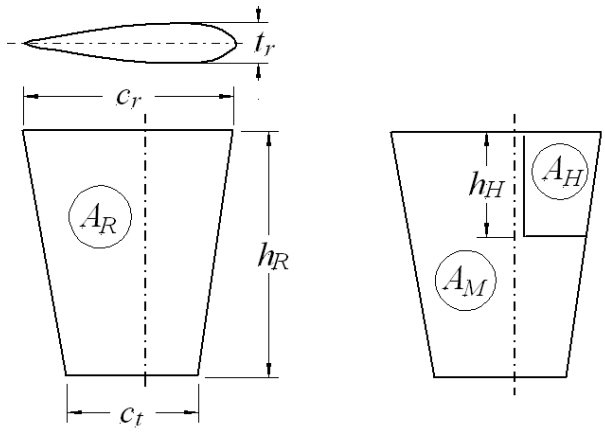

Figure 2.19: Rudders Geometric Parameters (vertical dash-dot lines represent stock axes)

area is typical for naval ships with the rudder located outside of the propellers' slipstreams) (Fig. 2.19). The rudder height h_R is in fact its span in terms of wing particulars (see Fig. 2.19). Many rudders have a trapezoidal form with the root chord c_r is and the tip[21] chord c_t. Then, the mean chord $c = \frac{1}{2}(b_r + b_t)$ and the rudder's aspect ratio is

$$k_R = \frac{h_R^2}{A_R}. \tag{2.158}$$

Most rudders have symmetric profiles NACA-0015, 0018, 0021 or similar (see [7] and [26] for more detailed information). The profile's thickness t_R must be large enough to accommodate the stock but is also influenced by hydrodynamic considerations.

In the case of the horn rudders (see (Fig. 2.19), right) several additional parameters appear:

- the movable part area A_M;
- the horn area A_H — it is clear that

$$A_R = A_M + A_H; \tag{2.159}$$

- the horn height h_H;
- the horn chord c_H .

The following dimensionless characteristics are also used:

- the relative movable area $A'_M = A_M/A_R$;
- the relative horn area $A'_H = A_H/A_R$;
- the relative horn height $h'_H = h_H/h_R$

(it is clear that in the case when $h'_H = 1$ we obtain a particular case when the horn is transformed into the rudder post).

[21] The ends of the rudder shown on Fig. 2.19 are both horizontal but in reality they can be inclined. However, for calculations it is usually convenient to replace them with horizontal edges conserving the rudder's area.

Kinematics and forces decomposition. During the manoeuvring motion, the deflected ship rudder produces, first, some **pure** rudder force $\mathbf{F}_{R0}$, which can be approximately assumed to be applied at some point on the stock axis[22], and, also—some *stock moment* (torque) Q_R, and some *stock bending moment* M_B. Although the information on the mentioned moments is very important for designing the steering gear and for the strength calculations, the ship manoeuvring motion depends just on the force $\mathbf{F}_{R0}$ and the following considerations will be concentrated on it.

Let us assume that the rudder is deflected by the angle δ_R and its instantaneous velocity with respect to the **water surrounding the rudder** is $\mathbf{V}_{RA}$ (Fig. 2.20). This velocity depends

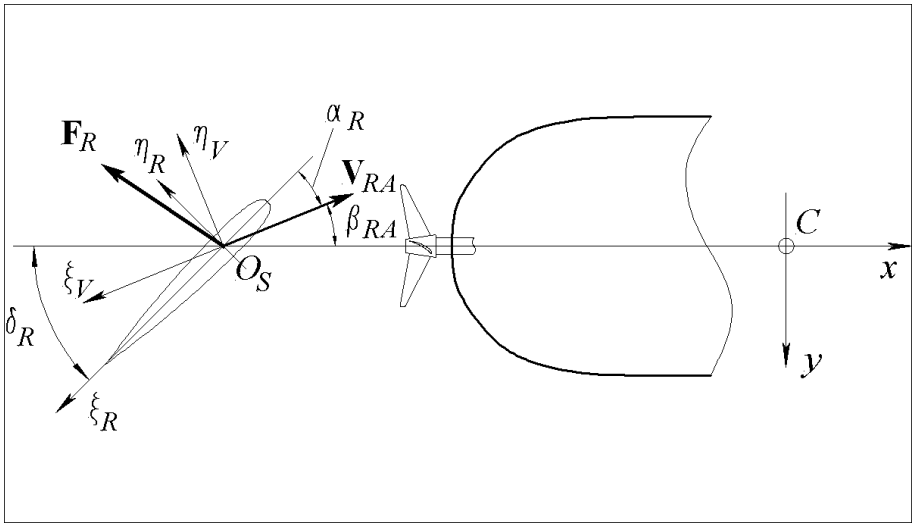

Figure 2.20: Rudder-Based Frames of Reference and Kinematic Parameters

on the rudder velocity with respect to the **undisturbed still water** $\mathbf{V}_R$ and also on velocities induced by the hull and by the propeller. The latter effect will be studied later and now we only suppose that $\mathbf{V}_{RA}$ is known and can be decomposed in the ship-fixed axes as

$$\mathbf{V}_{RA} = u_{RA}\,\mathbf{e_x} + v_{RA}\,\mathbf{e_y}. \tag{2.160}$$

Then, the effective rudder drift (sidewash) angle β_{RA} is defined by the equations

$$\begin{aligned} \cos\beta_{RA} &= \frac{u_{RA}}{V_{RA}} \\ \sin\beta_{RA} &= -\frac{v_{RA}}{V_{RA}}. \end{aligned} \tag{2.161}$$

In order to link the rudder hydrodynamic characteristics represented in the standard wing hydrodynamics way, with the rudder forces as they appear in the equations of motion, two rudder-blade-related additional coordinate systems must be introduced:

– the rudder-fixed axes $O_s\xi_R\eta_R$ and

[22]Of course, actually the force on the rudder blade is applied at the centre of pressure but the resulting error in the yaw moment will be insignificant.

– the rudder velocity axes $O_s\xi_V\eta_V$.

The both systems have a common origin O_s lying on the stock axis and the axes' directions are clear from Fig. 2.20. The decompositions of the rudder force in the body axes and these new frames are:

$$\mathbf{F}_{R0} = X_{R0}\mathbf{e_x} + Y_{R0}\mathbf{e_y} = F_T\mathbf{e}_{R\xi} + F_N\mathbf{e}_{R\eta} = F_D\mathbf{e}_{V\xi} + F_L\mathbf{e}_{V\eta}, \tag{2.162}$$

where the components' names are: F_T is the rudder tangential force, F_N — the rudder normal force, F_D — the rudder drag, and F_L is the rudder lift.

The body-axes projections of the pure rudder force can be expressed either through lift and drag

$$\begin{aligned} X_{R0} &= -F_D\,\cos\beta_{RA} - F_L\,\sin\beta_{RA} \\ Y_{R0} &= F_D\,\sin\beta_{RA} - F_L\,\cos\beta_{RA} \end{aligned} \tag{2.163}$$

or through normal and tangential components

$$\begin{aligned} X_{R0} &= -F_T\,\cos\delta_R - F_N\,\sin\delta_R \\ Y_{R0} &= F_T\,\sin\delta_R - F_N\,\cos\delta_R. \end{aligned} \tag{2.164}$$

The latter representation can be simplified because the tangential component is always small by its absolute magnitude compared to either the rudder normal force, or—to the total longitudinal force on the ship. Then,

$$\begin{aligned} X_{R0} &= -F_N\sin\delta_R, \\ Y_{R0} &= -F_N\cos\delta_R. \end{aligned} \tag{2.165}$$

No similar simplification can be applied to eq. (2.163) as the drag contribution may be comparable to that of the lift.

The pure rudder yawing moment can always be represented as

$$N_{R0} = x_R Y_{R0} \tag{2.166}$$

as the contribution of the longitudinal projection is negligible for any monohull.

The total rudder force $\mathbf{F}_R = X_R\mathbf{e_x} + Y_R\mathbf{e_y}$ can be represented like this:

$$\mathbf{F}_R = \mathbf{F}_{R0} + \mathbf{F}_{RH}, \tag{2.167}$$

where $\mathbf{F}_{RH}$ is the rudder–hull interaction force (it is induced on the hull due to the rudder's deflection).

In terms of the vector components we have:

$$\begin{aligned} X_R &= X_{R0}, \\ Y_R &= Y_{R0} + Y_{RH}, \\ N_R &= x_R Y_{R0} + x_{RH} Y_{RH}, \end{aligned} \tag{2.168}$$

where x_{RH} is the abscissa of the interaction transverse force application point and the interaction effect is considered negligible for the longitudinal component. The transverse rudder force and yaw moment can be alternatively represented as

$$\begin{aligned} Y_R &= Y_{R0}\,(1+a_H), \\ N_R &= x_R^* Y_R = (x_{R0} + a_H x_{RH})\,Y_{R0}, \end{aligned} \tag{2.169}$$

where $a_H = Y_{RH}/Y_{R0}$ is the rudder—hull interaction fraction and x_R^* is the effective rudder abscissa which is defined as

$$x_R^* = \frac{x_R Y_{R0} + x_{RH} Y_{RH}}{Y_{R0} + Y_{RH}}. \tag{2.170}$$

Both a_H and x_R^* can be determined experimentally and some general guidelines can be found in the literature. For instance, according to Söding [26, P. 87]

$$\begin{aligned} a_H &= \frac{1}{1 + (4.9\frac{e}{T} + 3\frac{c_R}{T})^2}, \\ x_R^* &= x_R + \frac{0.3T}{\frac{e}{T} + 0.46}, \end{aligned} \tag{2.171}$$

where T is the draught of the ship, e —the mean distance between the front edge of the rudder and the aft end of the hull, c_R — the mean rudder chord. However, such empiric recommendations may vary. For instance, according to Inoue's model [19] $x_R^* \equiv x_R$ and

$$a_H = 0.633 C_B - 0.153. \tag{2.172}$$

Open-water hydrodynamic characteristics of rudders. It follows from the dimensional analysis, as well as from the basic concepts of the wing theory that the pure rudder force components (drag, lift, and normal force) can be expressed like this:

$$\left.\begin{matrix} F_D \\ F_L \\ F_N \end{matrix}\right\} = \left\{\begin{matrix} C_{RD} \\ C_{RL} \\ C_{RN} \end{matrix}\right\} (\alpha_R, k_R, \mathsf{Rn}_R, \mathsf{Fn}_R) \frac{\rho V_{RA}^2}{2} A_R, \tag{2.173}$$

where C_{RD}, C_{RL}, and C_{RN} are respectively: drag, lift, and normal force coefficients; $\mathsf{Rn}_R = \frac{V_R c_R}{\nu}$ is the rudder Reynolds number; $\mathsf{Fn}_R = \frac{V_R}{\sqrt{g c_R}}$ — the rudder Froude number; α_R is the rudder attack angle defined as (see Fig. 2.20)

$$\alpha_R = \delta_R - \beta_{RA}. \tag{2.174}$$

The Strouhal number is not included into the set of arguments of the rudder forces coefficients as its influence is negligible for realistic deflection rates. The Froude number may affect the rudder force if the rudder intersects the water surface or its upper edge is only slightly submerged but such a situation must be avoided because of the aeration danger.

On the other hand, the mentioned arguments list can also be extended. For instance, the force on a horn rudder will depend not only on the attack angle but also directly on the deflection angle as it determines a certain "effective curvature". Also, the proximity of the rudder's root

to the hull can redistribute the spanwise loading and, hence, change the lift. This effect can be accounted for by means of correcting the aspect ratio k_R (according to the mirror image principle it must be doubled when there is no gap between the hull plate and the rudder but in fact the situation is complicated by the presence of the ship's boundary layer). Besides the aspect ratio, some another peculiarities of the rudder geometry can be relevant. The influence of the relationship between the root and the end chord lengths is not so strong but important is whether the tips are square or faired. The hydrodynamic characteristics of rudders depend also on the profiling.

The normal and tangential force coefficients can always be obtained as

$$C_{RN} = C_{RD} \sin \alpha_R + C_{RL} \cos \alpha_R, \tag{2.175}$$

$$C_{RT} = C_{RD} \cos \alpha_R - C_{RL} \sin \alpha_R \tag{2.176}$$

and it is sufficient to have information on the lift and drag.

The most accurate and reliable data on rudder hydrodynamics can be obtained experimentally, mainly from wind tunnel tests. In fact, all ship hydrodynamic centres have substantial databases of measured curves of the lift, drag, and stock moment coefficients for large varieties of rudder shapes. Some extracts from those databases can be found in the reference books [7, P. 294–308] and [26, P. 77–79].

The analysis of those data lead to the following summing-up guidelines and formulae for the approximate estimation of the free-stream hydrodynamic characteristics:

1. In the pre-stall range, i.e. at $|\alpha_R| \le \alpha_s$, the lift and drag coefficients practically do not depend on the Reynolds number and can be approximated as follows (the "quadratic" variant of the first equation can be found in [7, P. 306]):

$$C_{RL} = C^{\alpha}_{RL}\, \alpha_R + C^{\alpha\alpha\alpha}_{RL}\, \alpha_R^3, \tag{2.177}$$

$$C_{RD} = C_{RD0} + \frac{C^2_{RL}}{\pi a k_R}, \tag{2.178}$$

where

$$C^{\alpha}_{RL} = \frac{2\pi a k_R}{\sqrt{k_R^2 + 4} + 2a} \tag{2.179}$$

is the linear lift coefficient slope and a is the empiric correction factor;

$$C^{\alpha\alpha\alpha}_{RL} = \begin{cases} \frac{0.125 + 1.2 \frac{c_t}{c_r}}{k_R} & \text{with faired tips} \\ \frac{0.125 + 2.7 \frac{c_t}{c_r}}{k_R} & \text{with square tips} \end{cases} \tag{2.180}$$

is the nonlinear part's coefficient; C_{RD0} is the profile drag coefficient which is equal to 0.0065 for the NACA-0015 profile.

The correction factor a is in most cases recommended to be set equal to 0.9 [7] but experiment-based values exceeding unity (up to 1.1 [39]) have also been reported.

Another formulae for the rudder lift in the pre-stall region have been proposed. For instance, Söding [39] uses the following approximation:

$$C_{RL} = C_{RL}^{\alpha\prime} \sin\alpha_R + \sin\alpha_R |\sin\alpha_R| \cos\alpha_R, \tag{2.181}$$

where

$$C_{RL}^{\alpha\prime} = \frac{2\pi k_R (k_R + 0.7)}{(k_R + 0.7)^2}. \tag{2.182}$$

As can be seen, here it is assumed $a = 1$, the coefficient at the nonlinear part of the lift coefficient formula is always equal to 1 and although the formula (2.182) looks very different from eq. (2.179), its asymptotic behaviour at small and large k_R is similar and it gives close numerical results.

2. The maximum lift coefficient depends slightly on the aspect ratio having a smooth maximum at approximately $k_R = 1$ but it's dependence on the Reynolds number and on the rudder surface's roughness is substantial what can be seen from Table 2.1[23]. As the

Table 2.1: Typical Values of the Rudder Maximum Lift Coefficient: Reynolds Number's and Roughness' Influence

Rn	$7 \cdot 10^5$	$6 \cdot 10^6$
Smooth	1.08	1.6
Rough	0.86	1.04

roughness of the rudder surface is almost always known with sensible uncertainty, there is no sense in a too fine optimization and the aspect ratio is usually defined from another considerations (required rudder area, arrangement options, stock moment etc.).

3. The stall angle depends strongly on the aspect ratio typically varying, say, for a NACA-0015 profile from 14–22 degrees (infinite span) to 20–40 degrees ($k_R = 1$) varying also with the Reynolds number: lower values refer to model Reynolds number values while higher ones—to the full scale. The typical 35 deg maximum deflection angle is usually linked to those values of the stall angle. However, the attack angle can be very different from the deflection angle and in many cases increasing the maximum rudder deflection can augment a ship's turning ability at minimum expenses. On the other hand, it is recommended to restrict rudder deflections in model experiments to avoid a premature stall which is not expected in the full scale[24].

4. The magnitude of the stall angle in astern run is approximately 4–10 degrees smaller then in normal operation as the flow direction is unfavourable for the profile shape [7, P. 298].

[23] The data are borrowed from [7, P. Fig. 125] and are related to the infinite aspect ratio.

[24] However, according to some reported data, this danger is exaggerated for rudders in the propeller race as the stall is delayed in a highly turbulized flow field.

5. The section shape and thickness affect relatively weakly the forces in the pre-stall range but both the stall angle and the maximum lift depend on it significantly at least in the case of smooth surface. For instance, in Table 2.2 presented are some results obtained in wind-tunnel tests with rudders having different section shapes but with the same $k_R = 1$ and the same $\mathsf{Rn} = 0.78 \cdot 10^6$.

Table 2.2: Maximum Lift and Stall Angle

Profile	t/c, percent	$C_{RL\max}$	α_{stall}, deg
NACA-0015	15	1.06	34
NACA-0025	25	1.34	46
IfS 62 TR 25	25	1.47	46

6. After the stall, the lift is gradually (after a typical abrupt drop) decreasing until merely zero at $\alpha_R = 90$ degrees while the drag increases. The normal force, however, differing very little from the lift in the pre-stall region, remains approximately constant at the stall regime. This gives an idea of a simple straight-line approximation of the rudder normal force coefficient for arbitrary attack angles which can become useful for estimating rudder forces in hard manoeuvres.

Circular open-water rudder characteristics. Although free simulation of arbitrary manoeuvring motions requires all-round or circular hydrodynamic characteristics of the rudder and these can usually be obtained by means of wind-tunnel tests, there are very few published data of this kind. Drag and lift curves shown on Fig. 2.21 were obtained in the wind tunnel of

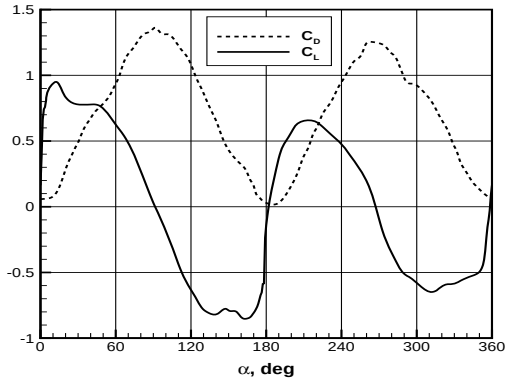

Figure 2.21: Airfoil drag and lift coeffcients circular data

the Krylov Ship Research Institute (St. Petersburg, Russia) for a wing with 5% profile [32] at $\mathsf{Rn} = 0.54 \cdot 10^6$. The data were brought to the aspect ratio 6 and as the study was propeller-oriented, the profile was not symmetric and the attack angle was defined in circular system i.e. was varying from 0 to 360 degrees. It is clearly seen that both lift and drag characteristics are

equally important. Curves for the corresponding normal and tangential force coefficients are shown on Fig. 2.22. Thsi plot confirms negligibility of the tangential force. The normal force

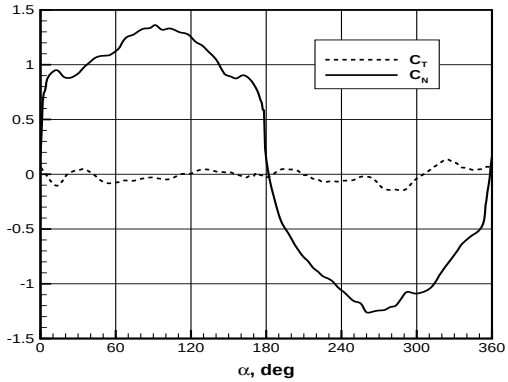

Figure 2.22: Airfoil tangential and normal force coefficients circular data

here drops immediately after the stall but then grows reaching its maximum value near $\alpha = 90°$ representing then in fact the cross-flow drag. However, it must be noticed that this profile is too thin for a rudder blade and its stall angle and maximum lift value are smaller than, say, on a 15% profile while the cross-flow drag remains almost the same. Hence, on a thicker profile it is possible to expect more constant normal force in the stall region.

On the rudder cavitation. Many rudders can cavitate and this is even not anything extraodinary. The rudder cavitation number σ can be defined as

$$\sigma = \frac{p - p_V}{\frac{\rho V_{RA}^2}{2}} \approx \frac{200}{V_{RA}^2}, \tag{2.183}$$

where p is the full minimum pressure in the undisturbed flow, p_v — vaporization pressure, and the last approximate equality is valid under assumption that p is equal to the atmospheric pressure. The inflow velocity V_{RA} must be taken in meters per second in the simplified version of the formula. Experiments show that some tangible changes in the lift coefficient can be observed at $\sigma < 2.0$. It means that for most merchant ships all cavitation effects can be neglected when assessing of the rudder effectiveness while some local cavitation still can occur damaging the painting and even eroding the rudder's plating. Rudders of naval ships often work at much lower cavitation numbers and the rudder force can drop severely. In those cases results of the cavitation tunnel tests are usually required for dependable manoeuvring predictions.

Direct influence of the hull. It was already mentioned that if the rudder's root chord contacts an approximately flat hull plating with a negligible gap, the effective rudder aspect ratio $k_{Re} = 2k_R$. However, some finite gap g_R always exists. this can be either the real gap, or the effective one caused by the boundary layer (then g_R is taken equal to the momentum thickness). The effective aspect ratio can then be estimated with the help of the following

formula approximating experimental results by Flügel [14]:

$$k_{Re} = \left(1 + \frac{1}{1 + 41.5\bar{g}_R - 98.5\bar{g}_R^2}\right) k_R, \tag{2.184}$$

where $\bar{g}_R = g_R/h_R$.

Lift on horn rudders. The following approximate method for estimating the lift coefficient C_{RL}^{horn} for a horn rudder was proposed in [42, P. 41–44] and it is based on the results of the lifting surface computations presented in [38].

According to this method

$$C_{RL}^{\text{horn}}(\delta_R, \beta_R) = C_{RL}(\alpha_{Re}), \tag{2.185}$$

where $C_{RL}()$ is the lift coefficient curve for the corresponding (with the same shape and dimensions) all-movable rudder as defined, for instance, by eq. (2.177); $\alpha_{Re} = \delta_{Re} - \beta_R$ is the *effective attack angle*; δ_{Re} —the *effective deflection angle* defined as

$$\delta_{Re} = c_H(A'_M, h'_H)\delta_R. \tag{2.186}$$

The horn correction factor c_H is calculated with the formula [38]

$$c_H = \tanh\left(\frac{3.2(A'_M + h'_H - 1)}{\sqrt{k_R h_H'^3}}\right) \tag{2.187}$$

which is valid for $k_R \in [1, 2.5]$ and $A'_M \geq 1 - 0.6h'_H$.

The formula (2.187) was initially obtained for the case of $\beta_R = 0$ i.e. when $\delta_{Re} = \delta_R$. Its continuation for non-zero values of the local sideslip angle was performed on the basis of the experimental fact that deflection of the flap (rudder blade in this case) approximately results in a parallel shift of the whole lift curve which can be accounted for through the zero lift (neutral) attack angle α_0 which is zero with symmetric profiles with undeflected flap. Then, the following steps can be followed:

1. Let the lift curve for the all-movable rudder be defined as

$$C_{RL}^{AM}(\alpha) = f_{AM}(\alpha), \tag{2.188}$$

   where $f_{AM}()$ is a known function.

2. As the horn reduction factor c_H is only defined at the horn attack angle $\alpha_H = -\beta_R = 0$, it can be written

$$C_{RL}(\delta_R, 0) = c_H(A'_M, h'_H)C_{RL}^{AM}(\delta_R). \tag{2.189}$$

3. The mentioned property of the lift curve shift yields in the case of a deflected blade

$$C_{RL}(\delta_R, 0) = C_{RL}^{AM}(\alpha - \alpha_0)|_{\alpha=0} = f_{AM}[-\alpha_0(\delta_R)]. \tag{2.190}$$

4. Any defined function $f_{AM}()$ can be inverted and then:

$$-\alpha_0(\delta_R) = f_{AM}^{-1}[C_{RL}(\delta_R, 0)]. \tag{2.191}$$

5. Combining (2.189) and (2.191) it is easy to obtain

$$\alpha_0(\delta_R) = -f_{AM}^{-1}[c_H(A'_M, h'_H)C_{RL}^{AM}(\delta_R)]. \tag{2.192}$$

6. The lift coefficient of the horn rudder is then

$$C_{RL}(\delta_R, \alpha_H) = C_{RL}^{AM}(\alpha_H - \alpha_0), \tag{2.193}$$

which can also be represented as

$$C_{RL}(\delta_R, \beta_R) = f_{AM}(\alpha_{Re}), \tag{2.194}$$

where

$$\alpha_{Re} = \delta_{Re} - \beta_R \tag{2.195}$$

is the equivalent attack angle and the equivalent deflection angle is:

$$\delta_{Re} = f_{AM}^{-1}[c_H(A'_M, h'_H)f_{AM}(\delta_R)]. \tag{2.196}$$

The formulae (2.194), (2.195), and (2.196) give the desired solution. This solution takes an especially elegant form defined by (2.186) if the function $f_{AM}()$ can be linearised i.e. represented as

$$f_{AM}(\alpha_R) = C_{RL}^{AM\alpha}\alpha_R, \tag{2.197}$$

where $C_{RL}^{AM\alpha}$ can be viewed as the lift coefficient gradient for an equivalent all-movable rudder. In this case the equivalent deflection angle is defined by (2.186) instead of (2.196).

The drag of the horn rudder can still be approximately estimated using the formula (2.177) but of course the evident increase of the profile drag is then neglected.

The equation (2.187) can be applied also to the case when $h'_H = 1$ i.e. for the rudder with the rudder post. In any case, $c_H \leq 1$ which complies with higher effectiveness of the all-movable rudders.

Rudder in the hull wake and in the propeller race.

There are several approaches to accounting for the hull and propeller wakes on the "engineering" level, which seems to be the most appropriate for the manoeuvring simulation applications . All of them are based on the basic assumption that none of the wakes is affected back by the rudder and, further, all the interaction effects can be described with a small number of simple parameters. So, the task is to define the function $\mathbf{V}_{RA} = f(\mathbf{V}_R, w_{aR})$, where $w_{aR} \equiv w_a(\xi_{PR})$ is the average propeller induced axial velocity .

A relatively consistent scheme for doing it looks as follows.

1. The longitudinal component of the effective rudder velocity is calculated as

$$u_{RA} = u_R\,(1 - w_R) + w_{aR}, \tag{2.198}$$

where w_R is the rudder wake fraction which is usually supposed to depend on the local "geometric" drift angle $\beta_R \equiv \beta(x_R)$ similarly to how it was described for the propeller. Again, according to [19]

$$w_R(\beta_R) = w_{R0}\,e^{-4\beta_R^2}, \tag{2.199}$$

where w_{R0} is the rudder wake fraction in straight run. Information on this parameter is still very scarce and the value 0.25 can serve as reasonable estimate for conventional single-screw merchant ships.

2. The transverse component of the effective rudder velocity is represented as

$$v_{RA} = \kappa_v v + \kappa_r x_R r, \tag{2.200}$$

where $\kappa_{v,r}$ are the so-called *flow straightening factors* reflecting the property of the near flow field to be governed by the hull geometry thus reducing the influence of the manoeuvring kinematics. These factors are supposed to be estimated with the help of model experiments. The accumulated generalized data are, again, not abundant and the recommendations are usually very uncertain. More or less sure is that on high-speed naval ships with nearly horizontal aft buttock branches, the both factors can be taken equal to unity (also, $w_R \equiv 0$ in this case). For typical merchant ships one can follow recommendations by Inoue [19]:

$$\kappa_v = \min\{0.5,\ 0.45\,|\beta_R - x'_R r'|\}; \qquad \kappa_r = 2\kappa_v. \tag{2.201}$$

For very full-bodied vessels, each of the factors can be taken equal to 0.3.

3. The magnitude of the effective rudder velocity is, evidently, equal to

$$V_{RA} = \sqrt{u_{RA}^2 + v_{RA}^2}. \tag{2.202}$$

4. The effective rudder drift angle is

$$\beta_{RA} = \begin{cases} -\arcsin\frac{v_{RA}}{u_{RA}} & \text{at} \quad u_{RA} \geq 0 \\ -\pi\,\mathrm{sign}\,v_{RA} + \arcsin\frac{v_{RA}}{u_{RA}} & \text{at} \quad u_{RA} < 0. \end{cases} \tag{2.203}$$

(it is clear that this angle is smaller for rudders in the propeller race and after full afterbodies, when smaller are the straightening factors).

5. When the rudder is partly immersed into the propeller slipstream, the following simple and effective though crude approach is followed in most practical methods. Let us suppose that the rudder area A_R^{inside} is that of part of the rudder blade inside the jet while $A_R^{\text{outside}} = A_R - A_R^{\text{inside}}$ corresponds to the part lying outside and subject to the hull influence only. If we append the same additional subscripts "inside" and "outside" to all variables related to the corresponding parts of the rudder, and if we assume that the force coefficient curves

will remain the same for each part as it was for the whole rudder (this is the most dubious assumption!), we can write as follows:

$$\begin{aligned} F_{R\,X,Y,N} &= \frac{\rho}{2}\,[C_{R\,X,Y,N}(\alpha_R^{\text{inside}})A_R^{\text{inside}}V_{RA\text{inside}}^2 \\ &+ C_{R\,X,Y,N}(\alpha_R^{\text{outside}})A_R^{\text{outside}}V_{RA\text{outside}}^2]. \end{aligned} \tag{2.204}$$

It can be seen that this method provides a linear interpolation between the two extreme cases: (1) full absence of the propeller race, and (2) —the rudder is supposed to be fully immersed into a slipstream of unlimited diametre. Although relatively large errors are possible in between, this approach used to be very popular in practical manoeuvring models (the formula (2.204) can be transformed to a more elegant form through introducing special correction factors).

Rudder Forces Estimation According to Inoue's Method

All the issues related to estimating rudder forces can be traced within the practical manoeuvring calculation method [19] but recognizing them is sometimes not easy due to another representation of certain relations, additional assumptions and some added empiric corrections. That is why, all the relations proposed by Inoue et al. are given below with brief comments linking them to the generic approach. No corrections for the presence of a horn or a rudder post are envisaged i.e. this method is primarily oriented towards all-movable rudders. Some elements of the Inoue methods have already been presented and its remaining components and features are:

1. The hull and propeller corrections are applied directly to the ship speed V and to $\beta'_R = \beta_R - x'_R r'$ (β'_R is the artificial effective rudder drift angle introduced to account for different hull/propeller influences in drift and yaw; β_R can be calculated by means of eq. (2.203) but with the subscript A removed everywhere). The defining equations are:

$$\begin{aligned} V_{RA} &= V(1-w_R)\sqrt{1+0.6\,(1-0.065\ \text{sign}\ \delta_R)\,S(s)}, \\ S(s) &= \frac{D_P(1-w_P)}{h_R(1-w_R)}\cdot\frac{s\left[2-s\left(2-0.6\frac{1-w_P}{1-w_R}\right)\right]}{(1-s)^2}, \\ \beta_{RA} &= \kappa_v\kappa_P\beta'_R, \end{aligned} \tag{2.205}$$

where κ_v is calculated with eq. (2.201) and κ_P is the propeller flow straightening factor computed as

$$\kappa_P = \frac{1}{\sqrt{1+0.6\,\frac{D_P}{h_R}\cdot\frac{s(2-1.4s)}{(1-s)^2}}}. \tag{2.206}$$

Pay attention to the function $\text{sign}\,\delta_R$ accounting for a part of the single-screw asymmetry.

2. The rudder attack angle

$$\alpha_R = \delta_R - \delta_{R0} - \beta_{RA} \tag{2.207}$$

is determined with another account for the asymmetry expressed through the neutral rudder angle δ_{R0} estimated as

$$\delta_{R0} = -0.035\, s_0, \tag{2.208}$$

where s_0 is the slip ratio at the approach speed in straight run.

3. The rudder normal force coefficient C_{RN} is taken in the form

$$C_{RN} = C_{RN}^{\alpha *} \sin \alpha_R, \tag{2.209}$$

where using $\sin \alpha_R$ instead of just α_R is not essential in the pre-stall range but the absence of a cubic or quadratic terms leads to significantly different results. However, the effective lift coefficient slope $C_{RN}^{\alpha *}$ is here calculated with the help of the formula

$$C_{RN}^{\alpha *} = \frac{6.13\, k_R}{k_R + 2.25} \tag{2.210}$$

which is a modification of the well-known Prandtl formula emerging from the lifting-line theory. This formula is known to overestimate considerably the lift slope of small aspect ratio wings. However, using it in combination with dropping the nonlinear term leads to numerical values of the lift which are practically identical to those obtained with eqs. (2.175)–(2.180) at 15–20 degrees attack angles. Hence, this approach provides some kind of chord linearisation.

4. Finally, the normal force F_{RN} is calculated from eq. (2.173) and its components in the body-fixed axes are:

$$\begin{aligned} X_R &= -F_{RN} \sin \delta_R, \\ Y_R &= -(1 + a_H)\, F_{RN} \cos \delta_R, \\ K_R &= -z_R Y_R, \\ N_R &= \quad x_R Y_R \end{aligned} \tag{2.211}$$

i.e. the hull—rudder interaction force is supposed to be applied in close vicinity of the rudder.

2.4 Mathematical Models for Computer Simulation of Manoeuvring Motion

2.4.1 Concept of Mathematical Model in Manoeuvring

The general concept of the mathematical model of some real physical object (or system, or phenomenon) is closely connected with the prediction problem. It can be said that a mathematical model is defined if it is possible to predict the behaviour of the modelled object without physical experiments, no matter be they full scale or model scale.

At the present state of the art in the ship manoeuvring, a manoeuvring mathematical model can be associated with some computer code capable to produce desired predictions. This code presumes existence of certain numerical algorithms developed on the base of some mathematical concepts. This description is somewhat restrictive as besides numerical, possible are also the so-called analogue mathematical models based on the fact that the same, say, differential equations describe various physical phenomena. As result, the ship as a manoeuvring object can be modelled by means of some suitable electric circuit where certain voltages would represent kinematic parameters of the ship's motion.

The analogue modelling was common until approximately 60s or 70s as it was capable to provide faster and cheaper solutions as the then available digital computers. Sometimes hybrid (i.e. digital + analogue) modelling systems were used. However, extremely rapid progress in digital hardware finally eliminated any need in the analogue or hybrid modelling.

Typically, a ship mathematical model's software consists of two main parts:

1. The core mathematical model
2. The graphic user's interface

The interface part is extremely important for interactive manoeuvring simulators where it includes visualisation of the instrument's panel and the simulated environment. The latter can include electronic charts on which the bird eye's view of the moving ship is projected and a simulated virtual reality panoramic view from the ship's bridge. The graphic interface can be highly simplified or even absent in research manoeuvring simulation codes where the off-line simulation is usually preferred. In any case, it is clear that design and development of the graphic interface lies well beyond the manoeuvring theory per se.

The core manoeuvring mathematical model encapsulates all simulated manoeuvring properties of the ship and it contains the following components:

1. Differential equations of motion
2. Auxiliary differential equations (those for propeller shafts and steering gears)
3. Methods for solving the initial-value problem for the differential equations
4. Numerical functions (procedures, subroutines) returning instantaneous values of all involved froces and moments at given values of the kinematic parameters

5. A computer code implementing all the previous components

It can be noticed that the first three components are more or less standard and common for all thinkable ship mathematical models although possible are small variations concerning, say, the effective number of the degrees of freedom and/or specifics of the frames of reference in use.

But the largest difference between various core mathematical models concerns representation of forces, especially the hydrodynamic forces. Practically, the corresponding force submodels almost completely define particular features of this or that mathematical model.

The described elements of a mathematical model can be not relevant for certain special simplified mathematical models which, however, are never used for simulation purposes. Some of these models called also input–output models will be considered later.

2.4.2 Example of Practical Mathematical Model

One of the most popular semi-empiric modular mathematical model was proposed in 1980 by Inoue et al. [19]. Some components of this model (hull and rudder forces) have already been partly presented and here its decription will be completed.

Equations of motion. The following set of equations is considered in the original model:

$$\begin{aligned}
(m+\mu_{11})\dot{u} - (m + C_m\mu_{22})vr &= X_H + X_P + X_R,\\
(m+\mu_{22})\dot{v} + mur &= Y_H + Y_R,\\
(I_{zz}+\mu_{66})\dot{r} &= N_H + N_R,\\
(I_{xx}+\mu_{44})\dot{p} + K_p p + mg\,GM\sin\varphi &= K_H + K_R,\\
\dot{\xi}_G &= u\cos\psi - v\sin\psi,\\
\dot{\eta}_G &= u\sin\psi + v\cos\psi,\\
\dot{\psi} &= r,\\
\dot{\varphi} &= p,
\end{aligned} \tag{2.212}$$

where C_m is a correcting factor commented in the next paragraph, the derivative K_p is the roll damping coefficient taken at zero frequency, GM is the transverse metacentric height. All the remaining symbols mean the same as in the previous material. This set of ordinary differential equations can be complemented with the steering gear equation as described below but the original model did not contain it.

Before elaborating the force and moment components at the right-hand sides, let us pay attention to some model's features:

1. The origin of the body axes lies in the centre of mass G, and the yaw and roll moments are around that point.

2. The model is technically 4DOF although it could be rather called (3+1)DOF because it was composed from the 3DOF with the roll equation added, not by descending from the

6DOF model as we had done before. This results in some additional difference with the 4DOF model devised earlier.

3. The side force developed by the propeller is neglected which is justified for moderate-speed merchant vessels.

Hull forces. The longitudinal quasi-steady hull force is represented as

$$X_H = -R_T(u), \tag{2.213}$$

where $R_T(u)$ is the total resistance curve for the given ship as function of the surge velocity. For any given ship, this curve must be known from the resistance calculations.

However, another part of the surge force is presented implicitly in the surge equation by the component $-C_m\mu_{22}vr$ in the lefthand side. In fact, it goes about the term $X_{vr}vr$ but the hydrodynamic derivative is expressed through the sway added mass by means of the correction factor C_m. Numerical values lying between 0.5 and 0.75 are recommended for the latter. Comparative calculations showed that its influence is not very strong and the mean value 0.625 can be used in absence of better information.

The sway force and yaw moment are described similarly to eq. (2.53):

$$\begin{aligned} Y_H &= Y'(v', r', \theta)\,\frac{\rho V^2}{2}LT, \\ N_H &= N'(v', r', \varphi, \theta)\,\frac{\rho V^2}{2}L^2T + Y_H x_{\mathrm{MID}}, \end{aligned} \tag{2.214}$$

where the dimensionless coefficients Y' and N' are estimated according to Subsection 2.3.5, and x_{MID} is the midship section's abscissa.

The roll moment is

$$K_H = -Y_H z_H, \tag{2.215}$$

where z_H is the applicate of the sway hydrodynamic force estimated from special experiments. The following approximation was obtained by Inoue et al.:

$$z_H = (0.95\frac{B}{T} - 2.66)T + z_{KG} - T, \tag{2.216}$$

where z_{KG} is the elevation of the ship's centre of mass (centre of gravity) above the baseline.

Propeller and rudder forces. The propeller is modelled as described above i.e. using normal propulsion equation with the surge velocity u playing the role of the propellers geometric velocity of advance. The wake fraction coefficient depends on the local geometric drift angle as prescribed by eq. (2.126) and it is assumed that just the surge force component is significant.

The main rudder forces have already been described in Subsubsection 2.3.6. The roll moment from the rudder will be

$$K_R = -Y_R z_R, \tag{2.217}$$

where z_R is the abscissa of the rudder's centre of pressure. For the ships with the Simplex rudder, as envisaged by the Inoue model, it can be assumed that $z_R = T/2$.

2.4.3 Additional Components of Manoeuvring Mathematical Models

Aside from the main part of any manoeuvring mathematical model mostly associated with the manoeuvring kinematics and hydrodynamic forces, some additional components can be (but not necessarily!) added. These are submodels describing dynamics of ship mechanisms, such that the steering gear and the main engine.

Description of Steering Gear Dynamics

The rudder is deflected with the help of a special engine or mechanism called *steering gear*. We are not going to get into details of the steering gear's design and construction: their are many particular engineering solutions but this must be the subject of a special course. Here, it is only enough to mention that most of modern marine steering gears are electro-hydraulic and, and, in the ideal case, their dynamics can be described with the simple first-order differential equation

$$T_R\dot{\delta_R} = \delta^* - \delta_R, \tag{2.218}$$

where T_R is the gear's time lag, and δ^* is the *ordered* rudder angle. It is clear that such gear will deflect the rudder with a decreasing rate up to the moment when the actual deflection angle is equal to the rudder order.

However, this description is not sufficient as any real steering gear has constraints imposed on the rudder angle

$$|\delta_R| \le \delta_m \tag{2.219}$$

and on the rudder deflection rate (due to power limitations)

$$|\dot{\delta_R}| \le \varepsilon_m. \tag{2.220}$$

Also, mechanical imperfections and tolerances result in a certain dead zone or insensitivity range of the width $2\delta_0$ which is described as

$$\dot{\delta_R} = 0 \quad \text{at} \quad |\delta^* - \delta_R| \le \delta_0. \tag{2.221}$$

The generalized mathematical model of a real steering gear can be described with a first-order nonlinear differential equation

$$\dot{\delta_R} = F_R(\delta^*, \delta_R), \tag{2.222}$$

where the right-hand side function is

$$F_R = \begin{cases} 0 & \text{at } \{|\delta^{**} - \delta_R| < \delta_0 \text{ or } [|\delta_R| \ge \delta_m \text{ and } \text{sign}\,(\delta^{**} - \delta_R) = \text{sign}\,\delta_R]\}; \\ \min\{\frac{1}{T_R}(|\delta^{**} - \delta_R| - \delta_0), \varepsilon_m\} \cdot \text{sign}\,(\delta^{**} - \delta_R) & \text{otherwise} \end{cases} \tag{2.223}$$

where δ^{**} is the auxiliary variable defined as

$$\delta^{**} = \begin{cases} (\delta_m + \delta_0)\ \text{sign}\,\delta^* & \text{at } |\delta^*| \ge \delta_m \\ \delta^* & \text{otherwise.} \end{cases} \tag{2.224}$$

Although it is preferable to use the most complete mathematical model of the gear, the linearized model as described by eq. (2.218) can often be used if the maximum rudder angle is not supposed to be reached, as in weak manoeuvres, and the rudder order is not changed too quickly, so that there is no saturation in deflection rate. Neglection of the deadband is also possible because on well maintained gears the δ_0 value does not exceed 0.5–1deg.

Moreover, as the gear's time constant T_R is smaller than any chracteristic time of the ship itself (lying in the interval 2–5s in most cases), it is even possible to apply the simplest mathematical model of the steering gear:

$$\delta = \delta^*. \tag{2.225}$$

It can be proven that this model, which is called the ideal steering gear, is a good approximation to the fullest model (2.222) when the the rate of change of the rudder order is small enough. The real gear is then working in the so-called sliding regime described by (2.225) with a very good approximation.

It is not difficult to notice that representation of the steering gear in form of a first-order aperiodic plant described by eq. (2.218) is not quite consistent physically: for a rudder order applied, the gear responds instantaneously with the maximum deflection rate i.e. the modelled angular acceleration of the rudder blade is infinite which is impossible. A physically more consistent model must be at least second order, it must be written in terms of actual torque and include the rudder blade's moment of inertia and the second time derivative of the rudder angle $\ddot{\delta}_R$. However, estimates showed that the additional time lag included in such a model will be very small that will make the whole dynamic system stiff and will complicate its numerical integration. On the other hand, the first-order model proved to be very convenient

Engine Dynamics

The equation of torque for each shaft is

$$2\pi I_{pp}\dot{n} = Q_E(n^*, n) + Q_P(u, n), \tag{2.226}$$

where I_{pp} is the equivalent polar moment of inertia of all the system Propeller–Shaft–Gearbox–Engine; n^* is the required (ordered) propeller rotation rate; n is the actual instantaneous rotation rate; Q_E is the torque produced by the engine; Q_P is the propeller torque.

Diesel Engines. A simple mathematical model for the Diesel engine torque is only applicable to the case of the natural revolutions stabilization or slowing down. In the first case, the rotation rate is maintained by the governor if the maximum permitted torque at the given rotation rate is not exceeded. When this is not the case, the governor reduces the fuel supply according to a pre-set program preventing from violation of the torque constraint. Such a simple model is defined by the equation:

$$Q_E(n^*, n) = \min\{Q_{Em}(n), -Q_P(n^*)\}, \tag{2.227}$$

where, in the simplest case of constant limiting torque,

$$Q_{Em}(n) = Q_{EM}, \tag{2.228}$$

where Q_{EM} is the engine's torque related to the rated rpm (rotation rate) n_M. This torque can also be expressed as

$$Q_{EM} = \frac{P_{MCR}}{n_M}, \tag{2.229}$$

where P_{MCR} is the maximum continuous rating of the engine.

The limiting characteristic of the engine defined by (2.228) presumes a torque limitation which is required by restriction of mechanical loads. However, many supercharged marine diesel engines require stricter limitations to avoid possible thermic overloads. In general, limiting characteristics are individually defined by the manufacturer and are supplied in engine operating manuals. It must be also taken into account that a Diesel engine cannot run at a rotation rate below certain value (usually around $0.3n_M$) and the engine torque then vanishes. Similarly, as the engine's rotation rate is also restricted by the governor independently of the load, the torque must be set equal to zero when $n > k_{\text{trial}} n_M$, where k_{trial} is the factor usually varying from 1.05 to 1.1 which reflects the fact that most engine manufacturers allow some overshoot of the design rpm in trials when the propeller is usually less loaded than in average operating conditions.

Steam and Gas Turbines. In the case of a steam or gas turbine, the torque can be accurately enough represented with the following equation based on the Flügel formula:

$$Q_E = \begin{cases} 0 & \text{at} \quad \kappa_V = 0 \quad \text{or} \quad n < n_{M-} \quad \text{or} \quad n > n_{M+}; \\ Q_0(1 - \frac{n}{n_0}) & \text{at} \quad \kappa_V \neq 0 \quad \text{and} \quad n \in [n_{M-}, n_{M+}], \end{cases} \tag{2.230}$$

where n_{M+} and n_{M-} are maximum permissible values of the turbine's rotation rate in the ahead and astern runs respectively (the rotation rate is considered negative in the latter case) and the remaining parameters are:

- The turbine torque at zero rotation rate:

$$Q_0 = \begin{cases} Q_{0s+}\kappa_V & \text{at} \quad \kappa_V \geq 0; \\ Q_{0s-}\kappa_V & \text{at} \quad \kappa_V < 0 \end{cases} \tag{2.231}$$

  where $Q_{0s\pm}$ is the zero rotation rate torque at the, respectively, "full ahead" or "full astern" main steam valve position (i.e. when $|\kappa_V| = 1$);

- The turbine free run rotation rate (i.e. at zero torque):

$$n_0 = \begin{cases} n_{0+} & \text{at} \quad \kappa_V > 0; \\ -n_{0-} & \text{at} \quad \kappa_V < 0 \end{cases} \tag{2.232}$$

  where $n_{0\pm}$ is the ahead (astern) free run rotation rate;

The current relative steam valve position κ_V must be determined from a differential equation

$$\dot{\kappa}_V = F_\kappa(\lambda_{Vm}, n, n^*) \tag{2.233}$$

with the right-hand side

$$F_\kappa = \begin{cases} 0 & \text{at} \quad |n^* - n| < \varepsilon_n; \\ \lambda_{Vm} \operatorname{sign}(n^* - n) & \text{at} \quad |n^* - n| \geq \varepsilon_n \end{cases} \tag{2.234}$$

where ε_n is the dead zone width for the rpm-governor, and λ_{Vm} is the valve opening rate which can be assumed constant in most cases.

Remarcs about electric drives. A relatively small number of ships have electric motors as main propulsion engines. These engines can have various characteristic curves depending of the motor's type, current (DC or AC) and on the controller. If the dependence of the torque on the rotation rate is documented, creation of the motor's mathematical model presents no difficulties.

2.4.4 Matrix Representation of Ship Mathematical Model

State variables and state space. Any physical variable describing the current state of any dynamic system can be called *state variable* or simply *state* (it is the same word in another meaning). It is usually said that if we know all the state variables *and* all the external (exogenous and control) actions, we will be able to predict the system's evolution. When the system is described by a set of ordinary differential equations (ODE), the number of state variables is equal to the order of the ODE set. It is also clear that it will be equal to the number of initial conditions necessary to define an initial-value problem for the mentioned ODE set. This number is designated further as k.

However, this description of state (variable) should not be viewed as a rigorous definition and the question whether this or that variable is a state variable or not is sometimes not so easy to answer. It is acknowledged that the notion of state was first introduced by Alan Turing in 1936 [3] and it can be assumed that its use came from a tendency to represent any physical system through a finite number of ordinary differential equations interrelating an equal number of variables which will then serve as states. For instance, in general mechanics part of the state variables are typically constituted by generalized coordinates and another part—by velocities or momenta. But there exists also a more general understanding of the state which can include thermic and electromagnetic phenomena. In the general theory of dynamic systems the state is treated as a fundamental notion which cannot be defined explicitly and is in this respect similar to the notion of "set" in mathematics. At the same time, in any specific case related to ship manoeuvrability it is relatively easy to understand which variables must serve as states.

Let us introduce a k-dimensional arithmetic space vector x which can be represented as a column matrix with k rows, i.e. $x = (x_1, x_2, \ldots, x_k)^T$. Each component of this vector is a real number representing the value of some state variable or it can be also understood as a real function of time t. In the case of the Inoue model, we can define the components of the state vector as follows:

$$\begin{aligned} x_1 &= u, \quad x_2 = v, \quad x_3 = r, \quad x_4 = p, \\ x_5 &= \xi_G, \quad x_6 = \eta_G, \quad x_7 = \psi, \quad x_8 = \varphi, \\ x_9 &= \delta_R, \quad x_{10} = n. \end{aligned} \tag{2.235}$$

It is cleare that the state variables include three distinct groups:

1. Quasi-velocities u, v, r, p
2. Generalized co-ordinates $\xi_G, \eta_G, \psi, \varphi$
3. Additional states δ_R, n

The two last states can be omitted when the engine and steering gear dynamics is not considered. For instance, these states are not needed in the case of constant rpm and ideal steering gear. The propeller rotation frequency n and the rudder angle δ_R become then *control variables* and the dimension of the state space comprising all state vectors reduces from 10 to 8. In a more complete case, control variables are also present but they are then the propeller rotation frequency order n^* and the rudder order δ_R^*. It can be noticed that the accelerations are not included in the number of state variables as they are not independent but are defined as functions of the states through the ODE set describing the system. This is typical when the equations of motion are taken in their natural mechanical form. However, the set of state variables is not unique for a given dynamic system and, as we shall see later, the equations of motion can be sometimes transformed in such a way that all the accelerations or part of them become state variables and the transformed equations contain their time derivatives.

Matrix equation of ship dynamics. Inspection of the equations (2.212), (2.222), and (2.226) indicates that they can be written in the following compact matrix form:

$$M\dot{x} = F(x, U), \tag{2.236}$$

where M is the generalized inertia square $k \times k$ matrix; $F(x, U) = (f_1(x, U), \ldots, f_k(x, U))^T$ is the vector right-hand side function; $U = (U_1, \ldots, U_\ell)$ is the control vector.

In the particular case of the Inoue model, $k = 10$, $\ell = 2$; the inertia matrix is diagonal (in the general case, it is not: see eq. (2.34)):

$$M = \text{diag}\,\{m + \mu_{11},\ m + \mu_{22},\ I_{zz} + \mu_{66},\ 1,\ 1,\ 1,\ 1,\ 1,\ 2\pi I_{pp}\} \tag{2.237}$$

The control vector is then $U = (\delta^*, n^*)^T$ i.e. $\ell = 2$. Finally, the components of the vector F are:

$$\begin{aligned}
f_1 &= (m + C_m\mu_{22})vr + X_H + X_P + X_R, \quad f_2 = -mur + Y_H + Y_R, \\
f_3 &= N_H + N_R, \quad f_4 = -K_p p - mgGM\sin\varphi + K_H + K_R, \\
f_5 &= u\cos\psi - v\sin\psi, \quad f_6 = u\sin\psi + v\cos\psi, \\
f_7 &= r, \quad f_8 = p, \quad f_9 = F_R(\delta^*, \delta_R), \quad f_{10} = Q_E(n^*, n) + Q_P(u, n).
\end{aligned} \tag{2.238}$$

The generalized inertia matrix M can always be inverted and the equation (2.236) becomes then:

$$\dot{x} = M^{-1}F(x, U) \equiv G(x, U). \tag{2.239}$$

It is worthwile to note that the matrix inversion must not be necessarily performed analytically. It is sufficient to be able to inverse it numerically for any particular set of data. This can be performed at each step of numerical integration.

2.4.5 Initial-Value Problem and Numerical Integration of Manoeuvring Equations

The most typical use of a ship manoeuvring mathematical model is reproduction (or simulation) of the ship motion in the time domain starting from its some initial state and with some predefined control program which means definition of the vector function $U(t)$. The initial state is defined through the initial conditions or initial values $x(0)$ of all state variables. In general, these initial values can be chosen arbitrarily within their permissible intervals but in practice it is usually convenient to assign to all of them zero values with a possible exception made for the surge speed $u = x_1$: it is often more practical to assume $u(0) = V_0$, where V_0 is then called the *approach speed*.

The set (2.239), together with the initial conditions defines an initial value problem for ODE which is well studied and supported by numerical analysis. Here, we shall only focus on certain peculiarities of applications of these numerical method to the stated specific problem:

1. The manoeuvring simulation problem is not too sensitive to the choice of integration method. Contrary to what is often stated, even the simplest Euler method works quite well in most cases. This method is described by the formula

$$x^{(i+1)} = x^{(i)} + hG(x^{(i)}, U(t_i)), \qquad i = 0, 1, \ldots, \tag{2.240}$$

where $h = t_{i+1} - t_i$ is the time integration step, and the subscript i at the state vector links it with the moment t_i. Another popular method is the Runge–Kutta 4th order method defined by the following set of equations:

$$\begin{aligned} k_1 &= G(x^{(i)}, U(t_i)), \\ k_2 &= G(x^{(i)} + \frac{h}{2}k_1, U(t_i + \frac{h}{2})), \\ k_3 &= G(x^{(i)} + \frac{h}{2}k_2, U(t_i + \frac{h}{2})), \\ k_4 &= G(x^{(i)} + hk_3, U(t_i + h)), \\ x^{(i+1)} &= x^{(i)} + \frac{h}{6}(k_1 + 2k_2 + 2k_3 + k_4). \end{aligned} \tag{2.241}$$

2. Most courses of numerical analysis claim that the Runge–Kutta method is far superior to the Euler method and is more economical as leads to the same accuracy at much greater values of the step h. However, this is not confirmed with the practice of manoeuvring simulations: equal accuracy is often obtained at equal steps but, as the Runge–Kutta method requires 4 times more computations of the right-hand side at each step, it loses. This happens because the superiority of the Runge–Kutta method is only guaranteed and proven theoretically when the right-hand side of the equations has continuous *fourth* derivatives. But this condition, as a rule, is not met in manoeuvring equations: the control variables can be discontinous and every function containing the absolute value operation has a discontinuous derivative. It can be also added that the manoeuvring simulation problem, in general, does not satisfy conditions of the classic Peano theorem

on the existence and uniqueness of the solution to the initial-value problem. But it practically always satisfies the Carateodori theorem [15] which guarantees the same in the generalized sense.

3. Various mathematical libraries and mathematical packages (like *Mathematica, MatLab, Maple, MathCAD*) usually offer sophisticated adaptive procedures with automatical adjustment of the integration step to obtain the desired accuracy. As a rule, it cannot be recommended to use such procedures as they can work too slowly, especially when discontinuities are present. More practical is to use simpler constant-step procedures which are very easy to code. The constant integration step is chosen by means of comparative simulations although some algorithms for its preliminary selection can be used. However, the step remains constant through all the simulation process.

4. As first approximation, it can be recommended to assume $h = 0.1T_{\text{ref}}$ for 3DOF manoeuvring models comprising just the motion in the horizontal plane. When the roll motion is included, the required integration step can be smaller by the order of magnitude. In this case, a faster integration procedure can result from using different steps for different state variables.

Simulation of particular manoeuvres

It goes here about off-line simulations of some typical manoeuvres already described verbally in Section 1.3. Unless defined otherwise, it will be assumed that $n^* = \text{const}$ i.e. there is no engine manoeuvre executed.

Turning circle. The control programme in turning manoeuvre can be written as

$$\delta^*(t) = \delta_{R0} + (\delta_s - \delta_{R0})H(t - t_0), \tag{2.242}$$

where δ_s is the ordered steady deflection angle; $H(t)$ is the Heaviside step function; $t(0)$ is the moment of the manoeuvre's start (in many cases it can be assumed $t_0 = 0$). It is supposed that the ship is going strait before the deflection order is given and that the rudder must be held in the neutral position.

The simulation continues until all relevant kinematic parameters are settled and some part of the steady turn is sailed. In most cases, the last variable to reach its steady turn value is the ship speed. On the other hand, 540deg of the heading change is a good rule of thumb in most situations. The main characteristics of the turning circle (advance, transfer, tactical diameter etc.) can be calculated automatically during the simulation process.

Pull-out manoeuvre. This is simply one of the possible endings of the steady turn. The rudder is returned to the neutral position and the simulation continues until a steady value of the rate of yaw is reached. As will be seen from the following material, this value is not necessarily zero. The control programme for the pull-out manoeuvre is:

$$\delta^*(t) = \delta_s + (\delta_{R0} - \delta_s)H(t - t_1), \quad t, t_1 > t_s, \tag{2.243}$$

where t_1 is the moment of the start of the pull-out's execute, t_s is the moment when the tuning can be considered as completed.

Helm check. This manoeuvre also serves for finishing the turn but the rudder is deflected to the opposite side at the maximum angle:

$$\delta^*(t) = -\delta_m \,\text{sign}\, \delta_s H(t - t_1), \quad t, t_1 > t_s. \tag{2.244}$$

If no further orders are given, the ship will finish with a steady tightest turn to the opposite side.

Zigzag manoeuvre. Assuming that δ_z and ψ_z are the zigzag parameters, the control for a zigzag starting at $t = 0$ will be described as:

$$\delta^*(\psi, r) = \delta_z \,\text{sign}\, (\psi_z \,\text{sign}\, r - \psi). \tag{2.245}$$

In this case, there is no explicit dependency of the rudder order on the time but, instead, it depends on instantaneous values of two state variables $\psi(t)$ and $r(t)$. It is usually said that in this case, we are dealing not with a control programme but with a *control law*. Introduction of a control law alters the nature of the dynamic system under consideration: instead of an *open-loop system*, we deal with a *closed-loop system*. In this case, the applied nonlinear control law results in the system's self-sustained oscillations showing up as the required zigzag manoeuvre.

Spiral manoeuvre. At the moment of writing this text, only the Dieudonné spiral as described in Subsection 1.3.4 can be simulated relatively easily. No reasonably simple formula for the control programme can be written down in this case but rather a loop over the grid of rudder orders $\Delta = \{\delta_1^* \equiv \delta_m, \delta_2^*, \ldots, \delta_{M-1}^*, \delta_M^* \equiv -\delta_m\}$ must be organized. At each $\delta^* \in \Delta$, the simulation continues until the steady values of r and u are reached. The interval between two consecutive values of the executed rudder angle must better depend on the region. This interval should be 1deg or even less for $|\delta^*| \leq 10$dg but it can be increased up to 5deg outside that domain. The set Δ must be scanned twice i.e. in the descending and ascending directions and the simulation must end again at $\delta^* \equiv \delta_m$. For some ships, this duplication does not bring any new information but in other cases it can reveal certain important details.

2.4.6 Examples of Simulated Trajectories and Time Histories.

Ship data.

The simulations will be carried out for a container ship *S175* whose main particulars are shown in Table 2.3 and the body plan—on (Fig. 2.23). The 4DOF Inoue mathematical model as

Table 2.3: Main Particulars of the Modelled Ship

Parameter	*Notation*	*Value*	*Unit*
Length	L_{pp}	175	m
Breadth	B	25.4	m
Draught	T	9.5	m
Mass	m	24571	t
Centre of mass' abscissa	x_G	0.82	m
Centre of mass' applicate	z_G	-0.02	m
Moment of inertia in roll	I_{xx}	$1.72 \cdot 10^6$	tm^2
Moment of inertia in pitch	I_{yy}	$4.36 \cdot 10^7$	tm^2
Moment of inertia in yaw	I_{zz}	$4.4 \cdot 10^7$	tm^2
Transverse metacentric height	GM	1	m
Design speed	V	16.7	kn
Propeller's diameter	D_P	5.3	m
Rudder area	A_R	48.5	m^2
Rudder relative area	$A_R/(LT)$	2.9	%
Rudder height	h_R	8.0	m
Rudder aspect ratio	k_R	1.38	
Maximum deflection angle	δ_m	35	deg
Maximum deflection rate	ε_m	2.33	deg/s
Steering gear's time lag	T_R	5	s

described above was used for all simulations. However, the origin C of the body axes lies in the midship plane and on the waterplane which implied some equivalent transformations of equations of motion.

Simulation of Turning Manoeuvres

First, a turning manoeuvre to the starboard with the full helm (35deg of the rudder's deflection) at approach speed 16kn and no retardation ($T_0 = 0$)was simulated. The trajectory with the ship's images corresponding to the main characteristic points is shown on Fig. 2.24 and the same trajectory with the image reproduced every 20s—on Fig. 2.25. The numerical characteristics of the turning manoeuvre were calculated by the simulation code and they are presented in Table 2.4 (this formatted table was generated by the code automatically). The time histories of main kinematic parameters are presented on Fig. 2.26. Analysis of these time histories leads to the following observations:

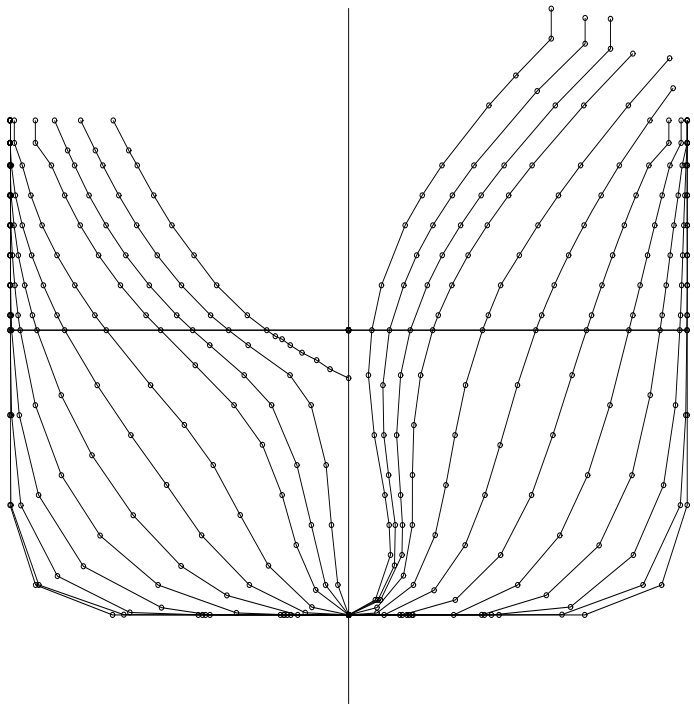

Figure 2.23: Body Plan of the Ship *S175*

Table 2.4: Parameters of a turn at the 35 deg helm order: actual final rudder deflection angle is 35 deg; approach speed is 16.7 knots; cumulated heading is 1.27e+03 deg

Parameter	Absolute value	Relative value
Advance, m	693.73	3.96
Transfer, m	370.22	2.12
Tactical Diameter, m	816.97	4.67
Steady Turning Diameter, m	707.25	4.04
Back Transfer, m	0.0991	0.000567
Steady Dimensionless Yaw Rate		0.495
Final Speed, kn	9.517	0.57

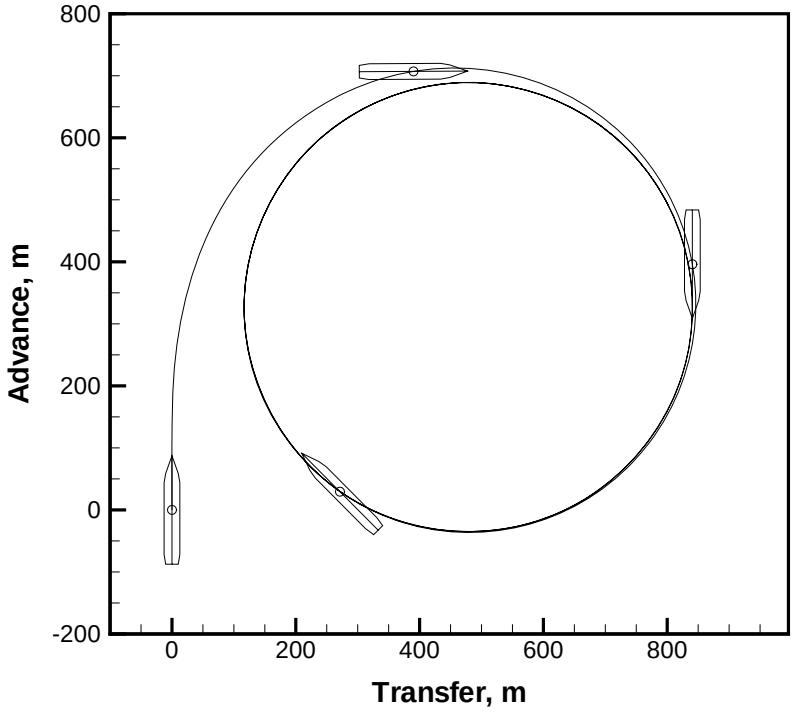

Figure 2.24: Trajectory in Turning Manoeuvre: Simulation until 1600s

1. At the initial phase of the right helm turn, the ship rolls to the starboard but very soon recovers and rolls to the portside i.e. outside of the turn. This behaviour is typical for all surface displacement ships. The initial heel to the starboard explains by the absence of the drift angle and of the hull force. The rudder force is directed to the portside and, as the rudder is located below the centre of mass, it will obviously heel the ship to the starboard. Then, the drift angle and the yaw develop and the hull force begins to dominate. It is also applied below the centre of mass but its direction is opposite to that of the rudder angle which results in the outboard heel.

2. While the static heel in steady turn is usually moderate, the dynamic roll can substantially exceed it and even reach worrying values. That is why, tight manoeuvres in rough seas are never recommended in good ship handling.

Time Histories for Forces. Time histories for the sway force, yaw moment and for the surge force are given on Fig. 2.27–2.30. Analysis of these data leads to the following observations:

1. The sway force in steady turn is mainly due to the hull and is directed inward thus compensating the centriphugal force (according to the d'Alembert principle). The steady value is substantially smaller than the maximum value reached around $t = 60$s mainly because of the ship speed drop. However, it can be seen that the rudder force dominates in the initial phase of turn which is clearly seen from the zoomed time histories (Fig. 2.28).

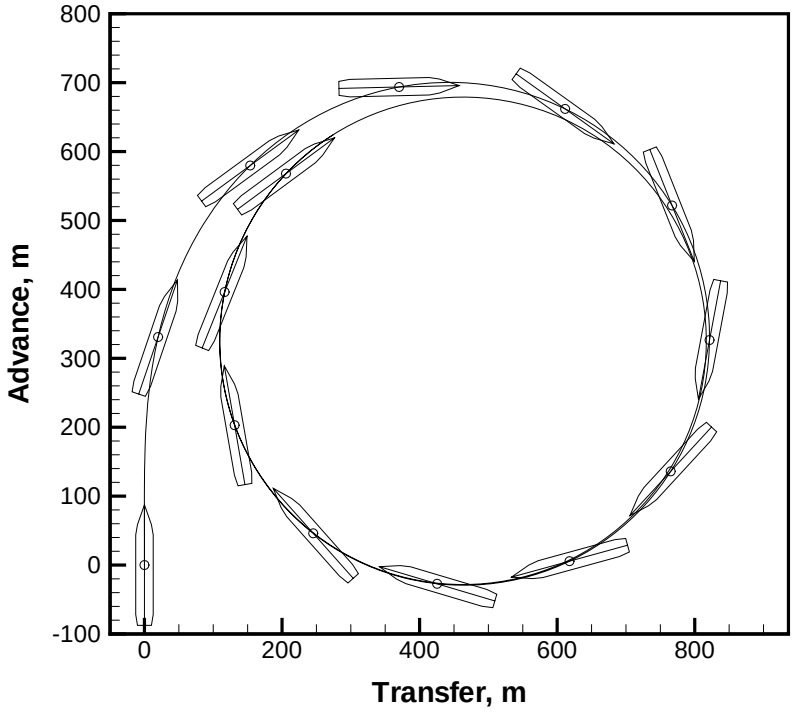

Figure 2.25: Trajectory in Turning Manoeuvre: Simulation until 1000s

This force is causing an insignificant back transfer of the ship.

2. The rudder sway force is directed opposite to the hull force thus, at first glance, reducing the ship's turning ability although the true role of the rudder can only be understood from anylysis of yaw moments.

3. The rudder yaw momement is almost counter-balancing the hull yaw moment (some residual total moment seen on the plot (Fig. 2.29) is caused by using non-central body axes in the current implementation; this residue is exactly zero in central axes). This is expectable as the rotation with a constant yaw rate can only be possible with the zero total yaw moment.

4. The residual total surge force in steady turn is necesary to counteract the x-projection of the centriphugal force. It is positive mainly due to the propeller's action. Under simulated condition (constant rpm is assumed) the propeller's thrust increases in comparison with the straight-run condition. The contribution of the hull and rudder to the surge force is close to each other in steady turn but at the initial phase i.e. immediately after the rudder got deflected, but before development of the drift angle, the rudder surge force (almost identical to the resistance) is twice the hull surge force which had been counter-balanced by the propeller at the approach phase. So, the rudder deflection is the main cause of the initial speed drop.

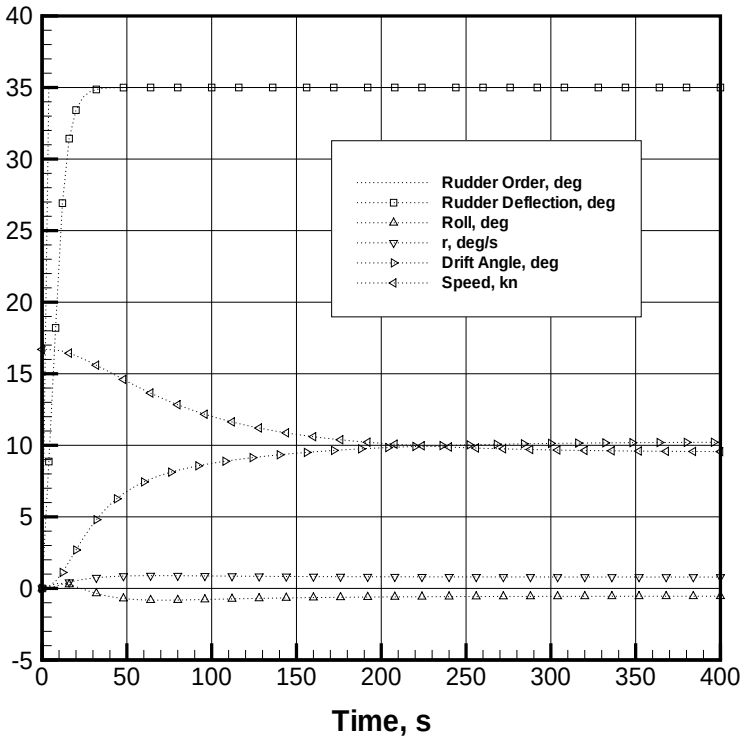

Figure 2.26: Time Histories of Kinematic Parameters in Turning Manoeuvre

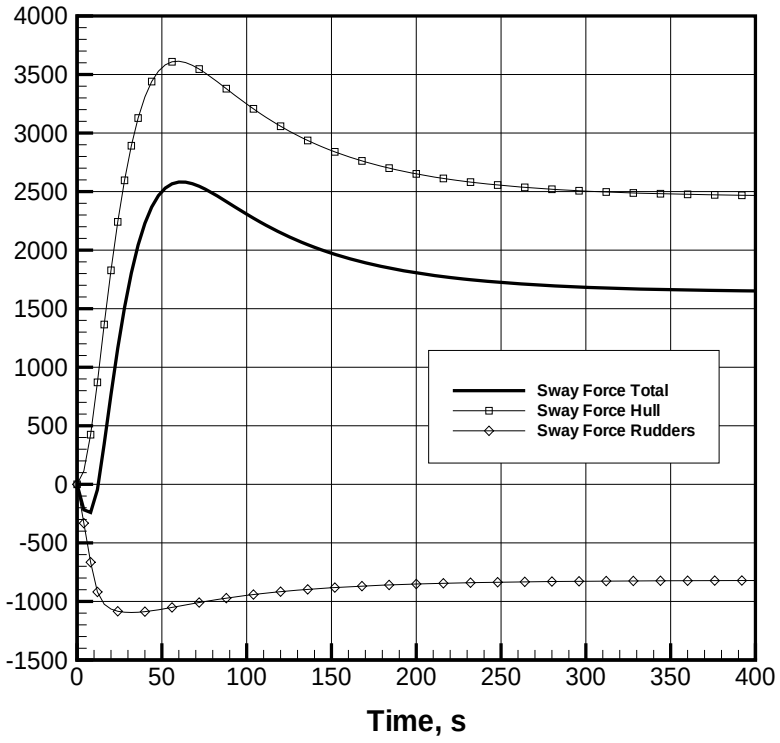

Figure 2.27: Time Histories of Sway Forces in Turning Manoeuvre

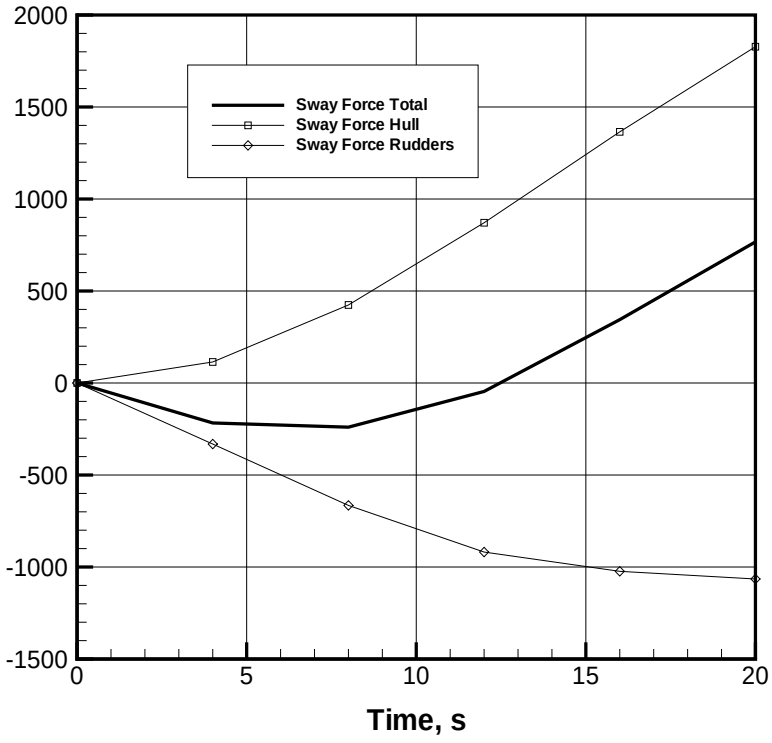

Figure 2.28: Time Histories of Sway Forces in Turning Manoeuvre (Zoomed)

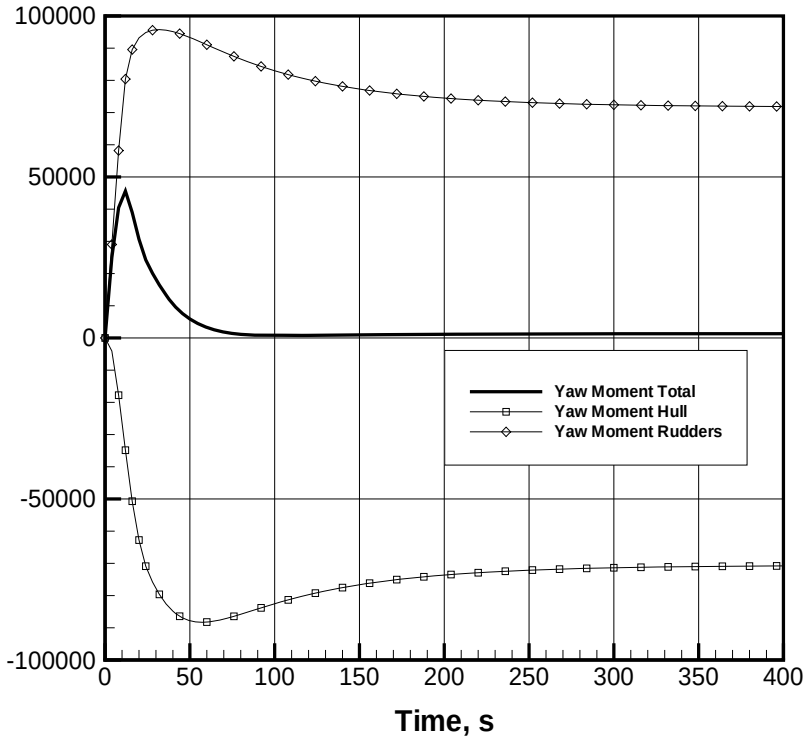

Figure 2.29: Time Histories of Yaw Moments in Turning Manoeuvre

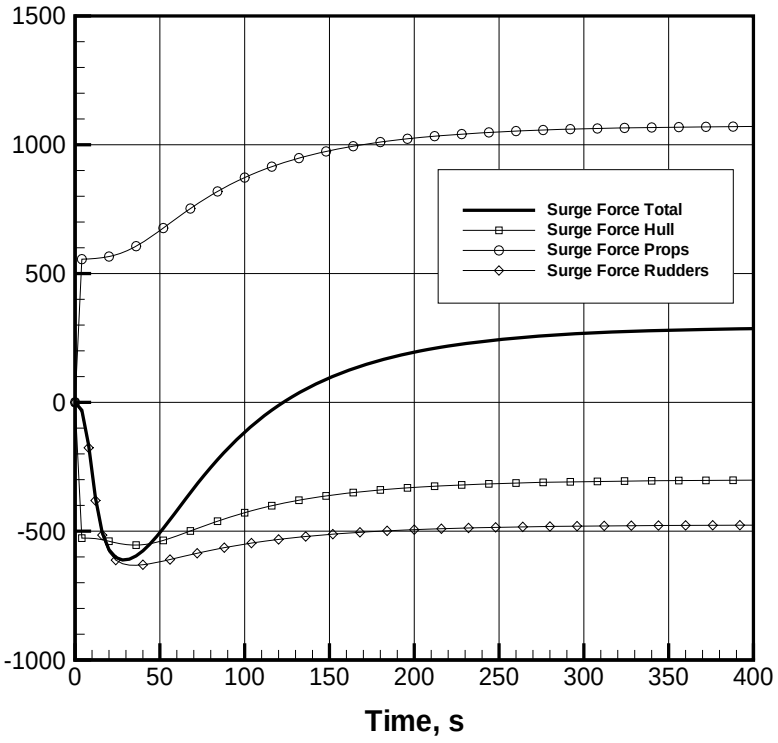

Figure 2.30: Time Histories of Surge Forces in Turning Manoeuvre

Simulation of Spiral Manoeuvre

The typical spiral curve i.e. the dependence of the steady turn dimensionless rate of yaw r'_s on the rudder angle δ_s is shown on Fig. 2.31 where the simulations were carried out in even keel condition. Plot of the steady-turn drift angle is shown on Fig. 2.32 and looks very similar to

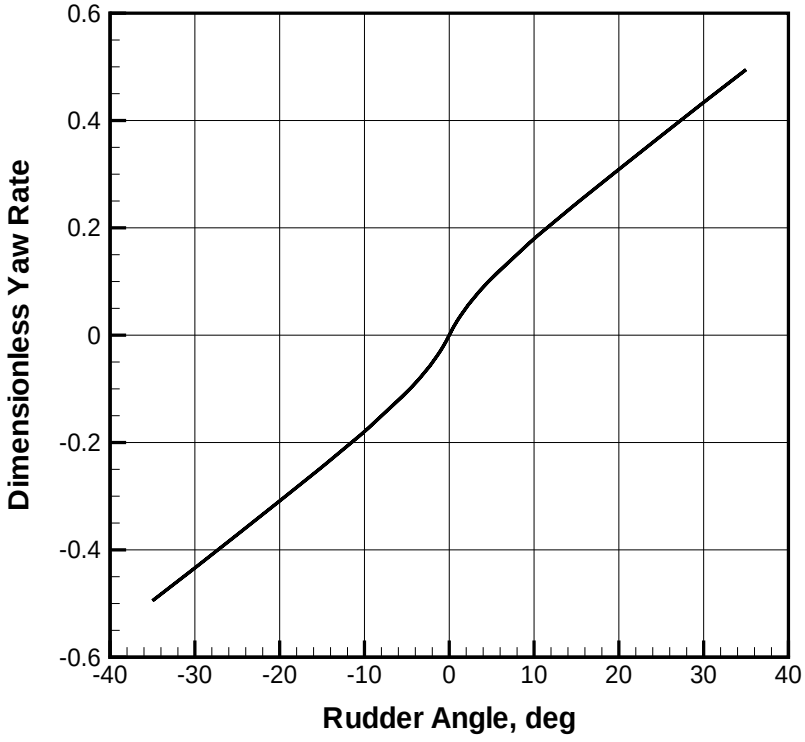

Figure 2.31: Spiral Curve: Even Keel

the main spiral curve. Finally, plots of the relative ship speed V_s/V_0 and of the pivot point's relative abscissa x'_{Ps} are presented on Fig. 2.33. All those dependencies do not show anything unexpected: the greater is the rudder angle, tighter is the steady turn, larger is the velocity drop and the drift angle. At the same time, the pivot point's abscissa is changing surprisingly little and sometimes this circumstance can be used for creating simplified mathematical models.

But the spiral curves obtained at the cosiderable (3m) trim by the bow presented on Fig. 2.34–2.36 demonstrate very different properties. The main peculiarity is presence of a hysteresis loop in the vicinity of the neutral rudder angle. It is clear then that the ship is unable to go straight with the rudder fixed even in its neutral position but instead it would rotate at the yaw rate $r_{s+}(0) > 0$ or $r_{s-}(0) < 0$ depending on the initial conditions. The last remark means that during the first half of the spiral simulation starting from $\delta_R = 35$deg with the following gradual reduction of the rudder angle the ship will rotate to the starboard at $\delta_R = 0$ and, after further reduction of the rudder angle to negative values, at certain $\delta_{0-} < 0$ the ship will suddenly change the direction of rotation. Then, outside the loop, the ship's reaction to changes in the rudder angle will be usual and during the second period of the spiral manoeuvre,

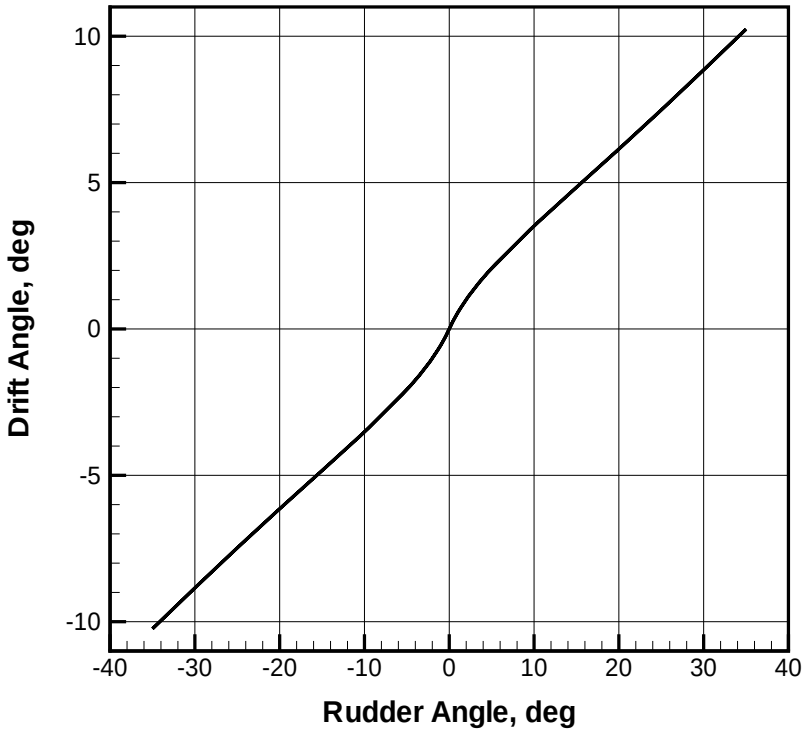

Figure 2.32: Drift Angle Spiral Curve: Even Keel

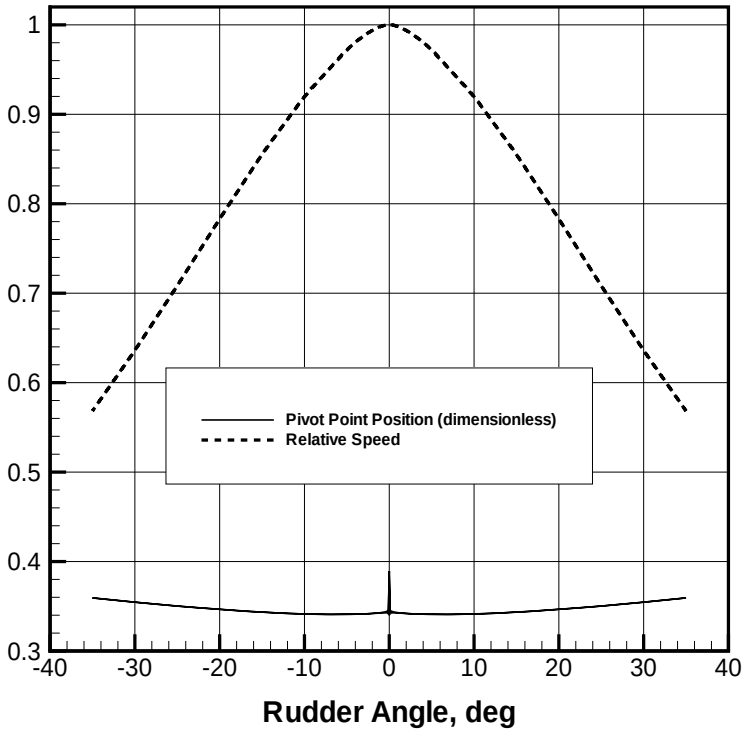

Figure 2.33: Auxiliary Spiral Curves: Even Keel

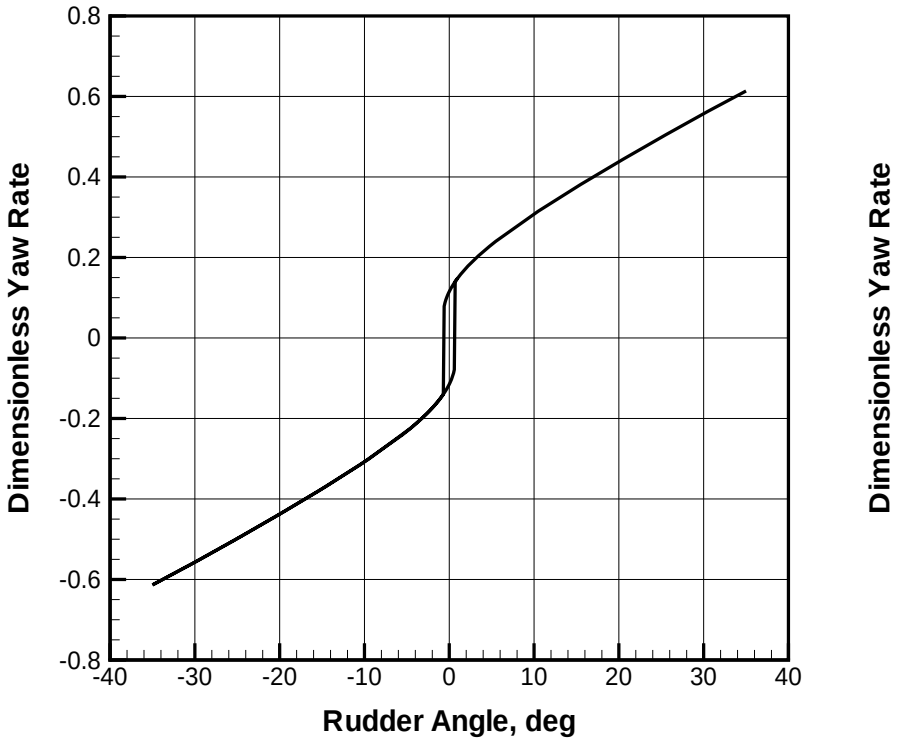

Figure 2.34: Spiral Curve: Trim by the Bow

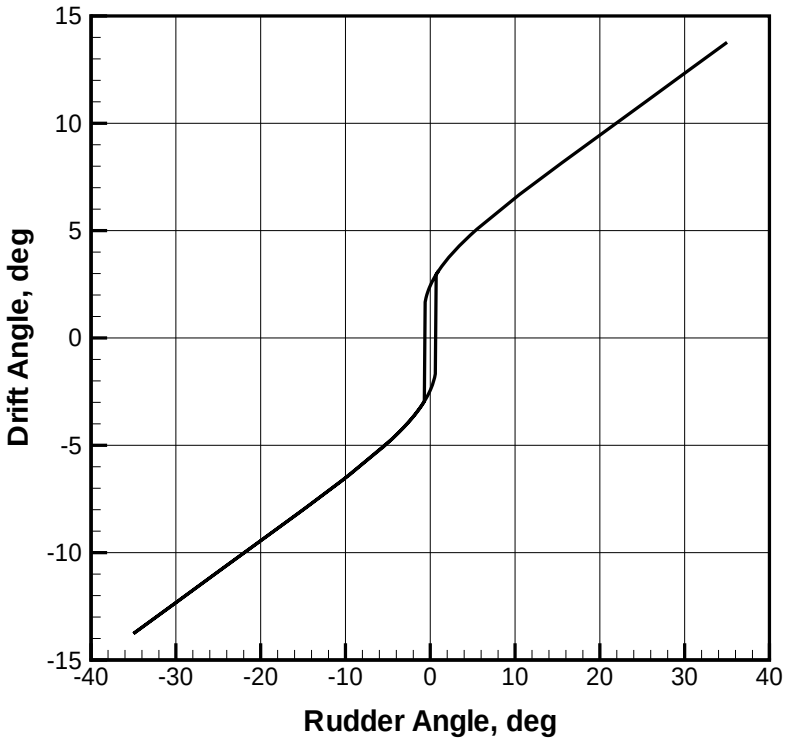

Figure 2.35: Drift Angle Spiral Curve: Trim by the Bow

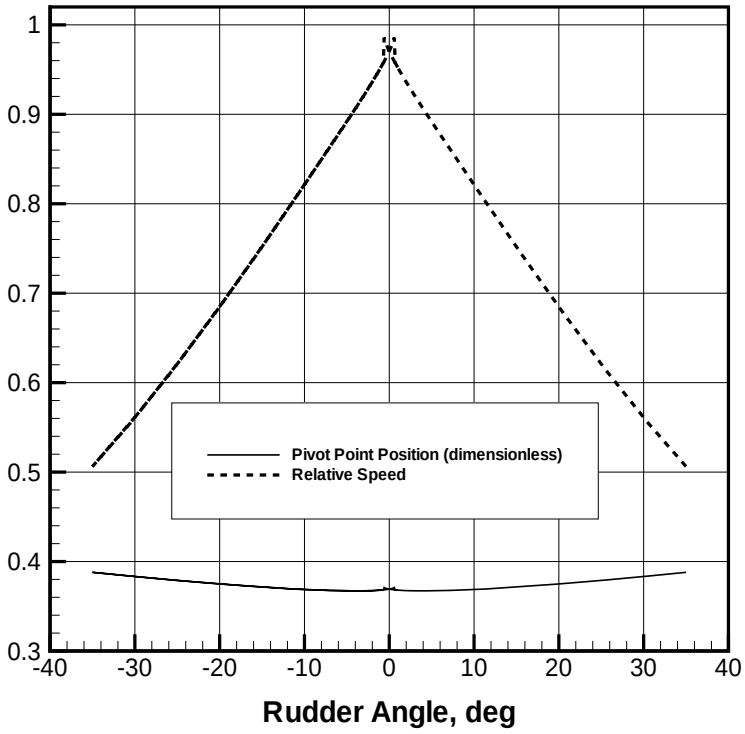

Figure 2.36: Auxiliary Spiral Curves: Trim by the Bow

similar things will happen with the opposite sign (the jump from negative to positive rotation will happen at $\delta_{0+} > 0$) which will result in the lower branch of the hysteresis loop. It is intuitively clear that such a ship cannot be stable on the straight course with the rudder fixed. Will elaborate this concept later.

The drift angle curve is similar to the main spiral curve while the salient feature of the speed drop curve is its separation from unity at the origin which is expectable as the straight motion regime is not present on this diagram.

The central part of the spiral curve on Fig. 2.34 is displayed stretched on Fig. 2.37 together with some additional curves. The hysteresis loop's "sidewalls" are not quite vertical because the spiral step is relatively large, equal to 0.1deg for small absolute values of the rudder angle. The height of the histeresis loop can be estimated as $r_{s+}(0) - r_{s-}(0) = 0.8$ and its width is $\delta_{0+} - \delta_{0-} = 2\text{deg}$. Such loops are considered high but relatively narrow.

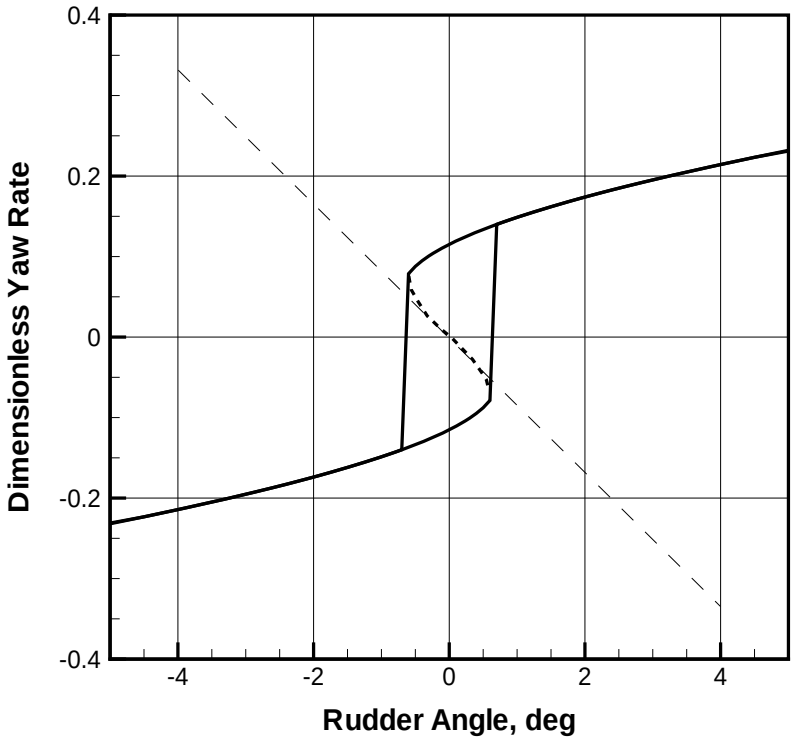

Figure 2.37: Spiral Curve at Trim by the Bow (Zoomed and with Sketches of Unstable Branch and of Linearised Response)

Calculation of the spiral curve by simulating the spiral manoeuvre is in fact equivalent to finding part of the solutions of the steady turn vector equation

$$F_1(x^{(1)}, \delta_R) = 0, \tag{2.246}$$

where F_1 and $x^{(1)}$ are the subvector of F and x respectively which only correspond to the dynamic part of the ship mathematical model. The kinematic equations and the models for

the steering gear and engine are not considered. It is clear that while outside the hysteresis loop the solution is unique, inside the loop there are at least two solutions for each value of the rudder angle seen as the upper and lower branch corresponding to different directions of the yaw. A more thorough analysis shows that there is always also, inside the loop, the third solution sketched on Fig. 2.37. Although this third solution also corresponds to an equilibrium of all forces and moments, that equilibrium is unstable and so is the solution itself. This branch of the spiral curve cannot be obtained with the usual spiral manoeuvre but a special Bech's spiral must be performed. The idea is to maintain some constant rate of yaw between r_{s-} and r_{s+}, to record the rudder angle's time history and—through averaging it over the time—to obtain the corresponding equilibrium value of δ_R. The expected unstable branch is traced on Fig. 2.37 with the dash line (it's just a sketch!). Also, shown is there with the long-dash straight line, the imaginary spiral "curve" which would be obtained with the linearised mathematical model. This straight line is tangent to the unstable branch of the spiral curve and, evidently cannot serve as a consistent approximation for the real spiral curve proving inapplicability of linearised models for simulation purposes, at least for directionally unstable ships. In the case of a directionally stable ship having no loop on the spiral curve, its approximation with the tangent also corresponding to the linearised model (Fig. 2.31) can be more successful but still very imprecise.

Influence of the rudder's size. It could be expected that substantial reduction of the rudder area would substantially impair the ship's turning ability and increasing that area would have the opposite effect. Technically, this is true but the effect can often be much less pronounced than expected. The ship with the bow trim was also simulated with the "large" rudder ($A_R = 100\text{m}^2$), "small" rudder ($A_R = 20\text{m}^2$), and "tiny" rudder ($A_R = 5\text{m}^2$). The resulting spiral curves are shown on Fig. 2.38–2.40. It is interesting that the ship's turning ability practically does not depend on the rudder's area although the width of the histeresis loop does. This is especially pronounced for the "tiny" rudder where one can expect bad controllability of the vessel.

The rudder area influences more the turning ability, especially at small and moderate rudder angles, in the case of a directionally stable ship (Fig. 2.41–2.43).

Simulation of Zig-Zag Manoeuvre

The 10deg–10deg zig-zag manoeuvres were simulated for the same ship at even keel, and also trimmed 3m by the bow. The results are presented on Fig. 2.44–2.45. It is clearly seen that the overshoot angles are much greater in the case of the ship trimmed by the bow when the spiral curve has a hysteresis loop. It can be expected that the ship is then poorly controllable.

Time histories obtained after simulated 20deg–20deg zig-zag manoeuvres are presented on Fig. 2.46–2.47.

In this case the difference in behaviour of a directionally stable and unstable ship is less pronounced. This leads to the idea that directionally unstable ships require larger helms to be controlled properly. In general, this is confirmed by the ship handling practice.

As directional instability of a ship can bring many troubles, it would be useful to establish

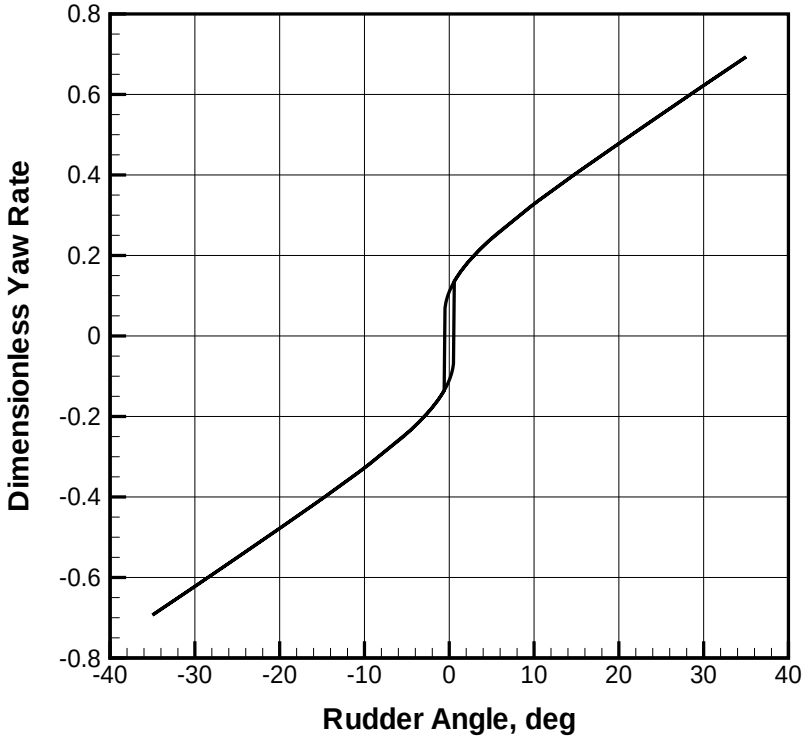

Figure 2.38: Spiral Curve: Trim by the Bow, "Large" Rudder

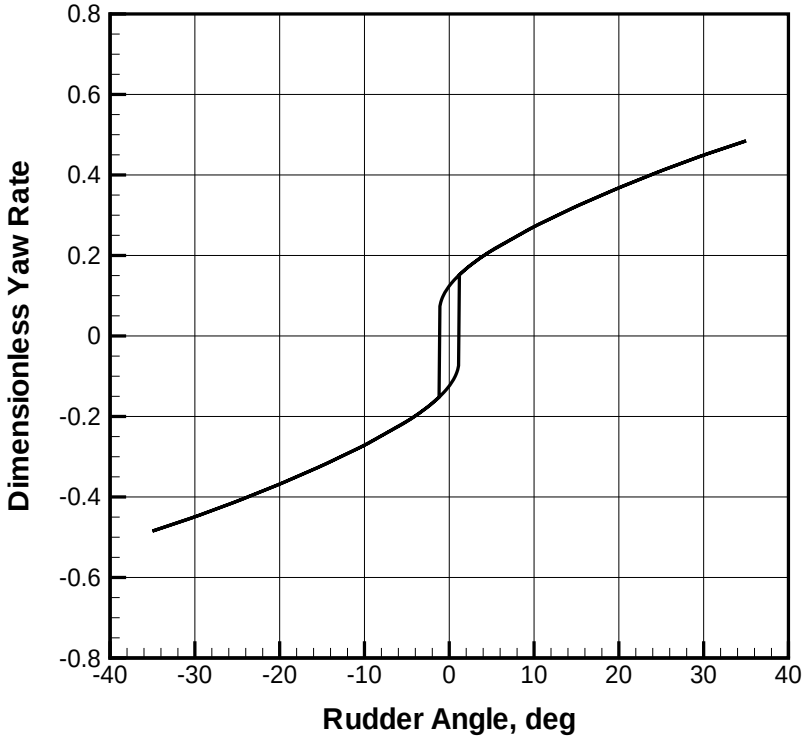

Figure 2.39: Spiral Curve: Trim by the Bow, "Small" Rudder

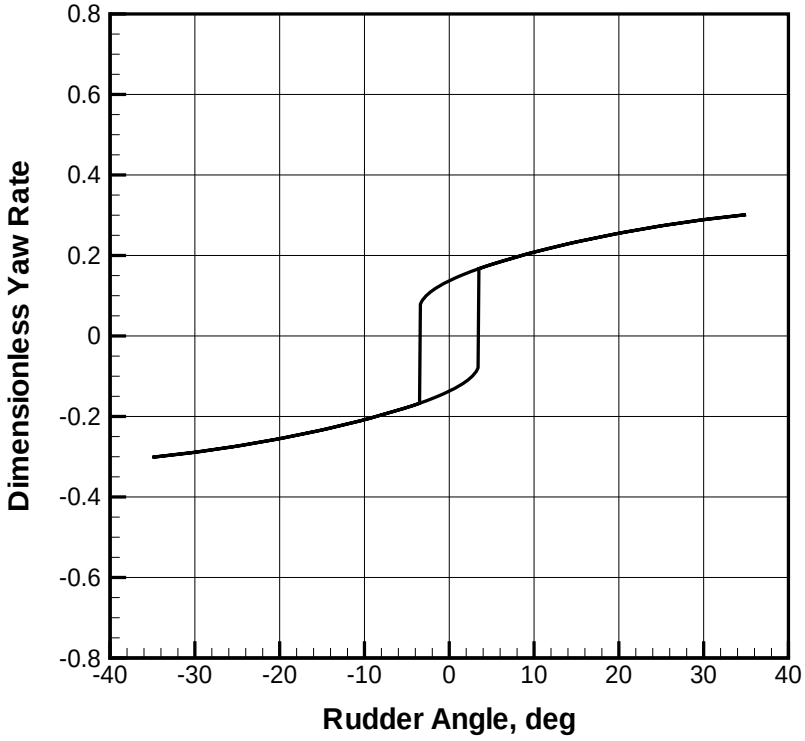

Figure 2.40: Spiral Curve: Trim by the Bow, "Tiny" Rudder

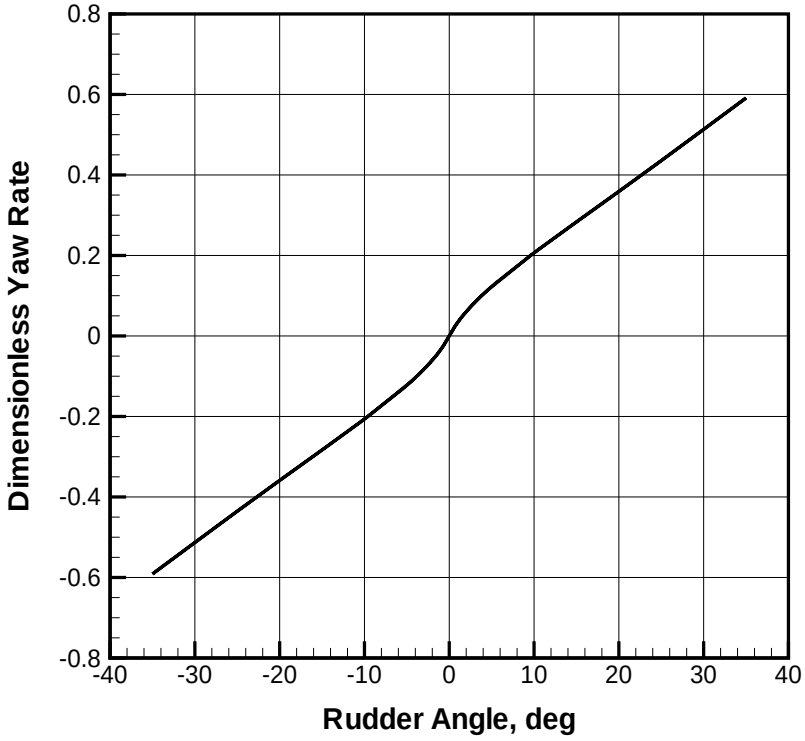

Figure 2.41: Spiral Curve: Even Keel, "Large" Rudder

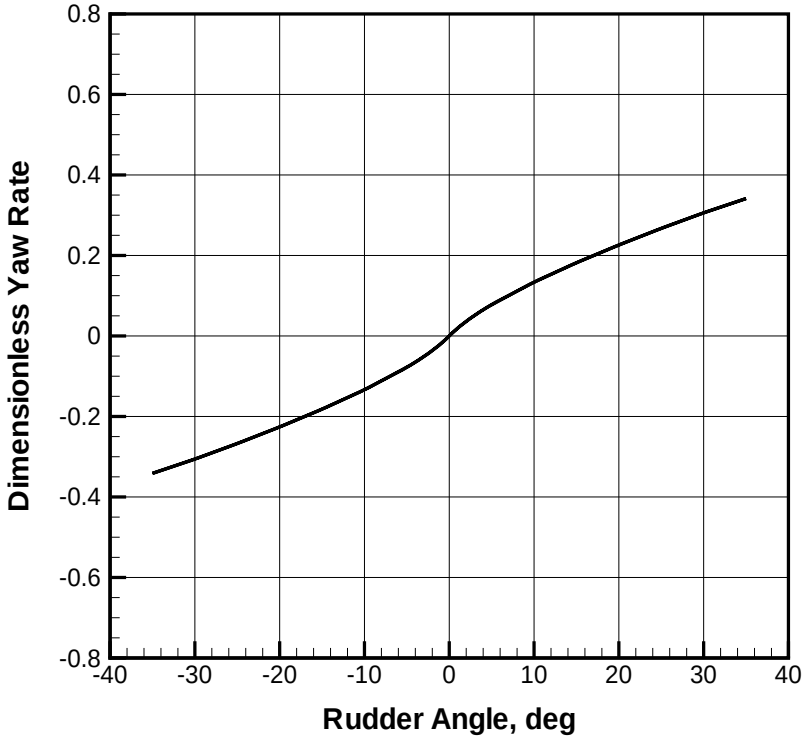

Figure 2.42: Spiral Curve: Even Keel, "Small" Rudder

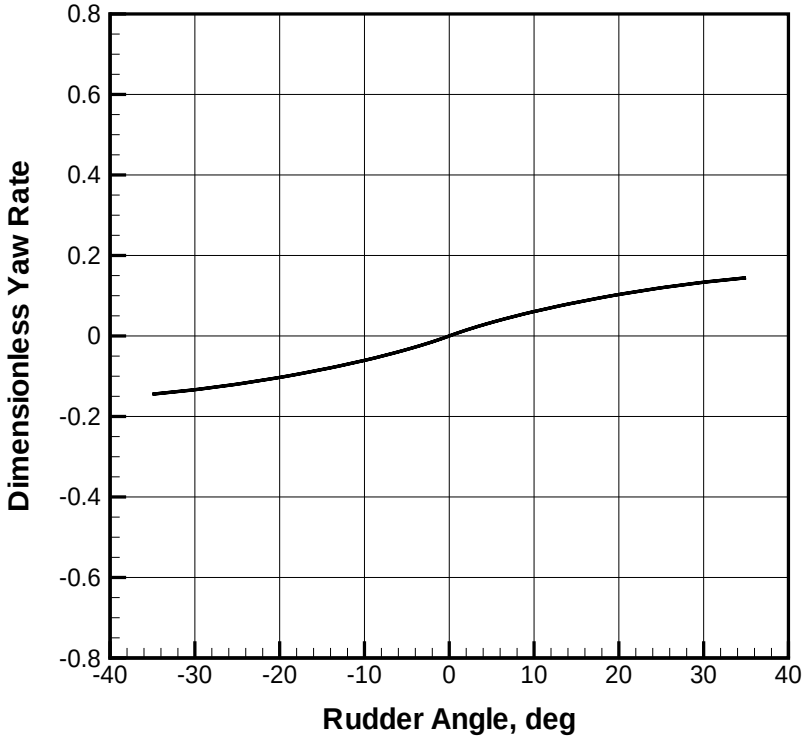

Figure 2.43: Spiral Curve: Even Keel, "Tiny" Rudder

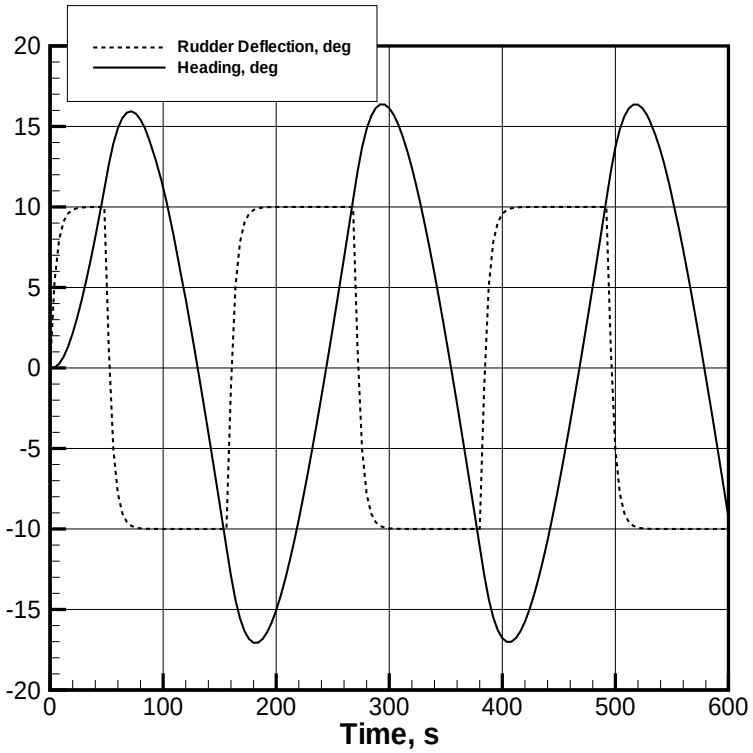

Figure 2.44: Zig-Zag Manoeuvre $10^o - 10^o$ Time Histories: Even Keel

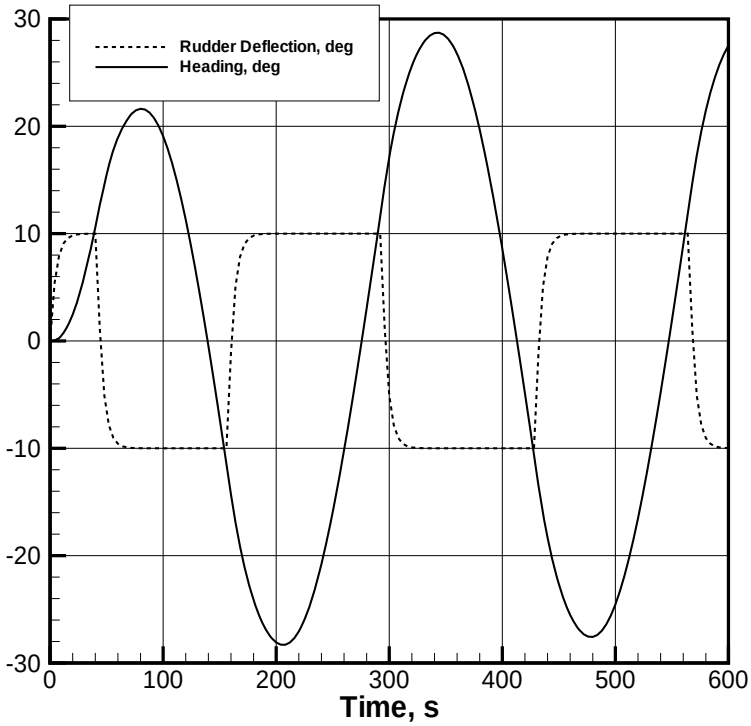

Figure 2.45: Zig-Zag Manoeuvre $10^o - 10^o$ Time Histories: Trim by the Bow

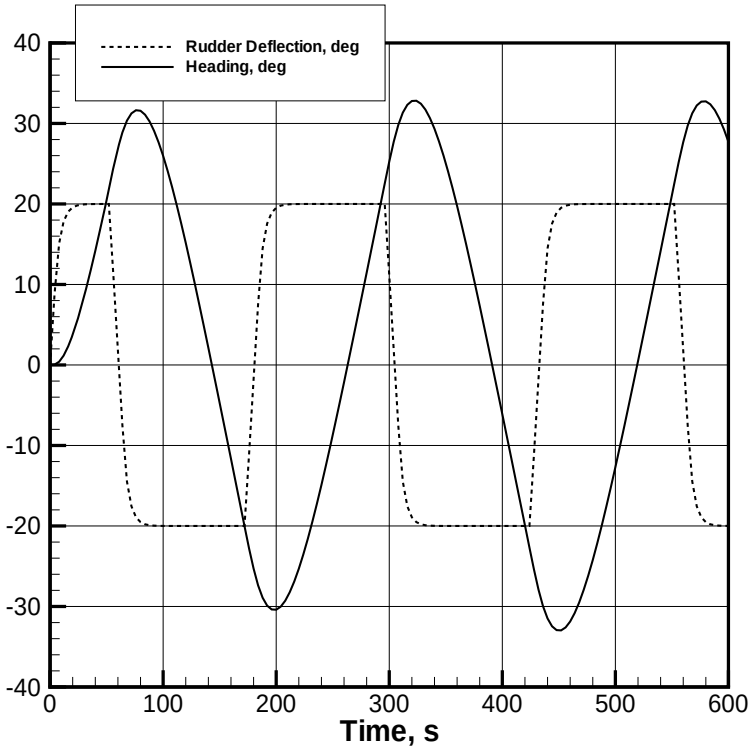

Figure 2.46: Zig-Zag Manoeuvre $20^o - 20^o$ Time Histories: Even Keel

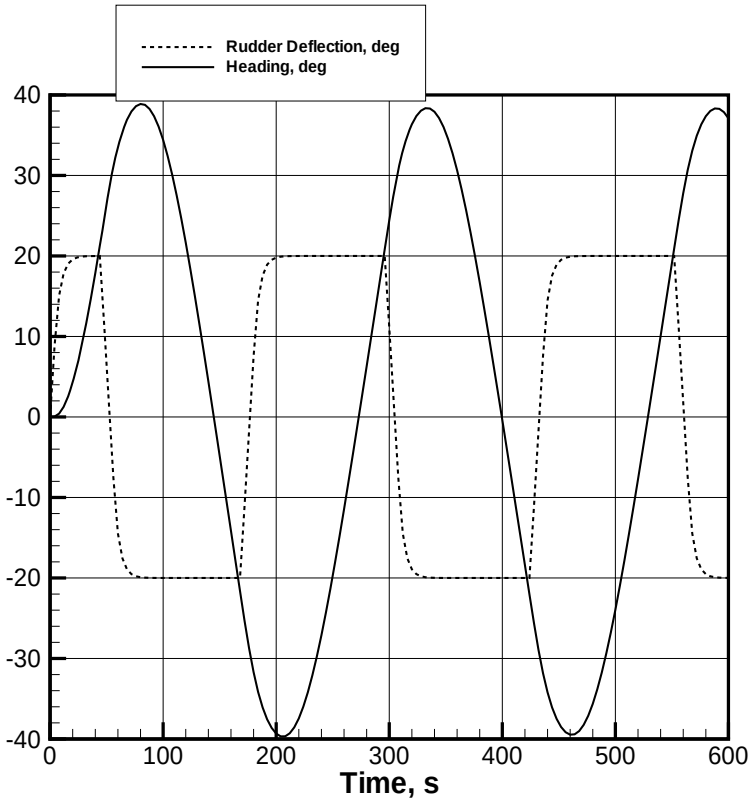

Figure 2.47: Zig-Zag Manoeuvre $20^o - 20^o$ Time Histories: Trim by the Bow

some crisp and simple criterion of directional stability. This will be done in the following material on the basis of linear model analysis.

Chapter 3

Ship Dynamic Properties: Linear Analysis

3.1 Linearised Ship Mathematical Models

General Case. The general ship manoeuvring mathematical model is nonlinear and described by eq. (2.236). Linearising this model means that we construct a linear matrix differential equation which would be equivalent to the primary nonlinear equation in some sense. The general form of the linearised model will be:

$$M\dot{x} = A_0 x + B_0 U, \tag{3.1}$$

where A_0 and B_0 are the system defining matrices with the dimensions $k \times k$ and $k \times \ell$ respectively.

Typically, to obtain the defining matrices, the nonlinear vector function $F(x, U)$ is expanded in Taylor series in the vicinity of some equilibrium point $(x^{(0)}, U^{(0)})$:

$$F(x,U) = F(x^{(0)},U^{(0)}) + \frac{\partial F}{\partial x}(x^{(0)},U^{(0)})(x - x^{(0)}) + \frac{\partial F}{\partial U}(x^{(0)},U^{(0)})(U - U^{(0)}) + \dots. \tag{3.2}$$

As at the equilibrium point $F(x^{(0)}, U^{(0)}) \equiv 0$, the equation (3.1) will follow from eq. (3.2) when $A_0 = \frac{\partial F(x,U)}{\partial x}(x^{(0)}, U^{(0)})$ and $B_0 = \frac{\partial F(x,U)}{\partial U}(x^{(0)}, U^{(0)})$ i.e. they are the Jacobi matrices and, further, x and U have the sense of their deviations from the equilibrium values i.e. $x := x - x^{(0)}$ and $U := U - U^{(0)}$. Usually the uniform straight motion is taken as the equilibrium state. Then, the surge velocity will be equal to the ship's speed and all the remaining parameters will be zero.

Of course, it is also possible to write the model (3.1) in the form:

$$\dot{x} = A_D x + B_C U. \tag{3.3}$$

Here: $A_D = M^{-1}A_0$ is called the system dynamics matrix and $B_C = M^{-1}B_0$ is the control matrix.

This representation of the linearised mathematical model is standard in the linear control theory and serves as basis for synthesizing automatic controllers and for investigation of the model's properties. The most evident possibility is to find eigenvalues of the matrix A which will make possible drawing important conclusions about the system's stability and apply some regular methods of the controller's synthesis.

However, not all the eigenvalues are of equal importance. It was found that the two eigenvalues corresponding to dynamics of the ship's lateral motion bring the most valuable information about the ship's dynamic properties. These eigenvalues will be found below with elementary means together with other useful information.

Linearised Model For Plane Lateral Motion. The first four dynamic equations of the set (2.212) are taken as basis. It can be easily demonstrated that within the linear approximation, the surge equation becomes independent from the remaining ones. Moreover, in most cases, account for the roll motion does not change significantly results of the analysis. So, it will only be necessary to consider the sway-yaw equations. In the linearised form they can be represented as

$$\begin{aligned}(m+\mu_{22})\dot{v}+mVr &= Y_{Hv}v+Y_{Hr}r+Y_{Rv}v+Y_{Rr}r+Y_{R\delta}\delta_R,\\ (I_{zz}+\mu_{66})\dot{r} &= N_{Hv}v+N_{Hr}r+N_{Rv}v+N_{Rr}r+N_{R\delta}\delta_R,\end{aligned} \tag{3.4}$$

where $Y_{Hv},\ldots,N_{R\delta}$ are linear hydrodynamic derivatives whose values must be obtained from the full mathematical model. It is convenient, for future applications, to introduce the following parameters:

$$\begin{aligned}Y_v &= -Y_{Hv}-Y_{Rv};\quad Y_r=mV-Y_{Hr}-Y_{Rr};\quad Y_\delta=Y_{R\delta},\\ N_v &= -N_{Hv}-N_{Rv};\quad N_r=-N_{Hr}-N_{Rr};\quad N_\delta=N_{R\delta}.\end{aligned} \tag{3.5}$$

Then, the linearised set is represented as

$$\begin{aligned}(m+\mu_{22})\dot{v}+Y_vv+Y_rr &= Y_\delta\delta_R,\\ (I_{zz}+\mu_{66})\dot{r}+N_vv+N_rr &= N_\delta\delta_R.\end{aligned} \tag{3.6}$$

3.2 Analysis and Transformations of the 2DOF Linear Model

Application of Laplace Transform and Transfer Functions. It is convenient to pass from the time domain to the domain of the complex variable s applying the Laplace transform $\mathcal{L}$ to all variables involved in the set (3.6):

$$V(s)=\mathcal{L}[v(t)];\quad R(s)=\mathcal{L}[r(t)];\quad \Delta(s)=\mathcal{L}[\delta_R(t)], \tag{3.7}$$

where the uppercase symbols are the Laplace transforms of the corresponding time variables.

The Laplace transforms for the time derivatives will be:

$$\begin{aligned} \mathcal{L}[\dot{v}] &= sV(s) - v_0, \\ \mathcal{L}[\dot{r}] &= sR(s) - r_0, \end{aligned} \tag{3.8}$$

where v_0 and r_0 are the intiual values of the sway velocity and yaw rate respectively.

Then, applying the Laplace transform to the both sides of the set (3.6) we will obtain, due to its linearity, the following set of linear algebraic equations with respect to $V(s)$ and $R(s)$:

$$\begin{aligned} [(m+\mu_{22})s + Y_v]V(s) + Y_r R(s) &= Y_\delta \Delta(s) + (m+\mu_{22})v_0, \\ N_v V(s) + [(I_{zz}+\mu_{66})s + N_r]R(s) &= N_\delta \Delta(s) + (I_{zz}+\mu_{66})r_0. \end{aligned} \tag{3.9}$$

This set can be easily solved analytically with the Kramer formulae. Namely,

$$\begin{aligned} V(s) &= D_V/D_0, \\ R(s) &= D_R/D_0, \end{aligned} \tag{3.10}$$

where the main determinant is

$$D_0 = \begin{vmatrix} (m+\mu_{22})s + Y_v & Y_r \\ N_v & (I_{zz}+\mu_{66})s + N_r \end{vmatrix} = As^2 + Bs + C, \tag{3.11}$$

and where

$$\begin{aligned} A &= (m+\mu_{22})(I_{zz}+\mu_{66}), \\ B &= (m+\mu_{22})N_r + (I_{zz}+\mu_{66})Y_v, \\ C &= Y_v N_r - Y_r N_v \end{aligned} \tag{3.12}$$

are the so=called hydrodynamic aggregates.

The remaining two determinants are:

$$\begin{aligned} D_V &= \begin{vmatrix} Y_\delta \Delta(s) + (m+\mu_{22})v_0 & Y_r \\ N_\delta \Delta(s) + (I_{zz}+\mu_{66})r_0 & (I_{zz}+\mu_{66})s + N_r \end{vmatrix}, \\ D_R &= \begin{vmatrix} (m+\mu_{22})s + Y_v & Y_\delta \Delta(s) + (m+\mu_{22})v_0 \\ N_v & N_\delta \Delta(s) + (I_{zz}+\mu_{66})r_0 \end{vmatrix}. \end{aligned} \tag{3.13}$$

After certain evident evaluations, the solutions $V(s)$ and $R(s)$ can be represented as:

$$\begin{aligned} V(s) &= W_{\delta v}(s)\Delta(s) + W_{v_0 v}(s)v_0 + W_{r_0 v}(s)r_0, \\ R(s) &= W_{\delta r}(s)\Delta(s) + W_{v_0 r}(s)v_0 + W_{r_0 r}(s)r_0, \end{aligned} \tag{3.14}$$

where $W(s)$ with various subscripts are the ship transfer functions from the rudder angle and initial conditions. Each of them is a regular rational function:

$$\begin{aligned} W_{\delta v}(s) &= \frac{Ds+E}{As^2+Bs+C}, & W_{v_0 v}(s) &= \frac{d_v s + e_v}{As^2+Bs+C}, \\ W_{r_0 v}(s) &= \frac{-(I_{zz}+\mu_{66})Y_r}{As^2+Bs+C}, & W_{\delta r}(s) &= \frac{Fs+G}{As^2+Bs+C}, \\ W_{v_0 r}(s) &= \frac{-(m+\mu_{22})N_v}{As^2+Bs+C}, & W_{r_0 r}(s) &= \frac{f_r s + g_r}{As^2+Bs+C}, \end{aligned} \tag{3.15}$$

and where

$$\begin{aligned} D &= (I_{zz} + \mu_{66})Y_\delta, & E &= Y_\delta N_r - N_\delta Y_r, \\ F &= (m + \mu_{22})N_\delta, & G &= N_\delta Y_v - Y_\delta N_v, \\ d_v &= f_r = A, & e_v &= (m + \mu_{22})N_r, \quad g_r = (I_{zz} + \mu_{66})Y_v. \end{aligned} \tag{3.16}$$

It can be easily established that $e_v + g_r = B$.

Eigenvalues, Ship Gain and Time Lags It can be demonstrated that the roots of the characteristic equation

$$D_0(s) = As^2 + Bs + C = 0 \tag{3.17}$$

are the eigenvalues of the matrix A_D as in eq. (3.3). These roots are:

$$\begin{aligned} s_1 &= \frac{-B + \sqrt{B^2 - 4AC}}{2A}, \\ s_2 &= \frac{-B - \sqrt{B^2 - 4AC}}{2A}. \end{aligned} \tag{3.18}$$

Analysis of the hydrodynamic aggregates A, B, C shows that for any surface displacement ship:

1. A and B are always positive (why?).
2. C can be positive, or negative, or zero.
3. The discriminant $B^2 - 4AC$ is always positive (even when $C > 0$).

It is known from the general stability theory (or, in particular—from the corresponding chapter of the control theory) that the neccessary condition of the stability (or, to be more precise, of the *asymptotic* stability) of any dynamic system described with ODE is that all the coefficients of the system's characteristic polynomial be of the same sign. It is also proven that for all first- or second-order systems this condition is also sufficient. Hence, the first criterion of the ship's directional stability is simply

$$C > 0. \tag{3.19}$$

Continuing analysis of the roots (eigenvalues) we shall easily establish that:

1. The both eigenvalues are always real.
2. The second eigenvalue s_2 is always negative.
3. The first eigen value s_1 can be either positive, or negative or zero and $\text{sign } p_1 = -\text{sign } C$.
4. The absolute value of s_2 is always sunstantially greater than that of s_1 or $|s_2| \gg |s_1|$.

When the characteristic polynomial's roots are known, it can be represented as

$$D_0(s) = A(s - s_1)(s - s_2). \tag{3.20}$$

The transfer function from the rudder angle to the angular velocity of yaw (see eq. (3.15)) is then

$$W_{\delta r}(s) = \frac{Fs + G}{A(s - s_1)(s - s_2)}. \tag{3.21}$$

This rational function can be also decomposed into sum of two partial fractions:

$$W_{\delta r}(s) = \frac{Q_1}{s - s_1} + \frac{Q_2}{s - s_2}, \tag{3.22}$$

where

$$Q_1 = \frac{Fs_1 + G}{A(s_1 - s_2)}, \qquad Q_2 = -\frac{Fs_2 + G}{A(s_1 - s_2)}. \tag{3.23}$$

From the viewpoint of the control theory, it means that a ship, as a linear dynamic system, can be represented as parallel connection of two first-order aperiodic plants, each connected consecutively with a proportional plant. To represent the aperiodic plants in the standard form, let us introduce the time lags T_1 and T_2 as

$$T_1 = -1/s_1, \qquad T_2 = -1/s_2. \tag{3.24}$$

Then,

$$W_{\delta r}(s) = \frac{K_1}{T_1 s + 1} + \frac{K_2}{T_2 s + 1}, \tag{3.25}$$

where $K_i = T_i Q_i, i = 1, 2$ are the new gains.

It is known from the general control theory that a transfer function can be interpreted as the Laplace transform of the system's time-domain reaction to a unity step excitation which means that in the considered case the excitation should be $\delta_R(t) = H(t)$, where $H(t)$ is the Heavyside step function. Then, applying the inverse Laplace transform to (3.25) we shall obtain for the ship's response to the instantaneous rudder deflection by a 1 radian angle:

$$r(t) = Q_1 e^{s_1 t} + Q_2 e^{s_2 t}. \tag{3.26}$$

The second term of the response always decays rapidly as $s_2 < 0$ and relatively large by its absolute value. This component does only contribute to the ship's behaviour during a short interval immediately after the rudder's deflection.

The first term in eq. (3.26) either decays (at $s_1 < 0$) though at much slower rate, or tends to infinity at $s_1 > 0$[1].

So, the behaviour of the whole solution (3.26) agrees well with the common understanding of the stable or unstable motion at $s_1 < 0$ and $s_1 > 0$ respectively.

Similar responses can be obtained using another transfer functions defined in (3.15) which permits, at least for the linear model, not to distiguish between the stability with respect to the control perturbations (rudder deflections) and with respect to initial conditions with the rudder fixed.

[1] At $s_1 = 0$ it will remain constant but this case is unlikely

Nomoto Equations.

Using the ship time lags as defined by eq. (3.24), it is possible to represent the transfer function $W_{\delta r}(s)$ in the following way:

$$W_{\delta r}(s) = \frac{K(T_3 s + 1)}{(T_1 s + 1)(T_2 s + 1)}, \tag{3.27}$$

where $K = G/C$ is the ship's gain, and $T_3 = F/G$ is the third ship time lag.

Analyzing definitions of F and G (eq. (3.16)) we can conclude that these parameters are always positive. Hence, T_3 is also always positive and sign K = sign C, i.e. the ship gain is positive for directionally stable ships and it is negative for unstable ships. It is also clear from the transfer function's structure that the ship can be represented as consecutive connection of 4 elementary plants: a proportional plant with the gain K, two first-order aperiodic plants with time lags T_1 and T_2 and with the forcing plant with the time constant T_3:

$$W_{\delta r}(s) = K \cdot \frac{1}{T_1 s + 1} \cdot \frac{1}{T_2 s + 1} \cdot (T_3 s + 1). \tag{3.28}$$

On the other hand, the same transfer function can be represented as

$$W_{\delta r}(s) = \frac{K(T_3 s + 1)}{T_1 T_2 s^2 + (T_1 + T_2)s + 1}. \tag{3.29}$$

Considering the zero-initial-condition case, we shall obtain the following connection between the Laplace image of the rudder angle $\Delta(s)$ and the rate of turn's image $R(s)$:

$$R(s) = W_{\delta r}(s)\Delta(s) = \frac{K(T_3 s + 1)\Delta(s)}{T_1 T_2 s^2 + (T_1 + T_2)s + 1} \tag{3.30}$$

or

$$[T_1 T_2 s^2 + (T_1 + T_2)s + 1]R(s) = K(T_3 s + 1)\Delta(s). \tag{3.31}$$

Applying now the inverse Laplace transform $\mathcal{L}^{-1}$ to the both sides of eq. (3.31) we shall obtain the following isolated differential equation of yaw:

$$T_1 T_2 \ddot{r} + (T_1 + T_2)\dot{r} + r = K(\delta_R(t) + T_3 \dot{\delta}_R). \tag{3.32}$$

This equation is usually called the Nomoto second-order equation of yaw and, as $\dot{\psi} = r$, can be also represented as

$$T_1 T_2 \dddot{\psi} + (T_1 + T_2)\ddot{\psi} + \dot{\psi} = K(\delta_R(t) + T_3 \dot{\delta}_R(t)). \tag{3.33}$$

The equation (3.32) can be also represented in the state-space form i.e. as a set of first-order equations:

$$\begin{aligned} \dot{r} &= a_r + \frac{KT_3}{T_1 T_2}\delta_R, \\ T_1 T_2 \dot{a}_r &= K\left(1 - \frac{T_3}{T_2} - \frac{T_3}{T_1}\right)\delta_R - (T_1 + T_2)a_r - r, \end{aligned} \tag{3.34}$$

where a_r is the auxiliary state variable defined in such a way that that the rudder angle derivative be removed from the right-hand side which benefits sensibly numerical integration of this equation.

All these transformations did not change the order of the linear mathematical model (2) of the sway–yaw motion and, moreover, the Nomoto equation or the set (3.34) are completely equivalent to the primary set (3.4). However, the vector of state variables is now diffferent: instead of $(v, r)^T$ we have $(r, a_r)^T$. That is, the new state includes the angular acceleration in yaw but the sway velocity is no longer present.

Applying a similar procedure to the transfer function $W_{\delta v}(s)$, it will be possible to obtain an isolated drift equation which, however, could not find applications comparable to those of the Nomoto equation. Probably, the main reason for this "non-symmetry" is a much better observability of the heading angle and of the rate of turn compared to observability of the velocity of sway or drift angle. Measuring any of the two latter parameters presented, until recently, serious problems. Nowadays, with application of high-precision GPS sensors, this is already possible but still costs and errors are substantially higher than when measuring the rate of turn. Also, the heading angle is a more important parameter from the viewpoint of ship navigation.

As $|T_1| \gg |T_2|$ for any surface diplacement ship, it was found reasonable to create a simpler, lower-order, yawing model neglecting the boundary-layer effects related to faster components of the transients.

It is known from theory of the Laplace transform that for any function $W(s) = \mathcal{L}[w(t)]$:

$$\lim_{s\to 0} sW(s) = \lim_{t\to\infty} w(t). \tag{3.35}$$

and also

$$\lim_{s\to \infty} sW(s) = \lim_{t\to +0} w(t). \tag{3.36}$$

These properties can be also interpreted as a similarity in the asymptotic behaviour of the function and its Laplace image. Namely, it can be said that asymptotics of the transfer function at $s \to 0$ corresponds to asymptotics of the transient at $t \to \infty$ and vice versa. So, if we want to get rid of faster components at large t, we must obtain a simpler asymptotic form of the transfer function at small $|s|$.

Consider now asymptotics of the transfer function $W_{\delta r}(s)$ at $s \to 0$:

$$W_{\delta r}(s) = \frac{K(1+T_3 s)}{1+(T_1+T_2)s+T_1T_2s^2} \sim \frac{K(1+T_3 s)}{1+(T_1+T_2)s} \sim \frac{K}{1+(T_1+T_2-T_3)s}. \tag{3.37}$$

Hence, the simplified (lower-order) transfer function $W^1_{\delta r}(s)$ is

$$W^1_{\delta r}(s) = \frac{K}{1+Ts}, \tag{3.38}$$

where $T = T_1 + T_2 - T_3$ is the equivalent time lag.

Returning now to the time domain, we obtain the following differential equation of yaw:

$$T\dot{r} + r = K\delta_R, \tag{3.39}$$

which is called the first-order Nomoto equation.

Numerical estimations show that for any surface displacement ship sign T = sign T_1 and, hence, $T > 0$ for directionally stable ships and $T < 0$ in the opposite case.

Within the range of applicability of the linear model, the first-order Nomoto equation provides, in spite of its simplicity, very resonable predictions of the ship's transient in yaw except for a very small initial time interval where the difference with the solution of the second-order equation can be considerable. Asymptotics at small time values can be explored separately.

Assume that the constant rudder angle δ_R is applied instantly. At first time moment, the angular velocity is still zero, the corresponding term in the Nomoto equation can be dropped and the initial angular acceleration is

$$\dot{r}(0) = \frac{K}{T}\delta_R. \tag{3.40}$$

It is interesting and important to notice that the initial angular acceleration parameter $P_1 = K/T$ is always positive as K and T are always of the same sign. It means that any ship, no matter directionally stable or unstable, will always react "correctly" to the rudder's execute performed from the straight-motion state.

The initial acceleration predicted by the second-order Nomoto equation (or by the primary linear model of the sway-yaw motion) is somewhat more difficult to evaluate. The simplest way is to find, first, asymptotics of the transfer function $W_{\delta r}(s)$ as $s \to \infty$ which corresponds to $t \to 0$:

$$W_{\delta r}(s) \sim \frac{KT_3 s}{T_1 T_2 s^2} = \frac{KT_3}{T_1 T_2 s}, \tag{3.41}$$

which will result in the following asymptotic form of the yaw equation:

$$T_1 T_2 \dot{r} = KT_3 \delta_R \tag{3.42}$$

and then

$$\dot{r}(0) = \frac{KT_3}{T_1 T_2}\delta_R. \tag{3.43}$$

Usually, $T_3 > T_2$ and the first-order equation will underestimate the ship response immediately after the rudder's deflection.

In steady turn, i.e. when $\dot{r} \equiv 0$, the both Nomoto equation and any other linear sway-yaw model will reduce to a proportional plant:

$$r = K\delta_R. \tag{3.44}$$

The equation (3.44) represents in fact spiral response according to the linearised model. The ship gain K defines the steepness and the direction of the straight line describing this response (Fig. 2.31 and 2.37). For directionally unstable ships, $K < 0$ and the steady turn response line goes from 4th to 2nd quadrant as shown on Fig. 2.37. It is clear that in this case, the linear-model approximation is in no way a good approximation to the actual nonlinear model although it can be used for stability analysis.

The Nomoto equations can also be re-written in the non-dimensional form:

$$//T_1'T_2'\ddot{r}' + (T_1' + T_2')\dot{r}' + r' = K'(\delta_R + T_3'\dot{\delta}_R)T_1'T_2'\ddot{r}' + (T_1' + T_2')\dot{r}' + r' = K'(\delta_R(t') + T_3\dot{\delta}_R(t')), \quad (3.45)$$

$$T'\dot{r}' + r' = K'\delta_R(t'), \quad (3.46)$$

where the upper dot means a derivative with respect to the dimensionless time t' and the dimensionless parameters are:

$$T_i' = T_i/T_{ref}, i = 1, 2, 3; \qquad K' = KT_{ref}. \quad (3.47)$$

Common Perception of Ship Directional Stability

Introductory remarks. All seaman know very well that different ships can behave very differently on the straight course, i.e. when the commnand "Steady as she goes!" is executed, even when they are sailing under similar conditions and are steered by equally trained and experienced helmsmen. Some ships are known to keep the straight course well while others are prone to excessive yawing. It would be natural to assume that in the first case the vessels possess good directional stability while in the second case the directional stability is poor. It is clear that reduced directional stability aggravates the helmsman's working conditions and finally can impair the navigational safety. Hence the concept of directional stability deserves a rather detailed and multi-aspect consideration.

For instance, any navigator in active duty can ask some very natural questions. For instance, what in general could be expected from ships with various degree of directional stability? What are specifics of their responses to the rudder deflections? What can be required in this respect from the ship owner from the navigators and helmsmen negotiating about jobs on this or that particular ship? Finally, why in general are built vessels with poor directional stability and in most cases these are not occasional design failures? If directionally stable vessels exist, why should not all the vessels be designed and built in this way?

In order to provide acceptable answers to these questions, it will be necessary to get a deeper insight into the problem. In particular, it will be necessary to introduce a few new concepts which already by themselves will somewhat clarify and complement the intuitive undestanding of the ship directional stability which served above as a starting point for our discussion.

Operational directional stability. The operational stability is a ship's ability to practically maintain the required heading with required precision with minimum rudder activity. That is, a ship possesses a better operational (or practical) stability when rarer and smaller (in average) rudder deflections under given environmental conditions are required to maintain the heading. Advantage of this concept is that it is in perfect agreement with the intuitive assessment of the stability being in fact its development. Certain quantitative measures of the operational stability, such as average frequency and amplitude of the rudder deflections, were also worked out. However, it is easy to see that all such measures not only will depend on the ship's properties but also on the helmsman's qualification, his fatigue, intensity of his work and, obviously on the sea state. That is why, the concept of operational stability turned out inconvenient for analyzing and comparing course-keeping properties of a given ship. A

more abstract but more robust concept of the *inherent* stability of a ship appeared to be much more suitable for such tasks. This concept will be introduced and analyzed in the following subsections.

Inherent Directional Stability and its Criteria

In fact, the concept of inherent directional stability of the ship in straight motion has already been mentioned more than once but here it will be treated in a more rigorous and systematic manner. The inherent stability can be also called "the rudder fixed stability" i.e. it is supposed that rudder is fixed at certain position and the ship in fact is not steered at all. In general, the rudder can be fixed at any deflection angle but the most interesting case directly linked with the straight course stability is when it is fixed in the neutral position and the ship is supposed to move straight without drift and rotation. In the ideal case of absence of disturbances, the ship must maintain this straight motion. Unfortunately, disturbances are always there and inspection of the rudder-fixed ship's reaction to a disturbance provides an initial insight into its inherent stability.

In the general stability theory, the most common is the concept of *local* stability of some base motion or equilibrium state as its particular case. Any process (motion, solution) $\bar{x}(t, x_0)$, where $x_0 = \bar{x}(0)$ is the initial condition, is called locally *stable* with respect to the initial conditions' perturbations if the process' perturbation $\delta x(t) = x(t, x_0 + \delta x_0) - \bar{x}(t, x_0)$ remains bounded as $t \to \infty$. If, on the contrary, $|\delta x(t)| \to \infty$ i.e. the perturbation motion is unbounded, the base motion is called *unstable* in the same sense. There is an important special case of the stable motion when $\delta x(t) \to 0$. The base motion is called then *asymptotically stable* i.e. stable and even more than that.

Observations and simulations of ship's behaviour on the straight course with the rudder fixed in neutral position show the following two variants of the ship's behaviour in terms of the angular velocity of yaw:

1. The angular velocity of yaw caused by a perturbation vanishes after the perturbation is lifted.
2. Under the same circumstances, the angular velocity of yaw does not tend to zero but to some final residual value $r_{0\pm}$.

The ship is called *directionally stable* in the first case. It means that it is asymptotically stable with respect to the rate of yaw. As the heading angle deviation is obtained from the rate of yaw process through integration, it is clear that the heading deviation will not tend to zero and the ship is not more than stable with respect to the heading angle. It means that once kicked out from the desired heading, a ship with the rudder fixed cannot restore that heading by itself.

In the second case, the ship remains stable with respect to the rate of yaw but not asymptotically: the angular velocity will not return to its zero value corresponding to the straight motion. As result, the ship will be unstable with respect to the heading angle as its perturbation will grow indefinitely as the ship is in a self-provoked steady turn. Naturally, such a ship is called *directionally unstable*.

Sometimes, wishing to emphasize that it goes about the rudder-fixed stability i.e. stability without intervention of a control system or human operator, used also is the term *inherently stable/unstable ship.*

While directionally stable ships behave more or less in accordance with the linear analysis' results, this is not quite so for unstable vessels: the linear theory predicts unbounded growth of the rate of yaw's absolute value (see eq. (3.26)) while in reality it remains finite. This happens because nonlinear components of the mathematical model come into action and stabilize the ship's motion though on a steady turn instead of a straight path. This steady turn, with the rudder amidship, is performed with the angular velocity $r_{s+}(0)$ or $r_{s-}(0)$ depending on the sign of the perturbation. A more detailed analysis demonstrates that any steady turn corresponding to a stable branch of the spiral curve is asymptotically stable.

Finally, let us sum up criteria of the directional stability/instability:

1. A ship is directionally stable on the straight path with the rudder fixed if $C > 0$, or $K > 0$, or $T_1 > 0$, or $s_1 < 0$, or $T > 0$, or the spiral curve does not show any loop (i.e. $r_{s+}(0) = r_{s-}(0) = 0$).

2. A ship is directionally unstable on the straight path with the rudder fixed if $C < 0$, or $K < 0$, or $T_1 < 0$, or $s_1 > 0$, or $T < 0$, or a hysteresis loop is present on the spiral curve.

3. A ship is called *marginally* stable on the straight path with the rudder fixed if $|C|$ and $|s_1|$ are close to zero. The linear steady response is then described with a vertical straight line.

The stability criterion $C > 0$ is sometimes given a more "physical" interpretation. It follows from definition of the parameter C (eq. (3.12)) that this criterion is equivalent to

$$Y_v N_r - Y_r N_v > 0. \tag{3.48}$$

As $Y_v > 0$ and $Y_r > 0$, this condition is, in its turn, equivalent to the following one

$$x_r > x_v, \tag{3.49}$$

where $x_r = N_r/Y_r$ and $x_v = N_v/Y_v$ are the arms of the yaw moments due to sway and yaw respectively. While the first moment is associated with the ship's deviation from initial path, the second one is associated with damping of this motion.

Finally, it must be emphasized that even directionally stable ships have a relatively small stability margin compared to many other moving objects. This makes possible reaching good turning ability with relatively small control surfaces. As, in practice, both stable and unstable ships require continuous rudder handling to maintain the required heading, there is no great difference in behaviour of slightly unstable and stable ships. In other words, merely all ships, except for a few pathological cases recorded in the shipbuilding history, are *practically* or *operationally* stable.

Chapter 4

External Factors in Ship Manoeuvring

Until now, we have mainly considered ship manoeuvring in absence of external perturbations, i.e. in calm weather and still, deep water. Most of time, sea-going vessels experience influence of a more or less strong wind and waves. When sailing in harbours and in approach channels, shallow-water condition is also possible, as well as hydrodynamic interaction with banks and other vessels. In berthing operations, tugs are often used for assistance. Current can be present in open sea, as well as in channels and rivers. Accounting for most of these factors constitutes subject of special areas of the ship manoeuvrability theory. Here, we shall only study effect of uniform current and constant wind which are the most important external factors.

4.1 Manoeuvring in Wind and Current

4.1.1 Kinematics

In general, three kinds of ship velocities can be considered:

1. Velocities with respect to water, or *water velocities*, or just velocities (by default) which determine hydrodynamic forces.
2. Velocities with respect to the sea bottom or *ground velocities*. These velocities define ship kinematics in the Earth-fixed frame and are necessary for computing the ship's position.
3. Velocities with respect to air or *air velocities*, or aerodynamic velocities. All aerodynamic forces will depend on them.

It is clear, that in absence of current and wind all three groups of velocities become identical. However, if this is not the case, it is necessary to establish relations between them. We shall assume that neither the current, nor the wind velocity fields do not contain rotational components and significant gradients. Then, it will be necessary to discriminate only between the linear velocities while all angular velocities with respect to water, ground and air remain identical.

We start with the same main frames as before (Fig. 2.1) assuming that present are: constant uniform current with the velocity $\mathbf{V}_c$ and uniform wind $\mathbf{V}_w$. These two vectors have angles χ_c and χ_w with respect to the ξ-axis respectively. The sign convention is the same as for other angles i.e. positive clockwise and the current and wind angles can be assumed to vary from 0 to 2π similarly to the heading and course angles. Also, shown are on the Figure the ground velocity $\mathbf{V}_G$ and the air velocity $\mathbf{V}_A$.

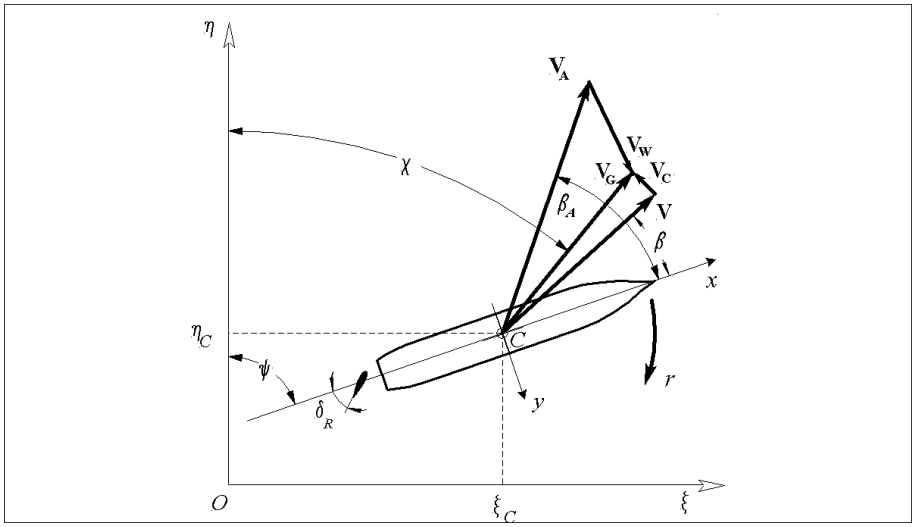

Figure 4.1: Main Kinematic Parameters in Presence of Wind and Current: all angles are positive; the current and wind angles are not shown

It is clear from the same figure that

$$\begin{aligned} \mathbf{V}_G &= \mathbf{V}_A + \mathbf{V}_w, \\ \mathbf{V}_G &= \mathbf{V} + \mathbf{V}_c \end{aligned} \tag{4.1}$$

and, hence,

$$\begin{aligned} \mathbf{V}_A + \mathbf{V}_w &= \mathbf{V} + \mathbf{V}_c, \\ \mathbf{V} &= \mathbf{V}_G - \mathbf{V}_c, \qquad (4.2) \\ \mathbf{V}_A &= \mathbf{V}_G - \mathbf{V}_w = \mathbf{V} + \mathbf{V}_c - \mathbf{V}_w. \qquad (4.3) \end{aligned}$$

All these velocities can be decomposed in Earth-fixed and body-fixed axes:

$$\begin{aligned} \mathbf{V}_w &= V_{w\xi}\mathbf{e}_\xi + V_{w\eta}\mathbf{e}_\eta = u_w\mathbf{e}_x + v_w\mathbf{e}_y, \\ \mathbf{V}_c &= V_{c\xi}\mathbf{e}_\xi + V_{c\eta}\mathbf{e}_\eta = u_c\mathbf{e}_x + v_c\mathbf{e}_y, \\ \mathbf{V}_A &= u_A\mathbf{e}_x + v_A\mathbf{e}_y, \\ \mathbf{V}_G &= u_G\mathbf{e}_x + v_G\mathbf{e}_y, \end{aligned} \tag{4.4}$$

where

$$\begin{aligned} V_{w\xi} &= V_w\cos\chi_w; \qquad & V_{w\eta} &= V_w\sin\chi_w, \\ V_{c\xi} &= V_c\cos\chi_c; \qquad & V_{c\eta} &= V_c\sin\chi_c, \end{aligned} \tag{4.5}$$

and $V_w = |\mathbf{V}_w|$ and $V_c = |\mathbf{V}_c|$ are the wind speed and the current speed respectively.

The water, air and ground quasi-velocities are connected to each other with the following relations:

$$\begin{aligned} u_G &= u + u_c; \qquad & v_G &= v + v_c, \\ u_A &= u_G - u_w; \qquad & v_A &= v_G - v_w, \end{aligned} \tag{4.6}$$

where

$$\begin{aligned} u_c &= V_{c\xi}\cos\psi + V_{c\eta}\sin\psi, \\ v_c &= -V_{c\xi}\sin\psi + V_{c\eta}\cos\psi, \\ u_w &= V_{w\xi}\cos\psi + V_{w\eta}\sin\psi, \\ v_w &= -V_{w\xi}\sin\psi + V_{w\eta}\cos\psi. \end{aligned} \tag{4.7}$$

Any of three couples of these quasi-velocities can be included into the state vector. In most cases, water-relative velocities u, v are preferred.

Useful will be the air drift angle β_A defined as

$$\beta_A = \begin{cases} -\arcsin v'_A & \text{at} \quad u_A \geq 0, \\ -\pi\,\mathrm{sign}\; v_A + \arcsin v'_A & \text{at} \quad u_A < 0, \end{cases} \tag{4.8}$$

where $v'_A = v_A/V_A$ and $V_A = |\mathbf{V}_A|$ is the ship's air speed equal to the relative wind speed as measured aboard the ship.

The generalized equations of motion according to the Inoue model will be:

$$\begin{aligned} (m+\mu_{11})\dot{u} - (m + C_m\mu_{22})v_G r &= X_H + X_P + X_R + X_A, \\ (m+\mu_{22})\dot{v} + mu_G r &= Y_H + Y_R + Y_A, \\ (I_{zz}+\mu_{66})\dot{r} &= N_H + N_R + N_A, \\ (I_{xx}+\mu_{44})\dot{p} + K_p p + mgGM\sin\varphi &= K_H + K_R + K_A, \\ \dot{\xi}_C &= u_G\cos\psi - v_G\sin\psi, \\ \dot{\eta}_C &= u_G\sin\psi + v_G\cos\psi, \\ \dot{\psi} &= r, \\ \dot{\varphi} &= p, \end{aligned} \tag{4.9}$$

The difference with the the original equations (2.212) is that the aerodynamic forces and moments X_A, Y_A, N_A, K_A are added to the right-hand sides and the ground velocities now enter into the right-hand sides of kinematic equations for the advance and transfer. The subscript at their symbols is replaced to avoid confusion with the the same subscript meaning "ground". No special current forces entered into the equations as the uniform homogeneous current is only acting kinematically: a moving inertial frame could have been attached to the moving water and the dynamic equations are identical for all such frames.

Finally the true course angle (i.e. the direction of the ground velocity) is defined as:

$$\chi = \begin{cases} \text{atan}\,\frac{\dot\eta_C}{\dot\xi_C} & \text{at} \quad \dot\xi_C > 0, \dot\eta_C > 0, \\ \pi + \text{atan}\,\frac{\dot\eta_C}{\dot\xi_C} & \text{at} \quad \dot\xi_C < 0, \\ 2\pi + \text{atan}\,\frac{\dot\eta_C}{\dot\xi_C} & \text{at} \quad \dot\xi_C > 0, \dot\eta_C < 0 \end{cases} \tag{4.10}$$

4.1.2 Aerodynamic Forces on a Ship

It is clear from general considerations that any aerodynamic force/moment component F_A must depend on the ship's air speed V_A, air drift angle β_A, air density ρ_A, heel angle ϕ and on some reference area which can be either the lateral above-water area A_L (used for any component), or the frontal above-water area (sometimes used for the surge force only). Then, the forces and moments are represented as

$$\begin{aligned} X_A &= C_X(\beta_A)\frac{\rho_A V_A^2}{2}A_L, \\ Y_A &= C_Y(\beta_A)\frac{\rho_A V_A^2}{2}A_L, \\ N_A &= C_N(\beta_A)\frac{\rho_A V_A^2}{2}A_L L_{OA}, \\ K_A &= C_K(\beta_A)\frac{\rho_A V_A^2}{2}A_L H_M, \end{aligned} \tag{4.11}$$

where C_X, C_Y, C_N, C_K are the force/moment aerodynamic coefficients, L_{OA} is the ship's length overall and $H_M = A_L/L_{OA}$ is the mean height of the lateral area.

The aerodynamic coefficients are mainly determined by means of wind tunnel tests. They can also depend on the Reynolds number and on the turbulence coefficient which in model tests can be different from those in the full scale. However, the above-water forms of most vessels are not streamlined, have relatively sharp edges and fixed separation regions which is reducing greately the scale effect. Hence, it is commonly believed that the coefficients obtained from model tests are trustworthy without any scale-effect corrections.

Data on aerodynamic characteristics of ships can also be found in the literature. For instance, a good collection of data obtained by Blendermann is presented in [26]. In general, the characteristic depend substantially on the confuguration of the above-water part of the ship but, as a first averaged approximation, the following formulae [38] can be used:

$$\begin{aligned} C_X(\beta_A) &= -C_{X0}\frac{A_T}{A_L}\cos\beta_A, \\ C_Y(\beta_A) &= C_{Y0}\sin\beta_A\cos\varphi, \\ C_N(\beta_A) &= C_Y(\beta_A)x'_A(\beta_A), \\ C_K(\beta_A) &= -C_Y(\beta_A)z'_A(\beta_A), \end{aligned} \tag{4.12}$$

where the dimensionless arms are:

$$\begin{aligned} x'_A(\beta_A) &= x'_{A0} + \frac{1}{4} - \frac{|\beta_A|}{2\pi}, \\ z'_A(\beta_A) &= \kappa_A(B/H_M)z'_{A0}, \end{aligned} \tag{4.13}$$

where $x'_{A0} = x_{A0}/L_{OA}$, $z'_{A0} = z_{A0}/H_M$, and x_{A0} and z_{A0} are the co-ordinates of the lateral area's centroid, and the coefficient κ_A depends also on the B/H_M ratio and on specifics of the form of superstructures and varies mostly between 0.8 and 2.0 for various hulls [26].

Calculations according to the presented formulae at $C_{X0} = 1.0$, $C_{Y0} = 1.05$ and $\varphi = 0$ were compared with the Blendermann data. In the case of surge and sway forces, comparison was made with all the models as the formulae do not contain any shape parameters and thus pretend to be universally applicable. As can be seen from the plots at Fig. 4.2 and 4.3, these formulae give reasonable estimates conservative for most ships although the errors for some particular models can be substantial. Predictions for the yaw moment depend substantially

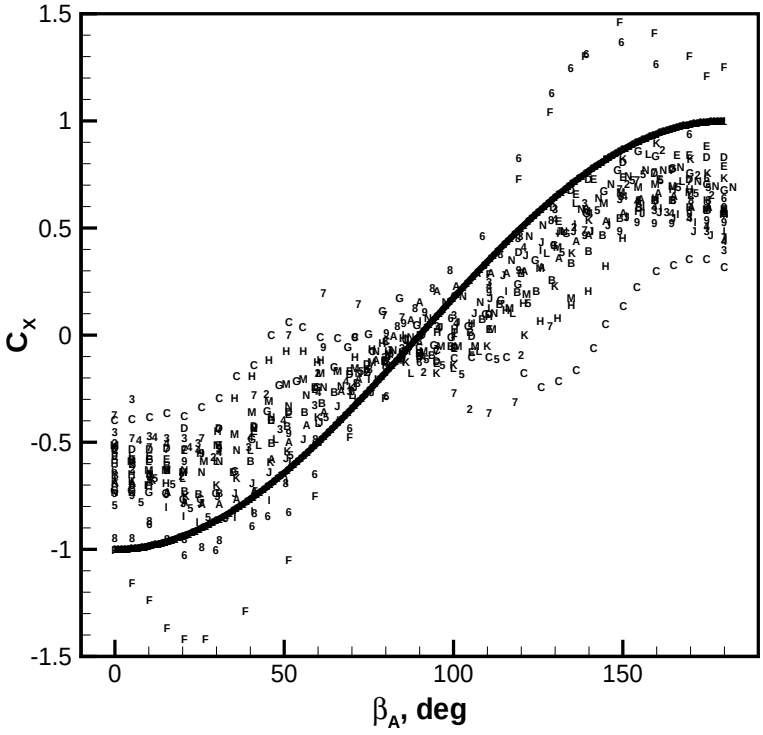

Figure 4.2: Aerodynamic surge force coefficient nondimensionalized by the frontal area: solid line—calculation; symbols—experimental data from [26]

on the longitudinal position of the lateral area's centroid and they were carried out for 5 values of this parameter and compared with the experimental data corresponding to models with similar characteristics (Fig. 4.4). Again, it is seen that the agreement is reasonable and the simple method catches the trend correctly.

Approximation of the heeling moment is the most problematic as in this case not only the vertical position of the centroid is important (z'_{A0} varies from -0.5 to -0.8 for practically all ships) but also the breath-to-height ratio and the shape's particulars accounted for by factor κ for which is difficult to develop a suitable regression model. So, in this case, the comparison (Fig. 4.5) is only shown for the model No. 18 from [26]. That model had $B/H_M = 1.82$ and,

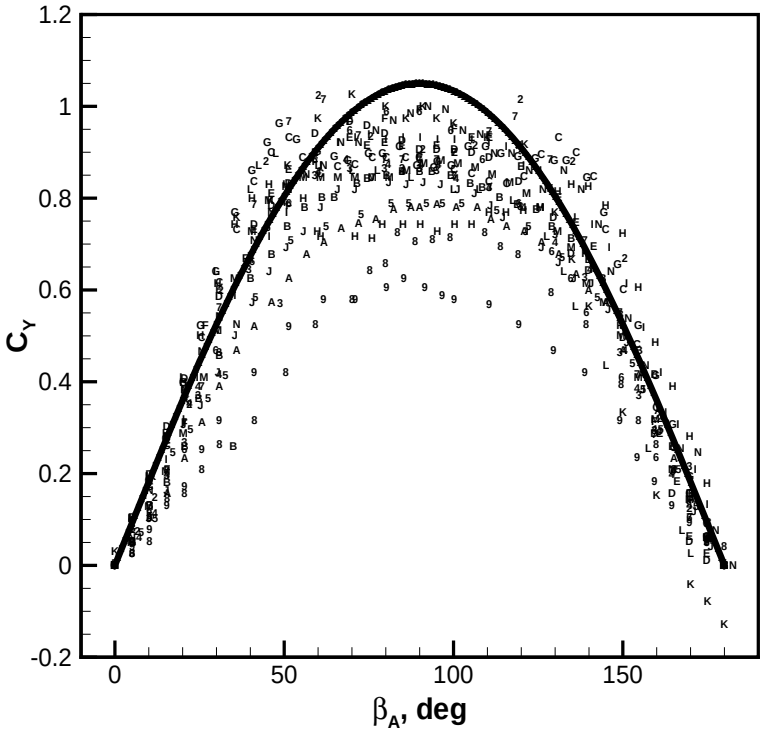

Figure 4.3: Aerodynamic sway force coefficient: solid line—calculation; symbols—experimental data from [26]

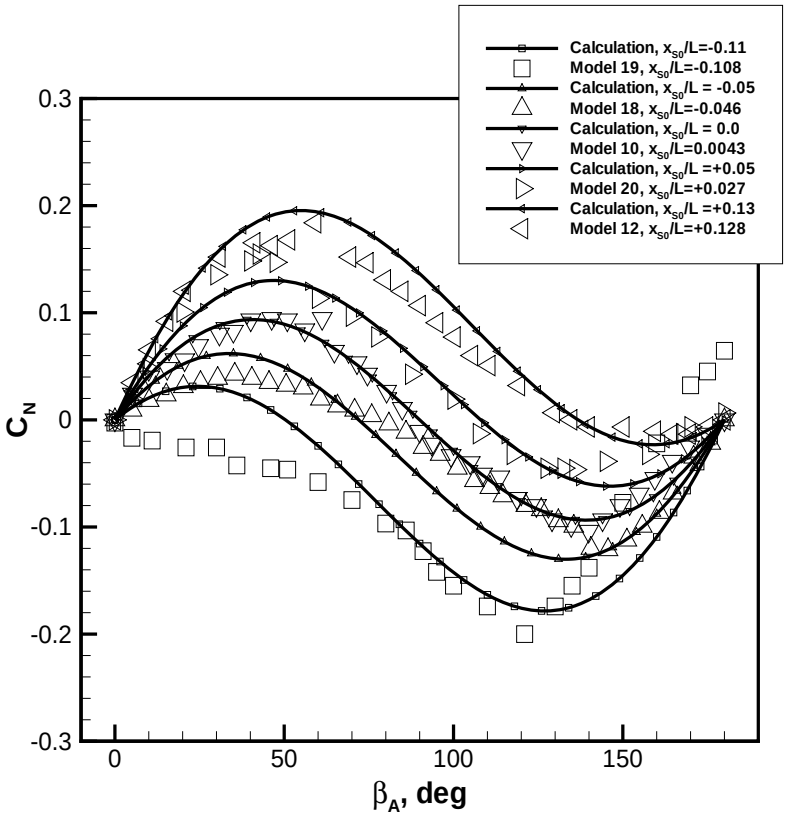

Figure 4.4: Aerodynamic yaw moment coefficient: solid line—calculation; symbols—experimental data from [26]

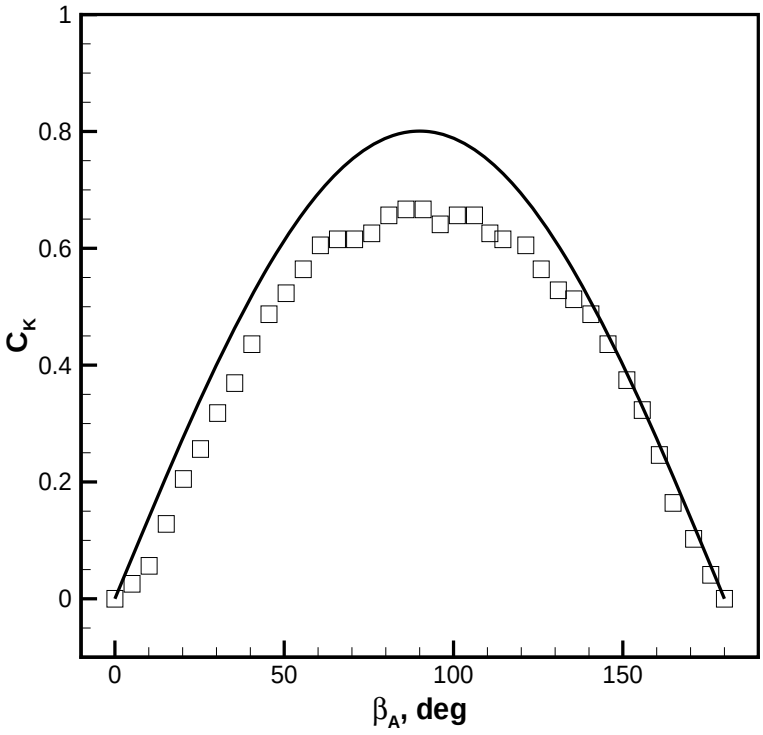

Figure 4.5: Aerodynamic heeling moment: solid line—calculation; symbols—experimental data from [26]

using Fig. 3.5 from [26], the value $\kappa = 1.25$ was chosen. The results of comparison still look acceptable although better fit would have been achieved at $\kappa = 1.0$. But in other cases the discrepancy can be much greater it can be rather recommended to find a suitable prototype from the experimental database.

4.1.3 Simulated Manoeuvring Motion Under Current and Wind Action

Current. Results of simulation of a turning manoeuvre are shown on Fig. 4.6. It is evident that the resulting motion is superposition of the plain turning and of the translation in direction of the current.

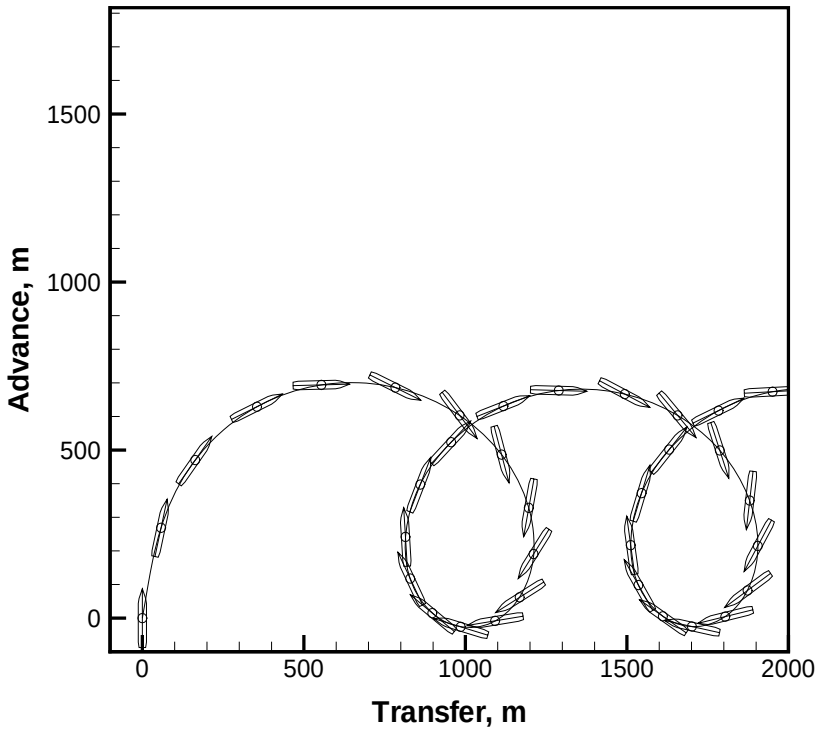

Figure 4.6: Trajectory at 35deg helm turning manoeuvre: current from left to right 3 knots

Wind. Action of the wind is much more complicated. A moderate wind corresponding to the force 5 Beaufort does not change the trajectory considerably (Fig. 4.7). A stronger wind corresponding to 11 Beaufort (Fig. 4.8) deforms the trajectory much more significantly but the centre of turn does not shift in the expected direction. This happens due to complicated nonlinear interaction of the wind action along various axes and of the propulsion active force. The result can be absolutely different for ships with different geometry and degree of directional stability/instability.

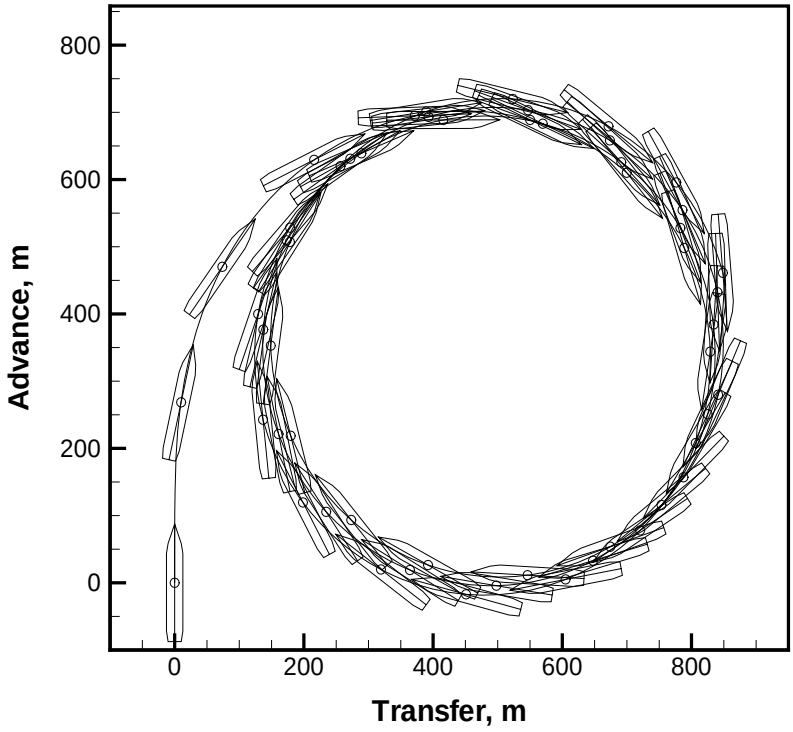

Figure 4.7: Trajectory at 35deg helm turning manoeuvre: wind from left to right 10m/s

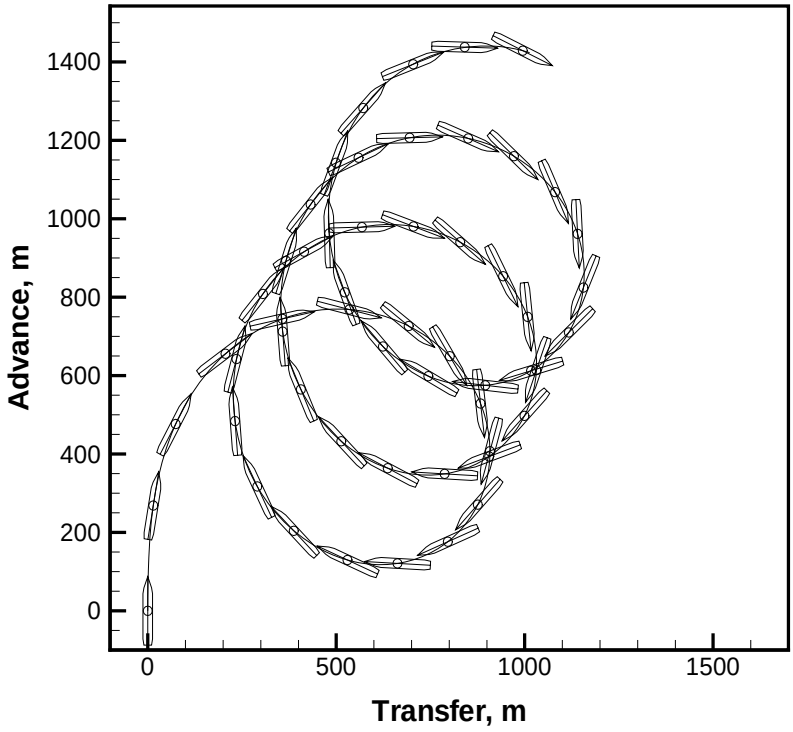

Figure 4.8: Trajectory at 35deg helm turning manoeuvre: wind from left to right 30m/s

Finally, the exceptional wind over 12 Beaufort (Fig. 4.9) causes partial loss of controllability:

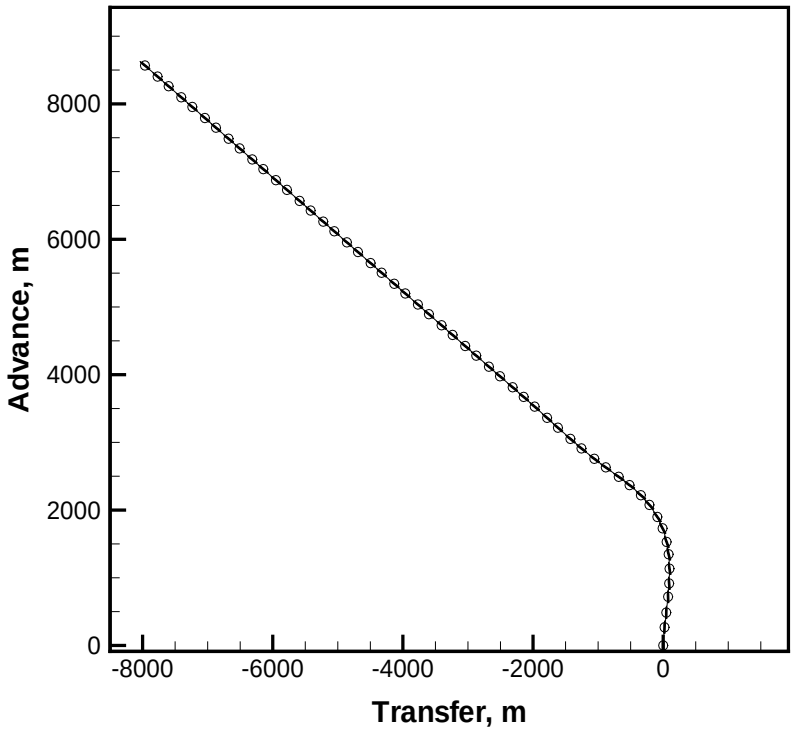

Figure 4.9: Trajectory at 35deg helm turning manoeuvre: wind from left to right 50m/s

the ship is not able to complete the initial turn but turns in the opposite direction instead. Later gaining additional velocity with the stern wind she makes the turn but then another loss of controllability follows.

In general, the ship's proneness to the controllability loss in wind depends on two parameters: the relative lateral wind area $A'_L = A_L/(LT)$ and on the relative wind speed $V'_w = V_w/V$, where V is the ship's approach speed. Hence, the most prone to wind are low-powered ships with large superstructures.

Chapter 5

Ship Control

5.1 General Principles of Ship Control

5.1.1 Preliminary Remarks

No one ship can sail uncontrolled during more or less significant time interval. This is clear from the fact that no one ship is asymptotically stable with respect to the heading angle and, even to maintain the straight course, let alone any prescribed path, continous rudder action is necessary.

It is possible to view the folowing levels of the ship control although the borders between them are not always crisp and well defined:

1. Route planning and working out headings required to follow the chosen itinerary. The problems considered on this level are exclusively kinematical and form content of the navigation science. The ship is here typically represented as a moving point, and in many formulations the curvature of the Earth spheroid must be taken into account.

2. Planning and execution of complicated practical manoeuvres. Many problems of this kind are considered in corresponding literature for navigators like, for instance, [8]. On this level, the ship's finite dimensions and her dynamic properties are often taken into account. Typically, considered task include berthing, unberthing, mooring, anchoring, station keeping, manoeuvring in formation (for the naval ships), replenishment of ships at sea, the man overboard manoeuvre etc. Weapons evasion manoeuvres can be also added to this list although these are usually studied in naval tactics. So far, solutions to any shiphandling problem were based exclusively on manual steering and practical experience although many issues of the ship manoeuvring theory, especially physical explanations of certain manoeuvring phenomena, were also taken into account.

3. Control in coursekeeping and basic manoeuvres, such as the course change or the lane change. Execution of standard trial manoeuvres already described earlier can be also associated with this basic level.

The third control level only can be considered in this course as in this case steering is most closely connected to the ship's inherent dynamic properties, the problems' statements are easily formalized and the applied mathematical models are detailed enough. On this level, steering can often be automatized. Any large ship is equipped with an autopilot used for the coursekeeping and, sometimes, for automated execution of course-changing manoeuvres. Lately, however, appeared a trend for formalization and automation of more complicated manoeuvres, even such as (un)berthing.

5.1.2 Control modes, programmes and laws

A ship can be steered in the manual or automatic mode. From the viewpoint of the control theory, the difference between these two modes is less dramatic than it could seem. In fact, in the both cases a ship is complemented with a *controller* which can be materialized either as an autopilot, or as a human operator.

On most ships, except for the small boats and high-speed craft, there are usually two concurrent human operators present: the conning officer and the helmsman. The task repartition between those two seamen is usually done in such a way that the officer is responsible for the level 1 and level 2 control tasks while the helmsman executes tasks of the level 3. For instance, the officer communicates a new heading to the helmsman and does not care how the latter executes the order. However, the officer has the right to override the helmsman's decisions and to give him direct orders of the type: "Rudder 20 degrees astarboard!". Regarding typically large reference time of a displacement ship, this override is equivalent to a virtual exclusion of the helmsman from the chain of command provided the orders are executed immediately and flawlessly. This means that considering the level 3 control it can be always assumed that we are dealing with a single controller.

Independently of the controller's nature, the control can be performed either through application of *control programmes* or implementing *control laws*.

Assuming that the only control variable is the required (ordered) rudder angle, the ship mathematical model can be taken in the form

$$\dot{x} = G(x, z, \delta^*). \tag{5.1}$$

Then, the programme control is defined if defined is the function

$$\delta^* = P(t) \tag{5.2}$$

which is called the control programme. It is essential that the list of arguments of the function P is complete and the rudder orders are pre-determined in advance. The typical and pure example of a control programme is that for the turning manoeuvre defined by eq. (2.242).

But the programme control is rarely applied in its pure form and is hardly applicable to more complicated manoeuvres as the external forces or exogeneous variables, such as the wind or sea waves action, cannot be predicted in advance and will introduce error into the ship's response. The only effective way to reduce this error is to monitor the actual ship response and

to correct the control according to the response. Explicit dependence of the control action on the time becomes then unnecessary.

In other words, instead of the control programme P applied must be a control law L which can be written as

$$\delta^* = L(y, x^*), \tag{5.3}$$

where $y = Cx$ is the vector of observable states (C is the observation matrix) and x^* is the vector of desired values of x.

The first introduced control law was that for the zigzag manoeuvre (2.245) and in this case: $y = (r, \psi)^T$ and $x^* = (\delta_z.\psi_z)^T$. In a more typical case of ship stabilisation on the given course, $x^* = (\psi^*, r^*)$, where $r^* = 0$ and the vector y will be considered later.

It is evident that the ship dynamics equation (5.1) describe, together with the control law equation (5.3), a so-called *closed-loop system* or a *feedback system* as the signal generated by the control law depends on the current values of the states while these, in there turn, depend on the control action. An appropriately designed feedback system sustains or executes the desired motion with acceptable errors under any disturbances within certain range. On the contrary, the set formed by eqs. (5.1) and (5.2) defines an open-loop system.

As the feedback control possesses, in application to the ship control, undiscutable advantages, only closed-loop controlled systems will be considered further on.

5.1.3 Control Requirements and Types of Control Laws

Any feedback controller, no matter human or automatic, must be trained or designed and adjusted to meet certain requirements. Some of these are about the operational hardware qualities (for instance, the helmsman must be alert and concentrated, the autopilot must be reliable and of reasonable size and mass, etc.) but many requirements are relevant to the ship dynamics. The most important of these are:

1. The closed-loop system must be stable.
2. The quality of control must be satisfactory.

It is evident that a controller destabilizing the system is useless and even harmful. On the other hand, the degree of stability of a ship with a good controller can be made much higher compared to what can be achieved with the rudder fixed. For instance, the ship can be made asymptotically stable not only with respect to the heading angle, which is mandatory for any type of controller, but also with respect to the lateral deviation from the desired path.

As to the quality of control, various criteria have been proposed. For instance, in a very typical case of the heading stabilisation, minimum average deviation from the desired heading can be required. On the other hand, the rudder deflections should not be too frequent and intense as well to avoid excessive wear of the steering gear and the mean drag's increase. Hence, the resulting criterion will be a compromise between these two.

Another typical quality criterion is the minimum time condition. For instance, it could be highly desirable to perform a course change as fast as possible. Typically, also, absence of an

overshoot can be required in this and other transient manoeuvres. It can be easily demonstrated that the no-overshoot requirements is in full compatibility with the minimum-time requirement.

As to the control law's nature and structure, they can be very complicated when the controller is human. In the case of an autopilot, real or simulated, the following options are followed in most cases:

1. *Fuzzy-Logic Control.* Autopilots of this type have been used in the simulation codes. They are designed to simulate the human operator's decision-making process. Such autopilots can only be implemented in form of a computer code i.e. the control system must be digital.

   A fuzzy-logic control algorithm is formulated in terms of the so-called linguistic variables. For instance, one of the rules constituting this algorithm can sound like this: "If the deviation from the desired heading is *large* and the ship is turning further with *moderate* rate, then apply a *considerable* helm to the opposite side". A set of such rules form the fuzzy-logic rule base which is linked to actual numerical values of the state variables and control orders by means of fuzzification/defuzzification interfaces [24]. Although fuzzy-logic controllers can be promising from the viewpoint of robustness and the gear's resource saving, still no successful real-life applications have been reported.

2. *Crisp Nonlinear Control.* Although nonlinear controllers may have a considerable potential, they are still mainly known in form of special particular cases as:

   (a) *Gain-Scheduling Control.* This is in fact a linear control law (see below) whose control gains are switched according to some auxiliary external-loop control law.

   (b) *Bang-Bang or Relay Control.* In this case, the control law does only produce rudder orders to maximum deflection angles i.e. any such law can be represented as

   $$\delta^* = \delta_m \operatorname{sign} \sigma(y, x^*), \tag{5.4}$$

   where $\sigma()$ is the *switching function.* This function is usually continuous but changes its sign depending on the combination of values of its arguments.

   It is proven that *any* time-optimal control law must be of bang-bang type but too energetic rudder executes are less suitable for the straight-course stabilization.

3. *Linear Control.* In the general case, linear control means that the control law can be represented as

   $$U = -Ky, \tag{5.5}$$

   where K is the control gain matrix (the minus sign is used partly for convenience in further evaluations, partly from tradition); $y = Ce$, where $e = x - x^*$ is the control errors vector and C is the observation matrix. Many well-developed methods exist for assigning appropriate values to the control gains [17]. Here, we shall only outline a simplified version of the so-called *pole-placement method.*

4. *Proportional-Integral-Derivative Control* or, shorter, the PID-control. This is in fact a particular case of the linear control which is, however, very important due to its simplicity

in implementation (can be easily realised on highly reliable analogue elements), fairly good performance, and because of an unmatched experience in its practical use: this law has been used during decades as the only control law in marine and aeronautical autopilots.

The PID-law is represented as

$$\delta^* = -k_\psi(\psi - \psi^*) - k_i \int_0^t (\psi(\tau) - \psi^*)\mathrm{d}\tau - k_r\dot{\psi}, \tag{5.6}$$

where k_ψ, k_i and k_r are the control gains. When some of these gains become zero, the law reduces to the PD-law or even to the P-law.

5.2 Examples of Controller Design: Pole-Placement Method

Full-state controller for sway-yaw motion. Typically, controllers are designed with the help of a linearised ship model although their performance is then verified on a full nonlinear model. So, combining this control law (5.5) with the equation of open-loop linear system (3.3) we have:

$$\dot{x} = \bar{A}x + \bar{B}x^*, \tag{5.7}$$

where the closed system's matrices are:

$$\bar{A} = A_D - B_C K C; \qquad \bar{B} = B_C K C. \tag{5.8}$$

In terms of the control errors, the equation of a feedback linear system will always have the form

$$\dot{e} = \bar{A}e. \tag{5.9}$$

Properties of the closed-loop system depend on the eigenvalues of the matrix $\bar{A}$. As this matrix depends on the gains matrix K, it can be imagined that it would be possible, adjusting the control gains, to assign desired values to the eigenvalues or, in other words, to place the poles of the transfer function to the desired loci. We shall show this process in the case when the ship's dynamics is described with eq. (3.6), the steering gear is ideal, i.e. $\delta_R \equiv \delta^*$, the control vector is one-dimensional, i.e. $U = (\delta^*)$ and the control law is full state, i.e.

$$\delta^* = -k_v v - k_r - k_\psi(\psi - \psi^*), \tag{5.10}$$

where ψ^* is the desired heading and the desired values of the remaining states are all zeroes which corresponds to the stabilisation on the direct course.

Inserting the law (5.10) into eq. (3.6) and adding the corresponding cinematic equation we have the following set of equations describing dynamics of the closed-loop system:

$$\begin{aligned} m_{22}\dot{v} + \bar{Y}_v v + \bar{Y}_r r + \bar{Y}_\psi \psi &= k_\psi Y_\delta \psi^*, \\ m_{66}\dot{r} + \bar{N}_v v + \bar{N}_r r + \bar{N}_\psi \psi &= k_\psi N_\delta \psi^*, \\ \dot{\psi} - r &= 0, \end{aligned} \tag{5.11}$$

where coefficients of the closed-loop system are:

$$\begin{array}{lll} m_{22} = m + \mu_{22}, & m_{66} = I_{zz} + \mu_{66}, & \\ \bar{Y}_v = Y_v + k_v Y_\delta, & \bar{Y}_r = Y_r + k_r Y_\delta, & \bar{Y}_\psi = k_\psi Y_\delta, \\ \bar{N}_v = N_v + k_v N_\delta, & \bar{N}_r = N_r + k_r N_\delta, & \bar{N}_\psi = k_\psi N_\delta. \end{array} \tag{5.12}$$

Applying the Laplace transform with zero initial conditions we get

$$\begin{array}{rcl} (m_{22}s + \bar{Y}_v)V + \bar{Y}_r R + \bar{Y}_\psi \Psi &=& k_\psi Y_\delta \Psi^*, \\ \bar{N}_v V + (m_{66}s + \bar{N}_r)R + \bar{N}_\psi \Psi &=& k_\psi N_\delta \Psi^*, \\ -R + s\Psi &=& 0. \end{array} \tag{5.13}$$

The characteristic equation is then

$$\hat{A}s^3 + \hat{B}s^2 + \hat{C}s + \hat{D} = 0, \tag{5.14}$$

where $\hat{A} = m_{22}m_{66}$, $\hat{B} = m_{22}\bar{N}_r + m_{66}\bar{Y}_v$, $\hat{C} = m_{22}\bar{N}_\psi + \bar{Y}_v\bar{N}_r - \bar{Y}_r\bar{N}_v$, and $\hat{D} = \bar{Y}_v\bar{N}_\psi - \bar{Y}_\psi\bar{N}_v$.

Explicit exact formulae for this equation's root, the Cardano formulae, exist but are very complicated and impractical. Let us suppose that the roots are found numerically (it is always possible) and they are: $\hat{s}_1$,$\hat{s}_2$, and $\hat{s}_3$. Then, according to the Vieta theorem:

$$\begin{array}{rcl} \dfrac{\hat{B}}{\hat{A}} &=& -(\hat{s}_1 + \hat{s}_2 + \hat{s}_3), \\ \dfrac{\hat{C}}{\hat{A}} &=& \hat{s}_1\hat{s}_2 + \hat{s}_2\hat{s}_3 + \hat{s}_1\hat{s}_3, \\ \dfrac{\hat{D}}{\hat{A}} &=& -\,\hat{s}_1\hat{s}_2\hat{s}_3. \end{array} \tag{5.15}$$

As the left-hand side depends on the control gains k_v, k_r, and k_ψ, eq. (5.15) can be viewed as a nonlinear algebraic system of equations with respect to those gains when the roots $\hat{s}_1$,$\hat{s}_2$, and $\hat{s}_3$ and, hence, the right-hand side of eq. (5.15) is pre-defined. Any real solution to this system will provide control gains resulting in the required loci of the poles.

To finalize the pole-placement method, it is only necessary to indicate which must be these loci. From the stability considerations, and we must require asymptotic stability of the controlled ship with respect to the heading angle, it is clear that all the poles, which can be complex, must be located on the left half of the complex plane.

Studies of the linear systems' behaviour showed that good quality of control is achieved when the poles correspond to the roots of the so-called Butterworth polynomials. The third-order Butterworth polynomial is

$$B_3(s) = s^3 + 2\omega_0 s^2 + 2\omega_0^2 s + \omega_0^3, \tag{5.16}$$

where ω_0 is a real parameter. This polynomial's roots satisfy the equation

$$\left(\frac{s}{\omega_0}\right)^6 = 1 \tag{5.17}$$

and lie all on the left half-plane. They are:

$$\hat{s}_1 = -\omega_0, \qquad \hat{s}_2 = \omega_0 e^{i\frac{2\pi}{3}}, \qquad \hat{s}_3 = \omega_0 e^{-i\frac{2\pi}{3}}. \tag{5.18}$$

Hence, the desired roots (poles) are all located on the circle with the radius ω_0 which remains a free parameter to be chosen by means of comparative simulations preferrably carried out not with the simplified linear model but using the complete nonlinear manoeuvring mathematical model including also the real steering gear.

Generally, larger values of ω_0 mean a faster response and better stabilisation but this can be at the expense of too energetic rudder deflections and frequent saturation of the rudder angle may happen. On the contrary, too small ω_0-values will mean a too slow response and bad accuracy of steering. Saturations will then never happen and such a system is then called "overdesigned". So, the optimal value of ω_0 corresponds to a moderately energetic response to expected perturbations with not frequent occasional saturations.

Simplified design of a PID controller. This kind of controller is expected to be best designed on the basis of the second-order Nomoto equation (3.33). Combining it with the PID-law (5.6), assuming that the rudder gear is ideal and changing for the Laplace-image representation, we'll obtain:

$$[T_1T_2s^3 + (T_1+T_2)s^2 + s]\Psi(s) = K(1+T_3s)[-k_\psi(\Psi-\Psi^*) - \frac{k_i}{s}(\Psi-\Psi^*) - k_r s\Psi]. \tag{5.19}$$

Transfering suitable terms to the left-hand part and multiplying both parts by s we shall get:

$$\begin{aligned}&[T_1T_2s^4 + (T_1+T_2+KT_3k_r)s^3 + (1+KT_3k_\psi)s^2 + K(k_\psi+T_3k_i)s + Kk_i]\Psi(s)\\ &= [K(k_\psi+T_3k_i)s + KT_3k_\psi s^2 + Kk_i]\Psi^*(s).\end{aligned} \tag{5.20}$$

This equation defines the transfer function of the closed-loop system from the desired heading ψ^* to the actual heading ψ. Stability of the system and quality of the control will mainly depend on the system's eigenvalues i.e. on the roots of the characteristic equation which, evidently, will be:

$$T_1T_2s^4 + (T_1+T_2+KT_3k_r)s^3 + (1+KT_3k_\psi+Kk_r)s^2 + K(k_\psi+T_3k_i)s + Kk_i = 0. \tag{5.21}$$

This equation, according to the principle theorem of algebra, has 4 roots. Although these roots can be expressed explicitly through the equation's coefficients by means of the Ferrari formulae, the resulting expressions are prohibitively complicated and this method is never used in practice. On the other hand, there is a number of reliable algorithms and codes for obtaining the roots at any values of the equation's coefficients. Let us assume that the desired values of these roots are: $\hat{s}_1$, $\hat{s}_2$, $\hat{s}_3$, $\hat{s}_4$. Then, the coefficients of eq. (5.21) and these roots' values will be connected with the following equations:

$$\begin{aligned} T_1+T_2+KT_3k_r &= T_1T_2S_1,\\ 1+KT_3k_\psi &= T_1T_2S_2,\\ Kk_\psi+KT_3k_i &= T_1T_2S_3,\\ Kk_i &= T_1T_2S_4, \end{aligned} \tag{5.22}$$

where

$$\begin{aligned} S_1 &= -(\hat{s}_1 + \hat{s}_2 + \hat{s}_3 + \hat{s}_4), \\ S_2 &= \hat{s}_1\hat{s}_2 + \hat{s}_1\hat{s}_3 + \hat{s}_1\hat{s}_4\hat{s}_2\hat{s}_3 + \hat{s}_2\hat{s}_4 + \hat{s}_3\hat{s}_4, \\ S_3 &= -(\hat{s}_1\hat{s}_2\hat{s}_3 + \hat{s}_1\hat{s}_3\hat{s}_4 + \hat{s}_2\hat{s}_3\hat{s}_4 + \hat{s}_1\hat{s}_2\hat{s}_4), \\ S_4 &= \hat{s}_1\hat{s}_2\hat{s}_3\hat{s}_4. \end{aligned} \tag{5.23}$$

However, if we consider eq. (5.22) as the linear algebraic set for defining the control gains, we shall see that the system is over-defined. It means that three control gains are nor sufficient to place all the roots to desired loci. However, it would be possible to find a solution in the least-square sense. Another possibility is to make the synthesis on the basis of the first-order Nomoto equation. In this case, the characteristuc equation is

$$Ts^3 + (1 + Kk_r)s^2 + Kk_\psi s + Kk_i = 0. \tag{5.24}$$

Applying again the Vieta theorem and assuming that the root loci's repartition corresponds to eq. (5.18), we shall easily obtain explicit formulae for the control gains:

$$\begin{aligned} k_r &= \frac{1}{K}(2T\omega_0 - 1), \\ k_\psi &= \frac{2T\omega_0^2}{K}, \\ k_i &= \frac{T\omega_0^3}{K}. \end{aligned} \tag{5.25}$$

It can be seen that all the control gains are inversely proportional to the ship gain which is quite natural. It must be emphasized that the obtained values of the control gains are in no way final. Further, they must be adjusted anyway, by using, say, the Ziegler–Nichols tuning procedure [16] or simply by means of comparative simulations on the full model.

Finally, it must be noted that the PID controllers are prone to the so-called *integrator windup* [16] which happens when a saturation occures in the chain of control. In the considered case of a steered ship, it corresponds to the case when the rudder angle attains its maximum absolute value. In this case, presence of the I-termsubstantially deteriorates transients and, to avoid this, the control must be reduced to the PD-control every time when the saturation happens.

Chapter 6

Manoeuvring Criteria and Standards

6.1 General Principles and Approaches

During centuries, vessels were built following traditions and empiric rules. This situation started to change gradually since the end of 18th century but natural technical progress and especially appearance of ships with mechanical power, of larger size and higher speed boosted that process. Currently, share of scientific knowledge in any new ship design is substantial. However, as many issues related to safety in ship operation are difficult to formalize, the empiric part is not rejected and, augmented with scientific results, is incorporated into Classification and Construction Rules of various classification societies. Most of the content of these Rules is dedicated to safety issues related to the ship strength, capsizing resistance and reliability and safety of ship engines and other mechanisms and their elements. Unfortunately, manoeuvring issues, with very few and uncertain exceptions (Det Norske Veritas, Russian Maritime Register of Shipping) have been so far neglected in these documents. However, as the naval production history contains cases of ships with unusually and dangerously bad manoeuvring performance though satisfying all existing rules, a work on elaboration of some manoeuvring standards was carried out, with alternating intensity, during last 50 years. This finally resulted in "Standards for Ship Manoeuvrability" adopted by the International Maritime Organization (IMO) [40]. These standards are based on certain combination of theoretical considerations and simulations (including those covered in the present manuscript) with statistical data on real ships. The latter was necessary because any viable rules or standards must comply with the majority of already existing successful vessels. Although the existing IMO standards are far from being perfect, they can help to eliminate ships with pathologically bad manoeuvring qualities and serve as good guidelines in the design process. In the present version, the Standards mean only displacement vessels and do not apply to ships shorter (between the perpendiculars) than 100m, except chemical tankers and gas carriers, and to the naval ships.

6.2 IMO Manoeuvring Standards

The standards are a legal document containing accurate definitions of all parameters and conditions. That is why, for any real-life application it can be advised to use the original text [40]. The material presented here is in full compliance with the standards but the formulations are simplified and commented and evident definitions are dropped.

All the criterial values correspond to the ideal test conditions: full-load, deep water, calm sea, absence of wind. The approach speed must be the ship's speed corresponding to the engine's output equal to 85 per cent of the maximum continuous rating. The maximum rudder angle is suppposed to be 35 degrees or less if there are speed-dependent restrictions.

All the criteria and their values required by the Standards are presented in Table 6.1

Table 6.1: IMO Manoeuvring Standards: Criteria and their Required Values

Quality	*Parameter*	*Criterion*
Turning ability	Advance	$\leq 4.5L$
	Tactical Diameter	$\leq 5L$
Initial Turning Ability	Travel Distance until $\Delta\psi = \pm 10$deg after $\delta_R = \pm 10$deg at maximum deflection rate	$\leq 2.5L$
Yaw Checking and Course Keeping Abilities	Zig-Zag 10–10 first overshoot	$\leq \begin{cases} 10\text{deg} & \text{if} \quad T_{ref} < 10\text{s} \\ \left(5 + \frac{T_{ref}}{2}\right)\text{deg} & \text{if} \quad T_{ref} \in [10\text{s}, 30\text{s}] \\ 20\text{deg} & \text{if} \quad T_{ref} > 30\text{s} \end{cases}$
	Zig-Zag 10–10 second overshoot	$\leq \begin{cases} 25\text{deg} & \text{if} \quad T_{ref} < 10\text{s} \\ \left(17.5 + \frac{3}{4}T_{ref}\right)\text{deg} & \text{if} \quad T_{ref} \in [10\text{s}, 30\text{s}] \\ 40\text{deg} & \text{if} \quad T_{ref} > 30\text{s} \end{cases}$
	Zig-Zag 20–20 first overshoot	≤ 25deg
Stopping Ability	Track reach at FULL ASTERN until stopped	$\leq \begin{cases} 15L & \text{if} \quad S < 1 \\ \min\{20L, (5 + 10S)L\} & \text{if} \quad S \geq 1 \end{cases}$
Remark: the ship inertial parameter $S = \frac{mV}{P_e}\mathsf{Fn}^2$, where P_e is the engine's maximum continuous rating in horsepower; mass m is in tonnes, approach speed V is in m/s.		

The travel distance and the track reach mentioned in the Table are measured with respect

to water along the ship's curvilinear path. Any standard ship log provides this reading directly.

6.3 Accounting for Manoeuvring Qualities in Ship Design

Usually manoeuvring issues are not of primary concern during the design process but should not be forgotten anyway. In accordance with the spiral nature of the engineering design process, manoeuvring issues are treated in several steps:

1. On the stages of conceptual and preliminary design, the steering arrangement can be taken (assumed to be) the same as on the prototype with appropriate scaling if necessary.

   In the case of a normal rudder as main control device, its area A_R can be approximately chosen as percentage of the approximate lateral submerged area LT. In most cases $\frac{A_R}{LT} = 1 - 3$ per cent where 1 per cent corresponds to the case of the rudder in the slipstream behind a moderately loaded propeller while higher values are typical for a rudder in the free stream on twin-screw ships. In case of arrangement problems, twin rudders can be used.

   Some national Classification and Construction Rules contain more elaborate recommendations. For instance, according to *Det Norske Veritas*

   $$\frac{A_R}{LT} \geq 0.01 \left[1 + 25 \left(\frac{B}{L}\right)^2\right]. \tag{6.1}$$

2. At the next design step, manoeuvring simulations by means of acknowledged methods (like the Inoue method described above) should be carried out. First of all, compliance with the IMO standards must be verified. If some of the standards are not met substantially, it is recommended to re-consider the steering arrangement's design. For instance, if the ship's turning ability is not satisfactory, the rudder's area should be increased or a twin-rudder arrangement must be applied. In some cases, a steering nozzle solves the problem.

   If excessive inherent directional instability is detected, it must be dealt with. When it is possible to adjust the hull form, it can be advised to design a sharper and better faired afterbody. However, very often the hull's shape is predetermined by hydrostatic and resistance consideration, and then adding stabilising fins or skegs can be the only available solution. In most cases, these are low-aspect ratio triangular wings, like, for instance the propeller shaft bossings.

3. In most cases, the design process is accompanied with manufacturing at least one scaled physical model and testing it in the towing tank primarily for resistance and propulsion purposes. The same model should, however, be subject to manoeuvring tests. If captive-model tests are performed, a more accurate mathematical model can be developed and all critical manoeuvres will then be simulated again. But often the manoeuvring performance is checked directly with the self-running model.

Again, if some signs of bad manoeuvring behaviour are revealed, additional corrections are introduced into the design. When possible, the scaled model is modified too and the tests are repeated.

It must be emphasized that, due to poorly studied scale effect, even a very thorough design does not guarantee that the manoeuvring qualities of a freshly built ship will be exactly as expected and predicted but at the present state of art severe mistakes are not likely to happen either.

Chapter 7

Afterword

We could only focus in these lectures on manoeuvring of classic surface displacement ships. Although such ships constitute prevailing part of the world tonnage, there are many others types of marine craft which have certain specifics in manoeuvring. Here we shall make a quick review of these specifics.

Planing and Semi-Planing Vessels. Typically, these are ships with the Froude number exceeding 0.6–0.7. There specifics are mainly related to the nature of the hull forces which are dependent on the asymmetry in spray formation. These vessels have typically greater relative turning radii then usual ships which, however, does not present much problems because of smaller dimensions of these craft. Unlike the displacement vessels, they all have an inward dynamic heel.

Air-Cushion Vehicles (ACV) and Surface-Effect Ships (SES). These vessels either have virtually no contact with the water surface (ACV) or have a very small one (SES) and the role of aerodynamic forces for them is higher than for displacement ships, especially in low-speed manoeuvring in wind. However, as the moving pressure field is interacting with water, hydrodynamic forces of wave nature dominate in manoeuvring over the sea surface. These forces can be effectively estimated with theoretical methods.

Submarines and Submersibles. Manoeuvrability of a surfaced submarine is quite similar to that of a surface displacement ship except for different hydrodynamic characteristics. But in submerged state, even the horizontal-plane dynamics requires recourse to a 6DOF model: if no counter-measures are taken, a submarine will not keep depth in the turning circle. Of extremely importance is manoeuvrability in the longitudinal plane which can be studied separately. Due to interaction between the hydrodynamic and hydrostatic forces, the submarine's eigenvalues in this plane will depend on the speed. Also, there exists a critical speed at which the stern planes lose there effectiveness and the submarine reacts to their deflection in the opposite way below and above that speed. Additional studied problems are related to the submarine balancing, main ballast tanks (MBT) operation, emergence surfacing, depth-change control etc.

Hydrofoils. Hydrodynamics is very different from that of displacement ships and simpler in some respects due to possibility of applying effectively the wing theory. On the other hand, the dynamic model should be 6DOF and the control problems can be very sophisticated. There are two different classes of hydrofoil craft: those with deeply submerged hydrofoils requiring an automatic control system for operation and those with little submerged or surface piercing foils using dependence on the foil submergence for natural stabilisation of the craft.

Bibliography

[1] Alessandrini B., Delhommeau G. *Viscous Free Surface Flow Past a Ship in Drift and in Rotating Motion*, 22nd Symposium on Naval Hydrodynamics: Washington, D.C. (USA), 9–14 August 1998, National Academy Press, Washington D.C., 1999, pp. 491–507.

[2] Arabshahi A., Beddhu M., Briley W., Chen J., Gaither A., Gaither K., Janus J., Jiang M., Marcum D., McGinley J., Pankajashan R., Remotigue M., Sheng C., Sreenivas K., Taylor D., Whitfield D. *A Perspective on Naval Hydrodynamic Flow Simulation*, 22nd Symposium on Naval Hydrodynamics: Washington, D.C. (USA), 9–14 August 1998, National Academy Press, Washington D.C., 1999, pp. 920–934.

[3] Arczewski K., Pietrucha J. *Mathematic Modelling of Mechanical Complex Systems. Vol. 1: Discrete Models, Ellis Horwood Ltd., Chichester, England, 1993.*

[4] Assenberg F. en Sellmeijer R. *Vier-kwadrant vrijvarende-schroef-karakteristieken voor B-serie schroeven. Fourier-reeks ontwikkeling en operationeel gebruik*, Maritiem Research Instituut Nederland (MARIN): Rapport No. 60482-1-MS. Wageningen: 1984. 30p.

[5] Bertram V. *Computational Fluid Dynamics for the Marine Industry: an Introduction*, "CFD for Ship and Offshore Design": 31st WEGEMT School, Hamburg, 3–7 May 1999. 15p.

[6] Bertram V. *Practical ship hydrodynamics*, Butterworth Heinemann, Oxford, 2000.

[7] Crane C.L., Eda H., Landsburg A. *Controllability*, In: Principles of Naval Architecture V.3/Ed. E.V. Lewis, Jersey City, NJ: SNAME, 1989. P. 191–365.

[8] Crenshaw R.S., Jr., Captain, USN *Naval Shiphandling*, Naval Institute Press, Annapolis, Maryland, 1972, 333p.

[9] Cura Hochbaum A. *Computation of the Turbulent Flow Around a Ship in Steady Turn and in Steady Oblique Motion*, 22nd Symposium on Naval Hydrodynamics: Washington, D.C. (USA), 9–14 August 1998, National Academy Press, Washington D.C., 1999, pp. 550–567.

[10] Draper N.R., Smith H. *Applied Regression Analysis*, Wiley Interscience Publ., 1998. 706 pp.

[11] El Moctar Ould M. *Numerical Computation of Flow Forces in Ship Manoeuvring*, Ship Technology Research/Schiffstechnik, 2001, Vol. 48, pp. 98–123.

[12] Eloot K., Vantorre M. *Alternative Captive Manoeuvring Tests: Possibilities and Limitations*, MAN'98: Proceedings of the Symposium on Forces Acting on a Manoeuvring Vessel. Val de Reuil, France. September 16–18, 1998. P. 89–100.

[13] *Explanatory Notes to the Standards for Ship Manoeuvrability*, International Maritime Organization (IMO) Circular MSC/Circ. 1053, 2002.

[14] Fedyaevsky K.K., Sobolev G.V. *Control and Stability in Ship Design*, U.S. Department of Commerce Translation, Washington, DC, 1964.

[15] Filippov A.F. *Differential Equations with Discontinuous Right-Hand Side*, Moscow: Nauka Publ., 1985 (Russian).

[16] Franklin G.F., Powell J. D., Emami-Naeini A. *Feedback Control of Dynamic Systems*, Addison Wesley Publishing Co., 1994, 778p.

[17] Friedland B. *Control System Design: An Introduction to State-Space Method*, McGraw-Hill Publ. Co., 1986, 513p.

[18] Inoue, S., Hirano, M., Kijima, K. (1981) *Hydrodynamic Derivatives on Ship Manoeuvring*, International Shipbuilding Progress. 1981. Vol. 28, No. 321. pp. 112–125.

[19] Inoue S. et al. *A Practical Calculation Method of Ship Maneuvering Motion*, Int. Shipbuild. Progr. 1981. Vol. 28. No. 325. pp. 207–222.

[20] Korn G.A., Korn T.M. *Mathematical Handbook for Scientists and Engineers*, McGraw-Hill Book Co., 1968.

[21] Kose K. *On a New Mathematical Model of Manoeuvring Motion of a Ship and its Applications*, Int. Shipbuild. Progr. 1982. Vol. 29. No. 336, pp. 205–220.

[22] Kuiper G. *The Wageningen Propeller Series*,MARIN Publication 92-001, May 1992.

[23] Landrini M. *CFD for Ship Manoeuvrability*, "CFD for Ship and Offshore Design": 31st WEGEMT School, Hamburg, 3–7 May 1999. 14p.

[24] Lin Ch.-F. *Advanced Control Systems Design*, PTR Prentice Hall, Englewood Cliffs, N.J., 1994, 664p.

[25] Lurie A.I. *Analytical Mechanics*. Springer Verlag, 2002. 864p.

[26] *Manoeuvring Technical Manual*/Ed. J. Brix, Hamburg: Seehafen Verlag, 1993.

[27] Myers R.H. and Montgomery D.C. *Response Surface Methodology*, Wiley-Interscience Publ., 1995.

[28] Newman J.N. *Theoretical Methods in Ship Manoeuvring*, Proceedings, th ONR Symposium on Naval Hydrodynamics, , 19.

[29] Nikolayev E. *Results of Rotating Arm Tests Carried out in Krylov Ship Research Institute*: Working Paper for the Manoeuvrability Committee Report. Proc. 19th ITTC, Madrid, Spain (1990), Vol. 1. p. 397.

[30] Oltmann P., Sharma S.D. *Simulation of Combined Engine and Rudder Maneuvers Using an Improved Model of Hull-Propeller-Rudder Interactions*. Proceedings, "15th ONR Symposium on Naval Hydrodynamics, Hamburg, September 2–7, 1984", National Academy Press, Washington D.C., 1985, pp. 83–108.

[31] Örnfelt M. *Naval Mission and Task Driven Manoeuvrability Requirements for Naval Ships*. Proceedings, 10th International Conference on Fast Sea Transportation FAST2009, Athens, Greece, 1984, pp. 505–518.

[32] Prishchemikhina T.Yu., Zlotin S.E.*Circular Wind-Tunnel Tests of Airfoils for Prediction of Four-Quadrant Characteristics of Screw-Propellers,* Transactions of the USSR Society of Naval Architects, Issue 296: "Means and Methods for Full Scale Studies of Seakeeping Qualities of Ships", Leningrad: Sudostroyeniye Publ., 1979, pp. 55–60 (in Russian).

[33] Roddy, R. F., D. E. Hess, and W. E. Faller *A tool to predict the four-quadrant performance of the Wageningen B-screw series for ship performance simulations* , Ship Technology Research, 2007, Vol. 54, No. 3, pp. 103-113.

[34] Santos, H. B., Sutulo, S., Guedes Soares, C. *Planning and Analysis of Maneuvering Tank Tests with Captive Models (in Portuguese: Planeamento e Análise de Ensaios de Manobrabilidade em Tanque com Modelos Fixos)*, In: O Mar Fonte de Desenvolvimento Sustentado/ C. Guedes Soares, J. Beirão Reis e M.B. Martins Guerreiro (Eds) , Edições Salamandra, Lisboa 2002, pp. 271–290.

[35] Sato T., Izumi K., Miyata H.*Numerical Simulation of Maneuvering Motion*, 22nd Symposium on Naval Hydrodynamics: Washington, D.C. (USA), 9–14 August 1998, National Academy Press, Washington D.C., 1999, pp. 724–737.

[36] Scragg C.A. *Determination of Stability Derivatives by Impulse-Response Techniques*, Marine Technology. 1978. Vol. 14. No. 3. P. 265–275.

[37] Simonsen Claus D., Stern Frederic *RANS Manoeuvring Simulation of* Esso Osaka *With Rudder and a Body-Force Propeller*, Journal of Ship Research, 2005, Vol. 49, No. 2, 99. 98–120.

[38] Sobolev G.V. *Ship Manoeuvring and Control*, Leningrad: Sudostroyeniye Publ., 1976 (Russian).

[39] Söding H. *Limits of Potential Theory in Rudder Flow Predictions*, 22nd ONR Symposium on Naval Hydrodynamics, Washington, D.C. (USA): August 9–14, 1998, National Academy Press, Washington D.C., 1999, pp. 622–637.

[40] *Standards for Ship Manoeuvrability*, International Maritime Organization (IMO) Resolution MSC.137(76)4, 2002.

[41] Sung Y.J., Lee S.Y., Rhee K.-P. *Estimation of Manoeuvring Coefficients from PMM Test by Genetic Algorithm*, MAN'98: Proceedings of the Symposium on Forces Acting on a Manoeuvring Vessel. Val de Reuil, France. September 16–18, 1998. P. 77–88.

[42] Sutulo S.V. *Hydrodynamic Properties of Ship Control Devices: Lecture Notes*, Leningrad Shipbuilding Institute Edition. Leningrad, 1988 (Russian).

[43] Sutulo S.V., Kim S.-Y. *Systematic Approach to PMM/Rotating Arm Experiment Planning, Parameter Estimation, and Uncertainty Analysis*, MAN'98: Proceedings of the Symposium on Forces Acting on a Manoeuvring Vessel. Val de Reuil, France. September 16–18, 1998. pp. 57–67.

[44] Sutulo S., Guedes Soares C. *Development of a multi-factor regression model of ship maneuvering forces based on optimized captive-model tests*, J. Ship Res., 2006. Vol. 50, pp. 311–333.

[45] Sutulo S., Guedes Soares C. *Contribution of higher-order harmonics for estimating manoeuvring derivatives from oscillatory tests*, Int. Shipbuild. Progr., 2007, Vol. 54, pp. 1–24.

[46] Tahara Y., Longo J., Stern F., Himeno Y. *Comparison of CFD and EFD for the Sries 60 $C_B = 0.6$ in Steady Yaw Motion*, 22nd Symposium on Naval Hydrodynamics: Washington, D.C. (USA), 9–14 August 1998, National Academy Press, Washington D.C., 1999, pp. 981–999.

[47] Van Mannen J.D., Van Oossanen P. *Propulsion*. In: Principles of Naval Architecture V.2/Ed. E.V. Lewis, Jersey City, NJ: SNAME, 1989. P. 127–254.